2007

Study Of Covalent And Non-Covalent Interactions In Ternary Systems Involving: Metal/DNA-RNA/Protein, Where Metal = Platinum(II), Palladium(II)

Anzellotti I. Atilio
Virginia Commonwealth University

STUDY OF COVALENT AND NON-COVALENT INTERACTIONS IN TERNARY SYSTEMS INVOLVING: METAL/DNA-RNA/PROTEIN, WHERE METAL = Pt(II), Pd(II).

A Dissertation submitted in partial fulfillment of the requirements for the degree of Ph.D. at Virginia Commonwealth University.

by

ATILIO I. ANZELLOTTI
M.Sc. in Chemistry, Venezuelan Institute for Scientific Research (IVIC) - Venezuela, 2004.
B.Sc. in Chemistry, Universidad de Los Andes – Venezuela, 1997.

Director: DR. NICHOLAS P. FARRELL
PROFESSOR AND CHAIR, DEPARTMENT OF CHEMISTRY, COLLEGE OF HUMANITIES AND SCIENCES, VIRGINIA COMMONWEALTH UNIVERSITY

Virginia Commonwealth University
Richmond, Virginia
November 2007

Acknowledgement

This dissertation, as every work, is a result of a joint effort from several people and the successful combination of different factors. I would like to thank God for giving me the opportunity to start and finish this Ph.D. program. My wife, for her loving support and company during the last ten years and her patience during my graduate work. My family and friends for sharing good times and happiness. My advisor Dr. Nicholas Farrell for the opportunity to work in such an interesting project and for providing me with the tools to make a good contribution towards its development. Dr. Yun Qu for helping me out in difficult moments and teaching me the underlying and importants details of spectroscopic techniques and important decisions. The members of my dissertation committee for their feedback and advice throughout my research project. Post-docs members Dr. Qin Liu, Dr. Seiji Komeda and Dr. Eva Montero, and present and past members in Dr. Farrell's group for interesting discussions and professional/personal lessons. I would also like to acknowledge the American Chemical Society for an International Activities Fellowship, which allowed me to start the research program.

Table of Contents

Page

List of Tables

Page

List of Figures

Page

List of Schemes

Page

List of Charts

Page

List of Abbreviations

A	Adenine
Å	Angstrom
ATZ	*trans*-dichloroamminethiazoleplatinum(II)
C	Cytosine, cysteine
Carboplatin	*cis*-diammine-1,1-cyclobutane dicarboxylateplatinum(II)
CD	Circular Dichroism
Cisplatin / cis-DDP	*cis*-diamminedichloroplatinum(II)
COSY	Correlation Spectroscopy
5'-CMP	5'-cytidine monophosphate
D_2O	Deuterium oxide
DFT	Density Functional Theory
Dien	Diethylenetriamine
DMF	Dimethyl formamide
DNA	Deoxy riboNucleic Acid
en	ethylenediamine
ENDOR	Electron-Nuclear Double Resonance
EPR	Electronic Paramagnetic Resonance
ESI-MS	Electro-Spray Ionisation Mass Spectrometry
9-EtGH	9-ethyl guanine
eV	Electron Volt
EXAFS	Extended X-ray Absorption Fine Structure
F	Phenylalanine
F2	C-terminal zinc finger in NCp7
G	Guanine
Guo	Guanosine
5'-GMP	5'-guanosine monophosphate

HDAC	Histone De-Acetylases
His	Histidine
HIV	Human Immunodeficiency Virus
HMG	High Mobility Group
HOMO	Highest Occupied Molecular Orbital
HPLC	High performance Liquid Chromatography
HSA	Human Serum Albumin
ICP	Inductively Coupled Plasma
Iq	Isoquinoline
ITC	Isothermal Titration Calorimetry
Ka	Association Constant
Kj	Kilo joule
LUMO	Lowest Unoccupied Molecular Orbital
MβL	Metallo-β lactamase
MD	Molecular Dynamics
1-MeCyt	1-Methyl Cytosine
MM	Molecular Mechanics
MMP	Matrix MetalloProteinase
MPN	Monofunctional Platinum-Nucleobase complexes
N-Ac Met	N-acetyl methionine
N-AcTrp	N-acetyl tryptophan
NCp7	Nucleocapsid Protein 7
NER	Nucleotide Excission Repair
NMR	Nuclear Magnetic Resonance
ns	Nanosecond
Oxaliplatin	[xalate(*trans*-L-diaminocyclohexane)platinum(II)
PDB ID	Protein DataBase IDentification
ppm	Parts per million
ps	Picosecond

PT	Prenyl Transferase
py	Pyridine
p53	Tumor protein 53 or protein 53
RMS	Root Mean Square
RNA	RiboNucleic Acid
SOD	Super Oxide Dismutase
T	Thymine
TPA	Trans-Planar Amine complexes
Transplatin, t-DDP	*trans*-diamminedichloroplatinum(II)
Trp	Tryptophan
Ub	Ubiquitin
W	Tryptophan
XANES	X-ray Absorption Near Edge Structure
ZF	Zinc Finger

Abstract

STUDY OF COVALENT AND NON-COVALENT INTERACTIONS IN TERNARY SYSTEMS INVOLVING: METAL/DNA-RNA/PROTEIN, WHERE METAL = Pt(II), Pd(II).

By Atilio I. Anzellotti

A Dissertation submitted in partial fulfillment of the requirements for the degree of Doctor of Philosophy at Virginia Commonwealth University.

Virginia Commonwealth University, 2007

Major Director: Nicholas P. Farrell
Professor and Chair, Department of Chemistry

Ternary systems comprising DNA/RNA, proteins and one (or more) metal ion are generating increased interest due to its biological relevance. The knowledge gained from the study of these sytems could provide important clues regarding the precise mechanism for transcription factors, repair proteins and metal complexes with anti-tumoral/anti-viral activities.

The interactions occurring among the components of these ternary systems can be broadly grouped into covalent and non-covalent. The first kind of interactions can lead to

the irreversible transformation of the components in the system, while the second is thought to be reversible leading to transient states and fluxionality. Both kinds of interaction are generally present in living systems, complementing the function of each other.

Monofunctional Platinum-nucleobase complexes (MPNs) are synthesized *via* substitution of a chloride ligand by a nucleobase in platinum complexes with *trans* geometry. MPNs are particularly interesting for the study of ternary sytems since they mimic the first step in the formation of a platinum-DNA adduct and their interaction with aminoacids/proteins provide a good first approach for more complex systems.

The presence of the nucleobase as a ligand, significantly modifies the biological activity of these complexes by reducing its cytotoxicity and generating a promising anti-viral activity, especially against HIV-1 virus. The specific role of the nucleobase ligand on these complexes as a non-covalent motif, important for protein recognition, was explored in models involving tryptophan/N-acetyl tryptophan and a small protein domain called zinc finger, containing also a tryptophan residue.

The coordination of the nucleobase to a metal ion such as Pt(II) or Pd(II) was found to increase its π-stacking interaction towards aromatic residues in proteins, specifically tryptophan. The enhancing effect was found to depend on the nature of the metal ion, nature of nucleobase and size/complexity of the protein model. Furthermore, DFT studies revealed an important change in the energy for the lowest unoccupied molecular orbital (LUMO) in the coordinated nucleobases, which could place this orbital in an favored position to interact with the highest occupied molecular orbital (HOMO) in

the tryptophan residue. Results from calculations showed a good correlation with experimental evidence and could indicate an important role for the frontier molecular orbitals (HOMO/LUMO) of the species involved in the π-stacking interaction

This study was extended to a zinc finger domain from an essential protein in HIV-1 virus, i.e. nucleocapsid protein NCp7. Findings showed that the nucleobase ligand in addition to modulate hydrolysis and reaction rates for MPNs can also be responsible for an initial non-covalent recognition towards a specific protein. This initial recognition has been proposed as the first stage in a two-step mechanism of action for these platinum complexes that ultimately can lead to zinc ejection from the zinc finger domain in the viral NCp7. The significance of the data presented show that is possible to modulate the ligand coordination sphere in metal complexes to can result in great differences in terms of biological effects.

The novel chemistry derived from DNA adducts with platinum complexes with a *trans* geometry was also explored *in silico*. The molecular dynamics of two free DNA 20-mer is compared with the corresponding metallated-adducts, namely monofunctional, 1,2-bifunctional interstrand and 1,3-bifunctional intrastrand. The differences in terms of structure and energy are ompared for these systems, in general the monofunctional adduct exhibited the most interesting feature in terms of structural change in the DNA double strand causing the destacking of the metallated nucleobase. Bifunctional adducts exhibited loss of Watson-crick bonds and localized change in sugar puckering. These results showed that important differences can be found for platinated DNA even at short simulation times < 1 ns.

CHAPTER 1 Introduction

1.1. General Overview:

Complex covalent and non-covalent interactions found in ternary systems involving metal ions, DNA/RNA, and proteins are ubiquitous in relevant biological processes that occur *in vivo*, such as gene expression/regulation, also DNA transcription and repair.[1,2] The understanding of these processes is one of the main objectives of *bioinorganic chemistry*, a relatively new and multidisciplinary field of research that studies the role and interactions of inorganic species (mainly metal ions) in living systems. Recent advances in biophysical/analytical techniques such as AE-ICP, nuclear/electronic resonance (NMR, EPR, ENDOR) and X-ray (XANES, EXAFS) spectroscopies, have allowed the proper determination and characterization of the coordination spheres in several metalloproteins, as well as the study of dynamic interactions involving metal centers.[3 - 5] The application of molecular model methods to explore the energetic profiles of a given proposed mechanism for metallo-enzymes, also expands the possibilities to study metal complexes with a very small lifetime and very distorted geometries (entatic state). The knowledge gathered so far has revealed some key aspects and basic concepts regarding the novel chemistry exhibited by these metallic species. In addition, simple models featuring mono- or bi-functional metal complexes have been extensively employed as an initial approach towards the understanding of either metal-DNA/RNA or metal-protein interactions.[6, 7] However the study of metal-protein-DNA/RNA ternary systems (MDP's) has remained a relatively

unexploited area of research,[8, 9] which could provide a deeper understanding in diverse bioinorganic applications including antisense strategies,[10] the mechanism of action of metallo-drugs, as well as metal ion homeostasis and heavy metal toxicity.

The interaction of zinc finger proteins, the largest family of regulatory proteins in mammals, complexed with DNA or RNA constitute a classical example of these kind of ternary MDP systems (Figure 1.1.).[11-13] Every zinc finger is made up of one zinc ion, which plays a structural role by coordinating two cysteine and two histidine residues[14] in a tetrahedral geometry, causing a particular tri-dimensional folding in the peptide. This compact unit can target specific nucleotide sequences with affinities in the nanomolar range[15], and a great amount of research has been devoted to developing therapeutic applications using engineered zinc fingers.[16, 17] Another example of the importance of ternary MDP systems include the metalloregulatory proteins, which bind metal ions and regulate cellular metabolism by functioning at the level of gene transcription, i.e., *Fur* (ferric uptake regulation) is a protein that binds Fe^{2+} to then function as a repressor of iron uptake. Metallothioneins in copper homeostasis provides another interesting example to this regard.[18]

The discovery of cytotoxic properties in platinum compounds, and specifically the complex *cis*-diamminedichloro platinum (II) or *cisplatin* (fig.1.2.), is considered one of the milestones for the development of bioinorganic chemistry as an independent discipline, even when platinum itself is not an essential inorganic element (i.e., is not found naturally in living systems).

Figure. 1.1. Metal/DNA/protein system: high resolution structrure of zinc finger (Znf) 268 with DNA, secondary structure of the 3 Znf's are depicted in yellow and zinc atoms depicted in green [19] (PDB ID: 1A1G).

Since its discovery in 1965 [20] and approval (1979)[21] by the U.S. FDA for use in anticancer treatment, *cisplatin* has become one of the most effective and widely used antineoplasic agents in the world. It has increased the percentage of survival in patients with testicular cancer from less than 5% to more than 95%.[22] Used in combination with other drugs such as paclitaxel, cisplatin makes it possible to treat other classes of syndromes such as ovarian, neck, gastric, bladder, breast and prostate cancer. The use of *cisplatin* and related complexes (carboplatin and oxaliplatin, fig. 1.2.) as antitumorals exceeded 2.2 billion U.S. dollars in sales just for 2004.[23] Therefore is understandable why cisplatin has generated a great amount of research aimed to understand its mechanism of action, and ultimately increase its therapeutic window (i.e., activity/toxicity ratio). Regarding the first point, a detailed understanding of the molecular basis of *cisplatin*'s mechanism is still out of reach, however it is accepted that the covalent interaction of the

partially hydrolyzed complex with DNA, forming adducts of the type $[Pt(NH_3)_2(N^7\text{-guanine})_2]$, is a key feature for the exhibited cytotoxicity.

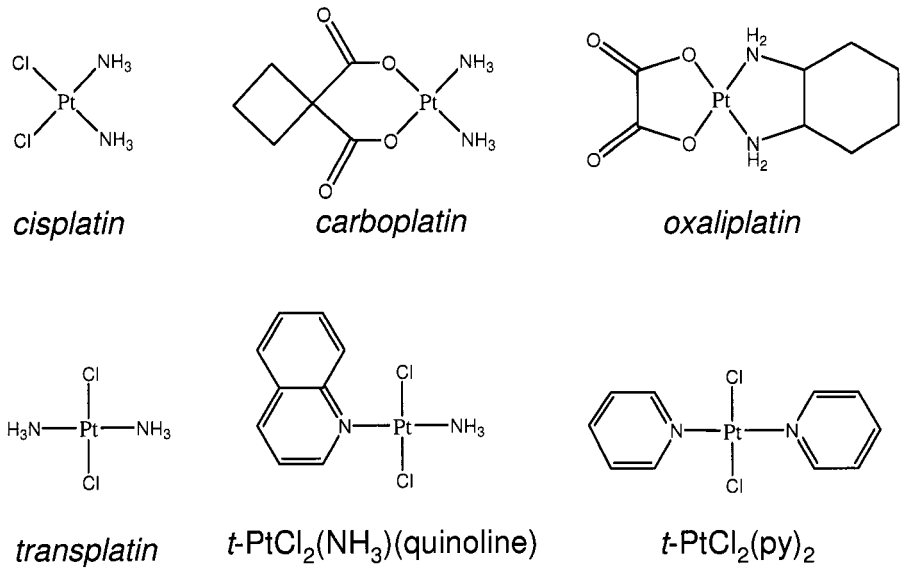

Figure 1.2. Structure of $PtCl_2(NH_3)_2$ isomers, and cytotoxic derivatives.

This fact has boosted greatly the study of metal-DNA/RNA interactions in general, [24, 25] because different metal ions other than platinum have also been studied as alternative anticancer agents.[26, 27] On the other hand side-reactions of *cisplatin* with sulphur residues in proteins (methionine/cysteine) have been long accepted as responsible for its toxicity,[28] as well as, a decrease on its activity due to detoxification mechanisms (i.e. glutathione) [29 - 31], or reduced uptake (i.e. enzymes: Ctr1 and ATP7A/ATP7B).[32, 33] The role of protein-platinum adducts as drug reservoirs have been also been studied, due to the fact that a final thermodynamically Pt-N stable products can be formed from the initial, kinetically preferred, Pt-S adducts.[34] However the study of ternary MDP adducts seems to be the most

promising way to reach an in depth understanding of *cisplatin* cytotoxicity; the $[Pt(NH_3)_2(N^7\text{-guanine})_2]$ fragment induces a particular bending in DNA's double helix that is recognized by High Mobility Group 1 (HMG1) or TATA-binding proteins (TBP),[35] eventually triggering the apoptotic pathway that lead into cell death.[36] Interestingly, not all platinum-DNA lesions lead to cell death and this is the reason why a large group of platinum compounds have been tested and discarded as alternative antitumorals. The way in which the cells handle the platinated lesion will ultimately dictate the activity of the complex or chemotherapeutic drug and this process will very likely involve ternary MDP systems. As an example, the main pathway for platinated-DNA repair is the nucleotide excision repair mechanism or NER which also involves a complex set of proteins. Notably, replication protein A (RPA) and xeroderma pigmentosum group A protein (XPA) have been studied recently and their synergistic affinity towards the DNA lesion understood in some detail.[37] Differences in binding specifities from these proteins between *cisplatin*- and *oxaliplatin*-DNA adducts is suggested as responsible for the efficacy of the latter platinum derivative in *cisplatin* resistant cell lines.[38]

Hydrolysis studies and structure-activity relationships provided the basis for the design of second and third generation of platinum compounds, capable of overcoming resistance and exhibiting a broad spectrum of activity, such as *oxaliplatin*. The study of MDP systems might be the next step towards a new generation of platinum compounds that can take advantage of more complex interactions downstream the cascade of cellular events following DNA lesion. After this brief highlight it is easy to understand how important

would be the study of MDP systems for new platinum compounds that interacts with DNA in a fundamentally different way compared to the classic *cisplatin*.

1.2. Metal-DNA/RNA-Protein (MDP) systems in *trans*-platinum biochemistry:

In spite of the success of *cisplatin* in the treatment of testicular tumors, there have been some serious drawbacks associated with this chemotherapeutic agent, such as, a narrow range of tumors treated, the development of resistance in some cell lines and severe side effects. These factors have created an area of improvement for the development of new anticancer agents based on transition metals. On this regard a broad range of metal ions have been tested, notably Ti^{II}, $Ru^{III/II}$ and Au^{III}, in search for alternative metal-DNA chemistry.[39, 40] In particular for platinum, the development of multinuclear complexes with more than one platinum (sometimes mixed Pt^{II}, Ru^{II})[41] capable of long range inter- and intrastrand DNA adducts,[42] less reactive Pt^{IV}, and mononuclear complexes with *trans*-geometry are so far the most promising alternatives in the search for a new molecular mechanism of action that could overcome the drawbacks of *cisplatin*.[43]

Mononuclear platinum complexes with *trans*- geometry are a very interesting case in the search for new anticancer agents, since they break with the initial paradigm for structure-pharmacologic activity establishing the isomer *trans*-diamminedichloro platinum (II) or *transplatin* as deprived of any therapeutic activity (fig.1.2.). It was found in the late 80's by Farrell, N. *et al.* that substitution of one or both of the ammonia ligands in *transplatin* by a planar aromatic amine, such as pyridine, thiazole or quinoline could change dramatically the biological activity of the complex enhancing its cytotoxicity even in

cisplatin resistant cell lines (fig. 1.2.). [44, 45] Since this initial discovery other research groups have reported on the enhanced cytotoxic properties of *transplatin*-modified complexes with at least one of the ammonia ligands substituted by an iminoether, [46] branched aliphatic amines[47] or heterocyclic non-planar amines.[48] Detailed studies on the molecular mechanism for *trans*-platinum complexes with planar amines (TPA) have shown that they exhibit a slower hydrolysis compared to parent *transplatin* due to the steric effect of the planar amine, this fact makes monofunctional DNA-adducts of these complexes particularly long-lived and prone to form novel bifunctional adducts. Biophysical assays have determined that a combination of monofunctional, interstrand and intrastrand bifunctional adducts are actually formed with DNA (none of them in major proportion), [49-51] in contrast to cisplatin were the major adduct (>70%)[52] is intrastrand bifunctional (fig. 1.3.).[53] This novel way of interaction with DNA might be an important factor to explain the distinctly different spectrum of activities of these complexes compared to *cisplatin* or *carboplatin*, and the relatively high cytotoxicity towards breast and colon tumor cell lines as a recent study against the NIH panel demonstrated. [54]

Another reason to consider the study of MDP systems as relevant in the mechanism of action of TPA's such as *t*-$PtCl_2(py)_2$, is the fact that the latter group of complexes produce protein-associated DNA strand breaks upon incubation with L1210 leukemia cells. Moreover the formation of ternary adducts of the type: platinum complex-DNA and the protein topoisomerase I have been also determined and is a fact not exhibited by *cisplatin* (or other active *trans*-platinum complexes such as the iminoether derivatives), suggesting that the presence of the planar aromatic amine is relevant for this biological feature.[55]

Induction of both DNA strand breakage and DNA-protein crosslinking in human breast (MCF-7) and human ovarian carcinoma cells (A2780) by the complex *t*-$PtCl_2(NH_3)$(thiazole) provides further support to consider MDP systems as a general feature in the biochemistry of TPAs. Again formation of ternary adducts platinated DNA-topoisomerase I was detected, thus confirming previous results.[56] Topoisomerase enzymes control the formation of DNA tangling structures during replication by catalyzing the transient breaking and rejoining of one (topoisomerase I) or both DNA strands (topoisomerase II).

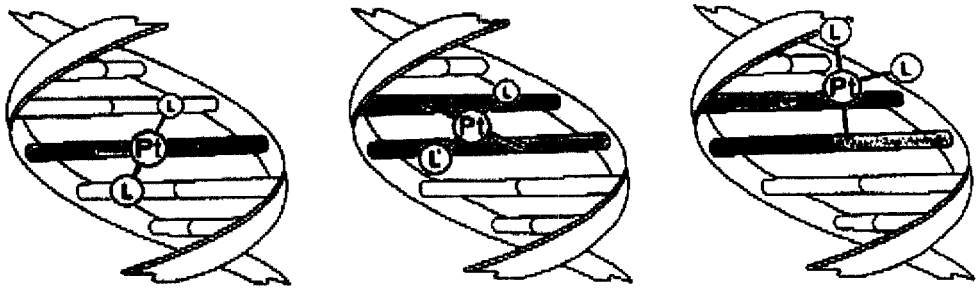

transplatin **t-$PtCl_2(NH_3)$(thiazole)** ***cisplatin***

Figure 1.3. Differences in interstrand crosslinks among platinum complexes.

The first model complex designed to study this class of novel chemistry comprised the nucleobase (9-EtGH) as a model of DNA: [SP-4-2]-$[PtCl(NH_3)$(quinoline)(9-Ethylguanine)$]^{2+}$, and its reactivity towards N-Acetyl methionine (N-AcMet) as a model of sulphur residues in proteins determined (Scheme 1.1.), this simple system was intended to mimic the behavior of the long-lived monofunctional Pt-DNA adducts aforementioned.

Results indicated a high affinity for N-AcMet compared to 5'-GMP (≈ 4:1), therefore confirming the tendency to form DNA-protein rather than DNA-DNA crosslinks.[57, 58]

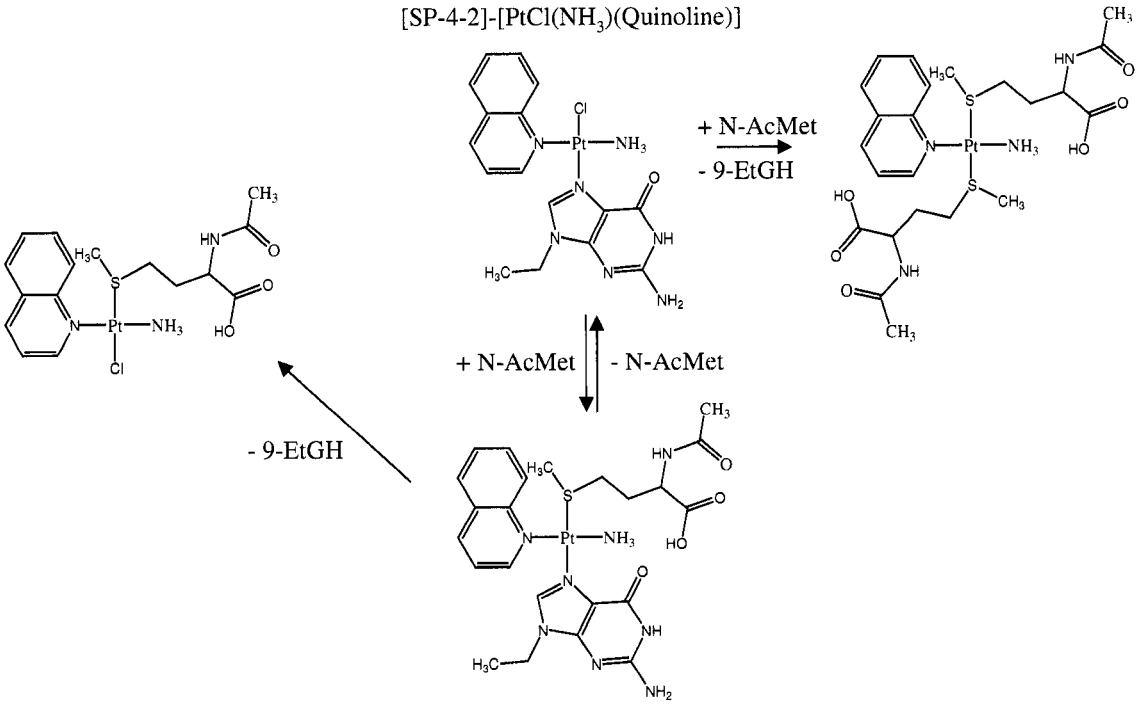

Scheme 1.1. Reactivity of model complex [SP-4-2]-[PtCl(NH_3)(Quinoline)(9-EtGH)]$^{2+}$ towards N-Acetyl methionine, as a first approach to ternary MDP systems.

1.3. Non-covalent (π-stacking) interactions in MDP systems:

Previous results have shown the importance of ternary MDP systems in the understanding of the mechanism of action for the novel TPA drugs; however it is necessary to notice that these studies have focused mainly on covalent interactions. An important consideration when studying macromolecular MDP systems is to assess the role

of molecular recognition elements directing DNA-DNA, protein-protein or protein-DNA (RNA is considered by extent) interactions.

Molecular recognition is a broad term that covers a set of intra- and inter-molecular interactions controlled by non-covalent interactions as hydrogen bonding, salt bridges or London dispersion forces. Usually the strength of these interactions is low (≤ 5kcal/mol) in comparison to covalent bonds (80 – 200 kcal/mol), but generally they occur in high numbers and with a mutual reinforcement in order to direct very specific and essential bio-chemical processes such as protein folding or antibody recognition. Among these kind of interactions, the so-called π-stacking or π- π involving two aromatic rings have recently gained an increased interest due to our relative poor understanding and its importance on several fields of applications, such as crystal engineering and supramolecular systems[59, 60], asymmetric synthesis[61, 62], separation science[63], and others as well. Specifically in living systems there are a large number of examples involving this kind of interaction, like the protein stability in cytochrome b5 [64] and the determination and stabilization of tertiary structure of proteins in general, [65] also of special interest for this work, the fundamental role played in DNA/RNA-protein selective recognition.[66 - 69]

To this regard important π-stacking interactions have been reported in the case of MDP systems involving *cisplatin*, which are highly relevant to its mechanism of activity. The first of these interactions is present in the ternary system that bent DNA forms with the HMG1 protein, a specific π-stacking interaction occurs when the phenylalanine residue in the protein enters in a hydrophobic cleft formed by the *cisplatin* kink in guanines 8 and 9 (Fig. 1.4.).

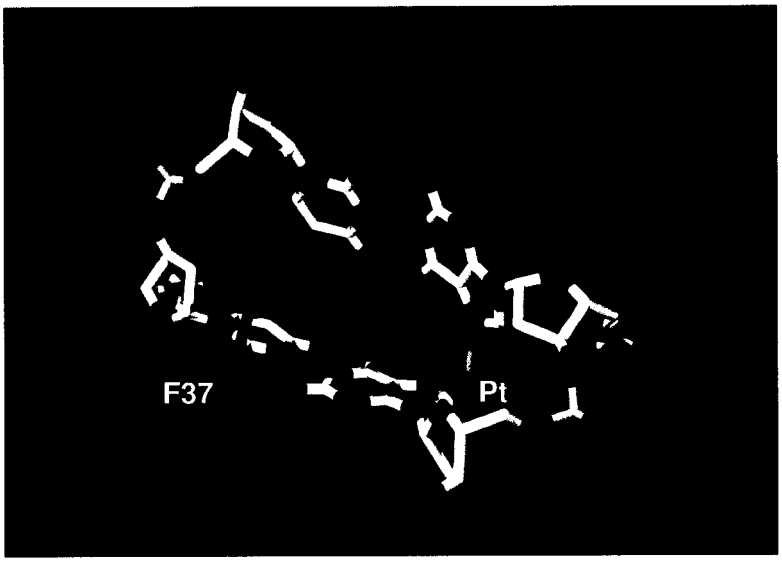

Figure 1.4. Detail of π-stacking interactions between phenylalanine residues in HMG1 protein (cyan) and guanines 8-9 in the oligonucleotide. (PDB ID: 1CKT)

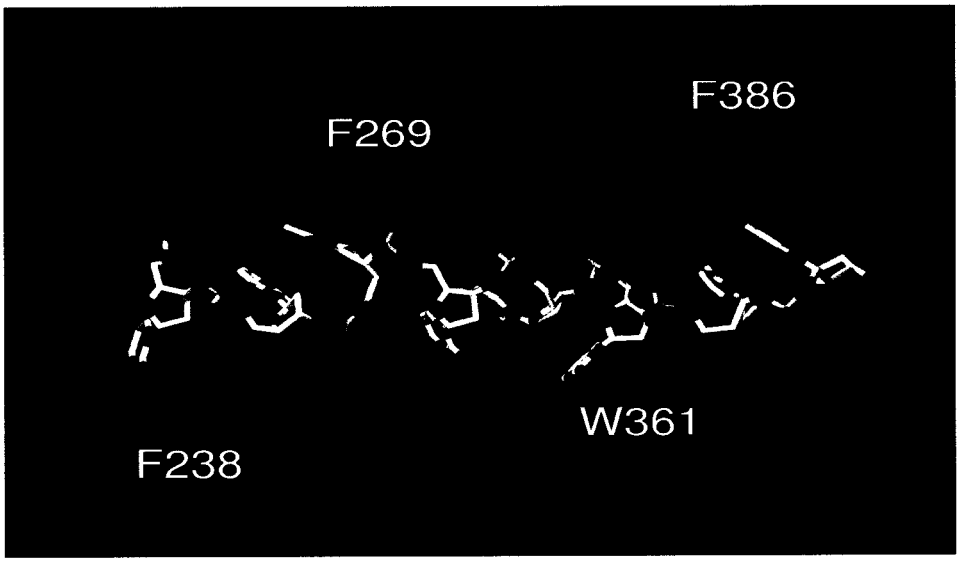

Figure 1.5. Detail of π-stacking interactions between aromatic residues in RPA protein (cyan) and the oligonucleotide C_8. The rest of the protein was omitted for clarity. (PDB ID: 1JMC)

Notably the mutation of phenylalanine residue by a non-intercalating alanine greatly reduced the binding of the protein to the bent DNA, thus suggesting the importance if this motif for ternary adduct formation.[70] The second of these interactions can be seen in the structure of RPA protein (important for NER mechanism) bound to DNA, where several π-stacking interactions between phenylalanine/tryptophan and cytosine bases can be seen as a recognition motif for single stranded DNA (Fig. 1.5.).[71]

The basic chemistry involved on this nucleic acid base / aromatic aminoacid motif has been studied with model compounds using several spectroscopic techniques including ^{1}H-NMR, Fluorescence and X-ray diffraction. It has been generally observed that N-quaternization of the nucleobase (i.e., N7 for purines and N3 for pyrimidines) by protonation or alkylation enhances the strength of the stacking interaction.[72, 73]

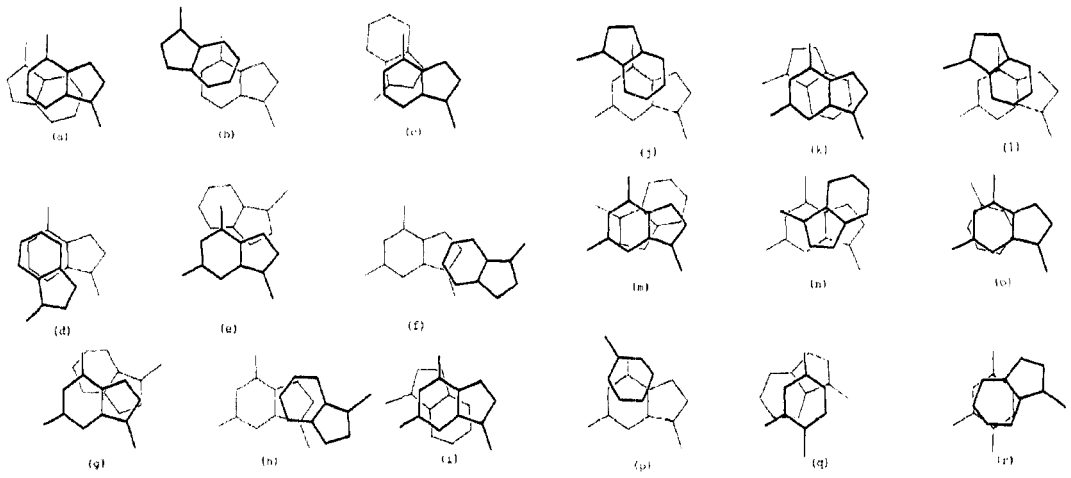

Figure 1.6. Different modes of π-stacking interaction for guanine, adenine, cytosine with indole.

The structural flexibility for the system has been explored using guanine, adenine and cytosine with indole as model compounds, the different modes of stacking interaction were characterized in solid state as seen in figure 1.6. [74]

It is worthwhile to draw the attention on the possibilities of similar interactions for N-quaternized nucleobases by platination, recalling that the carbonium CH_3^+ ion (and by extension other R^+) can be regarded as the isolobal analogous with the Pt^{2+} ion, since they exhibit similar frontier orbitals in terms of number, symmetry, electron occupation and radial extent[75]. Thus it is expected from this chemical species to exhibit a similar chemistry as indeed is shown in terms of DNA interaction, alkylating agents can bind to the nucleobases in similar fashion to cisplatin and related platinum drugs producing disruption of DNA function and cell death (apoptosis).

In the case of TPA complexes, there is a good amount of evidence that points towards a stacking interaction of the planar aromatic amine in *cis* position with the DNA coordination site. This kind of interaction will produce a similar kink in the double helix than the one produced by *cisplatin*, with the only exception of using a combined covalent/π-stacking interaction rather than purely covalent to this end. In fact the monofunctional adducts of *t*-$PtCl_2(NH_3)$(quinoline) and *t*-$PtCl_2(NH_3)$(thiazole) are recognized by HMG groups and repaired by the NER mechanism in a very similar way to *cisplatin*. The role played by the planar aromatic amine in the case of interstrand (35%) and intrastrand (30 %) DNA adducts and their relevance for further interactions with

diverse cellular proteins still have to be evaluated, of interest, a rapid and direct interaction of the telomerase enzyme with the complex *t*-$PtCl_2(py)_2$ was determined recently.[76]

The fact that topoisomerase I inhibitors such as adriamycin and camptothecin exhibit a similar profile of protein-associated DNA strand breaks could suggest some similarities in the mechanism of action between these two sets of compounds. Interestingly topoisomerase I inhibitors interact with the DNA-protein system mainly through non-covalent (π-stacking) interaction as can be seen in figure 1.7., from a crystal structure the inhibitor (in green) actually mimics the proximal base pair close to the DNA strand break impairing the repairing function of this enzyme.[77]

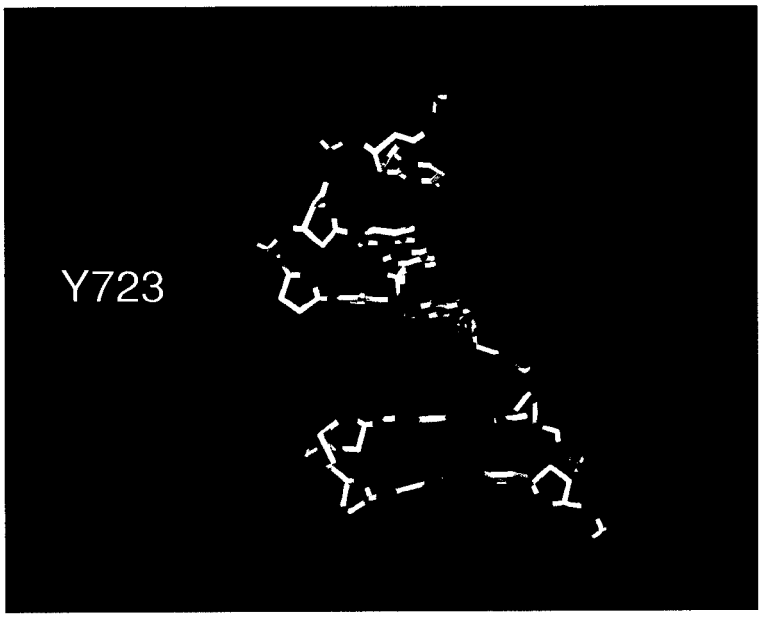

Figure 1.7. Detail of π-stacking interactions occurring in the adduct formed with inhibitor Topotecan (green), protein topisomerase I showing the active residue (cyan) and the DNA. (PDB ID: 1K4T)

1.4. *trans*-platinum nucleobase complexes as potential anti-virals.

In the case of complexes of the type: [SP-4-2]-[PtCl(L)(L')(nucleobase)]$^{2+}$ (where nucleobase = 9-ethylguanine or 1-methylcytosine and L = NH_3, 4-Mepy ; L' = quinoline, isoquinoline or thiazole) derived from the cytotoxic TPA's by substitution of a chloride ligand by the nucleobase, the role played by π-stacking interactions might be even more relevant for the mechanism of action. These complexes were found to display activity against several viral strains, included the Human Immunodeficiency Virus type 1 (HIV-1), it was also noticed that the cytotoxicity of these complexes was greatly reduced in comparison with the parent TPA's, this fact was very interesting and convenient for the design of a potential antiviral agent.[78] The change in biological activity (i.e., cytotoxic to antiviral) can be understandable taking into consideration that this kind of complex tends to react more with sulphur residues in proteins than with nucleobases (section 1.2.), moreover in the event of reaching DNA, they will produce only a monofunctional adduct, relatively easy to repair. The elucidation of the mechanism of action of this kind of complex has been an extensive line of research in Dr. Nicholas Farrell's group and there are several reasons and reported evidence pointing towards the nucleocapsid protein in HIV-1 virus (NCp7) as the main biological target:

- Monofunctional platinum complexes of the type [SP-4-2]-[PtCl(L)(L')(nucleobase)]$^{2+}$ have a high affinity towards sulphur residues (methionines or cysteines).[57, 58]
- NCp7 is composed of two zinc fingers with major content of cysteine residues (C_3H) compared to standard zinc fingers (C_2H_2).

- The cysteine residues in NCp7 are particularly activated towards electrophilic attack due to coordination to the zinc atom, thiol *vs.* thiolate.[79 - 82]
- Cobalt complexes have been proved to selectively interact with zinc finger models and cause zinc ejection, also inhibiting DNA binding by the Sp1 (Human Transcription Factor). [83]
- Release of zinc from the C-terminal knuckle of NCp7 was determined upon incubation with the complex [SP-4-2]-[PtCl(NH_3)(Quinoline)(9-EtGH)]$^{2+}$.[78]
- Gold complexes that share with platinum an intrinsic affinity for sulphur residues (HSAB principle[84]) have been proved to inhibit transcription factors from binding to DNA, such as the zinc finger from OB2-1[85] and the nuclear oncoproteins *Jun* and *Fos*.[86]
- Transplatin has been used as a crosslinking agent for the system involving tRNA and the protein amynoacyl-tRNA synthetase[87], also the nucleocapsid protein NCp15, closely related to NCp7, has been crosslinked to viral RNA (HIV-1). [88]

The possibility to target this enzyme is very promising since it plays important roles throughout several stages of the viral life cycle, [89 - 94] and its conserved sequence shows that there are not many possibilities for mutation.[95, 96] In other words if this protein can be selectively targeted, the chemotherapeutic agent will be effective even in the new mutated strains of this virus and would be a radically new approach to the compounds currently used to treat HIV.[97] An example of the interest generated by this protein is found on the number of publications devoted to its study and the development of inhibitors. [98 – 106]

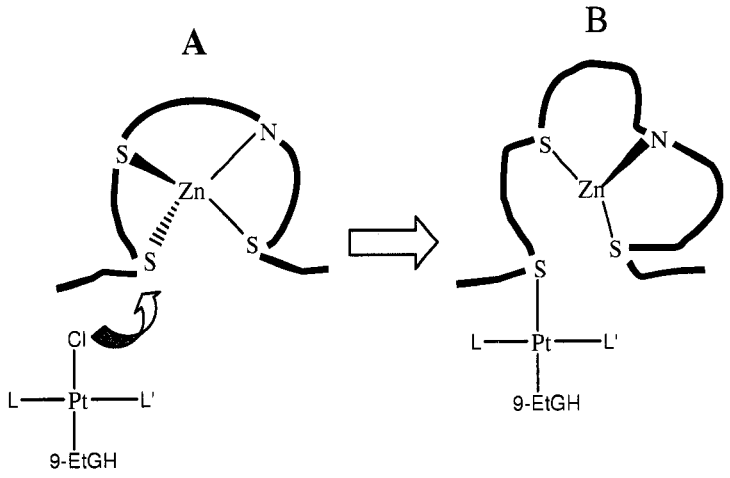

Scheme 1.2. Proposed mechanism of action of monofunctional [SP-4-2]-[PtCl(L)(L')(Nucleobase)]$^{2+}$ towards the zinc finger in NCp7.

Taking into account the supporting evidence a mechanism of action was proposed as can be seen in Scheme 1.2., where on a first step (A) the monofunctional [SP-4-2]-[PtCl(L)(L')(nucleobase)]$^{2+}$ complex would make an electrophilic attack on one of the cysteine residues of the NCp7 zinc fingers, in order to coordinate the sulfur atom through chloride substitution. As a result the tridimensional structure of the zinc finger will be greatly disrupted (B), eventually releasing the zinc atom to render useless the NCp7 protein and thus killing the virus.

Based on several studies of NCp7 interaction with its natural substrate, the Ψ-site in the viral RNA, it has been confirmed that π-stacking interactions play a very important role in terms of recognition and selectivity. Aromatic residues in the zinc fingers of NCp7, i.e. phenylalanine (F16) and tryptophan (W37) are specially suited for this kind of

interactions with oligonucleotides as shown by NMR structures (Fig. 1.8.). To this regard, it has been noticed that high affinities towards NCp7 generally required at least one guanine residue in the oligonucleotide.[107 -109] In addition, studies using either short oligonucleotides (5 or 6 base pairs long) or a model of the Ψ-site showed relevant π-stacking interaction between guanines nucleobases with F16 in the N-terminal zinc finger (F1) and with W37 in the C-terminal zinc finger (F2) of NCp7.[110 - 112] The actual mechanism for nucleic acid recognition in C_3H zinc fingers is different from the most common C_2H_2 and C_4 motifs found in human,[113] and this can be used to target specifically the NCp7. [114]

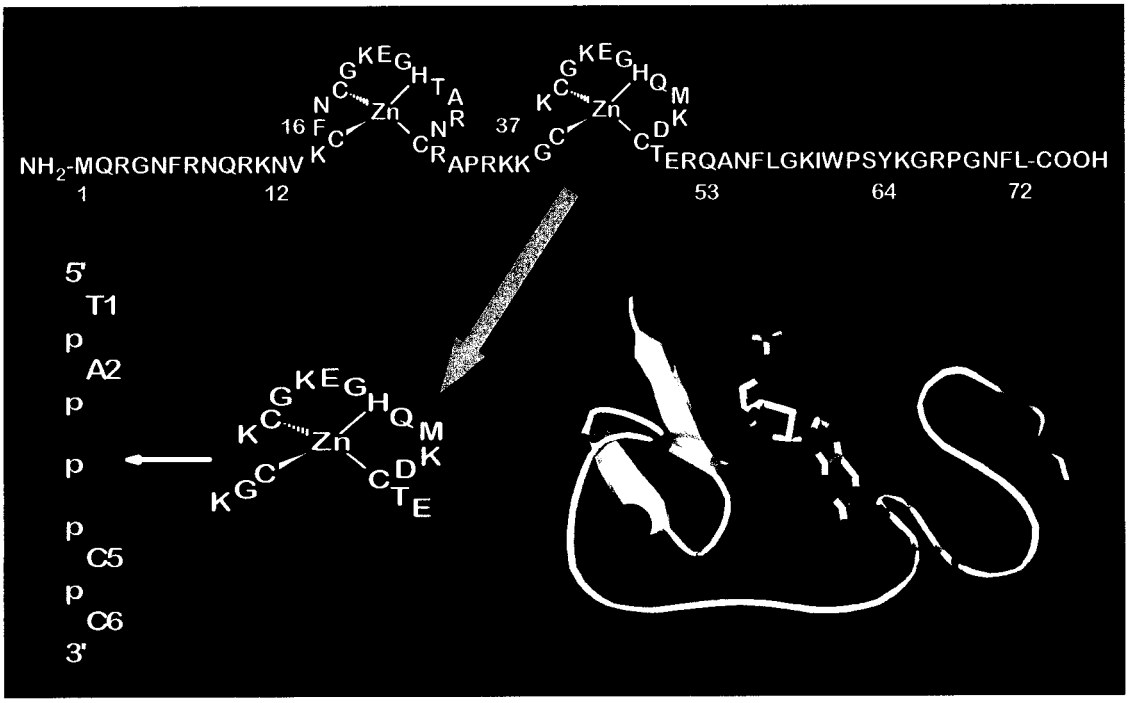

Figure 1.8. Aminoacid sequence for NCp7 (top); scheme of stacking interaction between guanine residue and tryptophan in F2 (bottom left); representation of the NCp7 interacting with oligonucleotide DNA. (PDB ID: 1BJ6)

For this reason it is logical to think that the nucleobase in complexes [SP-4-2]-[PtCl(L)(L')(nucleobase)]$^{2+}$, might be playing an important role as a molecular recognition motif, a factor that would account for the initial approach of both, NCp7 and the platinum complex *in vivo* and can give raise to the modulation in biological properties found for these complexes. This first recognition between the chemical species would dictate selectivity to the target in a previous step that would lead to A in Scheme 1.2.

1.5. Dissertation Outline.

It is the interest of the present work to study some basic aspects of the covalent and non-covalent interactions that can be exhibited by novel platinum complexes with *trans* geometry and containing planar amines. Given that the interaction with DNA and protein are a key new feature of this class of compounds, special emphasis will be dedicated to model this ternary system. The zinc finger motif will be taken as a representative example of protein in ternary systems, due to its potential implications in the antiviral activity exhibited by some of the platinum complexes studied. Chapter 2 reviews the importance of zinc metalloproteins in general as medicinal targets including zinc finger proteins.

The non-covalent interaction between model metal-nucleobase complexes with aromatic aminoacids like tryptophan is explored using fluorescence and ^{1}H-NMR spectroscopies, electrospray ionization mass spectrometry and theoretical methods (density functional theory) in Chapters 3 to 6. Important variables such as the nature of the metal ion and nucleobase, as well as, the complexity of the system (i.e., l-tryptophan to zinc finger) were studied trying to identify the origin of differences observed. This work is

complemented by the study of covalent interactions observed for the model metal-nucleobase and the active trans-platinum nucleobase complexes towards tryptophan and zinc finger models (Chapters 4 and 5).

The importance of understanding basic aspects of reactivity for *trans*-platinum complexes with planar amines (TPA) with DNA/protein as principal targets is underscored throughout this first chapter, the knowledge gained in this regard can provide important clues at the molecular level to explain downstream cellular signaling events leading to apoptosis. To this end the reactivity of two representative complexes is studied in Chapter 7 towards 5'-guanosine monophosphate and N-acetyl methionine and models for DNA and protein respectively, the extension of the study for the protein ubiquitin is also included. In addition, Chapter 8 is dedicated to the study of different DNA adducts of a representative TPA complex, namely *t*-[$PtCl_2(NH_3)$(thiazole)] using molecular dynamics to complement previous chemical and bio-physical findings on the DNA binding for this class of compounds.

Published work will be included in a format as close as possible to that in which it was published.

1.6. References.

(1) Finney, L.A.; O'Halloran, T.V., *Science*, **2003**, 300, 931-936.

(2) Silver, S.; Walden, W., In *Metal Ions in Gene Regulation*, Silver, S.; Walden,W. Eds.; ITP New York, NY, 1998; 1-10.

(3) Cowan, J.A., In *Inorganic Biochemistry: An introduction*, Wiley-VCH, Inc.: New York, 1997, pp. 65-132.

(4) Lippard, S.J., *Nature Chem. Biol.*, **2006**, 2, 504 – 507.

(5) Lu, Y., *Angew. Chem. Int. Ed.*, **2006**, 45, 5580 – 5601.

(6) Yamauchi, O.; Odani, A.; Takani, M., *J .Chem. Soc., Dalton. Trans.*, **2002**, 3411-3421.

(7) See Vols: 32, 33 and 38, *Met Ions Biol. Syst.*, Sigel, A., Sigel, H., Eds.; Marcel Dekker, Inc.: New York.

(8) Sabat, M., *Met. Ions Biol. Syst.*, **1996**, 32, 522-555.

(9) Reynolds, M.; Peterson, E.; Quievryn, G.; Zhitkovich, A., *J. Biol. Chem.*, **2004**, 279, 30419-30424.

(10) Leng, M.; Schwartz, A.; Giraud-Panis, M.-J., In Platinum-Based Drugs in Cancer Therapy, Kelland, L.R.; Farrell, N.P. eds., Humana Press: Totowa New Jersey, 2000; pp. 63-85.

(11) Klug, A., Schwabe, J., *FASEB J.*, **1995**, 9, 597-604.

(12) Branden, C.; Tooze, J., In *Introduction to Protein Structure*, Garland Publishing Inc.: NewYork, 1999; pp. 113-128.

(13) Iuchi, S., *Cell. Mol. Life Sci.*, **2001**, 58, 625-635.

(14) This is the general coordination (Cys_2His_2), but Cys_3His and Cys_4 are also possible.

(15) To achieve this kind of affinities the presence of at least two zinc-fingers is necessary. Vásquez, M.E.; Caamaño, A.M.; Mascareñas, J.L., *Chem. Soc. Rev.*, **2003**, 32, 338-349. So far only affinities in the micromolar level have been achieved with only one zinc finger. Michel, S.L.J.; Guerrerio, A.L.; Berg, J.M., *Biochemistry*, **2003**, 42, 4626-4630.

(16) Klug, A., *FEBS lett.*, **2005**, 579, 892-894.

(17) Nomura, A.; Sugiura, Y., *J. Am. Chem. Soc.*, **2004**, 126, 15374-15375.

(18) Cowan, J.A., In *Inorganic Biochemistry. An introduction*, Wiley-VCH, Inc.:New York, 1997; pp. 303-314.

(19) Elrod-Erickson, M.; Benson, T.E.; Pabo, C. O., *Structure*, **1998**, 6, 451-464.

(20) Rosemberg, B.; Van Camp, L.; Krigas, T., Nature, 1965, 205, 698-699.

(21) Roat-Malone, R.M., In *Bioinorganic Chemistry. A short course*, Wiley-Interscience: New Jersey, 2002; p. 281.

(22) O'Dwyer, P.J.; Stevenson, J.P.; Johnson, S.W. Cisplatin – How Good is it? In *Cisplatin*, Lippert, B.; Wiley VCH: New York, 1999; pp. 31-72.

(23) Medical World Communications: http://www.mwc.com/NewsfeedArticle.cfm?NewsID=13045.

(24) Johnson, N.P.; Butour, J.-L.; Villani, G.; Wimmer, F.L. Defais, M.; Pierson, V; Brabec, V, *Prog. Clin. Biochem. Med.*, **1989**, 10, 1-24.

(25) Jamieson, E.R.; Lippard, S.J., *Chem. Rev.*, **1999**, 99, 2467-2498.

(26) Clarke, M.J.; Zhu, F.; Frasca, D.R., *Chem. Rev.*, **1999**, 99, 2511-2533.

(27) Clarke, M.J., *Coord. Chem. Rev.*, **2003**, 236, 209-233.

(28) Montine, T.J.; Borcch, R.F., *Biochem. Pharmacol.*, **1990**, 39, 1751-1757.

(29) Timerbaev,A.R.; Aleksenko, S. S.; Polec-Pawlak , K.; Ruzik, R.; Semenova , O.; Hartinger, C. G.; Oszwaldowski, S.; Galanski, M.; Jarosz, M.; Keppler, B. K., *Electrophoresis*, **2004**, 25, 1988-1995.

(30) Peleg-Shulma, T.; Gibson, D., *J. Am. Chem. Soc.*, **2001**, 123, 3171 – 3172.

(31) Masters, J.R.; Thomas, R.; Hall, A.G., *et al.*, *Eur. J. Cancer*, **1996**, 7, 1248-1253.

(32) Samimi,G.; Safaei, R.; Katano, K., *et al.*, *Clin. Cancer Res.*, **2004**, 279, 46393-46399.

(33) Song, I.; Savaraj, N.; Siddik, Z.H., *et al.*, *Mol. Cancer Ther.*, **2004**, 3, 1543-1549.

(34) Reedijk, J., *Chem. Rev.*, **1999**, 9, 2499-2510.

(35) Jung, Y.; Mikata, Y.; Lippard. S.J., *J. Biol. Chem.*, **2001**, 276, 43589-43596.

(36) Kasparkova, J.; Farrell, N.; Brabec, V., *J. Biol. Chem.* **2000**, 75, 15789-15798.

(37) Farrell, N.P., *Semin. Oncol.*, **2004**, 31, 1-9.

(38) Kartalou, M.; Essigmann, J.M., *Mutat. Res.*, **2001**, 478, 1-21.

(39) See *Met. Ions in Biol. Syst.*, Marcel Dekker, Inc.:New York,2004, Vol. 42.

(40) Farrell, N., *Coord.Chem. Rev.*, **2002**, 232, 1-4.

(41) Van Houten, B.; Illenye, S.; Qu, Y.; Farrell, N., *Biochemistry*, **1993**, 32, 11794-11801.

(42) Farrell, N., In *Met. Ions in Biol. Syst.*, Marcel Dekker, Inc.:New York,2004, 42, pp. 251-290.

(43) Van Beusichem, M.; Farrell, N., *Inorg. Chem.*, **1992**, 31, 634-639.

(44) Farrell, N.; Ha, T. T. B.; Souchard, J.P. *et al.*, *J. Med. Chem.*, **1989**, 32, 2240-2241.

(45) Farrell, N.; Kelland, LR; Roberts J.D.; Van Beusichem, M., *Cancer Res.*, **1992**, 52, 5065-5072.

(46) Coluccia, M.; Nassi, A.; Loseto, F.; Bocarelli, A.; Mariggió, M.A.;Giordano, D.; Intini, F.P.; Caputo, P.A.; Natile, G., *J. Med. Chem.*, **1993**, 36, 510-512.

(47) Montero, E.I.; Diaz, S.; Gonzalez-Vadillo, A.M.; Perez, J.M.; Alonso, C.; Navarro-Ranninger, C., *J. Med. Chem.*, **1999**, 42, 4264-4268.

(48) Khazanov, E.; Barenholz, Y.; Gibson, D.; Najajreh, Y., *J. Med. Chem.*, **2002**, 45, 5196-5204.

(49) Zakovska, A.; Novakova, O.; Balcarova, Z., *et. al*, *Eur. J. Biochem.*, **1998**, 254, 547-557.

(50) Brabec, V.; Neplechova, K.; Kasparkova, J.; Farrell, N.; *J. Biol. Inorg. Chem.*, **2000**, 5, 364-368.

(51) Kasparkova, J.; Novakova, O.;Farrell, N.; Brabec, V., *Biochemistry*, **2003**, 42, 792-800.

(52) This considering both *cis*-GG and *cis*-AG intrastrand adducts.

(53) Fichtinger-Schepman, A. M. J.; van der Veer, J. L.; den Hartog, J. H. J., *et al.*, *Biochemistry* **1985**, *24*, 707-713.

(54) Fojo, T.; Farrell, N.; Ortuzar, W.; *et al.*, *Crit. Rev. Oncol. Hematol.*, **2005**, 53, 25-34.

(55) Farrell, N., In *Met. Ions in Biol. Syst.*, Marcel Dekker, Inc.:New York,1996, 32, pp. 603-639.

(56) Farell, N.; Povirk, L.F.; Dange, Y.; *et al.*, *Biochem. Pharmacol.*, **2004**, 68, 857-866.

(57) Bierbach, U.; Farrell, N., *Inorg. Chem.*, **1997**, 36, 3657-3665.

(58) Bierbach, U.; Farrell, N., *J. Biol.Inorg. Chem.*, **1998**, 3, 570-580.

(59) Lewis, M.; Barnes, C.L.; Glaser, R.; *Can. J. Chem.*, **1998**, 76, 1371-1378.

(60) Roesky, H.W.; Andruh, M., *Coord. Chem. Rev.*, **2003**, 1-2, 91-119.

(61) Jones, G.B., *Tetrahedron*, **2001**, 57, 7999-8016.

(62) Kishikawa, K.; Naruse, M.; Kohmoto, S.; *et al., J. Chem. Soc., Perkin Trans.*, **2001**, 1, 462-468.

(63) Pirkle, W.H.; Liu, Y., *J. Chromatogr., A.*, **1996**, 749, 19-24.

(64) Shan, L.; Jun-Xia, L.; Jian-Hua, G.;*et al.*, *Acta Cryst.*, **2005**, D61, 180-189.

(65) Burley, S.K.; Petsko, G.A., *Science*, **1985**, 229, 23-28.

(66) Meyer, E.A.; Castellano, R.K.; Diederich, F., *Angew. Chem. Int. Ed.*, **2003**, 42, 1210-1250.

(67) Nowakowski, J.; Shim, P.J.; Prasad, G.S.; *et al.*, *Nature Struct. Biol.*, **1999**, 6, 151-156.

(68) Hamilton, A.D.; Phillips, S.E.V.; Moras, D., *Curr. Opin. Struct. Biol.*, **1993**, 3, 11-16.

(69) Hélène, C.; Lancelot, G., *Prog. Biophys. Mol. Biol.*, **1983**, 39, 1-68.

(70) Ohndorf, U.; Rould, M.A.; He, Q.; Pabo, C.O.; Lippard, S.J., *Nature*, **1999**, 399, 708-712.

(71) Bochkarev, A.; Pfuetzner, R.A.; Edwards, A.M.; Frappier, L., *Nature*, **1997**, 385, 176-181.

(72) Ishida, T.; Doi, M.; Ueda, H.; Inoue, M.; Scheldrick, G. M., *J. Am. Chem. Soc.*, **1988**, 110, 2286-2294.

(73) Ishida, T.; Tarui, M.; In, Y.; Ogiyama, M.; Doi, M.; Inoue, M., *FEBS lett.*, **1993**, 333, 214 – 216.

(74) Ishida, T.; Ueda, H.; Segawa, K.; Doi M.; Inoue, M., *Arch. Biochem Biophys.*, **1990**, 278, 217-227.

(75) Hoffmann, R., *Science*, **1981**, 211, 995 - 1002

(76) Colangelo, D.; Ghiglia, A.L.; Vian, I.; *et al.*, *J. Inorg. Biochem.*, **2004**, 98, 61-67.

(77) Staker, B.L.; Hjerrild, K.; Feese, M.D.; et al., *Proc. Natl. Acad. Sci. USA*, **2002**, 99, 15387- 15392.

(78) Sartori, D.A.; Miller, B.; Bierbach, U.; Farrell, N., *J. Biol.Inorg. Chem.*, **2000**, 5, 575-583.

(79) Louie, A.Y.; Meade, T.J., *Proc. Natl. Acad. Sci. USA*, **1998**, 95, 6663-6668.

(80) Cheng, C-.C.; Lu., Y.L-., *J. Chem. Soc., Chem Commun.*, **1998**, 253-254.

(81) Smith, J.N.; Hoffman, J.T.; Shirin, Z.; Carrano, C.J., *Inorg. Chem.*, **2005**, 44, 2012-2017.

(82) Chuan, H.; Hua, W.; Verdine, G.L., *J. Am. Chem. Soc.*, **2003**, 125, 1450-1451.

(83) Liu, Q.; Golden, M.; Darensbourg, M.; Farrell, N., *J. Chem. Soc., Chem. Commun.*, **2005**, 34, 4360 - 4362.

(84) Pearson , R.G., *J. Am. Chem. Soc.*, **1963**, 85, 3533-3539.

(85) Hollywood, D.P.; Hurst, H.C., *Brit. J. Cancer*, **1995**, 71, 753-757.

(86) Handel, M.L.; Watts, C.K.; DeFazio, A.; *et al.*, *Proc. Natl. Acad. USA*, **1995**, 92, 4497-4501.

(87) Tukalo, M.A.; Kubler, M.; Kern, D.; *et al.*, *Biochemistry*, **1987**, 26, 5200-5208.

(88) Darlix, J.L-.; Gabus, C.; Nugeyre, M.T-. ; *et al.*, *J. Mol. Biol.*, **1990**, 216, 689-699.

(89) Darlix, J.L. ; Lapadat-Tapolsky, M.; de Rocquigny, H.; Roques, B.P., *J. Mol. Biol.*, **1995**, 254, 523-537.

(90) Rein, A.; Henderson, H. ; Levin, J.G., *Trends Biochem. Sci.*, **1998**, 23, 297-301.

(91) Huang, Y.; Khorchid, A.; Gabor, J.; *et al.*, *J. Virol.*, **1998**, 72, 3907-3915.

(92) Hargittai, M.R. ; Mangla, A.T. ; Gorelick, R.J. ; *et al.*, *J.Mol. Biol.*, **2001**, 312, 985-997.

(93) Tisné, C. ; Roques, B.P. ; Dardel, F., *J. Mol. Biol.*, **2001**, 306, 443-454.

(94) Bampi, C.; Jacquenet, S.; Lener, D.; Décimo, D. ; *et al.*, *Int. J. Biochem Cell Biol.*, **2004**, 36, 1668-1686.

(95) Dorfmann, T.; Luban, J.; Goff, S.P.; et al.; *J. Virol.*, **1993**, 67, 6159-6169.

(96) Ramboarina, S.; Druillennec, S.; Morellet, N.; *et al.*, *J. Virol.*, **2004**, 6682-6687.

(97) De Clercq, E., *Med. Res. Rev.*, **2002**, 22, 531-565.

(98) Druillenec, S.; Roques, B.P., *Drug News Persp.*, **2000**, 13, 337-349.

(99) Bombarda, E.; Cherradi, H.; Morrellet, N.; *et al.*, *Biochemistry*, **2002**, 41, 4312-4320.

(100) Goel, A.; Mazur, S. J.; Fattah, R.J.; *et al.*, *Bioorg. Med. Chem. Lett.*, **2002**, 12, 767-770.

(101) Pustowka, A. ; Dietz, J. ; Ferner, J. ; *et al.*, *ChemBioChem*, **2003**, 4, 1093-1097.

(102) Srivastava, P.; Schito, M.; Fattah, R.; et al., *Bioorg. Med. Chem.*, **2004**, 12, 6437-6450.

(103) Töszér, J.; Shulenin, S.; Louis, J.M.; *et al.*, *Biochemistry*, **2004**, 43, 4304-4312.

(104) Bampi, C.; Sandrine, J.; Lener, D.; Decimo, D.; Darlix, J.L., *Curr HIV Res.*, **2004**, 2, 79-92.

(105) Bombarda, E.; Roques, B.P.; Mély, Y.; Grell, E., *Biochemistry*, **2005**, 44, 7315-7325.

(106) Miller, L.M.; Calvin, J.; Hara, T.; *et al.*, *J. Med. Chem.*, **2005**, 48, 2847-2858.

(107) South, T.L.; Summers, M.F., *Prot. Sci.*, **1993**, 2, 3-19.

(108) Wu, J.Q.; Ozarowski, A.; Maki, A.H., *et al.*, *Biochemistry*, **1997**, 36, 12506-12518.

(109) Vuilleumier, C.; Bombarda, E.; Morellet, N., *et al.*, *Biochemistry*, **1999**, 38, 16816-16825.

(110) Morrellet, N.; Demene, H.; Teilleux, V.; Huynh-Dinh, T.; *et al.*, *J. Mol. Biol.*, **1998**, 283, 419-434.

(111) De Guzman, R.N.; Wu, R. Z.; Stalling, C.C. ; *et al.*, *Science*, **1998**, 279, 384-388.

(112) Amarasinghe, G.K.; De Guzman, R.N.; Turner, R.B.; *et al.*, *J. Mol. Biol.*, **2000**, 301, 491-511.

(113) Andreini, C.; Banci, L.; Bertini, I.; Rosato, A., *J. Proteome. Res.*, **2006**, 5, 196 - 201.

(114) Musah, R.A., *Curr. Top. Med. Chem.*, **2004**, 4, 1605 -16

CHAPTER 2 Zinc Metalloproteins as Medicinal Targets

Nicholas P. Farrell and Atilio I. Anzellotti

Department of Chemistry, Virginia Commonwealth University, 1001 W. Main St.

Richmond, VA 23284-2006, USA

Submitted to Chemical Society Reviews on January, 2007

2.1. Summary.

Proteins that need zinc as a cofactor are ubiquitously expressed in living organisms; they fulfill diverse and essential functions in the human proteome. Deviation from regulated protein function is correlated to disease states ranging from cancer to antibiotic resistance in bacteria. In this review, seven medically relevant zinc metalloproteins are discussed. Their structure and function relationships are summarized followed by an updated status of current and potential inhibitors with emphasis on the bioinorganic chemistry of the molecular target or metalloprotein's active site.

2.2. Introduction.

Zinc plays an essential role in biological systems with a diversity of functions performed by zinc-binding proteins. Up to 10% of the human proteome is potentially capable of binding zinc in vivo, with zinc-fingers being the most abundant class of metalloproteins.[1] The zinc ion (ZnII) displays a set of properties that make it suitable for catalytic and structural functions within proteins. Amongst these properties are: a) a great stability towards redox reactions; b) a d10 electronic configuration where the coordination geometry (4 - 6) is not dependent on ligand-field stabilization; c) an intermediate polarizability or borderline hardness allowing coordination of N, S, and O donor atoms and d) a Lewis acid character useful to activate coordinated substrates, whilst maintaining ligand nucleophilicity.[2, 3] Altogether these properties make zinc the most common transition metal observed in proteins[4] even while its total concentration in the human body (2 -3 g.) does not make it the most abundant.

Table 2.I. Representative biological function of zinc and zinc proteins.

Zinc protein	Biological function
Alcohol dehydrogenase	Oxidoreductase, alcohol breakdown.
Farnesyl transferase	Transferase, signal transduction
Carboxypeptidase A	Hydrolase, peptide cleavage
Carbonic anhydrase	Lyase, activation of small molecules
Phosphomannose isomerase	Isomerase, isomerization of fructose-6-phosphate
DNA ligase III	Ligase, DNA repair
Zinc $^{2+}$	Growth, neurotransmission

Classification of zinc sites in proteins is broadly divided into (a) catalytic sites with the presence of a labile water ligand coordinated to the zinc (i.e. hydrolases)[5] and (b) structural

sites with no coordinated water and only protein residues in the coordination sphere, which has as its purpose the creation or maintenance of an appropriate secondary/tertiary structure in the protein (i.e. zinc fingers).[6] A cocatalytic site is also recognized where a zinc ion is bridged with a second metal usually by a single protein residue; the second metal can be zinc (i.e. β-lactamses) or another metal (i.e. Cu,Zn-Superoxide dismutases). Finally a fourth, protein interface zinc site can be defined, which influences the quaternary structure of proteins. The coordinating residues for this type of zinc site are supplied by two proteins (i.e. nitric oxide synthase, superantigens).[7] Additionally, roles for the zinc metal ion can be extended to regulatory (i.e. metallothioneins) and neuromodulation (i.e. presynaptic vesicles) functions, Table 2.I. This last topic has recently gained increasing attention due to the involvement of free zinc in neurological signaling and neurodegenerative disorders.[8-11] Zinc deficiency is detrimental in many aspects for the normal function of the organism, with notable effects on growth and immune systems. [12-14]

Given the importance and the diversity of zinc-containing metalloproteins and enzymes, perturbation of zinc homeostasis, either through zinc diet deficiency or genetic alterations in zinc proteins, is correlated with the onset of many life-threatening diseases such as cancer[15] and diabetes.[16] These advances have resulted in the recognition of zinc enzymes and proteins in their own right as molecular targets for disease intervention. The understanding of the molecular basis of zinc biochemistry in medicine and disease has been further facilitated by advances in molecular biology and spectroscopic techniques such as fluorescence, which may overcome the lack of spectroscopic properties of the metal ion and allow development of probes of zinc metabolism even under real-time conditions.[17]

The purpose of this review is to summarize recent information on the relevance of key zinc metalloproteins in current and important diseases for public health ranging from neurodegenerative disorders to antibacterial drug resistance (Table 2.II.). The review focuses on the bioinorganic viewpoint, emphasizing the structure of the zinc active sites; the effect of mutation or alteration of the active site on enzyme and protein mechanism; the role of the zinc protein as medicinal target as well as design and current clinical status of experimental inhibitors. For the purposes of the review the zinc sites will be broadly grouped into catalytic and structural.

Table 2.II. General comparison among zinc metalloproteins considered in this review.

Enzyme	Function	Zn coordination sphere	Medical Relevance
Catalytic Zinc			
MMPs	Degradation of extracellular matrix proteins.	HHH/HHD-H_2O	Cancer, diabetes, neurodegenerative disorders, arthritis, infectious diseases.
HDACs	Deacetylation of lysines residues in histone N-terminal tails.	HDD-H_2O	Cancer, neurodegenerative disorders, inflammatory related diseases, diabetes.
PTs	Prenylation of proteins involved in signal transduction.	CHD-H_2O	Cancer, rheumatoid arthritis, parasitic infections, multiple sclerosis.
SOD	disproportionation of superoxide ion.	HHDH	Familial Amyotrophic Lateral Sclerosis (fALS).
MβLs	Hydrolysis of β-lactam ring in antibiotics.	HHH/HHN (Zn1) DCH/DHH (Zn2)	Bacterial resistance to antibiotics.
Structural Zinc			
ZFs	Structural, DNA/RNA/protein recognition.	CCHH CCCH CCCC	Applications in human gene therapy, cancer, inflammatory conditions, antiviral therapy.
p53	Tumor suppressor	CCCH	Cancer, neurodegenerative disorders.

2.3. Catalytic Zinc as Target.

2.3.a. Matrix Metalloproteinases (MMPs):

2.3.a.1. Metzincin structure.

Matrixins or Matrix Metalloproteinases (MMPs) along with astacins, serralysins, adamalysins, leishmanolysins and snapalysins are members of the metzincin superfamily, which involves > 770 zinc endopeptidases. All members of this superfamily share a common zinc environment in their catalytic domain, the binding sequence motif HEXXHXXGXX(H/D) (where X is any aminoacid). In the active site, the three histidines from the sequence are coordinated by the metal ion in a trigonal pyramidal coordination sphere completed by a catalytic water molecule as a fourth ligand. For the astacin and serralysin families, there is also a fifth coordinated ligand from the hydroxyl oxygen of a conserved tyrosine which increases the coordination number around Zn^{2+} to five in a trigonal-bipyramidal geometry.[18] A second structural zinc site exists in the catalytic domain of MMPs, where the central zinc coordinates three histidines and one aspartic acid in a tetrahedral geometry.

In general, peptide cleavage is achieved through polarization of the zinc-bound water molecule (by H-bonding interactions with a conserved glutamate residue) followed by attack on the scissile carbonyl group from the peptide substrate that is oriented to the catalytic site (Scheme 2.1). The importance of the glutamate residue for this general-base mechanism was confirmed when mutants with aspartate and alanine residues, resulted in a reduced and low catalytic activity respectively.[19]

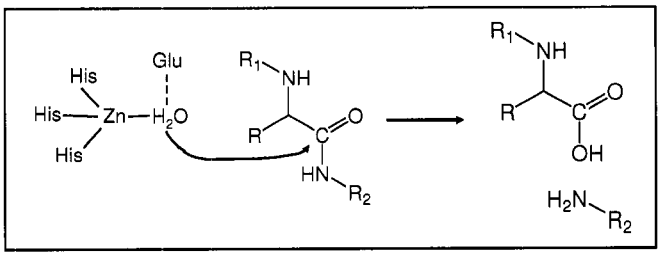

Scheme 2.1. General hydrolysis mechanism of peptide bonds by MMPs

MMPs are initially synthesized as a pro-enzyme or zymogen, where the catalytic water in the active site is substituted by a cysteine residue. This cysteine residue is included in a pro-peptide domain which must be cleaved by other MMPs or proteases in order to activate the enzyme and provide access to the substrate, in what is called a "cysteine switch" mechanism of activation.[20] This "cysteine switch" is an interesting example of nature's use of structural and catalytic zinc properties to achieve highly specific and controlled functions. Other important domains on MMPs are the haemopexin-like C-terminal, connected to the catalytic domain by the hinge region which can be up to 75 aminoacids long (Fig.1); both these regions are implicated in substrate specificity and activation.

Another common feature shared by this superfamily is the presence of a conserved methionine as a part of a tight 1,4-β-turn that forms a hydrophobic floor to the Zn^{2+} ion binding site. The presence of the methionine residue gives the name to the superfamily but its role for catalytic activity is still a matter of debate. Experiments using protease C from E. chrysanthemi found a decreased activity for the mutant forms M226A, M226I and M226L; although the crystal structure of M226L was found to be isomorphous to the wild type, the authors attribute a small rearrangement of the histidine ligands as a cause for the difference in activity.[21] Another study using mutants M392L and M392S from the human MMP-2

(gelatinase A) showed that the activity of the mutants was comparable in terms of kcat/Km to the wild-type MMP-2. Moreover, in addition to cleave the physiological substrates: native type I collagen and the chemokine monocyte chemoattractant protein-3, the mutants were also inhibited by MMP-2 inhibitors indicating a preserved active site.[22] Substitution of methionine 214 in P. aeruginosa by a nonnatural l-difluoromethionine also resulted in little effect on protein structure and function.[23]

Besides the active site and the methionine turn, the six aforementioned metzincin families share several topological characteristics despite an overall low sequence similarity among them (≈ 20% homology).

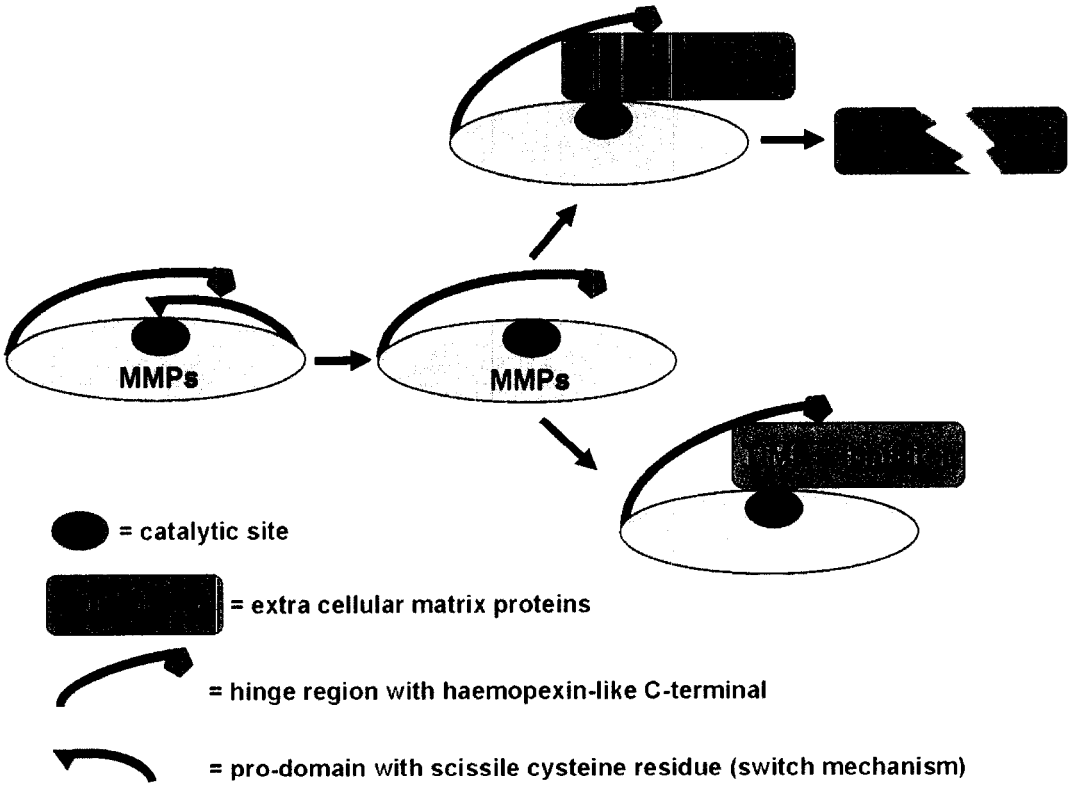

Figure 2.1. Schematic representation of MMPs function and Inhibition.

The common presence of a substrate binding crevice that subdivides the metalloprotein into an upper and lower domain provides an example of this (Fig. 2.1.); a detailed structural analysis for this superfamily can be found in the literature.[18, 24]

Zinc metalloproteins in the metzincin superfamily are in general capable of degrading all kinds of extracellular matrix proteins, in addition to being involved in cell-extracellular matrix and cell-cell interactions such as cleavage of cell surface receptors or chemokine activation/inactivation which are correlated to several diseases. The extracellular matrix (ECM) or connective tissue is a complex structure of insoluble macromolecules consisting primarily of collagen, proteoglycans and glycoprotein molecules such as fibronectin and laminin that surrounds the cells and provides them with support. This review will focus on the MMPs or matrixin family which was first discovered about 40 years ago and is currently considered as part of the future for molecular medicine.[25]

2.3.a.2. MatrixMetalloproteinase function and role in diseases.

There are 23 MMPs in humans from 24 genes due to a duplicated MMP-23 gene. These metalloproteins are tightly regulated and their expression is transcriptionally controlled by inflammatory cytokines and growth factors within the ECM, as well as hormones and cell-matrix interactions. A list of substrates cleaved and resulting biological effects produced by MMPs is given in Table 2.III., where a very diverse role in biological events can be appreciated. Deviations from MMP normal expression and behavior can lead to pathological disorders, as has been reviewed for the following diseases:

2.3.a.2.1.) Cancer. Due to the key role of MMPs in tissue remodeling and angiogenesis, a direct link with cancer invasion and metastasis is recognized;[26] there is a general correlation between the levels of MMP expression and the stage of tumor progression. Specific members of the subfamily such as matrilysin (MMP-7)[27, 28] and neutrophil collagenase (MMP-8)[29] are especially linked to human cancers. The function of MMPs in apoptosis remains paradoxical since pro-apoptotic and anti-apoptotic effects have been reported so far for MMP-1, -2, -3, -7, -9, -11. Recent evidence points also to novel substrates for MMPs beyond ECM and intracellular bioactive molecules, the ability to cleave the DNA repair enzyme poly-ADP-ribose-polymerase (PARP) suggests a role for MMPs in the nucleus.[30]

2.3.a.2.2.) Neurodegenerative disorders. Upregulation of MMPs is observed in all diseases of the Central Nervous System (CNS) including spinal cord injury, multiple sclerosis and stroke. However, also beneficial roles such as neurogenesis, axonal growth and myelinogenesis can be ascribed to MMPs during development and in response to insults in adulthood.[31]

2.3.a.2.3.) Arthritis. MMPs as well as other metzincins such as A disintegrin metalloproteinases (ADAMs) and the disintegrin metalloproteinase with thrombospondin type 1 like repeats (ADAM TSs) are generally secreted by many cell types and are involved in extra cellular matrix degradation of cartilage and bone. Their role in a range of human joint pathologies including ostheoarthritis has been identified and studied,[32] even the role of MMP in human caries have been recently examined.[33]

Table 2.III. Representative biological activities mediated by MMP cleavage.

Biological effects	MMP	Substrate
Tumor cell resistance	MMP-9	ICAM-1
Mammary epithelial cell apoptosis	MMP-3	Basement membrane
Osteoclast activation	MMP-13	Type I collagen
Adipocyte differentiation	MMP-7	Fibronectin
Cell migration	MMP-1, -2, -3	Fibronectin
Anti-inflammatory	MMP-1, -2, -9	IL-1β degradation
Disrupted cell aggregation and increased cell invasion	MMP-3, MMP-7	E-cadherin
Reduced cell adhesion and spreading	MT1-MMP, MT2-MMP, MT3-MMP	Cell surface tissue transglutaminase
PAR1 activation	MMP-1	Protease activator receptor 1
Vasoconstriction and cell growth	MMP-7	Heparin-binding EGF

2.3.a.2.4.) Infection and inflammation. The ambivalent role of MMPs in infectious diseases has also been reviewed recently. Beneficial roles involved in the normal immune response to infection include facilitation of leucocyte recruitment, cytokine/chemokine processing and matrix remodeling. However the detrimental aspect of increased MMP activity following the infection is correlated to onset of HIV, endotoxin shock, tuberculosis, hepatitis B and other diseases.[34] Pathologies derived from inflammatory cells are proposed to take part in various lung diseases including asthma, lung fibrosis and cancer.[35]

2.3.a.2.5.) Diabetes. An abnormal vascular ECM surrounding large and small arteries has been observed in diabetes mellitus (DM) cases, which has been called diabetic vasculopathy and can affect coronary/cerebral arteries, as well as, retinal and renal microcirculation. Hyperglycemia itself modulates the cellular secretion of MMPs and a role for these zinc metalloproteins in the pathophysiology of cardiovascular diseases in DM has been studied and described.[36]

2.3.a.3. MMP inhibitors (MMPIs).

The appropriate regulation of ECM degradation and turnover depends also on endogenous MMPs inhibitors called TIMPs (tissue inhibitors of metalloprotease)[20] and α2-macroglobulin. Specifcially α2-macroglobulin is a general inhibitor for endoproteinases but not astacins; this 725 kDa glycoprotein tetramer entraps the protein and further clears the complex by endocytosis. Recently novel inhibitors of MMPs have been described such as the reversion inducing cysteine-rich protein with Kazal motifs or RECK protein; the tissue-factor-pathway-inhibitor 2, TFPI2 and the procollagen C-terminal proteinase enhancer, CT-PCPE) although their mechanisms of action are not completely understood. [37]

TIMPs are wedge-like proteins, 184 - 194 aminoacids long. There are four mammalian variants (TIMP-1 to -4), each with its own profile of selectivity (MMPs, ADAMs and ADAM TSs).[38] Essentially, TIMPs have a two domain structure with N- and C-terminal regions; TIMPs interact with the subtrate cleft in the MMPs by slotting its ridge composed of the first four N-terminal residues C1-TC-V4 (aminoacid symbol and position in the sequence) linked by a disulfide bond with E67-SV-C70 (Fig. 2.2.A). In this way C1 expels the catalytic water in the active site (thus deactivating the MMP) by chelating the zinc ion through its N-teminal amino and carbonyl groups. The C-terminal domain is important for protein-protein interactions and binding to pro-MMPs, an important step in the activation process of MMPs. In addition, TIMPs exhibit MMP-dependent and -independent actions that complicate a complete understanding of their cell signaling process.[39] The determination of the crystal structures of TIMP-MMP complexes has helped significantly to elucidate the types of interactions needed to design specific inhibitors which will fit in the so-called S1'

pocket of the active site, which is conserved within MMPs and highly relevant for substrate specificity (Fig. 2.2.B).[37] The majority of MMPIs have been developed via structure-based design which in some regards mimic the natural substrate to obtain sequence-specific binding and incorporate carboxylate, hydroxamate, phosphonate, or phosphinate as chelating groups for the active zinc ion.[40] Figure 2.2.B exemplifies this for batimastat, one of the earliest MMP inhibitors to reach clinical trials.

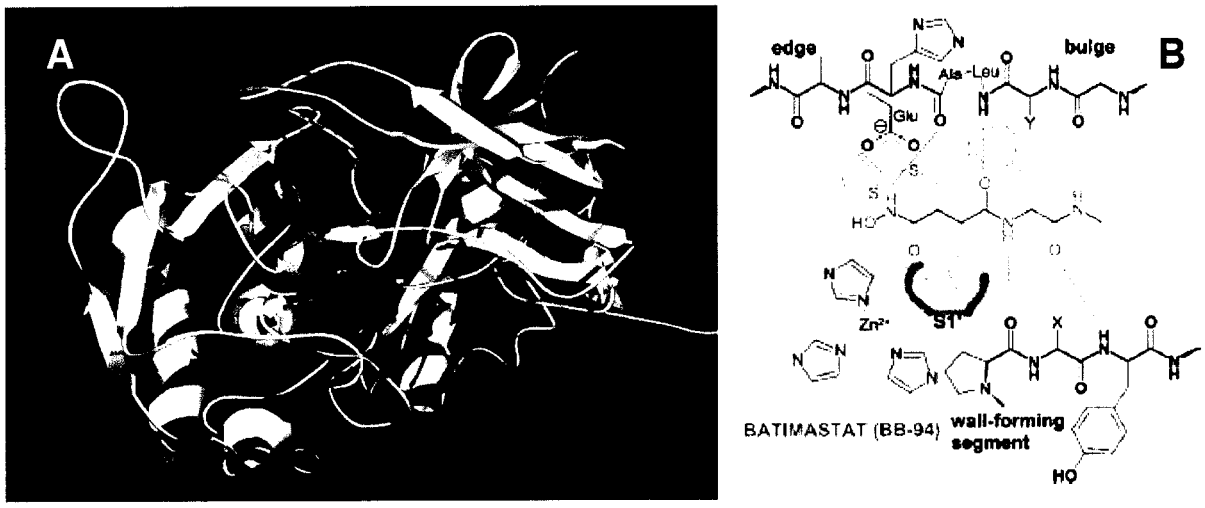

Figure 2.2. A. Crystal structure of the complex formed by the membrane type 1-matrix metalloproteinase (white) with TIMP-2 (yellow). Catalytic zinc with coordinating residues is colored green while structural zinc with coordinating residues is colored cyan (PDB ID: 1BUV).[41] B. Schematic drawing of the non-peptide inhibitor batimastat (red) with the active site (black) is shown, substrate binding pocket S1' is indicated in green.[37]

Nonpeptide inhibitors have also been described[42] and currently the search is focused on anti-succinates and sulfonamides. However the clinical efficacy of these inhibitors has been limited so far, in part due to the inability to discriminate a specific MMP substrate. Most of the MMPIs that have advanced into phase III clinical trials have failed to increase the

survival of patients. Two main causes for this failure have been indicated as an incorrect target validation and a lack of information regarding in vivo MMP substrates or physiological roles.[43] Moreover, comparison of x-ray and NMR structures obtained for MMPs indicates the flexibility of the protein backbone as one of the problems towards the development of specific inhibitors.[44] In order to increase specificity, recent pyrimidinetrione-based compounds have been reported to discriminate between MMP-13 and -14 with high selectivity.[45] In addition, small heterocyclic zinc-binding groups have been found to have a broad therapeutic window and an enhanced zinc binding as measured through IC50 values from an MMP-3 fluorescence assay.[46] Novel chelating groups can contribute to overcoming observed side-reactions in hydroxamate-based MMPIs such as the production of nitric oxide. A change in MMPI design philosophy has pointed out the importance of a moderate zinc affinity in order to improve specificity in other parts of the compound.[47] In the context of medicinal inorganic chemistry, it should be noted that the antimetastatic properties of NAMI-A (imidazolium trans-tetrachlorodimethylsulfoxideimidazoleruthenate (III)) have been linked with its interaction with MMPs, specifically MMP-2 and MMP-9 action `is inhibited in vitro by the Ru complex.[48]

Alternative biological strategies to inhibit MMP activity include RNA interference (RNAi)-mediated gene targeting, where a double-stranded RNA is used to degrade and homologous mRNA. This novel approach has been used for inhibition of MMP-1[49] and MMP-9[50], but so far the only MMPI which is widely available clinically is the antibiotic doxycycline with therapeutic efficacy for MMP mediated ocular surface diseases and for

periodontal disease. This semisynthetic tetracycline has been found to inhibit MMP-9 activity in a wide variety of cells including prostate cancer and endothelial cells.[51]

2.3.b. Histone Deacetylases (HDACs).

2.3.b.1. Structure and function.

DNA organization and gene expression is tightly regulated by epigenetic modifications such as DNA methylation, and histone modification.[52, 53] Histone DeACetylases (HDACs) are one of the several families of proteins responsible for epigenetic control since they catalyze the deacetylation of ε-amino groups of lysine residues in histone N-terminal tails (Scheme 2.2.).

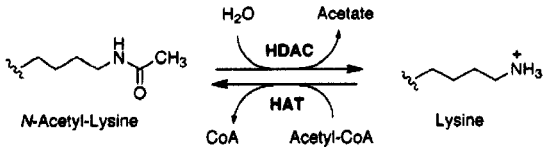

Scheme 2.2. General mechanism for acetylation/deacetylation of histone lysines.

The reverse process is performed by Histone Acetyl Transferases (HATs) and any deviation from the delicate balance of both processes (acetylation homeostasis) results in aberrant transcriptional activity correlated with a variety of diseases including cancer, diabetes and neurodegenerative disorders. The HAT-HDAC system is also considered to modulate replication, site specific recombination and DNA repair. The mechanism for lysine acetylation in HATs can vary within subfamilies but generally involves the transfer of an acetyl group from acetyl-coenzyme A to the specific lysine residue.

Modification of histone tails, termed the histone code, by reactions such as acetylation, phosphorylation, ubiquitination, methylation, and poly-ADP-ribosylation regulates

accessibility of transcription factors to DNA.[54] Histone deacetylation in particular, is generally associated with a compact chromatin structure and gene inactivation. So far 18 different HDACs have been identified and divided into four classes based on homology. Specifically for eukaryotes, 11 HDACs of Classes I (HDAC-1, -2, -3 and -8) and II (HDAC-4 to -7 and -9,-10) have been identified so far. HDAC-11 is classified as the sole member of class IV and sometimes included in class II (class III is a structurally unrelated subfamily found in yeast).[55] Class I HDACs are localized exclusively in the nucleus and are ubiquitously expressed, whereas the proteins in class II are larger and are shuttled between the cytoplasm and the nucleus and display a tissue-specific expression. To the present day only three-dimensional structures for HDAC-8 have been reported,[56, 57] and previous studies regarding HDAC structure and catalytic mechanism were based on the histone deacetylase like protein (HDLP) which shares basically the same catalytic site.[58]

HDAC-8 shares 30% homology with HDLP although important variations in the loops for both proteins are present, specifically HDAC-8 comprises a single compact α/β domain with an eight-stranded parallel β sheet sandwiched between 13 α helices (insert A in figure 2.3.). The active site is thought to be essentially identical for HDACs classes I, II and IV since key catalytic residues are conserved in the overall sequence. One of the main characteristics featured in this family of zinc metalloproteins is the presence of a narrow hydrophobic tunnel that leads into the active site: a zinc ion coordinating one histidine (H180) and two aspartic acids (D178, D267) along with a water molecule to complete the first or inner coordination sphere. Additional key residues in the active site comprise one tyrosine (Y306) and two histidines (H142, H143) in the second or outer coordination sphere (*vide infra*).

Recently it has been suggested that Fe(II) instead of Zn(II) as the active metal ion for HDAC-8; confirmation of this result would have profound implications for metal cofactor assignment *in vivo*.[59]

A.

1.

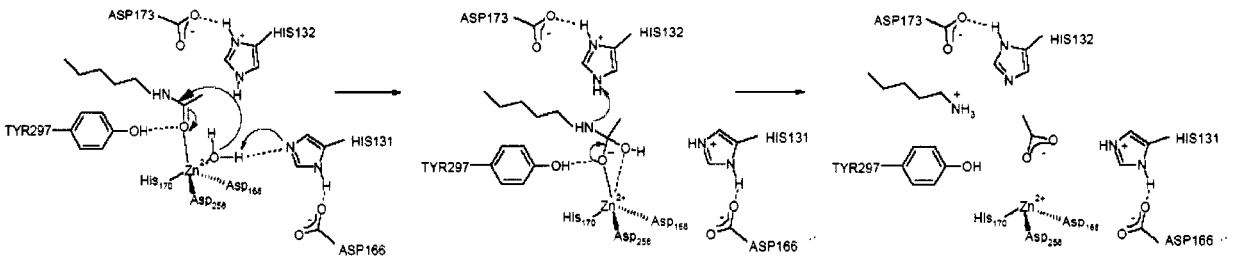

2.

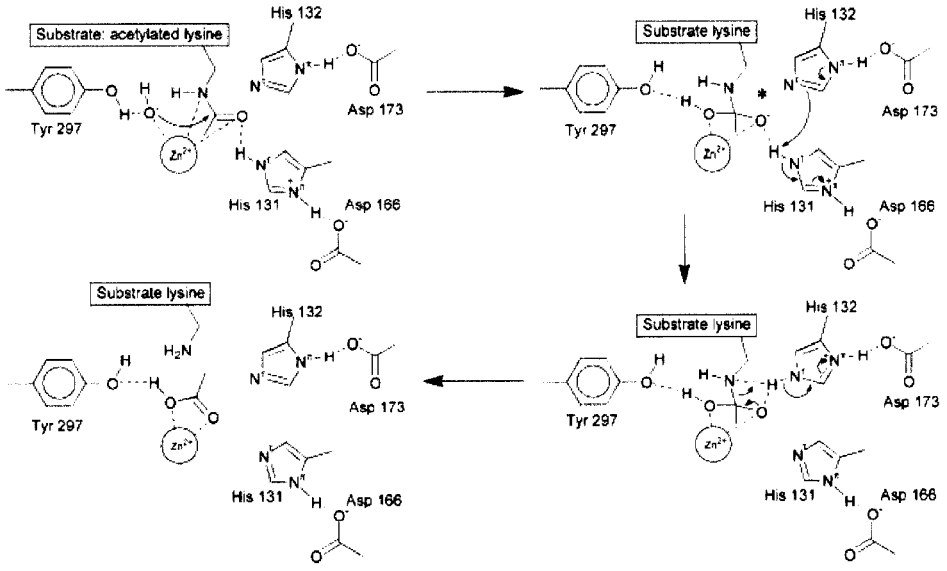

3.

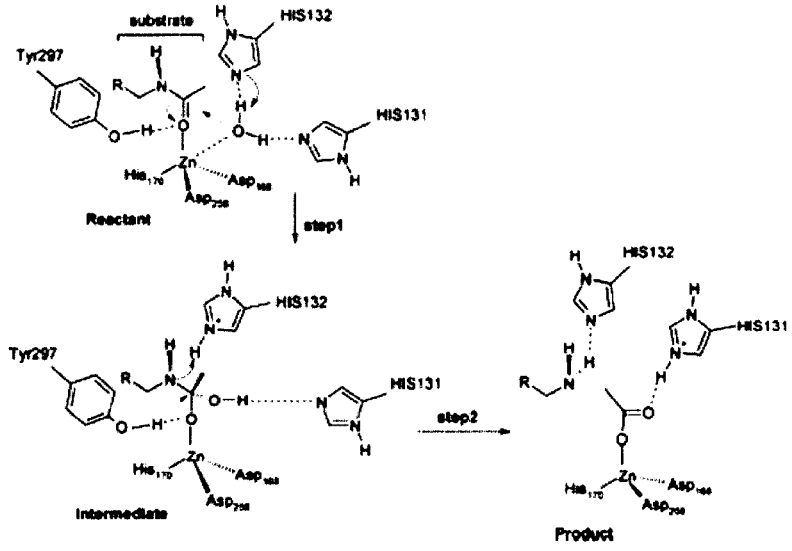

Figure 2.3. HDAC-8 complexed with inhibitor MS-344 (in green), chelating the zinc ion (in red) PDB ID: 1T67 (A). Proposed mechanisms for HDAC activity (1 -3).

The catalytic mechanism of HDACs has been the subject of frequent updates in recent years with contributions from DFT and QM/MM calculations. The first postulated mechanism considered the water as a nucleophile due to polarization between the zinc ion and a histidine residue (H131). This activated water can attack the acetyl group causing cleavage from the lysine residue (mechanism 1 in figure 2.3.). This mechanism assumes a five-coordinate transition state and the key residues histidine H143 (H132 for HDLP) and H142 (H131 for HDLP) as doubly and singly protonated respectively, acting as an acid and a base to assist in the stabilization of the bound water molecule.[58] These features are closely related to the one found generally for zinc proteases (i.e. MMPs). Recent results have suggested that the transition state could differ significantly in the case of HDACs. [60]

One of the important and novel features that differentiate the active site is the presence of two adjacent histidine-aspartate (H-D) dyads where the imidazole ring in histidine residues H142 and H143 is hydrogen bonded with the carboxylate moiety of the aspartate residues D176 and D183 respectively. The strength of the hydrogen bonding causes a modification (usually a reversal) in the pKa for H and D in what is called a charge-relay mechanism. [61] These dyads are different in structure according to hydrogen bond distance between the carboxylate oxygen in D and the N^{π} atom in H, and relative orientation between the imidazole ring (H) and the carboxylate group (D). Additional energetic features including proton affinity, along with an analysis of histidine/aspartate distances led to the formulation of a second mechanism, which postulates an inverse protonation for the histidines H142 and H143 present in the second coordination sphere. In addition Y297 is proposed to help in the stabilization of the water molecule in the first step, although the zinc ion maintains the

pentacoordinated intermediate (mechanism 2, figure 2.3.). A third and more recent postulated mechanism consider both histidines singly protonated and acting to stabilize the coordinated water molecule in the first step of the reaction, this feature is indicated to decrease the energy for the reactant state in 5 kcal/mol^{-1}. The zinc ion is tetracoordinated in the intermediate state and in the rest of the reaction process with its principal role the activation of the carbonyl group of the amide (mechanism 3, figure 2.3.). [62]

Another interesting member of this family of zinc metalloproteins is HDAC-6, the largest class II protein (1215 residues) which exhibits two potential catalytic domains. This rather uncommon feature for an HDAC has been actively studied and *in vitro* studies using mutations in the histidine residue reported that only the second domain (C-terminal) is the active one, not only towards acetylated histone, but acetylated α-tubulin as well. [63] These findings conflict with the results which found both domains to be responsible for deacetylation activity, and where the spatial arrangement of HDAC-6 domains is of main importance for the catalytic activity *in vivo*. [64]

2.3.b.2. Clinical Relevance.

A growing number of non-histone proteins can serve as substrates for HDACs including nuclear and cytoplasmic factors (p53, CREB, HMGB1) and the importin family.[55] Given the importance of the acetylation process for gene regulation and the type of substrates that HDACs modulate, it is therefore straightforward to imagine the profound implications of this zinc metalloproteins in multiple diseases, notably cancer.

Deviation from the delicate acetylation homeostasis maintained between HDACs/HATs produces a disturbed genome pattern which is a common molecular mechanism used by

oncogenes. Moreover, loss of histone acetylation leads to gene silencing and decreased DNA repair.[52, 65] On the other hand, hyperacetylation of HDAC substrates can induce growth arrest, cell differentiation, and apoptosis of tumor cells. [66] The first model disease that demonstrated HDAC involvement was acute promyelocytic leukaemia (APL), where transcriptional silencing is produced by aberrant HDAC behavior. Administration of retinoic acid, the substrate for the transcription factor retinoic acid receptor-α (RAR), along with HDAC inhibitors has proven to cause remission in transgenic models of therapy-resistant APL. [67] Specific forms of lymphoma also involve aberrant recruitment of HDACs and the mechanism for regulation of these metalloenzymes has been understood in some detail specially for class II. [68, 69] Hormone-dependent cancers such as breast and prostate, are thought to be associated with a group of coregulator proteins which modulate the nuclear receptor transactivation function and carry HDACs - as an example the coregulator testicular zinc finger protein has been shown to recruit HDAC-2 to this end. [70] It is generally accepted that imbalances in epigenetic modification play a basic role in cancer development and progression, and thus the efforts towards the development of HDACinhibitors as anticancer agents have flourished in the last years (*vide infra*), [71] even though the molecular basis for their anticancer selectivity remains largely unknown. [72]

An acetylation balance is important also for neuronal vitality, and an increasing amount of evidence show that this balance is greatly impaired during neurodegenerative conditions, in line with the fact that HDACs inhibitors prevent oxidative neuronal death and ameliorate the conditions associated with Alzheimer's , Parkinson's and Huntington's disease, multiple sclerosis and Friedreich's ataxia. [73]

The correlation of HDACs in diabetes has also been reviewed recently. Multiple genes that are defective in the various form of diabetes, so-called diabetogenes, have been shown to associate both with HATs and HDACs. Moreover, the regulation of insulin expression by glucose has been demonstrated to be under the control of histone hyperacetylation, further confirming links between HDACs and this disease. [74]

Chronic Obstructive Pulmonary Disease (COPD) refers to chronic bronchitis and emphysema, two lung diseases that are characterized by obstruction of airflow due to a specific pattern of inflammation. The correlation between a reduced HDAC activity (particularly HDAC-2 > HDAC-3, HDAC-5) and the production of inflammatory genes in patients with COPD have been observed[75] In this regard class I HDACs have been reported to have inflammatory properties (specially HDAC-1, -2 and -3), and HDAC inhibitors exhibit anti-inflammatory effects apparently due to: 1) inhibition of cytokine and NO production, 2) inhibition of key transcription factors such as NF-κB and STAT, 3) inhibition of proliferation or induction of differentiation of normal cells during differentiation. The potential use of HDACs inhibitors for inflammatory diseases has been reviewed recently. [76]

2.3.b.3. HDACs Inhibitors (HDACIs).

The precise molecular mechanism for inhibition of the class I and II zinc-HDACs is not clearly understood, and the genes responsible for the biological response have not been identified. However several three-dimensional structures of HDLP and HDAC-8 complexed with HDACIs (hydroxamate type) have been determined and the general features observed involve first the obstruction of the substrate pocket (rim) and hydrophobic binding tunnel that leads into the catalytic site and secondly the chelation of the active zinc ion, as seen in

Fig 2.2. The net effect is similar to a long cork that hinders the entrance of the putative substrate, and displaces the nucleophilic water molecule from the active site, while simultaneously saturating the coordination sphere of the zinc ion. Therefore three main characteristics are generally present in common HDACIs, beginning with a metal binding site for zinc chelation, followed by a linker or spacer that mimics the substrate and fills the hydrophobic tunnel, and lastly a hydrophobic cap that closes the entrance to the tunnel and ideally should exhibit good interaction with the outer rim.

The HDACI literature have been reviewed thoroughly, [55, 66, 68, 71, 77, 78] and these compounds can be categorized into six different chemical classes[79] as:

II.b.3.1.) carboxylates, including short-chain fatty acids like butyric and valproic acids, which has undergone phase II oncology trials. [80] Although being generally weak inhibitors and highly unspecific, they are still a valuable (i.e. valproic acid) tool to study the structure and mechanism of HDACIs. Some of these compounds can be acquired through some foods like, broccoli and garlic and could achieve the necessary concentration to have an important therapeutic impact. [81]

II.b.3.2.) small-molecule hydroxamates, including early HDACIs like Trichostatin A (TSA), PXD101 and SAHA, this group exhibits an unfavorable pharmacokinetic behavior resulting from glucuronidation and sulfation, and from metabolic hydrolysis, decreasing the half-life of the hydroxamic group. Alternatives compounds with a different chelation group are an active area of research, recent α-mercaptoketone and α-thioacetoxyketone analogs of SAHA are reported to have higher potency on *in vitro* and *in vivo* tests than the parental HDACIs. [82]

2.3.b.3.3.) electrophilic ketones (epoxides), including AOE and trapoxin B, make use of the epoxy group to modify or alkylate the active site in the HDAC.

2.3.b.3.4.) cyclic peptides, generally the macrocyclic peptide portion of the inhibitor is used to bind to the rim of the active site, while an aliphatic linker anchors in the hydrophobic tunnel, example depsipeptide or FK228 is considered a pro-drug that needs intracellular reduction, is in phase III oncology trials.[80]

2.3.b.3.5.) benzamides, two examples of this type being MS-275 and CI-944. The former is undergoing clinical phase II trials as an anticancer agent and its use in the treatment of epigenetically induced psychiatric disorders has been suggested. [83] CI-944 on the other hand, has been used in several clinical phase I trials. Their mechanism of action remains uncertain.

2.3.b.3.6.) other hybrid compounds, where recent examples include short-chain fatty acids with Zn^{2+} chelating binding motifs[84] and a cyclic tetrapeptide (chlamydocin) with an epoxyketone surrogate, [85] which combines the inhibition mechanisms of both cyclic peptides and epoxides and are sometimes active at the nanomolar level.

HDACIs constitutes a novel class of cancer chemotherapeutics already in clinical Phase I/II trials, which are used in an effort to reestablish the acetylation balance that is disturbed in pathological diseases. Although there is some evidence that there is certain degree of specificity among HDACi, (i.e. capable of discriminate between HDACs classes I and II) and recent results from clinical trials are encouraging, a greater specificity even among members within a class is preferable to increase the therapeutic window of HDACIs, because key cellular functions could be disrupted by its indiscriminate use. In this regard, a

correlation between HDACI activity and teratogenic properties for valproic acid has been described. [86]

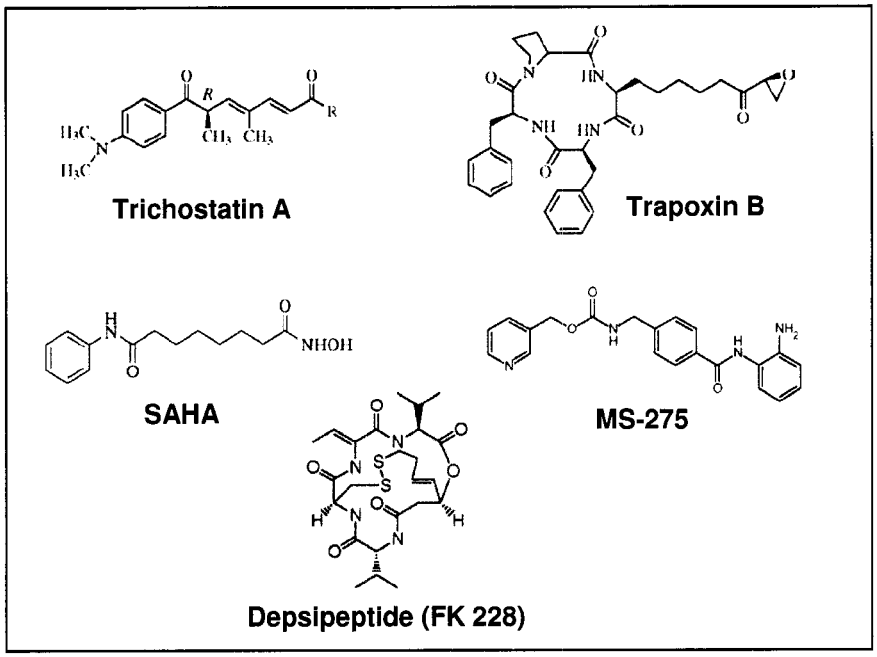

Figure 2.4. Structure of different type of HDACIs

The success of HDACIs as anticancer agents relies on an apparent selectivity in apoptosis induction for cancer cell lines, compared to normal cells. Attempts to explain this fact point to a preferential up regulation of pro-death genes or down regulation of pro-survival genes at the transcriptional level, or a different cascade of events produced in normal and cancer cells. HDACIs can also increase reactive oxygen species preferentially in transformed cells which would explain the selectivity towards cancer cells. [87] The need to understand in more depth the mechanism of action (anticancer, anti-inflammatory, diabetes) of these compounds is critical since non-histone substrates might be playing a more important role in the

therapeutic activity, and the almost random up/down regulation of genes remains far from being controlled.

2.3. c. Prenyl Transferases.

2.3.c.1. Structure and Function.

Protein prenyltransferases (PTs) catalyze the covalent attachment of a polyisoprene group, from an appropriate prenyldonor i.e. farnesyldiphosphate (C_{15}) or geranylgeranyldiphosphate (C_{20}), to a cysteine at or near the carboxyl termini of proteins involved in signal-transduction pathways and cell growth (Scheme 2.3.). This post-translational modification is necessary not only for subcellular localization but also plays a direct role in protein-protein and protein-membrane interactions.

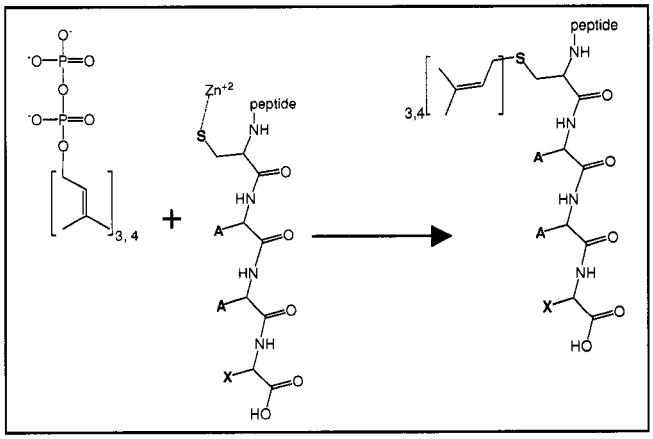

Scheme 2.3. General mechanism for protein prenylation.

As can be seen in Table 2.IV., there are three different PTs in humans: farnesyl transferase (FT) and geranylgeranyl transferase type I (GGT-I) recognize a similar motif at the C-termini of the substrate proteins, while geranylgeranyl tranferase type II (GGT-II) does not require a specific motif as long as there is one or two cysteines available. However it does

require an escort protein called Rab escort protein (REP) in order to transfer two geranylgeranyl moieties to a flexible motif with two cysteines in the sequence. [88]

The heterodimeric structure of the three enzymes is very similar composed of α/β subunits; with one zinc ion per dimer harbored in the β subunit. [89] The α subunit is encoded by the same gene (FNTA) and is identical for FT and GGT-I with a molecular mass of 48 kDa. It is composed of α-helical pairs that form a crescent-shaped super helix and wraps around the compact α-α barrel of the β subunit. The α subunit in GGT-II (60kDa) is composed of three domains: a helical domain which is structurally similar to the α subunit in FT and GGT-I (22% identity), an immunoglobulin (Ig)-like domain and a leucine-rich repeat (LRR) domain. The functions of these two latter domains remain unknown so far, but apparently are not directly involved in substrate or REP interactions.[89]

Table 2.IV. Comparison among PTs in terms of recognition motif and protein substrate.

Enzyme	Protein substrate	Recognition motif
Farnesyl transferase	Ras (H-, N-, K-); prelamin A, HDJ2, PTP-CAAX/PRL tyrosine phosphatases, Rho-B, Rheb, CENP-E, -F	CAAX, X = S, M, Q, A.
Geranylgeranyl transferase type I	Rac1,-2; RalA, Rap1A,-1B; Rho-A,-B,-C; Rab 8, Cdc42,	CAAX, X = L, F
Geranylgeranyl transferase type II	Rab	-CC, -CXC, -CCX, -CCXX/REP

The β subunit of the three enzymes shares a very similar structure (Fig. 2.5.), in spite of a low sequence identity between them, i.e. 25% for GGT-I and 30% for GGT-II, compared to FT. Basically 12 to 14 α-helices form a compact α-α barrel which is closed at one end by a loop from the C-terminus, creating a deep funnel-shaped cavity at the center of the barrel

lined with hydrophobic residues which is the proposed binding site for the hydrophobic tail of the prenyl diphosphate. The diphosphate head group in turn, faces to a positively charged cluster or cleft found at the rim of this cavity close to the α/β interface. The active zinc ion is coordinated by three conserved residues: aspartate, cysteine and histidine and the nature of the fourth ligand is still in controversy between a tightly water ligand or a second oxygen from the aspartate. Results from computational studies have pointed out the close energetic proximity between both possibilities, although favoring the second alternative at least in the case of FT.[91] Both α/β subunits exhibit a extensive interface with an unusually high polar/charged residue content therefore increasing significantly the number of hydrogen bonds.[91] Apparently the role of zinc in these metalloproteins is purely catalytic since studies with zinc depleted FT have shown that the overall structure is identical to the original, and binding of the farnesyldiphosphate has been also observed in the absence of zinc.

It can be seen from Table 2.IV. also that there is some overlap of the protein substrates for these enzymes but particular features on each one contribute to further selectivity. Regarding the catalytic mechanism for prenylation, an important distinction between the FT and GGT-I mechanism on one side and GGT-II on the other can be made due to specific structural differences. In the former case the binding of the prenyl diphosphate to the hydrophobic α-α barrel from the β subunit in FT or GGT-I constitutes the first step of the catalytic cycle.

As determined by X-ray diffraction using model lipid substrates and mutation experiments, the depth of the cavity in the α-α barrel is an important factor to modulate selectivity between FT and GGT substrates. Specifically at the bottom of the cavity there is a steric constraint in FT that does not exist in GGT-I, constituting the presence of a tryptophan and

tyrosine residues limiting the entrance of only three isoprene units present in the farnesyl diphosphate substrate. These residues are instead threonine and a phenylalanine respectively in the case of GGT-I, allowing the entrance of the fourth isoprene unit in geranylgeranyl diphosphate.

Figure 2.5. Overlay of the β subunit (Cα only) in farnesyl transferase (white, PDB ID: 1FT2), geranylgeranyl transferase type I (yellow, PDB ID: 1N4P) and geranylgeranyl transferase type II (green, PDB ID: 1DCE). First sphere of zinc coordination is shown is square, except for water (right) .Zinc atoms are drawn as grey CPK balls.

A proper fit within the hydrophobic α-α barrel will place the C1 carbon of the prenyl diphosphate in proximity to the active zinc center allowing or enhancing the prenylation transfer. The second step in the cycle is the peptide binding, the CAAX moiety making extensive van der Waals contacts with all the isoprene moieties but the first, and the cysteine sulphur is coordinated to the zinc ion producing a five coordinate intermediate. The exact nature of the cysteine before coordination (thiol vs. thiolate) is another matter of debate since

the pKa of the thiol depends on several factors such as the nature of residues surrounding the cysteine, presence of substrate, etc... After cysteine coordination to the zinc ion and rotation of the first isoprenoid unit to facilitate approach of the activated cysteine to the C1 carbon in the prenyl diphosphate, an associative mechanism (Sn_2) with dissociative character is followed. The thioether formation proceeds with configuration inversion of C1, the developing charge in the diphosphate group is stabilized with the help of either a magnesium ion in FT or a positive lysine residue in GGT-I.

A second factor for substrate specificity, in addition to the depth of the cavity in the α-α barrel, is given by the last AX pair of residues in the recognition motif (CAAX) of the protein terminus. Since the cysteine is coordinated to the zinc and the next A residue is basically open to the solvent, the interaction of the last two residues with the tranferase enzyme have been found to play an important role according to tri-dimensional structures obtained for models of the recognition motif. Notably the X-residue binding pocket in FT was found to be more polar than GGT-I, explaining the differences in affinity observed for the X residue among both enzymes (Table 2.IV.). The rate-limiting and last step in the cycle is the product release, which occurs with the help of a new entering prenyl diphosphate displacing the final product to an exit groove.

The catalytic cycle for GGT-II on the other hand has not been studied in so much detail, and so far two different mechanisms have been proposed, which under *in vivo* conditions are thought to depend on the concentration of the proteins involved. In a first pathway REP associates with an unprenylated Rab protein, then GGT-II can recognize this complex and prenylates twice the Rab protein probably *via* consecutive independent steps (although some

Rab are only monoprenylated, i.e. Rab 8). The binding of a new prenyl diphosphate ligand to GGT-II stimulates the release of the product in a similar fashion with the last step in the catalytic cycle for FT and GGT-I. Since there is only one geranylgeranyl diphosphate binding site it has been suggested that the second prenyl diphosphate ligand could be harbored in an alternative hydrophobic tunnel analogous to the exit groove in FT and GGT-I. A second pathway proposes the formation of a complex between REP and GGT-II prior to the binding of Rab and further prenylation.

Findings regarding structural and mechanistic aspects of PTs have provided essential information for the development of inhibitors with diverse potential therapeutic applications as will be discussed in the next sections. However some key questions regarding the prenylation mechanism in FT and GGT-I are yet to be confirmed, and this situation is also the case for GGT-II which only recently has received a more focused attention.

2.3.c.2. Clinical Relevance.

The clinical relevance of PTs stems from the fact that proteins involved in cell proliferation, signal transduction and malignant transformation, need to be prenylated in order to exert their vital functions. Small GTPases in Ras, Rho and Rab families in addition to nuclear lamins, cGMP phosphodiesterase are amongst the substrates for PTs. The involvement of mutated forms of *ras* genes and farnesylated Ras proteins in human tumors has been observed for 30% - 40% of cases. The mutated Ras have suppressed GTPase activity and remain active (GTP bound) independently of upstream activation, therefore relaying a signal for tumor growth. There are three *ras* proto-oncogenes that encode for four proteins H-Ras, K-Ras (two splice variants) and N-Ras. H-Ras mutations are rare, however have been

observed in bladder cancers (15 – 20 %), mutated K-Ras are prevalent in some adenocarcinomas including pancreatic (> 90 %), colorectal (50 %) and lung cancer (30 %), while mutated N-Ras occur in melanoma (10 – 20 %) and some hematologic malignancies. Also a correlation between the kind of cancer developed with mutations in a specific Ras protein have been suggested.[92]

The development of inhibitors for PTs and specially FT has been sought as an effective noncytotoxic anticancer strategy. However N-Ras and K-Ras can act as substrates for GGT-I upon FT inhibition, due to the aforementioned substrate overlap between these two enzymes (albeit N-Ras in a less efficient way), becoming geranylgeranylated and recovering functionality in an equivalent way to the farnesylated analogues. These facts have suggested the need for dual FT and GGT-I inhibitors to achieve better anticancer results, although some pre-clinical data indicates a potential toxicity if both enzymes are inhibited.[93] FT inhibition has also been shown to prevent collagen-induced arthritis by downregulating inflammatory gene expression.[94]

Inhibition of FT in patients with myelodysplastic syndromes (i.e. refractory anemia, preleukemia) has shown some promise in Phase I/II studies, although issues related to toxicity also indicate the need for further studies to establish dose optimization and correlation between response and molecular targets among others.[95, 96] FT inhibition has also been employed for the treatment of parasitic diseases caused by pathogenic protozoa, like malaria and trypanosomyasis. A very promising efficacy has been found and the development of a proper pharmacokinetic profile seems to be the next step towards a parasitic chemotherapy. Interestingly, there appears to be an inherent cytotoxic selectivity for

pathogenic protozoa compared to normal mammalian cells which could be due to a lack of an analogue of GGT-I or a higher sensitivity for farnesylation inhibition in the parasite.[97]

In the last decade GGT-I inhibitors have also shown potential in the treatment of smooth muscle hyperplasia, multiple sclerosis, parasitic infections, osteoporosis, atherosclerosis/restenosis and hepatits C virus infection.[98] Statins, inhibitors of hydroxy-methylglutaryl-coenzyme A reductase (HMG-CoA), can act as indirect PTs inhibitors by blocking the synthesis of farnesyl- and geranylgeranyldiphosphate. The biological implication of lipophilic statins that can inhibit geranylgeranylation for use as therapeutic agents in rheumatoid arthritis has been discussed recently.[99]

2.3.c.3. Prenyltransferase inhibitors.

Due to the aforementioned involvement of Ras farnesylation in cancer, initial efforts focused greatly in developing inhibitors for FT enzyme (FTIs). Findings derived from x-ray characterization of FT interaction with model tetrapeptides, indicated the possibility of using modified tetrapeptides with aromatic residues in the A position next to the X residue in the CAAX motif as inhibitors. Allegedly the aromatic portion in the residue would block access to the prenyl diphosphate binding site thus inhibiting the enzyme, and this approach has been investigated until recently.[100] Although generally these peptidomimetic compounds have drawbacks relating to their pharmacokinetics (i.e. rapid intracellular degradation and deficient cellular uptake), the substitution of the aliphatic AA portion of the motif by benzodiapine or aminomethylbenzoic acid significantly increases the stability (non-peptidomimetics). Basically the currently known FTIs can be classified according to their mechanism of action - by competing with farnesyldiphosphate, the CAAX motif or both.

Nowadays there are at least six FTIs that have been tested in clinical trials: 1) BMS-214662 from Bristol-Myers Squibb; 2) L778123 from Merck & Co., Inc.; 3) tipifarnib or R115777 from Ortho Biotech Products; 4) lonafarnib or SCH66336 from Schering-Plough Corporation; 5) FTI-277 Calbiochem and 6) L744832 from Biomol International L.P (Figure 6).[101] All these compounds display a high selectivity with FT IC_{50} in the nanomolar range although inhibition of other prenyl transferases cannot be ruled out. Recently the inhibition of GTT-II by analogs of BMS-214662 was reported, in spite of being considered structurally unrelated with FT. Generally the pre-clinical results were very promising, Results of Phase I/II clinical trials confirmed a significant therapeutic window (anticancer activity/toxicity), but unfortunately Phase III trials clearly indicate the failure of FTIs as single-agent anticancer drugs in solid cancers. The clinical and pre-clinical activity has been reviewed thoroughly in recent publications. [93, 102]

However the use of FTIs in combination with other antitumor agents such as taxanes and antiestrogens might present more potential, and FTIs have also shown a very good activity against hematologic cancers such as chronic myelogenous leukemia, myelodisplastic syndrome and acute myelogenous leukemia. The inhibition of other proteins besides Ras can provide a clue to the therapeutic activity observed for FT inhibitors, especially those which are FT substrates only like the Rheb, CENP-E/CENP-F and PTP-CAAX/PRL involved in tuberous sclerosis, taxane synergy and antitumor activity respectively. The quest for a specific target protein is complicated by the fact that there are more than 30 proteins that are known to be farnesylated pointing to a quite complicate mechanism of biological activity.

This lack of knowledge in terms of molecular pharmacology for FTIs has been pointed out as one of the factors contributing to the poor clinical trial results. In this regard an alternative Ras-independent antitumor mechanism has been reported for FTI inhibitors like FTI-277, where sole FT inhibition was not sufficient to mediate G_1 arrest and proteasome inhibition and up-regulation of p21 may be implicated.[104]

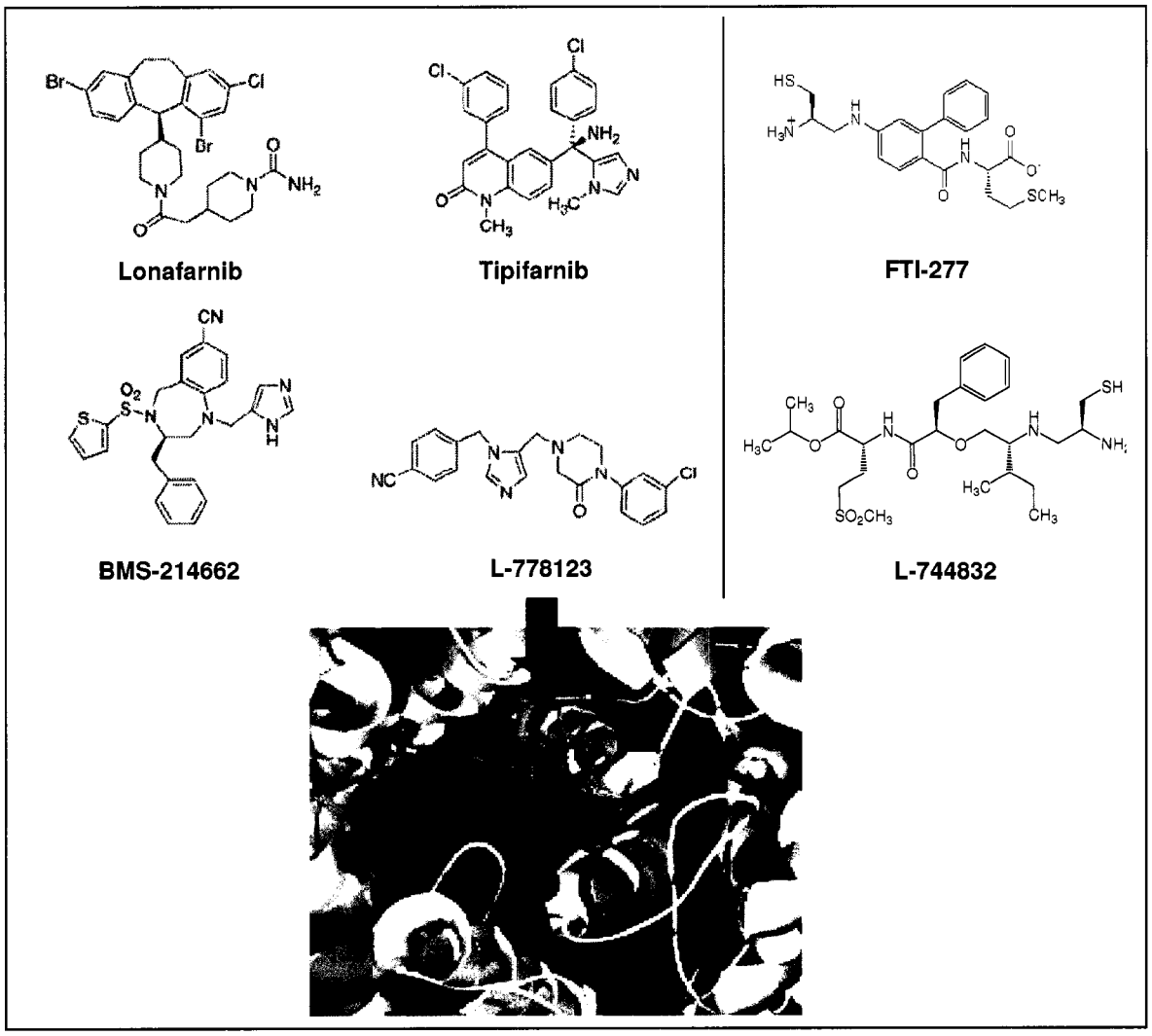

Figure 2.6. Representative structures of farnesyl tranferase inhibitors (top). Zoom from the active site of human FT (white ribbon) showing the imidazol moiety of L-778123 (green) coordinated by the zinc ion (red). The farnesyl diphosphate molecule can also be seen (orange). PDB ID: 1S63[104]

2.3.d. metallo-β-Lactamases (mβLs).

2.3.d.1. Structure and Function.

β-lactams are the oldest, least expensive and most used family of antibiotics which include penicillins, cephalosporins and carbapenems (Scheme 2.4.B). These antibiotics act by interfering with cell wall peptidoglycan biosynthesis, using their four membered beta-lactam moiety to deactivate the key enzyme transpeptidase. This chemotherapeutic approach, although very selective, is hampered by a special class of enzymes that hydrolyzes the important C-N bond within the β-lactam ring, hence the name β-lactamases. These enzymes represent the most common mechanism of resistance to antibiotics[105] and they are mainly classified as serine-β-lactamases (classes A, C and D) or metallo-β-lactamases, mβLs, (class B) depending on the sequence homology (Ambler), although an alternative classification based on substrate specificity also exists, which places mβLs under group 3 (Bush-Jacoby-Medeiros).[106] Depending on the catalytic mechanism employed however, serine-β-lactamases use an activated serine nucleophile to attack the carbonyl carbon atom in the beta-lactam ring, while mβLs employ a water (hydroxide) molecule coordinated to one or two zinc ions (scheme 2.4.A). Based on aminoacid sequence and substrate affinities mβLs are further divided in three subclasses (B1 – B3) but general features in the active site are somewhat conserved, that is one of the zinc ions (Zn1) has a tetrahedral geometry and the other (Zn2) is trigonal bipyramidal.

Both zinc ions are usually within 3.6 Å bridged by a hydroxide group which is thought to act as the nucleophile in the hydrolytic reaction, although some results points to Zn2 as intimately involved in the hydrolytic reaction.[107] The nature of the coordinated residues for the zinc ions vary with the subclass. Accordingly Zn1 will coordinate three Hs for B1 and B3 subclasses, while two Hs and an N will be the coordinating residues for B2. Zn2 on the other hand coordinates a D, C, H triad in B1, B2 while the C is substituted by another H in B3; the coordination is completed by the bridging OH^- and a water molecule in Zn2. The affinities for zinc in the two coordinating sites are different, and it is accepted that B1 and B3 mβLs are active through Zn1 while the presence of Zn2 typically enhances their activity. On the contrary for B2 mβLs the presence of Zn1 causes an inhibition in function and usually the active position is Zn2.[108]

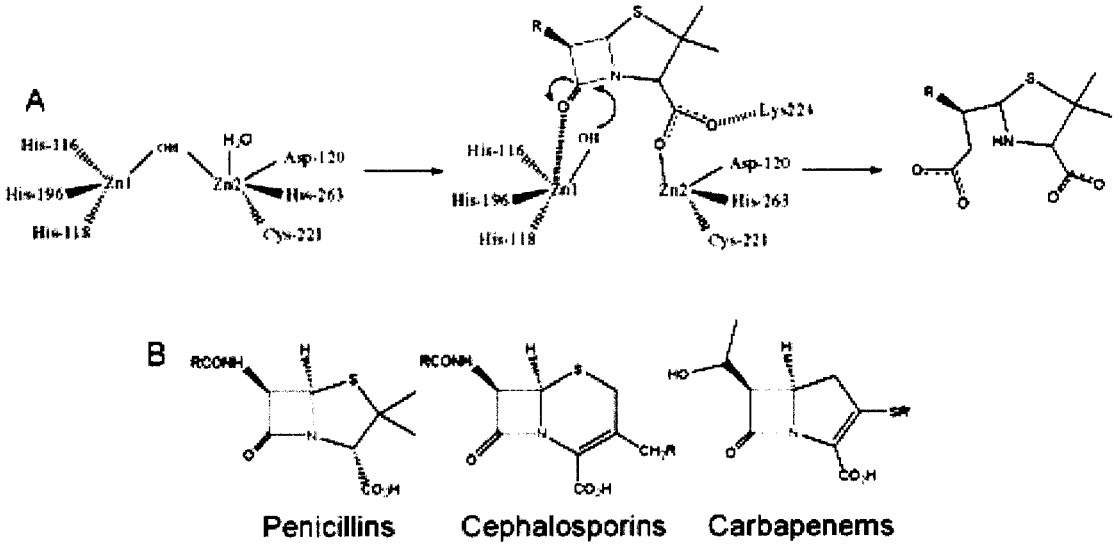

Scheme 2.4. Hydrolysis of β-lactam ring (red) in a penicillin derivative by a dinuclear zinc site (subclasses B1 and B3).

In general the physiologically relevant metal content has not been clearly established, and some radical possibilities have been suggested such as to consider mβLs as apoenzymes *in vivo* that only bind zinc in the presence of substrate. The synergy in zinc binding was recently demonstrated for L1 mβL in *S. maltophilia*, where binding of the Zn1 helps in reorganizing the ligands in the second site Zn2 for binding.[109] Additional experimental/computational evidence towards the zinc ion being distributed between the two active sites has also been presented.[110] The two halves of the core β-sandwich are generally joined by a two-turn α-helix α3, which is extended in subclass B2, followed by an open coil structure. A flexible motif in the metalloprotein (i.e. a loop or an extended helix) is present to close over the active site groove when inhibitors or substrates are bound, thereby promoting the hydrolysis reaction. A network of H-bond and ionic interaction has been observed mainly in the active site of sub-class B1, and a disruption of this structural network has been implicated for reduction of zinc affinity in the Zn2 site.[111]

In terms of the mechanism employed by these enzymes it is accepted that the zinc ions are primarily responsible for substrate binding and catalysis, leaving to the surrounding ligands (with a few exceptions) the role of mainly maintaining the zinc ions in position. For mβLs sub-classes B1 and B3 with two zinc ions in the active site it is generally accepted that Zn2 and K224 (according to the standard numbering scheme for mβLs[113]) help to stabilize the substrate by interaction with the carboxylate moiety in the ring adjacent to the β-lactam, while Zn1 coordinates the carbonyl in the β-lactam ring and assists in the nucleophilic attack by the hydroxide ligand. For sub-class B2 with only one zinc, it has been proposed that the

residue D120 acts as a general base that activates a water nucleophile for its attack to the β-lactam ring. Further steps in the cycle involve proton transfer and intramolecular arrangements to regenerate the active site.[111]

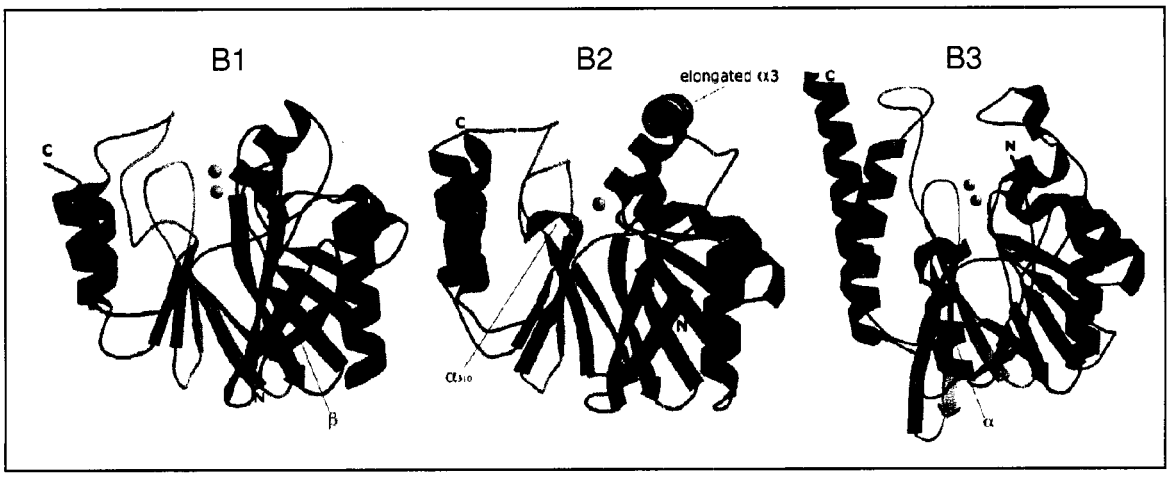

Figure 2.7. Structural comparison among the three subclasses of metallo-β-lactamases from[112] different features within each sub-class are highlighted.

2.3.d.2. Clinical Relevance.

β-lactam antibiotics are the main front line against opportunistic Gram-negative bacterial pathogens that can affect severely the life expectancy in patients with compromised immune system, i.e. HIV, chemotherapy, and advanced age For this reason, and the important public health problem associated with resistant bacteria, β-lactamases are an important target for chemotherapy.[114] mβLs in particular, despite representing a small group of β-lactamases, display a very broad substrate spectrum hydrolyzing almost all β-lactam antibiotics and especially carbapenem-derivatives, which are the newest and most powerful generation of β-lactams. In addition, there are no clinically useful inhibitors for mβLs, in contrast to serine-β-lactamases where inhibitors such as clavulanic acid or sulbactum can be used effectively.

The production of mβLs by major pathogens in the near future is also a very likely event due to the current abuse of antibiotics in clinical and agricultural purposes.[115] Worldwide surveillance programs such as the SENTRY, MYSTIC have confirmed an escalated rate of occurrence of mβL-mediated resistance for different gram-negative bacilli like the *P. aeruginosa* since 2000.[116] mβLs can be either chromosomally mediated or encoded by transferable genes, the most recognized among the latter are IMP-1, VIM-1, SPM-1 and GIM-1, and especially the first two types are the most frequent. The fact that genes encoding for these four mβLs can be associated with integrons and other genetic elements such as transposons or plasmids means a higher probability for worldwide dissemination.[117]

2.3.d.3. metallo-β-Lactamases inhibitors (mβLIs).

A variety of chemical classess have been tested as mβLIs (B1 – B3), among them trifluoromethyl alcohols and ketones, biphenyl tetrazoles, succinic acids, peptides, cephamycins and several thiol compounds. The most potent known inhibitors so far are 2, 3-disubstituted succinic acids and mercapto-carboxylic acids, with inhibition constants in the 3 - 90 nM range (Fig. 2.8.). One of the key steps in the mechanism of action for mβLIs is the displacement of the bridging hydroxyl ligand or water by an appropriate sulphur or oxygen atom in the thiol or carboxylate moiety respectively. Formation of disulfides with the C ligand in Zn2 has been also observed leading to irreversible inhibition. The approach to design of an ideal mβLI however is by no means straightforward, since the wide distribution of dinuclear active sites in enzymes (i.e. human glioxalase II) could lead to the issue of a high toxicity due to inhibition of essential enzymes in the host. Also it has been shown that

the affinity of any given mβLI can vary vastly among mβLs due to important differences in sequence diversity - the mutation of the highly conserved K224 to a Y224 in the important VIM-2 is a clear example of this affirmation. However, the role of two key aminoacids has been highlighted in terms of design of more specific mβLIs, namely K224 and D120. The former residue and specifically the N_ε has been implicated by mutagenic and structural data as contributing to binding and orientation of substrates by hydrogen bonding to the carboxylate group usually present adjacent to the β-lactam ring (scheme 2.4B). A novel class of inhibitors takes into account interactions with this residue in order to target the active site in IMP-1, a B1 mβL.[118]

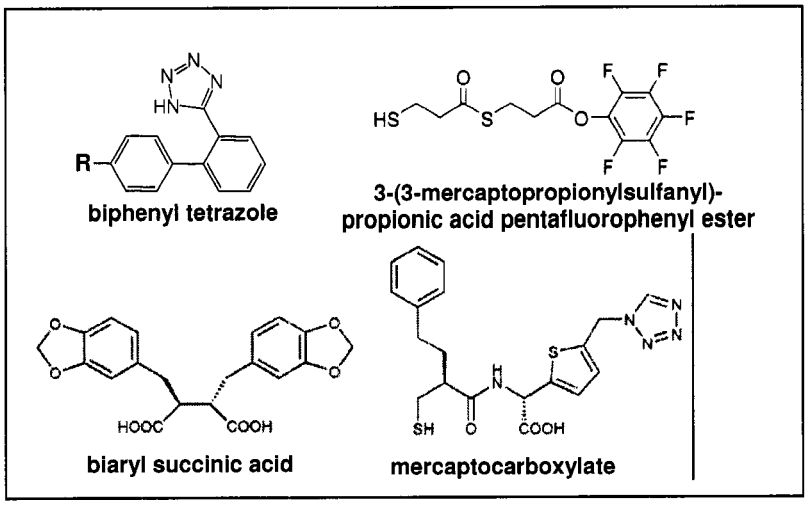

Figure 2.8. Structures of representatives metallo-β-lactamases inhibitors MBLIs

Another potentially relevant residue in the active site is Trp64 present in the flexible loop of mβLs that could be involved in hydrophobic/non-covalent interactions with the substrate. Additional residues in the active site, besides the already mentioned here, could play a determinant role as recognition motifs and modulators of mβLIs efficacy. Therefore its

consideration should be taken into account in the design of novel inhibitors. [119] Up to now none of the mβLIs reported have been developed into drugs. In this regard structure-based pharmacophore design has been also employed in order to identify new leading compounds.[120]

Additional mechanisms of resistance further decrease the possibilities for mβLIs to reach the target in different gram-negative bacteria, such as outer membrane protein mutations modifying or decreasing the porin channels and thus minimizing the permeability in the membrane or by the expression of active efflux pumps decreasing the half-time of the antibiotic within the bacteria.

2.3.e. Cu,Zn-Superoxide Dismutase (SOD-1).

2.3.e.1. Structure and Function.

The SOD-1 protein found in the cytosol is a homodimeric protein with 32kDa molecular mass. Two other forms SOD-2 (Mn) and SOD-3 (Cu,Zn) are found in the mitochondria and outside the cell respectively forming tetramers. Basically each sub-unit in SOD-1 containing 158 aminoacids folding as a flattened eight-stranded β-barrel containing one catalytic copper and one structural zinc ion in the active site. The residues coordinating the metal ions are strictly conserved: H44, H46 and H118 for copper and H69, H78 and D81 for zinc. Residue H61 acts as a bridging ligand between the two metal centers that are approximately 6 Å apart, completing the tetrahedral coordination sphere for zinc and the square pyramidal coordination sphere for copper together with a solvent molecule that is not involved in the catalytic cycle (fig. 2.9.). An additional stabilization of the dinuclear site is made by the

residue D122, in the second coordination sphere, which connects *via* hydrogen bond residues H44 and H69. The metal ions together with an important intramolecular disulfide bridge (C57-C146) are post-translational modifications that greatly stabilize the metalloprotein. Indeed the stability of wild type SOD-1 is remarkable, being active even after harsh conditions such as 4% SDS, 10M urea or 80°C. Several studies have highlighted the importance of the disulfide presence for dimer stability and further relevance in pathogenic aggregation.[121] SOD-1 presents a funnel-like cavity or cone with a 24 Å diameter at the surface of the metalloprotein ending in a narrow 4 Å channel that leads to the active copper ion partly exposed to the solvent.

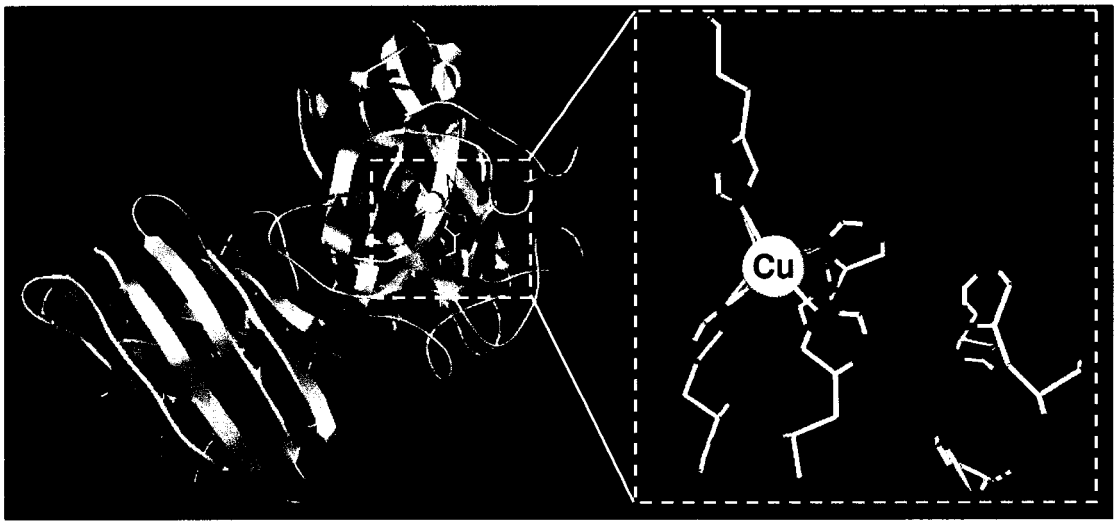

Figure 2.9. Ribbon structure of Cu,Zn-SOD homodimer, showing the metal ions Cu^{2+} in yellow and Zn^{2+} in green (left). Zoom of the active site showing the coordinating residues (right).

There is a net positive electrostatic potential close to the active site involving residues K120, D130, E131 and K134, that helps in binding and guidance of the substrate to the copper site. SOD-1 functions as an antioxidant metalloprotein catalyzing the dismutation or

disproportionation of the superoxide anion ($O_2^{\bullet-}$) into hydrogen peroxide and oxygen (scheme 2.5.), the overall reaction is done in two steps both first-order with respect to $O_2^{\bullet-}$. This reaction is extremely efficient, basically limited by substrate diffusion thus enabling SOD-1 to shorten the lifetime of the superoxide radical by a factor of $\approx 10^{10}$.

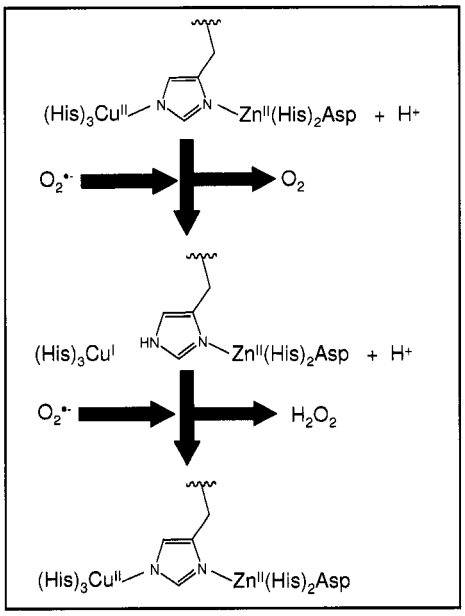

Scheme 2.5. Dismutation of two molecules of superoxide anion ($O_2^{\bullet-}$) by the Cu,Zn-SOD. The scheme shows successive breaking and formation of the inter-metallic bridge formed by H61, upon changes in copper oxidation state (Cu^{II} – Cu^{I}).

The zinc ion is indirectly involved in the accepted catalytic mechanism with an important role for electronic polarization and electrostatic stabilization due to the H61 coordination. The two steps in SOD-1's catalytic cycle correspond to a first half-reaction where copper is reduced (Cu^{II}-Cu^{I}, inner sphere mechanism) upon binding of a first superoxide anion, this is coupled to protonation of H61 and concomitant rupture of the Cu/Zn bridge. The resulting cuprous ion with a trigonal planar coordination releases dioxygen as the first product, diffusing out of the electrostatic cone thanks to its neutral charge. Initial protonation of the first superoxide molecule by a donor in the cone has been proposed. In the second half-

reaction, a subsequent superoxide anion enters the cone and oxidizes the Cu^{I} by an outer-sphere mechanism to its initial state, protonation of the substrate to form and release of hydrogen peroxide reestablishing the bridge from H61.A high relevance of D122 for stabilization of the reduced state has been shown through theoretical calculations at the DFT level.[122]

2.3.e.2. Clinical Relevance.

Interest in the medical relevance of SOD-1 derives from the presence of mutants associated with Amyotrophic Lateral Sclerosis (ALS) or Lou Gehrig's disease, which is a neurodegenerative disorder characterized by the selective death of motor neurons in the spinal cord, brain stem and brain. This disease is one of the most common neurodegenerative disorders, with a prevalence of 4 - 6 per 100,000 and affecting more than 35,000 people only in USA. This disease is frequently diagnosed between the ages of 40 and 70, being 20% more common in men than women. Specifically, point mutations in SOD-1 have been linked to a sub-set of the familial form of ALS or fALS, which constitutes approximately 1/5 of the cases. The concentration of wild-type SOD1 (wtSOD-1) does not influence either the aggregation nor the motor neuron toxicity of the mutant forms, as demonstrated using specific antibodies for the mutant forms in spinal cords (Fig. 2.10.). 120 point mutations in SOD-1 (almost 1/3 of protein sequence!) have been identified so far. They are evenly distributed throughout the tri-dimensional structure of the metalloprotein and have been classified mainly in two groups based on their position and metal content (see http://www.alsod.org).[123] The first group is called wild-type-like mutants with an almost intact metal content compared to the wtSOD-1. The second group exhibits mutations in the

metal-binding region involving coordinating residues or close neighbors in the vicinity generating mutants with zinc/copper deficiency. Since some mutant forms of SOD-1 retain the dismutase activity of the wild type, the toxicity arising from mutations is rather ascribed to a gain in function.

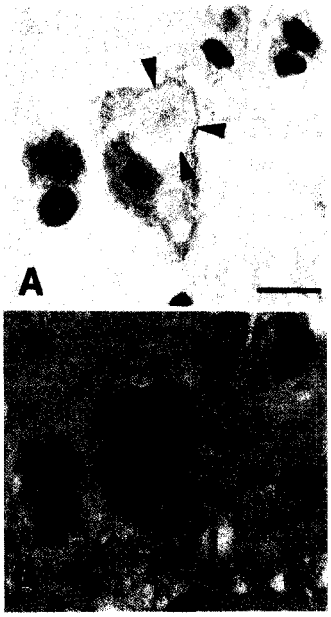

Figure 2.10. Microphotographs showing H&E staining of the ventral portion from an end-stage mouse with mutant SOD1 (A). The presence of mutant SOD-1 aggregates (arrows) is revealed through an immunoreactive essay even in the absence of endogeneous wt-SOD1 (B).[128]

Several hypotheses have been suggested in this regard but so far two main views are predominant in theliterature, although these are not necessarily mutually exclusive. One of the hypotheses states that mutant SOD-1 toxicity is due to an enhanced oxidative activity which contributes to oxidative damage, supported by evidence of the high level of oxidative-stress in presence of SOD-1 mutants and stimulation of oxidative damage in the presence of physiological bicarbonate.[124, 125] In addition although an increased peroxidase and thiol oxidase activity has been found for Zinc-deficient SOD-1,[126] and a certain correlation between wild-type-like mutants and this hypothesis has been found;[127] the majority of SOD-1

mutants do not exhibit such an enhanced activity compared to the wild type further complicating support for this hypothesis.

A second hypothesis has gained overwhelming support and involves basically the misfolding and aggregation of mutant SOD-1, a common point also for other neurodegenerative diseases such as Alzheimer's and transmissible spongiform encephalopathies. A multistep process has been suggested for the mechanism of aggregation, involving sequential dimer dissociation, metal loss from the monomer and oligomerization of the apo-monomers.[129] This contrasts with the sequence of post-translational modifications involved for activation of the metalloprotein i.e. copper and zinc binding, disulfide formation and dimerization. Several techniques have been employed to support these findings. Recently the equilibrium between the native dimer, monomer intermediate and the unfolded monomer was observed and studied for various mutants, with favorable conditions for the last two monomer states.[130, 131] Different conformations in living cells have been also observed for SOD-1 mutants compared to wild type metalloprotein, thanks to a fluorescent assay using green fluorescent protein.[132] Determination of melting temperature in fALS relevant SOD-1 mutants by differential scanning calorimetry has been extensively used to compare relative stabilities in the apo-protein and various reports evidenced a net destabilization for the mutants compared to the wtSOD-1.[133] However another recent study using a bigger universe of mutants (20) found that some of them can actually exhibit higher stability compared to the wtSOD-1 compromising to some extent the general agreement, the results were confirmed by hydrogen-deuterium exchange.[134] Clarification of this point is

important since the nascent SOD-1 apo-monomer is regarded as the main fALS relevant toxic specie.

As mentioned before the metal ions are important for kinetic stability in SOD-1, and in this regard it has been determined that copper contribution is greater than Zn.[135] The other important stabilizing key feature is the sulfide bridge, where it has been shown that mutants are more susceptible to reduction on this sulfide bridge and recent *in-vivo* experiments points to an incorrect disulfide cross-linking in the mutant SOD-1 as a cause for aggregation. Aberrant intra- to inter-molecular reactivity from these immature of disulfide-reduced forms in mutants can lead to insoluble high molecular mass species containing even wild type SOD-1.[136] Overall evidence points to stability issues generated in the SOD-1 homodimer by the mutants, and this is a biologically relevant point in the mechanism. In this regard molecular dynamics has contributed with significant findings, first by identifying disruptions in the inter-monomer dynamics in all mutants tested. Moreover, the wtSOD-1 dimer was shown to be a complex network exhibiting two main motions that are disrupted for mutants, where it was observed that the high connectivity region in the dimer interface and metal-binding loops was altered significantly.[137] Second, sequence fragments in SOD-1 mutant have been identified by molecular mechanics as prone to aggregation and/or intermolecular interactions, namely the β-strands 4 and 7 and the crossover loops I (linking β-strands 3 and 4) and II (linking β-strands 6 and 7).[138] An additional study involving kinetic measurements of folding behaviour suggest that misfolding issues in the SOD-1 apo-monomer could arise from β-strands 1 – 3.[139]

The aggregation hypothesis is thus the most actively studied regarding mutant SOD-1 toxicity, although it is worth mentioning however alternative hypotheses such as an aberrant copper chemistry describing mutations that can lead to catalytic nitration of tyrosine residues close to the copper ion.[140] So far only scarce evidence both against and in favor of this affirmation has been presented, and clearly new evidence is necessary to support it as an alternative mechanism of toxicity.

2.3.e.3. SOD inhibitors.

In spite of the important biological function of SOD-1 in depleting the reactive superoxide anion, a selective targeting of this metalloprotein could be important for anticancer applications. Due to the exacerbated metabolism in cancer cells the production of reactive oxygen species in general is increased and thus they could exhibit a higher dependence on SOD activity. It has therefore been suggested that inhibition of this metalloprotein could have potential therapeutic interest as an antitumor strategy.[141] On the other hand a recent report describes the screening of small molecules that can enhance SOD-1 dimer stability as an alternative to fight SOD-1 aggregation and amyeloid formation in ALS.[142] In general, results obtained for animal models of SOD1-linked fALS have helped in the development of novel chemotherapeutic approaches for ALS.[143] Current treatment for ALS includes 2-amino-6-(trifluromethoxy)benzothiazole or rilutek(riluzole) which has an inhibitory effect on glutamate release and ability to interfere with intracellular events that follow transmitter binding at excitatory amino acid receptors. This drug prolongs survival by only three months and improvement on quality of life or muscle strength is not clear. Additionally valproic acid, which has been mentioned earlier as an HDACI, has also been implicated in ALS

suppression in mice models.[144] SOD-1 inhibitors such as diethyldithiocarbamates could have potential as antiparasitic agents specifically Chaga's disease.[145]

2.4. Structural Zinc as Target.

2.4.a. Zinc Fingers (ZFs)

2.4.a.1. Structure and function.

The zinc finger (ZF) motif, first discovered in the transcription factor TFIIIA from the clawed toad *Xenopus laevis* some 20 years ago,[146, 147] is a very interesting protein domain due to the notably diverse array of structure and functions exhibited, the latter involving important cellular processes such as transcription, DNA repair, cellular signaling, metabolism and apoptosis. Typically the term ZF involves a definite number of aminoacid residues within the protein, usually 30 to 40, with suitable metal binding sites composed of cysteines (C) and histidines (H). A key component of this system is the zinc ion (Zn^{2+}) which binds to the residues in a tetrahedral environment providing essential elements of structure. Zinc finger motifs are highly conserved and thus either release or substitution of the central zinc ion, as well as, mutation of coordinating residues can result in a loss or impairment of the biological function. In ZFs the Zn^{2+} ion is thermodynamically preferred to other metal ions such as Co^{2+}, Ni^{2+} or Fe^{2+}, attributed to contributions from ligand field stabilization energy and other entropic factors.[148] However the affinity of ZFs for Cd^{2+} appears to depend on the number of coordinating cysteines such that the latter is preferred over Zn^{2+} for ZFs with four cysteine metal-binding residues.[149] Formation and dissociation of ZFs has been postulated to be a multistep process, and the presence of an equilibrium between a tri- and

tetra-coordinate zinc could exist.[150,151] This fact is in agreement with the reported non-equal contribution from the coordinating residues to the formation of ZFs.[152]

Typically ZFs can be classified according to the type of residues coordinated by the metal ion, i.e. C_2H_2, C_3H or C_4 (Figure 2.11.), although this classification might be extended to include more complex domains that need more than one zinc ion for structure stabilization. Double ZFs like the estrogen receptor (C_8) require eight binding residues which predominantly are cysteines, and the mode of Zn coordination can vary between a simple one, with the first four residues coordinating Zn1 and the second four Zn2, to an intertwined or an interleafed coordination, and in addition bridging cysteines can be found for C_6-ZFs[6, 153]. Within this review we will use the term zinc finger for functional and independent zinc sites with at least two cysteines as binding residues, but it is useful to keep in mind that the versatility of zinc-protein complexes for modulation of biological functions depends largely on the type of secondary structure or fold formed by the ZFs. More than 10 different topologies for the ZF motif have been reported, although in general it features a C_2H_2 - like, treble clef or zinc ribbon structure. [154]

Naturally occurring C_2H_2-ZFs are the most frequently used class of transcription factor, accounting for about 3% of genes in the human genome.[155] Their structural framework comprises a $\beta\beta\alpha$ fold where the cysteine residues are within the β-turn and the histidines in the α-helix, additional interactions from hydrophobic residues further stabilize this structure. C_2H_2-ZFs have been methodically designed and used in an array of ZF modules (n x C_2H_2) to further increase the sequence-specific recognition of DNA.[156-159]

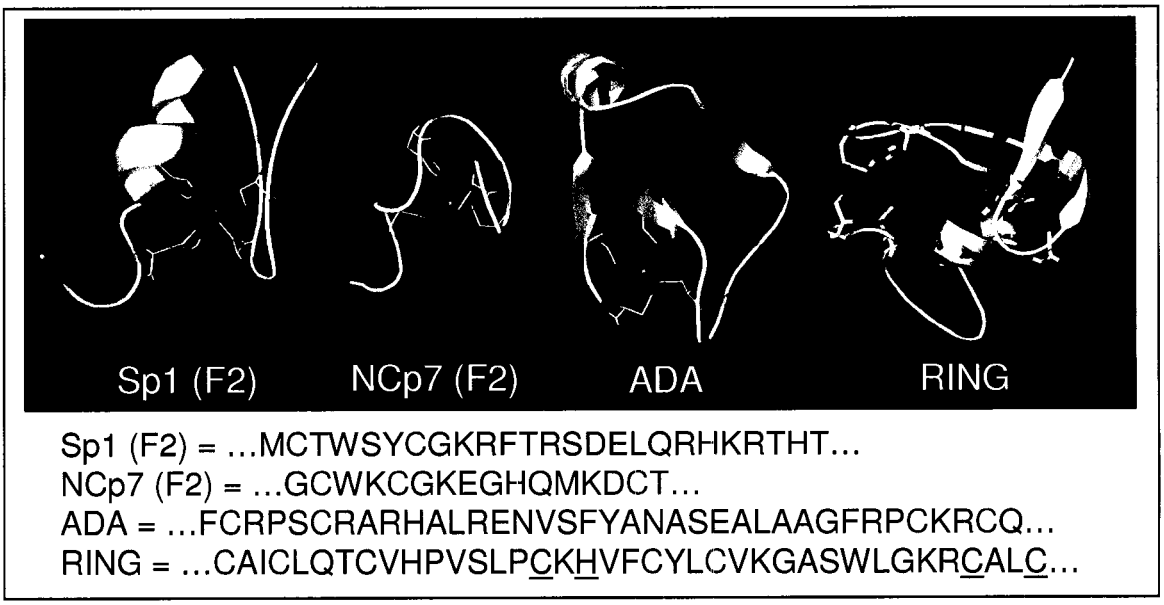

Figure 2.11. 3D structures of different ZFs showing coordinating residues. PDB ID: 1ESK (Sp1), 1VA2 (NCp7), 1ADN (ADA), an intertwined dinuclear domain is also shown PDB ID: 2D8T (RING). Sequences for the domains shown are at the bottom with coordinated residues in red (coordinating residues for the second zinc in RING are underlined).

\Generally studies have focused on the direct DNA recognition α-helix but recent results attribute a significant role also to the β-hairpin region which may suggest new directions for ZF design in terms of recognition and specificity.[160] The classical role of C_2H_2-ZFs as transcription factors has focused attention towards the mode for DNA recognition, which classically involves mainly hydrogen bond interactions between side chains of α-helical residues (frequently at positions -1, +2, +3 and +6) and base pairs in the DNA major groove (preferences for arginine/guanosine; aspartic acid/adenosine, cytidine; leucine/thymidine). Every ZF recognizes 3 or 4 consecutive base pairs and some of the ZF units in a larger array can be used as spacers. This is true for Sp1 and Zif268 (both 3 x C_2H_2) but a slightly different DNA recognition pattern can be found for other C_2H_2-ZFs, i.e. GLI (5 x C_2H_2).

The interaction of C_2H_2-ZFs with RNA on the other hand, has gained increased interest thanks to crystal structures of TFIIIA in complex with a core 5S rRNA, where two different modes of interaction are observed depending on the substrate DNA/RNA. It was found that fingers used as spacers for DNA interaction, ZF4 and ZF6, are strongly involved in the interaction with RNA. The former by interactions of a histidine residue with two guanines (H119-G75, G99) in the internal loop region E, and the latter by stacking of a tryptophan residue into an adenine (W177-A11) in loop A. ZF5 only interacts with backbone atoms in helix V. [161, 162] This latter type of interaction involving stacking of aromatic residues in the zinc finger, mostly tryptophan, with nucleobases has been reported for the HIV Nucleocapsid 7 protein (NCp7).[163] In the particular case of an C_3H-ZF, exposed guanine bases bind to hydrophobic clefts in both ZFs of the protein, and additionally the ZFs form hydrogen bonds to groups in the RNA that normally engage in Watson-Crick hydrogen bonding in A helices.[164] C_4-ZFs are another motif for DNA recognition as exemplified in the typical DNA binding domain (DBD) for nuclear receptors like the human estrogen related receptors (hERR1-hERR3) or the glucocorticoid receptor, both involving two sets of C_4-ZFs in tandem (2 x C_4). The basic recognition of a canonical 6 base pair sequence in the hormone response element (HRE) by the DBD is considered essential, although additional interactions have been shown to be needed for high-affinity interactions.[165] In contrast to C_2H_2-ZFs which bind DNA as monomers, C_4-ZFs bind as homodimers or heterodimers, in the former case they exhibit twofold rotational symmetry.

ZFs can also act as protein recognitions motifs as exemplified by the LIM domain consisting of a double ZF motif (1 x C_3H -1 x C_4), [166] and similar RING (i.e. mouse double minute 2,

MDM2, Fig. 2.11) and PHD domains.[167] Of particular interest is the GATA-1/Friend of GATA (FOG) interaction, where the structure of the N-terminal C_4-ZF in the former protein with one of the C_3H-ZFs in the latter has been characterized. The two protein domains interact *via* both polar and hydrophobic interactions, mainly through the first and second β-hairpin in GATA-1 to the α-helix in FOG.[168]

2.4.a.2 Clinical Relevance. One of the interesting features regarding ZFs is the high specificity and affinity in substrate binding that they can achieve, and for this reason they have been proposed as key building blocks in the design of proteins towards human gene therapy.[169, 170] One of the potential applications is to use ZFs in combination with endonuclease proteins to selectively produce DNA double strand breaks, because the presence of these lesions is reported to increase the frequency for homology recombination events thus favoring gene targeting to a specific mutation. This is a very promising area of research with recent examples of viability in targeting specific genes. In addition several libraries of ZFs have been developed to discriminate DNA sequences, and are available for the design of novel polydactyl ZFs.[171 - 174]

Alternatively the sequence specificity of ZFs can also be coupled to a transcription activation or repression domain to regulate gene expression.[175] An example is the use of a designed zinc finger to inhibit gene expression in the virus of herpes simplex 1 using a six-finger peptide to partially repress the replication cycle in the virus.[176] This strategy has also been applied to inhibit transcription and replication of HIV-1.[177] Moreover the use of designed ZFs to regulate endogenous genes promotes expression of the natural splice variants of that

gene, in contrast to standard gene therapy where only a single variant of the gene is expressed. This point has been illustrated recently for the human endothelial growth factor (VEGF), where an engineered 3 x C_2H_2 ZF-protein was used to induce angiogenesis in advanced-age mice.[178] Monogenic diseases like sickle-cell anemia, haemophilia, Gaucher's disease could benefit greatly from this approach.

C_2H_2-ZFs belonging to the Sp (specificity protein) and KLF (Krüppel-like factors)[179, 180] are recognized as targets for development of new anticancer drugs. Their involvement in tumorigenesis stems from a variety of reasons including its interaction with oncogenes and tumor suppressors. Sp1 alone is thought to regulate several hundreds of genes and is the most characterized transcriptional activator in mammalian cells. The importance of this family of transcription factors in gene regulation for tumor development, growth and metastasis has been reviewed.[181] In addition, elevated expression of Sp5, have been detected for human cancers.[182] Deviations from normal behavior in cancer cells can also induce a down regulation of certain zinc fingers as in the case of ZFp-42, a transcription factor encoded by the Rex-1 gene which has been found significantly decreased in renal cell carcinoma specimens compared to normal cells.[183] More striking is the reported down-regulation of the protein TRPS1 expression by androgens in human prostate cancer, this protein is on the contrary highly expressed in breast cancer. TRPS1 is a multiple ZF protein consisting of nine C_2H_2-ZF units and one GATA C_4-ZF.[184] Aberrant activation of yet another C_2H_2 transcription factor, the GLI-ZF, is proposed to be involved in the growth and maintenance of a wide range of cancers, including prostate and basal cell carcinoma.[185]

The LIM superfamily of transcription factors briefly mentioned before features a double ZF motif involved mostly in protein/protein interactions, related to cellular architecture, intracellular signaling and transcriptional processes. [186] Their involvement in multiple human diseases has been addressed. [187] Another important superfamily exhibiting double ZF motifs (2 x C_4) in their DNA binding domain is the nuclear receptor. Its protein members are activated as transcription factor after binding of small lipophilic molecules such as lipids, metabolites or steroid hormones. Specifically, the steroid hormone glucocorticoid produces glucocorticoid receptor (GCR) proteins, whose clinical importance stems from the anti-inflammatory/immunosupresive effects exhibited by glucocorticoid hormones. The relevance of GCR on both of its isoforms (α, β) as the sole mediator of glucocorticoid's actions has been reviewed for inflammatory conditions.[188] Also the involvement of coregulators in the mediation of GCR action is yet another layer of complexity that has to be taken into account for an adequate understanding of biological function modulation by glucocorticoids, and this aspect with respect to brain function has been reviewed recently.[189]

2.4.a.3. Zinc Fingers Inhibitors (ZFIs). In contrast to catalytic zinc, where inhibition is usually through blocking of an active site, inhibition of structural zinc must involve chemical modification of the coordinating residues (oxidation/alkylation) with metal ion removal. Inhibition of ZFs, as in the case of MMPs and HDACs, is a double-edge sword since although beneficial responses can be achieved, the potential risk of impairing or disturbing essential cellular functions is also high. In fact the damage of zinc fingers in DNA repair proteins such as the xeroderma pigmentosum group A (XPA), one of the proteins involved in

the nucleotide excision repair pathway, by oxidizing agents or redox-active metals has been regarded as a novel mechanism of carcinogenesis.[190] In this regard it has been shown that human DNA polymerase-α is inhibited by cis-diamminedichloroplatinum (II), by covalent interaction with the cysteine residues on its C_4-ZF motif.[191] Other important zinc metalloproteins involved in DNA/RNA repair could be potentially inhibited, as in the case of the bacterial sacrificial protein Ada whose C_4-ZF motif located in the N-terminal domain repairs the methyl phosphotriester lesion in DNA. In this mechanism an alkyl group is transferred from the damaged DNA to an activated cysteine (C38) residue in the ZF.[192, 193] In addition, the interaction from the DNA/ZF interaction in Sp1 and TFIIA has been reported to be disrupted by selenite ion.

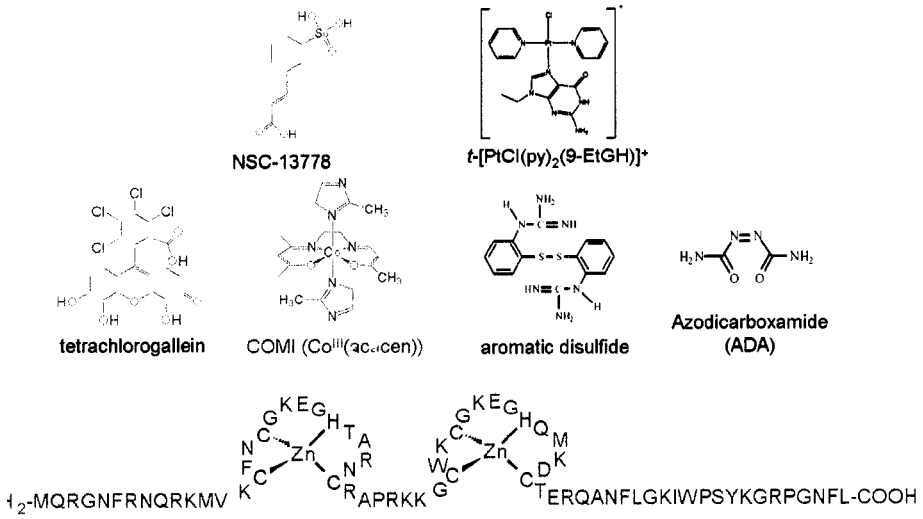

Figure 2.12. Structure of representative organic and metal compounds used to target the Nucleocapsid protein (NCp7, top). Sequence of NCp7 showing coordinating residues in red (bottom).

However, there are cases in which structural differences between the target substrate to be inhibited and alternatives substrates can be exploited, as in the case of key ZFs within retroviruses and arenoviruses[194] , in addition the possibility to extend this strategy to other viruses is feasible given the importance of zinc domains for virus stability.[195] The nucleocapsid protein NCp7 (HIV-1) in particular, has been the subject of an in-depth study in the last years including characterization and substrate interaction.[196]

This small protein with two C_3H-ZFs, plays many essential roles along the viral life cycle (such as RNA packaging, reverse transcription and integration). Iin addition it is remarkably mutation intolerant, therefore making it an attractive target for the development of novel and complementary HIV chemotherapeutic agents. Several molecules with electrophilic functional groups have been employed to oxidize or methylate cysteine residues within the ZFs causing inhibition of normal NCp7 functions. Specifically thiosulfonate and azodicarboxamide (ADA, Phase I trials) have been shown to promote zinc ejection from NCp7 at concentrations that do not impact other important human ZFs such as Sp1, PARP or GATA-1; this fact shows that key differences in terms of ZF reactivity could lead to an appropriate discrimination of inhibition targets (i.e. C_3H in NCp7 vs. C_2H_2 or C_4 which are more common in human ZFs).[197] Additional non-covalent motifs can also be exploited for an additional increased selectivity towards NCp7; recently platinum-nucleobase complexes explored this area by the use of nucleobase recognition from the C-terminal ZF, reporting zinc displacement and loss of tertiary structure (Fig. 2.12).[198]

2.4.b. p53.

2.4.b.1. Structure and Function. The tumor suppressor gene *Tp53* codes for the p53 protein with a molecular mass of 53kDa (hence its name), corresponding to 393 aminoacids in four domains: a N-terminal transactivation domain, a central DNA-binding core domain, an oligomerization domain and a C-terminal regulatory domain as follows:

2.4.b.1.1.) The N-terminal domain (residues 1-93) can be further differentiated into a transactivation domain (residues 1 - 60) and a proline-rich regulatory domain (residues 64 - 92); this domain is natively unfolded but exhibits the formation of a helix in the region 15 - 30 upon binding to MDM2. Recruitment of transcriptional machinery like the TATA box and TFIID occurs in the N-terminal domain, in addition the key interaction with the C-terminus of the histone acetyltransferase CREB binding protein (CBP) allows acetylation of the terminal lysine residues and provides p53 with additional stabilization towards ubiquitin, further stimulating its DNA-binding activity. Binding of p53 to the replication protein A (RPA) and the MDM2 protein also occurs predominantly on this domain, the former case results in transcription inhibition, p53 export to the cytoplasm and eventual degradation of the p53. In the latter case inhibition of RPA binding to DNA occurs, being RPA one of the key proteins involved in the nuclear excision repair pathway. Interestingly p53, RPA and MDM2 are all zinc metalloproteins and this is a brief example of their biological relevance in cell processes. The involvement of critical residues tryptophan, methionine and phenylalanine as a motif for p53's protein-protein interaction, especially for the N-terminal domain has been discussed in detail recently.[199]

2.4.b.1.2.) The central DNA-binding core domain (DBD) with a molecular mass of 25 kDa comprises residues 94 - 312, this domain is natively folded into a β-sandwich, composed of two antiparallel β-sheets with a small β-hairpin closing the access to the hydrophobic core. A total of three helices can be distinguished on this domain; the first (166 -168) corresponds to a small 3_{10} helix, the second (177 - 181) to the C_3H-ZF motif, and the third corresponding to the C-terminal helix (278 - 291). The zinc ion coordinates the residues C176, C238, C242 and H179 in a pseudo-tetrahedral coordination geometry (fig. 2.13.), that connects loops L2 and L3 in the domain. The zinc ion has proven to be required for structural reasons, since the apo-protein exhibits a DBD significantly different with reduced DNA-binding specificity and prone for aggregation.

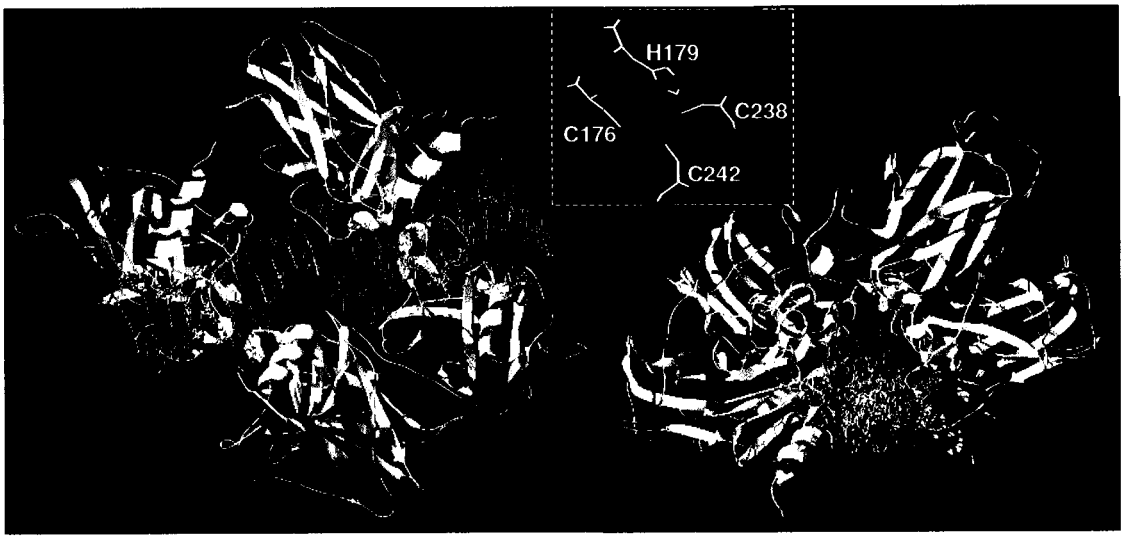

Figure 2.13. Two different views of a p53 tetramer (white ribbon) with DNA (yellow), the structure was determined using the DNA-binding site only. Zinc ions are represented in green. First coordination sphere in p53-zinc site is shown inside square. PDB ID: 2AC0, 2FEJ

The role of zinc in p53 function extends beyond this domain and has been shown to coordinate the movements of different structural elements in the protein required for DNA binding.[200]

The stability of the DBD is relatively low with a melting temperature of about 43 °C (aggregation occurs at 37 °C). NMR studies have revealed a very mobile structure compared to reported crystal structures and more importantly the presence of buried polar groups in the core of the structure like tyrosine and threonine on positions 236 and 253 respectively, that affects the domain's dynamics. The majority of mutations on p53 occurs on this domain and given its inherent instability it is understandable how these mutations can lead to a loss of p53 functions and subsequent cancer development. However specific mutations on the aforementioned buried polar groups, to key hydrophobic residues like phenylalanine and isoleucine can actually lead to a gain in stabilization (up to 3 kcal/mol) for the core, allowing for a better study and characterization.[201]

2.4.b.1.3.) The oligomerization domain comprises residues 324 – 355, being one of the smallest known protein oligomerization domains, and sometimes is considered as part of the C-terminal domain. It enables p53 to adopt its biologically active tetrameric form and is composed of an α/β secondary structures which upon dimerization forms an antiparallel β-sheet and a pair of antiparallel helices. The extensive hydrophobic surface formed by the antiparallel helices is the main driving force for the association of dimers in a reversible process leading to the tetramer. Binding to DNA breaks the initial dimer subunit interaction causing the rotation of one of the dimers by 70° to grip the DNA double helix.[202] *In vitro* studies have shown that tetramerization is post-translational while dimerization occurs

cotranslationally. Mutagenesis studies made on this domain have shown that due to structural symmetry present in wild type p53, point mutations can reduce the stability of the tetramer significantly, leading to tumorigenesis.

2.4.b.1.4.) The C-terminal domain (residues 367 -393) is as the N-terminal domain natively unfolded, and important proteins interact mainly with this domain including the breast cancer tumor suppressor protein (BRCA1), cyclin A and helicases such as the WRN and BLM involved in the Werner and Bloom syndrome respectively. Interaction of p53 with the matrix attachment region, which are DNA sequences responsible for anchor chromatin fiber to the nuclear matrix, occur to some extent in this p53 domain.

The p53 metalloprotein has a central role in one of the major signal transduction pathways in the cell which regulates its response to environmental and internal cues. At the same time this pathway is intimately linked to others and their inter-coordinaton has been proposed to be regulated by loops which involves proteins such as P38, COP1, PIRH2, AKT, etc. [203] In addition, p53 has been called guardian of the genome due not only to its role as a tumor suppressor but also as a regulator of more than a hundred sixty genes in response to various types of stress - in fact microarray experiments have suggested 500 up-regulated and 260 down-regulated p53 target genes!. In the presence of diverse stress signals that can be classified as genotoxic (DNA adducts or breaks), oncogenic (activation of proto-oncogens) or non-genotoxic (ribonucleotide depletion or oxygen oversupply), the p53 protein is activated mainly by post-translational modifications which include phosphorylation, acetylation, methylation and others.[204] These changes increase p53 concentration in the cell by several ways (p53 modifier/partner relationship) including MDM2 degradation.

Subsequently, the modified p53 can bind to specific DNA sequences, tetramerize and enhance the transcription rate of required genes (fig. 2.8.). The details of such p53/DNA interaction involving the tetramer were characterized recently for different DNA sequences, a correlation between differential binding affinities for the sequences studied and protein-DNA contact geometry was demonstrated.[205]

The type of genes activated by p53 will depend on the initial stress signal produced, cell type and context. As an example, upon DNA damage p53 will activate the transcription of XPC and DDB2 genes initiating the nucleotide excision repair mechanism.[206] The resulting cellular outcomes driven by p53 also vary accordingly to the stress signal, being cell cycle arrest the one exhibited upon genotoxic stress which allows the cell to repair damaged DNA For oncogenic stress or non-reparable DNA damage the usual outcome is apoptosis and for non-genotoxic stress p53 activation is mediated by a subspecies of the Jun-N-terminal kinase (JNK2), although this pathway has been poorly characterized.[207] Both transcription-dependent[208] and -independent activities are ascribed to p53 in apoptosis and precisely the second mode of action has been extensively studied recently. The body of evidence points out to p53 activating the mitochondrial pathway apparently by two different mechanisms (mitochondrial vs. cytosolic p53).[209] In this regard, the possibility of p53 functioning as an homologue of the Bcl2 related protein belonging to the group III (BH3) has been suggested by experimental data.[210]

2.4.b.2. Clinical Relevance. The evidence showing an involvement of p53 in human tumors is overwhelming. Mutations of the gene encoding for this metalloprotein are found in

approximately 50% of tumor cases, causing either a loss of activity or a gain in function producing p53 capable of cellular transformation.[211] In the latter case two types of pathways are differentiated, the first corresponding to aberrant interactions with DNA as shown for p53 mutants interacting with different DNA regions compared to wild type p53 (wt-p53). The other type of aberrant interaction observed for mutants is with diverse cellular proteins such as with p73, an homologue protein that does not interact with wt-p53 but its reactivity with mutated p53 have been shown otherwise, moreover this interaction correlating with resistance to anticancer agents.[212] In addition germline mutation or inheritance of only one functional copy of the *p53* gene results in the syndrome known as Li-Fraumeni which predisposes its bearer to cancer development. Mutations in p53 can be categorized on two different classes on the basis of *in vitro* essays and tri-dimensional structure of the protein: class I affect aminoacids directly involved in the protein-DNA interaction, they feature a wild type conformation and lack of binding to the chaperone hsp70. Class II on the other hand affects the aminoacids involved in stabilizing the tertiary structure in the protein; these mutants exhibit an altered conformation and an intense binding to hsp70. A great percentage of mutations are located in the DNA-binding domain, although evidence for an important number of mutations also in the oligomerization domain is currently being reported.[213]

The whole picture of p53 function is by no means straightforward since a multitude of variables tends to complicate the correlation between the p53 status, tumor phenotype and clinical study interpretation. These variables are listed as follows:

2.4.b.2.1.) Point mutations, more than 1,500 mutations have been reported for 15,000 tumors, this heterogenic factor and its implications for human cancer as been reviewed.[214]

The involvement of p53 mutations in human tumors in general and in specific cholangiocarcinoma,[215] breast cancer[216], skin cancer,[217] bone differentiation and development,[218] as well as, other diseases such as Alzheimer's, Parkinson's, stroke and traumatic injury[219], has been also reviewed.

2.4.b.2.2.) Two different p53 proteins can be expressed due to an intragenic polymorphism either with arginine ($p53_{arg}$) or proline ($p53_{pro}$) in codon 72, the distribution of these two variants in the general population has proven to vary in a rather broad range (16 - 63%). These polymorphs along with the one exhibiting the mutation P47S have been discussed recently.[220] It has been shown that patients exhibiting mutant $p53_{arg}$ exhibit a poor response to chemotherapy and have shorter survival; a higher resistance to cytotoxic agents was also confirmed in mutant $p53_{arg}$ polymorphs. In addition the wild type version of $p53_{arg}$ seems to exhibit a greater antiapoptotic activity compare to wt-$p53_{pro}$.

2.4.b.2.3.) Two highly homologous proteins p63 and p73 together with its isoforms as well, have been found to complete the p53 family of transcription factors. The function of these isoforms are different from p53 despite a substantial sequence and structure homology, p63 is a putative oncogene, and is required for the development and maintenance of stratified epithelium while p73 is implicated in neurogenesis, neuron survival and the inflammatory response. [221] In addition aberrant function for the $p53_{arg}$, $p53_{pro}$ polymorphs mentioned early can also interact and affect both p63 and p73 further complicating the understanding of p53 function.

2.4.b.2.4.) Multiple lower molecular mass isoforms can be generated when the p53 gene is transcribed; the existence of two promoters for the *p53* gene and three transcription initiation

sites produces isoforms species differing on its N and C termini.[222] The cellular functions of these isoforms differ in some aspects to the wt-p53 protein, being in some cases opposite and future studies could change dramatically the actual understanding of p53.[223]

2.4.b.2.5.) Several pathways. p53 is at the junction of several interrelated pathways in the cell. Due to the wide variety of stress signals that activates p53 and the interrelation between intermediates on these pathways, an understanding of the extent of p53 roles could require a more holistic approach, involving new strategies that minimize methodological issues.[224] Moreover an additional role has been suggested for p53 as suppressor of angiogenesis and cell migration, thus inhibiting the one of the late stages in tumorigenesis which involve the ability to migrate and invade different tissues.[225]

2.4.b.3. p53 inhibitors (p53Is) Taking into account the preceding section the potential for p53-based therapies in treating a wide range of malignancies is understandable. The development of p53Is is just one of the ways to interrupt p53 signaling but two other approaches have been also pursued to this same end and will also be mentioned, namely caspase inactivation to inhibit the MDM2/p53 complex and disruption of the MDM2/p53 interaction.

Pifithrin is the most representative of p53Is and acts at the post-transcriptional level; it was discovered in 1999 in a screening study for compounds that block the transcriptional activity of p53. This compound can rescue wt-p53 cells from apoptosis induced by irradiation and cytotoxic drugs, therefore has been widely used as a protector against secondary effects from chemotherapy and radiotherapy. However a careful balance between the treatment and the dose of pifithrin needs to be maintained to avoid mutagenesis. As an exception to the rule, it

has been reported an activating effect on the p53 pathway when Pifithrin is used together with doxorubicin.[226] Moreover pifithrin and derivatives (fig. 2.13.) have shown promising results as neuroprotective agent in both *in vitro* and *in vivo* stroke models. In addition since experimental evidence have suggested a link between p53-mediated pathways and neurodegenerative processes occurring in some pathological cases (notably HIV), the use of p53Is should be potentially relevant for HIV-associated dementia and related diseases sharing common events (i.e. increased oxidative stress or activation of apoptotic program), such as ischemia or Alzheimer's.[227] The design of improved P53Is based on pifithrin's moiety has been published recently, an additional *in vivo* cyclization from the precursors is suggested to increase the activity in this novel compounds.[228]

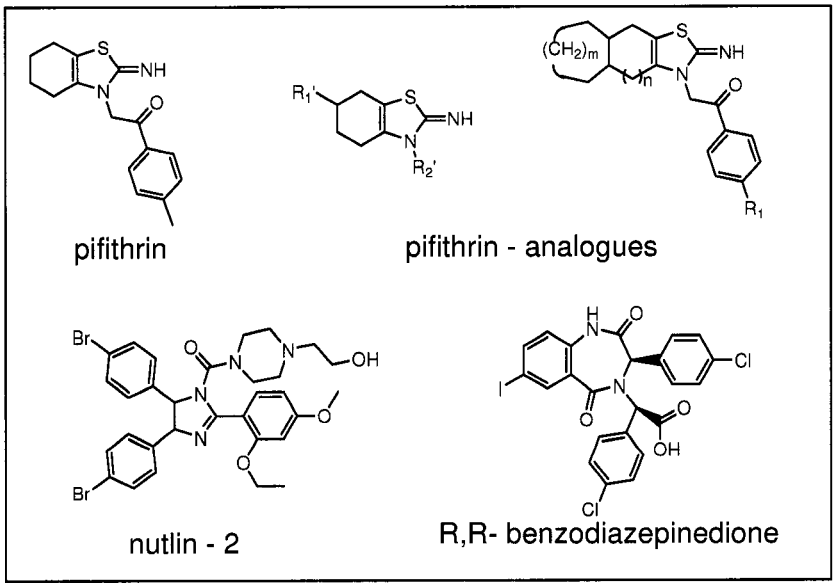

Figure 2.14. p53 inhibitors (top) and mdm2/p53 inhibitors (bottom).

To date no P53Is has been approved for use; so far the mechanism of action of pifithrin and derivatives remains largely unknown, although there is strong evidence suggesting that its antiapoptotic action is p53 dependent and does not affect the ubiquitin pathway. To this

regard the consideration of p53-independent therapeutic effects should also be taken into account for pifithrin and analogue compounds.

The second p53-based therapy involves the inhibition of caspases, which are a family of specialized proteases central to the apoptotic program, their current status of their inhibitors have been reviewed.[229] On the other hand disruption of the MDM2/p53 interaction as been achieved by the use of cis-imidazoline analogues called nutlins or benzodiazepinediones (Fig. 2.14.), these inhibitors need to basically inhibit the formation of the MDM2/p53 adduct by mimicking three key residues from p53: L26, W23 and F19 (Fig.2.15.), which are in close proximity at the same end of a helix and bind in a hydrophobic cleft of MDM2. Efforts towards the development of enhanced affinity derivatives are currently under way.[230, 231] Novel strategies aiming to restore or control p53 function in cancer patients have been made use of viruses to either destroy wt-p53 deficient cells or in a gene therapy approach to replace wt-p53.[232] An additional and complementary approach to the design of p53Is is the concept of reactivation or rescuing of mutant p53 by small molecules. The rationale is to shift the equilibrium towards a properly folded state or wild-type conformation by a molecule that will bind strongly to this form of p53 rather than to the unfold mutant. Examples of this approach involves a great variety of chemical entities including pieces of sequences from the very C-terminal domain in p53.[233] It has been reported that even with peptide sequences small as nine residues, is possible to bind and stabilize p53 mutants with subsequent restoration of DNA binding activity.[234]

The MDM2 protein needs special attention on this section due to its importance in tumorigenesis and cell growth regulation with p53-dependent and -independent functions.

MDM2 basically presents an N-terminal p53 binding domain and a C-terminal RING finger domain (C_4).

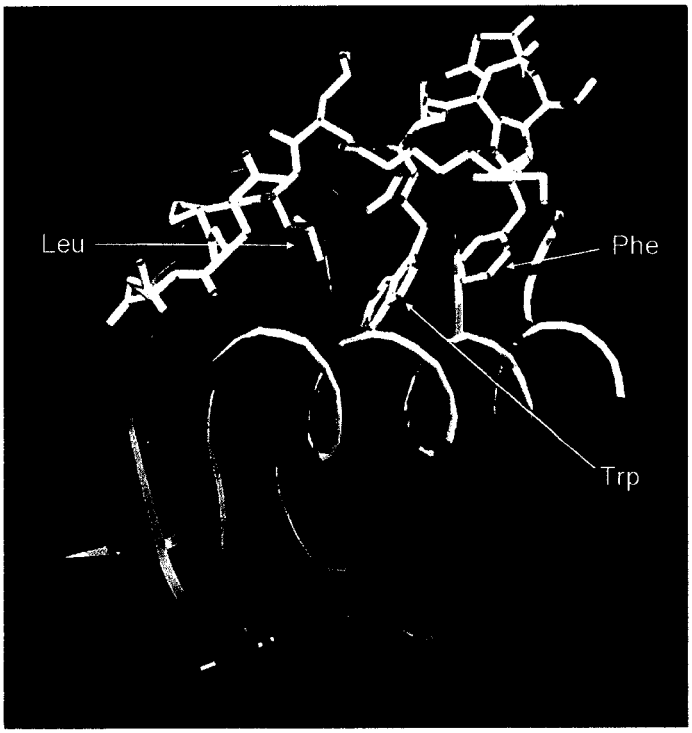

Figure 2.15. Crystal structure of the 109-residue amino-terminal domain of MDM2 (green) bound to a 15-residue transactivation domain of p53 (yellow). Potential inhibitors of the p53/MDM2 interaction generally mimic the interaction of the key residues Phe19, Trp 23 and Leu26 indicated with the arrows.[235] PDB ID:1YCR

The MDM2 protein needs special attention on this section due to its importance in tumorigenesis and cell growth regulation with p53-dependent and -independent functions. MDM2 basically presents an N-terminal p53 binding domain and a C-terminal RING finger domain (C_4). The solution structure of the C_4-ZF of the human counterpart HDM2 as been reported recently,[236] exhibiting a 3_{10} helix followed by four β-strands, its function is not completely clear but it has been suggested that could negatively regulate the level of M2MD (or HDM2) with implications for the development of tumors. The interest in the design of

MDM2 inhibitors stems from the fact that this protein is overexpressed in some tumors and its inhibition has been shown to restore p53 function and prevent cancer growth. Also MDM2 is a mediator of survival signaling in the PI3K/Akt pathway; it activates certain steroid hormone receptors and can inhibit the TGF-beta growth restrictive pathway further increasing its potential as a target.[237] Moreover the use of anti-HDM2 antisense oligonucleotides has demonstrated chemo- and radio-sensitizing effects and antitumor activity in several human cancer models, regardless of their p53 status.[238] Other inhibitors for MDM2 are either small hydrophobic molecules or oligomeric molecules that can reproduce the natural substrate site in p53, although novel peptoids where the side chain is directly attached to the backbone nitrogen atom rather than to the α-carbon have also been tried recently.[239]

2.5. Conclusions

This review provides a basic outlook on seven key zinc-metalloproteins with proven relevance in the medicinal arena, for which a great amount of effort has been made in the structural characterization of active sites and design of inhibitors. Other zinc-metalloproteins are expected to join this selective group in the future, given the central role played by zinc in the proteome. As commonly found in living systems, zinc-metalloproteins either with catalytic and/or structural sites can have a close interrelationship in their actual function *in vivo*. As an example, p53 can be a substrate for HDACs while MDM2 (a zinc finger containing protein) is a major regulator of p53 levels inside the cell. In addition, zinc finger proteins have been reported to recruit HDACs to modulate nuclear receptor transactivation. In this regard the importance of zinc, as a trace element, for living systems can be correlated

to a large extent to the broad variety of functions exerted by the enzymes and structural proteins that need it as a cofactor.

The interrelationship exhibited by zinc-metalloproteins is further emphasised by the overlap between different diseases linked to them, as was observed in the clinical relevance section presented on this review. Cancer being a notable example where the influence of several zinc-metalloproteins appears to play diverse but critical roles. Further deviations from the proper regulation on zinc-metalloproteins has been linked to other important public health issues such as diabetes and neurodegenerative diseases.

A common theme for disease regulation is interference with the essential zinc ion of the protein/enzyme. A thorough characterization of the active site for these zinc-metalloproteins has provided important clues towards their mechanism and function. This knowledge in turn has contributed to the development of more specific inhibitors that takes into account not only the first-coordination sphere in the active site but also the secondary and tertiary structural features of the metalloprotein, necessary for drug selectivity. This approach is a fruitful and essential joining of fundamental bioinorganic chemistry with structural biology and medicinal chemistry.

2.6. References

(1) Andreini, C.; Banci, L.; Bertini, I.; Rosato, A., *J. Proteome Res.*, **2005**, 5, 196-201.

(2) G. Parkin, *Chem. Rev.*, 2004, **104,** 699-767.

(3) Lipscomb W.N.; Sträter, N., *Chem. Rev.*, **1996**, 96, 2375 – 2433.

(4) Shi, W.; Zhan, C.; Ignatov, A.; Manjasetty, B.A.; N. Marinkovic; Sullivan, M.; Huang, R.; Chance, M.R., *Struct.*, **2005**, 13, 1473 -1486.

(5) Turner, A.J., *Biochem. Soc. Trans.*, **2003**, 31, 723 – 727.

(6) Laity, J.H.; Lee B.M.; Wrigth, P.E., *Curr. Opin. Struct. Biol.*, **2001**, 11, 39 – 46.

(7) Auld, D.S., *BioMetals*, **2001**, 14, 271 - 313.

(8) Hirzel, K.; Müller, U.; Latal, A. T.; Hülsmann, S.; Grudzinska, J.; Seelinger, M.W.; Betz H.; Laube, B., *Neuron*, **2006**, 52, 679 – 690.

(9) Mocchegiani, E.; Bertoni-Freddari, C.; Marcellini, F.; Malavolta, M., *Prog. Neurobiol.*, **2005**, 75, 367-390.

(10) S.C. Burdette and S.J. Lippard, *Proc. Natl. Acad. Sci. USA*, **2003**, 100, 3605 - 3610.

(11) Frederickson, C.J.; Bush, A.I.; *BioMetals*, **2001**, 14, 353-366.

(12) Stefanidou, M.; Maravelias, C.; Dona, A.; Spiliopoulou, C., *Arch. Toxicol.*, **2006**, 80, 1-9.

(13) Vallee, B.L.; Falchuk,K.H., *Physiol. Rev.*, **1993**, 73, 79-118.

(14) Hambidge, M., *J. Nutr.*, **2000**, 130, 1344S - 1349S.

(15) Ho, E., *J. Nutr. Biochem.*, **2004**, 15, 572 – 578.

(16) Quraishi, I.; Collins, S.;. Pestaner, J.P; Harris, T.; Bagasra, O., *Med. Hypotheses*, **2005**, 65, 887 – 892.

(17) Jiang, P.; Guo, Z., *Coord. Chem. Rev.*, **2004**, 248, 205 - 229.

(18) Stocker, W.; Bode, W., *Curr. Opin. Struct. Biol.*, **1995**, 5, 383 - 390.

(19) Maskos, K.; Bode, W., *Mol. Biotech.*, **2003**, 25, 241 - 266.

(20) Nagase, H.; Visse, R.; Murphy, G., *Cardiovascular Res.*, **2006**, 69, 562 - 573.

(21) Hege, T.; Baumann, U., *J. Mol. Biol.*, **2001**, 314, 181-186.

(22) Butler, G.S.; Tam, E.M.; Overall, C.M., *J. Biol. Chem.*, **2004**, 279, 15615 – 15620.

(23) Walasek, P.; Honek, J.F., *BMC Biochem.*, **2005**, 6, 21-32.

(24) Gomis-Ruth, F.X., *Mol. Biotech.*, **2003**, 24, 157-202.

(25) Brinckerhoff, C.E.; Matrisian, L.M., *Nat. Rev. Mol. Cell Biol.*, **2002**, 3, 207-214.

(26) Deryugina, E.I.; Quigley, J.P., *Cancer Metastasis Rev.*, **2006**, 25, 9-34.

(27) Shiomi, T.; Okada, Y., *Cancer Metastasis Rev.*, **2003**, 22, 145-152.

(28) Ii, M.; Yamamoto, H.; Adachi, Y.; Maruyama Y.; Shinomura, Y., *Exp. Biol. Med.*, **2006**, 231, 20-27.

(29) Van Lint, P.; Libert, C., *Cytokine Growth Factor Rev.*, **2006**, 17, 217-223.

(30) Mannello, F.; Luchetti, F.; Falcieri, E.; Papa, S., *Apoptosis*, **2005**, 10, 19-24.

(31) Yong, V.W., *Nat. Rev. Neurosci.*, **2005**, 6, 931-944.

(32) Murphy, G.; Lee, M.H., *Ann. Rheum. Dis.*, **2005**, 64, 44 – 47.

(33) Chaussain-Miller, C.; Fioretti, F.; Goldberg, M.; Menashi, S., *J. Dental Res.*, **2006**, 85, 22-32.

(34) Elkington, P.T.G.; O'Kane, C.M.; Friedland, J.S., *Clin. Exp. Immun.*, **2005**, 142, 12 – 20.

(35) Gueders, M.M.; Foidart, J-. M.; Noel, A.; Cataldo, D.D., *Eur. J. Pharm.*, **2006**, 533, 133 – 144.

(36) Tayebjee, M.H.; Lip, G.Y.H.; MacFayden, R.J., *Diabet. Med.*, **2005**, 22, 1628 – 1635.

(37) Maskos, K., *Biochimie*, **2005**, 87, 249-263.

(38) Lee, M.-H.; Rapti, M.; Murphy, G., *J. Biol. Chem.*, **2004**, 279, 45121-45129.

(39) Chirco, R.; Liu, X-. W.; Jung, K-. K.; Kim, H-. R. C., *Cancer Met. Rev.*, **2006**, 25, 99 – 113.

(40) Baker, A.H.; Dylan, R.E.; Murphy, G., *J. Cell. Sci.*, **2002**, 115, 3719 – 3727.

(41) Fernandez-Catalan, C.; Bode, W.; Huber, R.; Turk, D.; Calvete, J.J.; Lichte, A.; Tschesche, H.; Maskos, K., *EMBO J.*, **1998**, 17, 5238 – 5248.

(42) Pavlovsky, A.G.; Williams, M.G.; Ye, Q.Z.; Ortwine, D.F.; Purchase, C.F. 2nd; White, A.D.; Dhanaraj, V.; Roth, B.D.; Johnson, L.L.; Hupe, D.; Humblet, C.; Blundell, T.L., *Protein Sci.*, **1999**, 8, 1455-1462.

(43) Overall, C.M.; Kleifield, O., *Nat. Rev. Cancer*, **2006**, 6, 227-239.

(44) Bertini, I.; Calderone, V.; Cosenza, M.; Fragai, M.; Lee, Y-.M.; Luchinat, C.; Mangani, S.; Terni, B.; Turano, P., *Proc. Natl. Acad. Sci. USA*, **2005**, 102, 5334 – 5339.

(45) Blagg, J.A.; Noe, M.C.; Wolf-Gouveia, L.A.; Reiter, L. A.; Laird, E. R.; Chang, S-.P.; Danley, D. E.; Downs, J. T.; Elliott, N. C.; Eskra, J. D.; Griffiths, R. J.; Hardink, J. R.; Haugeto, A. I.; Jones, C. S.; Liras, J. L.; Lopresti-Morrow, L. L.; Mitchell, P. G.; Pandit, J.; Robinson, R. P.; Subramanyam, C.; Vaughn-Bowser, M. L.; Yocum, S. A., *Bioorg. Med. Chem. Lett.*, **2005**, 15, 1807 – 1810.

(46) Puerta, D.T.; M.O. Griffin, J.A. Lewis, D. Romero-Perez, R. Garcia, F.J. Villareal and S.M. Cohen, *J. Biol. Inorg. Chem.*, 2006, **11**, 131-138.

(47) Overall, C.M.; Kleifeld, O., *Br. J. Cancer*, **2006**, 94, 941 – 946.

(48) Sava, G.; Zorzet, S.; Turrin, C.; Vita, F.; Soranzo, M. R.; Zabucchi, G.; Cocchietto, M.; Bergamo, A.; DiGiovine, S.; Pezzoni, G.; Sartor, L.; Garbisa, S., *Clin. Cancer. Res.*, **2003**, 9, 1898 -1905.

(49) Yuan, J.; Dutton, C.M.; Scully, S.P., *J. Orthop. Res.*, **2005**, 23, 1467-1474.

(50) Lakka, S.S.; Gondi, C.S.; Dinh, D.H.; Olivero, W.C.; Gujrati, M.; Rao, V.H.; Sioka, C. ; Rao, J.S., *J. Biol. Chem.*, **2005**, 280, 21882 – 21892.

(51) De Paiva, C.S.; Corrales, R.M.; Villareal, A.L.; Farley, W.J.; Li, D-.Q.; Stern, M.E.; Pflugfelder, S.C., *Exp. Eye Res.*, **2006**, 83, 526 – 535.

(52) Yoo, C.B.; Jones, P.A., *Nat. Rev. Drug Discovery*, **2006**, 5, 37-50.

(53) Rodenhiser, D.; Mann, M., *Can. Med. Assoc. J.*, **2006**, 174, 341-348.

(54) Cosgrove, M.S.; Wolberger, C., *Biochem. Cell Biol.*, **2005**, 83, 468-476.

(55) Minucci, A.; Pelicci, G., *Nature Rev. Cancer*, **2006**, 6, 38-51.

(56) Somoza, J. R.; Skene, R. J.; Katz, B. A.; Mol, C.; Ho, J. D.; Jennings, A. J.; Luong, C.; Arvai, A.; Buggy, J. J.; Chi, E.; Tang, J.; Sang, B.; Verner, E.; Wynands, R.; Leahy, E. M.; Dougan, D. R.; Snell, G.; Navre, M.; Knuth, M. W.; Swanson, R. V.; McRee, D. E.; Tariet, L. W., *Structure*, **2004**, 12, 1325-1334.

(57) Vannini, A.; Volpari, C.; G. Filocamo, E. C. Casavola, M. Brunetti, D. Renzoni, P. Chakravarty, C. Paolini, R. De Francesco, P. Gallinari, C. Steinkühler and S. Di Marco, *Proc. Natl. Acad. Sci. USA.*, **2004**, 101, 15064 -15069.

(58) Finnin, M.S.; Donigian, J.R.; Cohen, A.; Richon, V.M.; Rifkind, R.A.; Marks, P.A.; Breslow, R.; Pavletich, N.P. *Nature*, **1999**, 401, 188 - 193.

(59) Gantt, S.L.; Gattis, S.G.; Fierke, C.A. *Biochemistry*, **2006**, 45, 6170 – 6178.

(60) Kapustin, G.V.; Fejer, G.; Gronlund, J.L.; McCafferty, D.G.; Seto, E.; Etzkorn, F.A. *Org. Lett.*, **2003**, 5, 3053 – 3056.

(61) Vanommeslaeghe, K.; De Proft, F.; Loverix, S.; Tourwé, D.; Geerlings, P. *Bioorg. Med. Chem.*, **2005**, 13, 3987-3992.

(62) Corminboeuf, C.; Hu, P.; Tuckermann, M.E.; Zhang, Y. *J. Am. Chem. Soc.*, **2006**, 128, 4530-4531.

(63) Zou, H.; Wu, Y.; Navre, M.; Sang, B. *Biochem. Biophys. Res. Comm.*, **2006**, 341, 45-50.

(64) Zhang, Y.; Gilquin, B.; Khochbin, S.; Matthias, P. *J. Biol. Chem.*, **2006**, 281, 2401-2404.

(65) Matsumoto, H.; Hawke, D.; Kobayashi, R.; Verreault, A. *Nature*, **2005**, 436, 294 - 298.

(66) Yoshida, M.; Matzuayama, A.; Komatsu, Y.; Nishino, N. *Curr. Med. Chem.*, **2003**, 10, 2351-2358.

(67) He, L.; Tolentino, T.; Grayson, P.; Zhong, S. ; Warrell, R. P.; Rifkind, Jr., R. A.; Marks, P. A.; Richon, V. M.; Pandolfi, P. P. *J. Clin. Invest.*, **2001**, 108, 1321-1330.

(68) Hess-Stumpp, H. *Eur. J. Cell Biol.*, **2005**, 84, 109-121.

(69) Han, A.; He, J.; Wu, Y.; Liu, J.O.; Chen, L. *J. Mol. Biol.*, **2005**, 345, 91-102.

(70) Tao, R.-H.; Kawate, H.; Wu, Y.; Ohnaka, K.; Ishizuka, M.; Inoue, A.; Hagiwara, H.; Takayanagi, R. *Mol. Cel. Endocrinol.*, **2006**, 247, 150 -165.

(71) Acharya, M.R.; Sparreboom, A.; Venitz, J.; Figg, W.D. *Mol. Pharmacol.*, **2005**, 68, 917-932.

(72) Liu, T.; Kuljaca, S.; Tee, A.; Marshall, G.M. *Cancer Treat. Rev.*, **2006**, 32, 157 - 165.

(73) Saha, R.N.; Pahan, K. *Cell Death Diff.*, **2006**, 13, 539-550.

(74) Gray, S.G.; De Meyts, P. *Diabetes Metab. Res. Rev.*, **2005**, 21, 416 – 433.

(75) Barnes, P.J. *Chest*, **2006**, 129, 151-155.

(76) Blanchard, F.; Chipoy, C. *Drug Discov. Today*, **2005**, 10, 197-204.

(77) Dokmanovic, M.; Marks, P.A. J. Cell. Biochem., **2005**, 96, 293-304.

(78) Monneret, C. *Eur. J. Med. Chem.*, **2005**, 40, 1 -13.

(79) Drummond, D.C.; Noble, C.O.; Kirpotin, D.B.; Guo, Z.; Scott, G.K.; Benz, C.C. *Annu. Rev.Pharmacol. Toxicol.*, **2004**, 45, 495-528.

(80) Carey, N.; La Thangue, N.B. *Curr. Op. Pharmacol.*, **2006**, 6, 369 -375.

(81) Dashwood, R.H.; Myzak, M.C.; Ho, E. *Carcinogenesis*, **2006**, 27, 344 -349.

(82) Gu, W.; Nusinzon, I.; Smith Jr., R.D.; Horvath, C.M.; Silverman, R.B. *Bioorg. Med. Chem.*, **2006**, 14, 3320 - 3329.

(83) Simonini, M.V.; Camargo, L.M.; Dong, E. ; Maloku, E.; Veldic, M. Costa, E.; Guidotti, A. *Proc. Natl. Acad. Sci. USA.*, **2006**, 103, 1587-1592.

(84) Lu, Q.; Yang, Y.-T.; Chen, C.-S.; Davis, M.; Byrd, J. C.; Etherton, M. R.; Umar, A.; Chen, C-. S. *J. Med. Chem.*, **2004**, 47, 467-474.

(85) Bhuiyan, M.P.I.; Kato, T.; Okauchi, T.; Nishino, N.; Maeda, S.; Nishino, V; Yoshida, M. *Bioorg. Med. Chem.*, **2006**, 14, 3438-3446.

(86) Eikel, D.; Lampen, A.; Nau, H. *Chem. Res. Toxicol.*, **2006**, 19, 272-278.

(87) Marks, P.A.; Jiang, X. *Cell Cycle*, **2005**, 4, 549-551.

(88) Maurer-Stroh, S.; Washietl, S.; Eisenhaber, F. *Genome Biol.*, **2003**, 4, 212 - 212.9.

(89) Leung, K.F.; Baron, R.; Seabra, M.C. *J. Lipid Res.*, **2006**, 47, 467 -475.

(90) Sousa, S.F.; Fernandes, P.A.; Ramos, M.J. *J. Biol. Inorg. Chem.*, **2005**, 10, 3 – 10.

(91) Lane, K.T.; Beese, L.S. *J. Lipid Res.*, **2006**, 47, 681 – 699.

(92) Brunner, T.B.; Hahn, S.M.; Gupta, A.K.; Muschel, R.J.; McKenna, W.J.; Bernhard, E.J. *Cancer Res.*, **2003**, 63, 5656 – 5668.

(93) deSolms, S.J.; Ciccarone, T.M.; MacTough, S.C.; Shaw, A.W.; Buser, C.A.; Ellis-Hutchings, M.; Fernandes, C.; Hamilton, K. A.; Huber, H. E.; Kohl, N. E.; Lobell, R. B.; Robinson, R. G.; Tsou, N. N.; Walsh, E. S.; Graham, S. L.; Beese, L. S.; Taylor. J. S. *J. Med. Chem.*, **2003**, 46, 2973 – 2984.

(94) Na, H-. J.; Lee, S-.J.; Kang, Y-.C.; Cho, Y-.L.; Nam, W-.D.; Kim, P.K.M.; Ha, K-. S.; Chung, H-.T.; Lee, H.; Kwon, Y-.G.;.Koh, J. S.; Kim, Y-.M. *J. Immunology*, **2004**, 173, 1276 – 1283.

(95) Catenacci, D.V.T.; Schiller, G.J. *Blood Rev.*, **2005**, 19, 301 – 319.

(96) Faderl, S.; Kantarjian, H.M. *Cancer*, **2004**, 101, 226 – 241.

(97) Eastman, R.T.; Buckner, F.S.; Yokoyama, K.; Gelb, M.H.; Van Voorhis, W.C. *J. Lipid Res.*, **2006**, 47, 233 – 240.

(98) Oualid, F. E.; van den Elst, H.; Leroy, I. M.; Pieterman, E.; Cohen, L. H.; Burm, B. E. A.; Overkleeft, H. S.; van der Marel, G. A.; Overhand. M. *J. Comb. Chem.*, **2005**, 7, 703 - 713.

(99) Nagashima, T.; Okazaki, H.; Yudoh, K.; Matsuno, H.; Minota, S. *Arthritis & Rheumatism*, **2006**, 54, 579 - 586.

(100) Santagada, V.; Caliendo, G.; Severino, B.; Lavecchia, A.; Perisutti, E.; Fiorino, F.; Zampella, A.; Sepe, V.; Califano, D.; Santelli, G.; Novellino, E. *J. Med. Chem.*, **2006**, 49, 1882 – 1890.

(101) Appels, N.M.G.M.; Beijnen, J.H.; Schellens, J.H.M. *The Oncologist*, **2005**, 10, 565 – 578.

(102) Basso, A.D.; Kirschmeier, P.; Bishop, R. *J. Lipid Res.*, **2006**, 47, 15 - 31.

(103) T.S. Reid, S.B. Long and L.S. Beese, *Biochemistry*, 2004, **43**, 9000 - 9008.

(104) Efuet, E.T.; Keyomarsi, K. *Cancer Res.*, **2006**, 66, 1040 - 1051.

(105) Thomson, J.M.; Bonomo, R.A. *Curr. Opin. Microbiol.*, **2005**, 8, 518 - 524.

(106) Helfand, M.S.; Bonomo, R.A. *Curr. Op. Pharmacol.*, **2005**, 5, 452 - 458.

(107) Garrity, J.D.; Bennett, B.; Crowder, M.W. *Biochemistry*, **2005**, 44, 1078 - 1087.

(108) Xu, D.; Xie, D.; Guo, H. *J. Biol. Chem.*, **2006**, 281, 8740 - 8747.

(109) Costello, A.; Periyannan, G.; Yang, K-. W.; Crowder, M.W.; Tierney, D.L. *J. Biol. Inorg. Chem.*, **2006**, 11, 351 - 358.

(110) Heinz, U.; Adolph, H.-W. *Cell. Mol. Life Sci.*, **2004**, 61, 2827 - 2839.

(111) Murphy, T.A.; Catto, L.E.; Halford, S.E.; Hadfield, A.T.; Minor, W.; Walsh, T.R.; Spencer, J. *J. Mol. Biol.*, **2006**, 357, 890 - 903.

(112) Garau, G.; Bebrone, C.; Anne, C.; Galleni, M.; Frère, J.M.; Dideberg, O. *J. Mol. Biol.*, **2005**, 345, 785 - 795.

(113) Garau, G.; Garcia-Saez, I.; Bebrone, C.; Anne, C.; Mercuri, P.; Galleni, M.;, Frère, J.M.; Dideberg, O. *Antimicrob. Agents and Chemother.*, **2004**, 48, 2347-2349.

(114) Jacoby, G.A.; Munoz-Price, L.S. *N. Engl. J. Med.*, **2006**, 352, 380 - 391.

(115) Levy, S.B. *Adv. Drug. Delivery Rev.*, **2005**, 57, 1446 - 1450.

(116) Fritsche, T.R.; Sader, H.S.; Toleman, M.A.; Walsh, T.R.; Jones, R.N. *Clin. Infect. Diseases*, **2005**, 41, S276- S278.

(117) Walsh, T.R.; Toleman, M.A.; Poirel, L.; Nordmann, P. *Clin. Microbiol. Rev.*, **2005**, 18, 306 - 325.

(118) Kurosaki, H.; Yamaguchi, Y.; Higashi, T.; Soga, K.; Matsueda, S.; Yumoto, H.; Misumi, S.; Yamagata, Y.; Arakawa, Y.; Goto, M. *Angew. Chem. Intl. Ed.*, **2005**, 44, 3861 - 3864.

(119) Spencer, J.; Walsh, T.R. *Angew. Chem. Int. Ed.*, **2006**, 45, 1022 -1026.

(120) Olsen, L.; Jost, S.; Adolph, H-. W.; Pettersson, I.; Hemmingsen, L.; Jørgensen, F.S. *Bioorg. Med. Chem.*, **2006**, 14, 2627 - 2635.

(121) Hart, P.J. *Curr. Op. Chem. Biol.*, **2006**, 10, 131 -138.

(122) Pelmenschikov, V.; Siegbahn, P.E.M. *Inorg. Chem.*, **2005**, 44, 3311 - 3320.

(123) Radunovic, A.; Leigh, P.N., *Amyotrophic Lateral Scler. Other Mot. Neuron Disord.*, **1999**, 1, 45 - 49.

(124) Karunakaran, C.; Zhang, H.; Joseph, J.; Antholine, W.E.; Kalyanaraman, B. *Chem. Res. Toxicol.*, **2005**, 18, 494 - 500.

(125) Miller, A.F. *Curr. Op. Chem. Biol.*, **2004**, 8, 162 - 168.

(126) Medinas, D.; Augusto, O. *Free Radical Biol. Med.*, **2005**, 39, S26 - S27.

(127) Valentine, J.S.; Hart, P.J. *Proc. Natl. Acad. Sci. USA.*, **2003**, 101, 15094 -15099.

(128) Bruijn, L.I.; Houseweart, M.K.; Kato, S.; Anderson, K.L.; Anderson, S.D.; Ohama, E.; Reaume, A.G.; Scott, R.W.; Cleveland, D.W. *Science*, **1998**, 281, 1851 - 1854.

(129) Khare, S.D.; Caplow, M.; Dokholyan, N.V. *Proc. Natl. Acad. Sci. USA.*, **2004**, 101, 15094 - 15099.

(130) Vassall, K.A.; Stathopulos, P.B.; Rumfeldt, J.A.O.; Lepock , J.R.; Meiering, E.M. *Biochemistry*, **2006**, 45, 7366 -7379.

(131) Rumfeld, J.A.O.; Stathopulos, P.B.; Chakrabarrty, A.; Lepock, J.R.; Meiering, E.M. *J. Mol. Biol.*, **2006**, 355, 106 - 123.

(132) Zhang, F.; Zhu, H. *Biochim. Biophys. Acta*, **2006**, 1760, 404 - 414.

(133) Furukawa, Y. ; O'Halloran, T.V. *J. Mol. Biol.*, **2005**, 280, 17266 -17274.

(134) Rodriguez, J.A.; Shaw, B.F.; Durazo, A.; Sohn, A.H.; Doucette, P.A.; Nersissian, A.M.; Faull, K.F.; Eggers, D.K.; Tiwari, A.; Hayward, L.J.; Valentine, J.S. *Proc. Natl. Acad. Sci. USA.*, **2005**, 102, 10516 - 10521.

(135) Lynch, S.M.; Colón, W. *Biochem. Biophys. Res. Comm.*, **2006**, 340, 457 - 461.

(136) Furukawa, Y.; Fu, R.; Deng, H-.X.; Siddique, T.; O'Halloran, T.V. *Proc. Natl. Acad. Sci. USA.*, **2006**, 103, 7148 - 7153.

(137) Khare, S.D.; Dokholyan, N.V. *Proc. Natl. Acad. Sci. USA.*, **2006**, 103, 3147 - 3152

(138) Khare, S.D.; Wilcox, K.C.; Gong, P.; Dokholyan, N.V. *Proteins: Struct. Funct. Inform.*, **2005**, 61, 617 - 632.

(139) Nordlund, A.; Oliveberg, M. *Proc. Natl. Acad. Sci. USA.*, **2006**, 103, 10218 - 10223.

(140) Liochev, S.I.; Fridovich, I. *Free Radical Biol. Med.*, **2003**, 34, 1383 1389.

(141) Hileman, E.A.; Achanta, G.; Huang, P. *Exp. Op. Ther. Targets*, **2001**, 5, 697 – 710.

(142) Ray, S.S.; Nowak, R.J.; Brown Jr., R.H.; Lansbury Jr., P.T. *Proc. Natl. Acad. Sci. USA.*, **2005**, 102, 3639 - 3644.

(143) Carri, M.T.; Grignaschi, G.; Bendotti, C. *Trends Pharm. Sci.*, **2006**, 27, 267 - 273.

(144) Sugai, F.; Yamamoto, Y.; Miyaguchi, K.; Zhou, Z.; Sumi, H.; Hamasaki, T.; Goto, M.; Sakoda, S. *Eur. J. Neurosc.*, **2004**, 20, 3179 - 3183.

(145) dePaula, C.H.T.; Sanches, S.M.; Taft, C.A. *J. Mol. Graphics Model.*, **2004**, 23, 89 - 97.

(146) Hanas, J.S.;. Hazuda, D.J ; Bogenhagen, D.F.; Wu, F.Y.-H.; Wu, C. *J. Biol. Chem.*, **1983**, 23, 14120 - 14125.

(147) Miller, J.; McLachlan, A.D.; Klug, A. *EMBO J.*, **1985**, 4, 1609-1614.

(148) Lachenmann, M.J.; Ladbury, J.E.; Dong, J.; Huang, K.; Carey, P.; Weiss, M.A. *Biochemistry*, **2004**, 43, 13910 - 13925.

(149) Kopera, E.; Schwerdtle, T.; Hartwig, A.; Bal, W. *Chem. Res. Toxicol.*, **2004**, 17, 1452 -1458.

(150) Bombarda, E.; Cherradi, H.; Morellet, N.; Roques, B.P.; Mély, Y. *Biochemistry*, **2002**, 41, 4312 - 4320.

(151) Bombarda, E.; Roques, B.P.; Mély, Y.; Grell, E. *Biochemistry*, **2005**, 44, 7315 - 7325.

(152) Nomura, A.; Sugiura, Y. *Inorg. Chem.*, **2002**, 41, 3693 -3698.

(153) Maret, W. Exploring the zinc proteome. *J. Anal. At. Spectrom.* , **2004**, 19, 15 - 19.

(154) Krishna, S.S.; Majumdar, I.; Grishin, N.V. *Nucl. Acids Res.*, **2003**, 31, 532 - 550.

(155) Bateman, A.; Birney, E.; Cerruti, L.; Durbin, R.; Etwiller, L.; Eddy, S.R.; Griffiths-Jones, S.; Howe, K.L.; Marshall, M.; Sonnhammer, E.L.L. *Nucl. Acids Res.*, **2002**, 30, 276-280.

(156) Dhanasekaran, M.; Negi, S.; Sugiura, Y. *Acc. Chem. Res.*, **2006**, 39, 45-52.

(157) Papworth, M.; Kolasinska, P.; Minczuk, M., Gene, **2006**, 366, 27-38.

(158) Jantz, D.; Amann, B.T.; Gatto, G.J.; Berg, J.M. *Chem. Rev.*, **2004**, 104, 789-799.

(159) Vazquez, M.E.; Caamaño, A.M.; Mascareñas, J.L. *Chem. Soc. Rev.*, **2003**, 32, 338 - 349.

(160) Shiraishi, Y.; Imanishi, M.; Morisaki, T.; Sugiura, Y. *Biochemistry*, **2006**, 44, 2523 - 2528.

(161) Hall, T. M. T. *Curr. Op. Struct. Biol.*, **2005**, 15, 367-373.

(162) Brown, R.S.*Curr. Op. Struct. Biol.*, **2005**, 15, 94 - 98.

(163) Morellet, N.; Demene, H.; Teilleux, V.; Huynh-Dinh, T.; De Rocquigny, H.; Fournie-Zaluski, M.C.; Roques, B.P. *J. Mol. Biol.*, **1998**, 283, 419-434.

(164) De Guzman, R.N.; Wu, Z.R.; Stalling, C.C.; Pappalardo, L.; Borer, P.N.; Summers, M.F. *Science*, **1998**, 279, 384-388.

(165) Little, T.H.; Zhang, Y.; Matulis, C.K.; Weck, J.; Zhang, , Z.; Ramachandran, A.; Mayo, K. E.; Radhakrishnan, I. *Mol. Endocrinol.*, **2006**, 20, 831-843.

(166) Algirdas, V.; Jun, Q. *Zinc Finger Prot.*, **2005**, 9, 99 -105.

(167) Bienz, M. *TRENDS Biochem. Sci.*, **2006**, 31, 35 - 40.

(168) Liew, C.K.; Simpson, R.J.Y.; Kwan, A.H.Y.; Crofts, L.A.; Loughlin, F.E.; Matthews, J.M.; Crossley, M.; Mackay, J.P. *Proc. Natl. Acad. USA.*, **2005**, 102, 583 - 588.

(169) Klug, A. *FEBS Lett.*, **2005**, 579, 892-894.

(170) Beerli, R.R.; Barbas, C.F. *Nat. Biotech.*, **2002**, 20, 135-141.

(171) Porteus, M.H. *Mol. Ther.*, **2006**, 13, 438 - 446.

(172) Cathomen, T.; Weitzman, M.D. *Gene Ther.*, **2005**, 12, 1415 - 1416.

(173) Porteus, M.H.; Carroll, D. *Nat. Biotech.*, **2005**, 23, 967 - 973.

(174) Dreier, B.; Fuller, R.P.; Segal, D.J.; Lund, C.; Blancafort, P.; Huber, A.; Koksch, B.; Barbas III, C.F. *J. Biol. Chem.*, **2005**, 280, 35588 - 35597.

(175) Gommans, W.J.; Haisma, H.J.; Rots, M.G. *J. Mol. Biol.*, **2005**, 354, 507 - 519.

(176) Papworth, M.; Moore, M.; Isalan, M.; Minczuk, M. ; Choo, Y.; Klug, A. *Proc. Natl. Acad. Sci.*, **2003**, 100, 1621-1626.

(177) Kim, Y.-S.; Kim, J.-M.; Jung, D.-L.; Kang, J.-E.; Lee, S.; Kim, J. S.; Seol, W.; Shin, H.-C.; Kwon, H. S.; Van Lint, C.; Hernandez, N.; Hur, M.-W. *J. Biol. Chem.*, **2005**, 280, 21545 - 21552.

(178) Yu, J.; Lei, L.; Liang, Y.; Hinh, L.; Hickey, R. P.; Huang, Y.; Liu, D.; Yeh, J. L.; Rebar, E.; Case, C.; Spratt, K.; Sessa, W. C.; Giordano, F. J. *FASEB J.*, **2006**, doi 10.1096/fj.04-3670fje.

(179) G. Lomberk and R. Urrutia, *Biochem. J.*, 2005, **392**, 1-11.

(180) Bieker, J.J. *J. Biol. Chem.*, **2001**, 276, 34355 - 34358.

(181) Safe, S.; Abdelrahim, M. *Eur. J. Cancer*, **2005**, 41, 2438-2448.

(182) Chen, Y.; Guo, Y.; Ge, X.; Itoh, H.; Watanabe, A.; Fujiwara, T.; Kodama, T.; Aburatani, H. *Biochem. Biophys. Res. Commun.*, **2006**, 340, 758 - 766.

(183) Raman, J.D.; Mongan, N.P.; Liu, L.; Tickoo, S.K.; Nanus, D.M.; Scherr, D.S.; Gudas, L.J. *Carcinogenesis*, **2006**, 27, 499 - 507.

(184) Chang., G.T.G.; Jhamai, M.; van Weerden, W.M.; Jenster, G.; Brinmann, A.O. *Endocr. Rel. Cancer*, **2004**, 11, 815 - 822.

(185) Kasper, M.; Regl, G.; Frischauf, A.-M.; Aberger, F. *Eur. J. Cancer*, **2006**, 42, 437 - 445.

(186) Kadrmas, J.L.; Beckerle, M.C. *Nature Rev. Mol. Cell Biol.*, **2004**, 5, 920 - 931.

(187) Hunter, C.S;. Rhodes, S.J. *Mol. Biol. Reports*, **2005**, 32, 67 - 77.

(188) Goecke, A.; Guerrero, J. *Immunobiology*, **2006**, 211, 85 - 96.

(189) Meijer, O.C.; van der Laan, S.; Lachize, S.; Steenbergen, P.J.; de Kloet, E.R. *Neuroscience*, **2006**, 138, 891-899.

(190) Witkiewicz-Kucharczyk, A.; Bal, W. *Toxicol. Lett.*, **2006**, 162, 29 - 42.

(191) Evanics, F.; Maurmann, L.; Yang, W.W.; Bose, R.N. *Biochim. Biophys. Acta*, **2003**, 1651, 163 - 171.

(192) Mishina, Y.; Duquid, E.M.; He, C. *Chem. Rev.*, **2006**, 106, 215 - 232.

(193) He, C.; Hus, J-. C.; Sun, L.J.; Zhou, P.; Norman, D.P.G.; Dötsch, V.; Wei, H.; Gross, J.D.; Lane, W.S.; Wagner, G.; Verdine, G.L. *Mol. Cell*, **2005**, 20, 117 - 129.

(194) García, C. C.; Djavani, M.; Topisirovic, I.; Borden, K. L. B.; Salvato, M. S.; Damonte, E. B. *J. Gen. Virol.*, **2006**, 87, 1217 - 1228.

(195) Chaturvedi, U.C.; Shrivastava, R. *FEMS Immunol. Med. Microbiol.*, **2005**, 43, 105 - 114.

(196) Amarasinghe, G. K.; De Guzman, R. N.; Turner, R. B.; Chancellor, K. J.; Wu, Z. R.; Summers, M.F. *J. Mol. Biol.*, **2000**, 279, 384 - 388.

(197) Musah, R.A. *Curr. Top. Med. Chem.*, **2004**, 4, 1605-1622.

(198) Anzellotti, A.I.; Liu, Q.; Bloemink, M.; Scarsdale, J.N.; Farrell, N. *Chem. Biol.*, **2006**, 13, 539-548.

(199) Ma, B.; Pan, Y.; Gunasekaran, K.; Keskin, O.; Venkataraghavan, R.B.; Levine, A.J.; Nussinov, R. *Phys. Biol.*, **2005**, 2, S56 - S66.

(200) Duan, J.; Nilsson, L. *Biochemistry*, **2006**, 45, 7483 - 7492.

(201) Perez-Cañadillas, J.M.; Tidow, H.; Freund, S.M.V.; Rutherford, T.J.; Ang, H.C.; Fersht, A.R. *Proc. Natl. Acad. Sci. USA.*, **2006**, 103, 2109 - 2114.

(202) Veprintsev, D.B.; Freund, S.M.V.; Andreeva, A.; Rutledge, S.E.; Tidow, H.; Perez-Cañadillas, J.M.; Blair, C. M.; Fersht, A.R. *Proc. Natl. Acad. Sci. USA.*, **2006**, 103, 2115 - 2119.

(203) Harris, S.L.; Levine, A.J. *Oncogene*, **2005**, 24, 2899 - 2908.

(204) Levine, A.J.; Feng, Z.; Mak, T.W.; You, H.; Jin, S. *Genes & Delop.*, **2006**, 20, 267 - 275.

(205) Kitayner, M.; Rozenberg, H.; Kessler, N.; Rabinovich, D.; Shaulov, L.; Haran, T.E.; Shakked, Z. *Mol. Cell*, **2006**, 22, 741 – 753.

(206) Ford, J.M. *Mut. Res.*, **2005**, 577, 195 – 202.

(207) Krauss, G. (2003). Biochemistry of Signal Transduction and Regulation. 3° Ed., Wiley-VCH Weinheim, Ch. 14, pp. 504 - 505.

(208) Liu, G.; Chen, X. *J. Cell. Biochem.*, **2006**, 97, 448 - 458.

(209) Moll, U.M.; Wolff, S.; Speidel, D.; Deppert, W. *Curr. Op. Cell Biol.*, **2005**, 17, 631 - 636.

(210) Yee, K.S.; Vousden, K.H. *Carcinogenesis*, **2005**, 26, 1317 - 1322.

(211) Soussi, T. *Brit. J. Surgery*, **2005**, 92, 1331 - 1332.

(212) Ozaki, T.; Nakagawara, A. *Cancer Sci.*, **2005**, 96, 729 - 737.

(213) Chong, L.T.; Swope, W.C.; Pitera, J.W.; Pande, V.S. *J. Mol. Biol.*, **2006**, 357, 1039 - 1049.

(214) Souzi, T.; Lozano, G. *Biochem. Biophys. Res. Commun.*, **2005**, 331, 834 - 842.

(215) Khan, S.A.; Thomas, H.C.; Toledano, M.B.; Cox, I.J.; Taylor-Robinson, S.D. *Liver Int.*, **2005**, 25, 704 - 716.

(216) Lacroix, M.; Toillon, R-. A.; Leclercq, G. *Endocr. Rel. Cancer*, **2006**, 13, 293 - 325.

(217) Latonen, L.; Laiho, M. *Biochim. Biophys. Acta*, **2005**, 1755, 71 - 89.

(218) Zambetti, G.P.; Horwitz, E.M.; Schipani, E. *J. Cell Biol.*, **2006**, 172, 795 - 797.

(219) Pietracosta, N.; Garino, C.; Laras, Y.; Quelever, G.; Pierre, P.; Clavarino, F.; Kraus, J.-L. *Drug Develop. Res.*, **2005**, 65, 43 - 49.

(220) Pietsch, E.C.; Humbey, O.; Murphy, M.E. *Oncogene*, **2006**, 25, 1602 - 1611.

(221) Barbieri, C.E.; Pietenpol, J.A. *Cancer Biol. Ther.*, **2005**, 4, 419 - 420.

(222) Prives, C.; Manfredi, J.J. *Mol. Cel.*, **2006**, 19, 719 - 721.

(223) Scoumanne, A.; Harms, K.L.; Chen, X. *Cancer Biol. Ther.*, **2005**, 4, 1178 - 1185.

(224) Hall, P.A.; McCluggage, W.G. *J. Pathol.*, **2006**, 208, 1 - 6.

(225) Roger, L.; Gadea, G.; Roux, P. *Biol. Cell*, **2006**, 98, 141 - 152.

(226) Kaji, A.; Zhang, Y.; Nomura, M.; Bode, A. M.; Ma, W-.Y.; She, Q-.B.; Dong, Z. *Mol. Carcinog.*, **2003**, 37, 138 - 148.

(227) Gudkov, A.V.; Komarova, E.A. *Biochem. Biophys. Commun.*, **2005**, 331, 726 - 736.

(228) Pietrancosta, N.; Moumen, A.; Dono, R.; Lingor, P.; Planchamp, V.; Lamballe, F.; Bähr, M.; Kraus, J-. L.; Maina, F. *J. Med. Chem.*, **2006**, 49, 3645 - 3652.

(229) Linton, S. D. *Curr. Top. Med. Chem.*, **2005**, 5, 1697-1716.

(230) Parks, D. J.; LaFrance, L. V.; Calvo, R. R.; Milkiewicz, K. L.; Marugán, J. J.; Raboisson, P.; Schubert, C.; Koblish, H. K.; Zhao, S.; Franks, C. F.; Lattanze, J.; Carver, T. E.; Cummings, M. D.; Maguire, D.; Grasberger, B. L.; Maroney, A. C.; Lu, T. *Biorg. Med. Lett.*, **2006**, 16, 3310 - 3314.

(231) Tovar, C.; Rosinski, J.; Filipovic, Z.; Higgins, B.; Kolinsky, K.; Hilton, H.; Zhao, X.; Vu, B. T.; Qing, W.; Packman, K.; Myklebost, O.; Heimbrook, D. C.; Vassilev, L. T. *Proc. Natl. Acad. Sci. USA.*, **2006**, 101, 15094 - 15099.

(232) Bouchet, B.P.; de Fromentel, C.C.; Puisieux, A.; Galmarini, C.M. *Crit. Rev. Oncol. Hematol.*, **2006**, 58, 190 - 207.

(233) Bykov, V.J.N.; Selivanova, G.; Wiman, K.G. *Eur. J. Cancer*, **2006**, 39, 1828 - 1834.

(234) Friedler, A.; Hansson, L.O.; Veprintsev, D.B.; Freund, S.M.V.; Rippin, T.M.; Nikolova, P.V.; Proctor, M.R.; Rüdiger, S.; Fersht, A.R. *Proc. Natl. Acad. Sci. USA.*, **2002**, 99, 937 - 942.

(235) Kussie, P.H.; Gorina, S.; Marechal, V.; Elenbaas, B.; Moreau, J.; Levine, A.J.; Pavletich, N.P. *Science*, **1996**, 274, 921- 922.

(236) Yu, G.W.; Allen, M.D.; Andreeva, A.; Fersht, A.R.; Bycroft, M. *Prot. Sci.*, **2006**, 15, 384 - 389.

(237) Levav-Cohen, Y.; Haupt, S.; Haupt, Y. *Growth Factors*, **2005**, 23, 183 - 192.

(238) Zhang, Z.; Zhang, R.W. *Curr. Cancer Drug Targets*, **2005**, 5, 9 - 20.

(239) Hara, T.; Durell, S.R.; Myers, M.C.; Apella, D.H. *J. Am. Chem. Soc.*, **2006**, 128, 1995 - 2004.

CHAPTER 3 Platination of nucleobases to enhance non-covalent recognition in protein-DNA/RNA complexes

Atilio I. Anzellotti, Erin S. Ma and Nicholas P. Farrell

Department of Chemistry, Virginia Commonwealth University, 1001 W. Main St.

Richmond, VA 23284-2006, USA

Inorganic Chemistry, **2005**, 44 (3), 483 - 485

3.1. Abstract:

Fluorescence quenching experiments show that the stacking interaction between nucleic acid bases and l-tryptophan is enhanced significantly upon base coordination to a metal center such as Pt(II) and the biological implications of such enhancement are discussed.

3.2. Introduction:

Stacking π-π interactions play a fundamental role in DNA/RNA-protein selective recognition.[1] These interactions generally involve the planar protein residues tryptophan(phenylalanine) and guanine(cytosine) on the nucleic acid. Methylation of purine and pyrimidine nucleic acid bases enhances π-π stacking interactions to l-tryptophan (Trp) in both solid state and solution, attributable to a lowering in energy for the π-acceptor LUMO in the methylated nucleobase, thus improving the acceptor properties toward the π-donor HOMO of the amino acid.[2] In this contribution we report that the analogy between the electrophiles Me^+ and Pt^{2+} may be extended so that platination of simple nucleic acid bases exerts a similar enhancement in stacking interactions. The results suggest a novel

structural motif for design of metallodrugs capable of selective ternary DNA(RNA)-protein interactions and as novel probes for the tryptophan environment in protein systems.

3.3. Results and Discussion:

The systems examined were [Pt(dien)(L)]2+ (where L = 9-Ethylguanine, (9-EtGH, 1), 5'-guanosine monophosphate (5'-GMP, 2), 1-MethylCytosine (1-MeCyt, 3) and 5'-cytidine monophosphate (5'-CMP, 4). In the absence of a reactive leaving group only non-covalent hydrogen-bonding and stacking interactions need to be taken into account (Fig. 3.1).

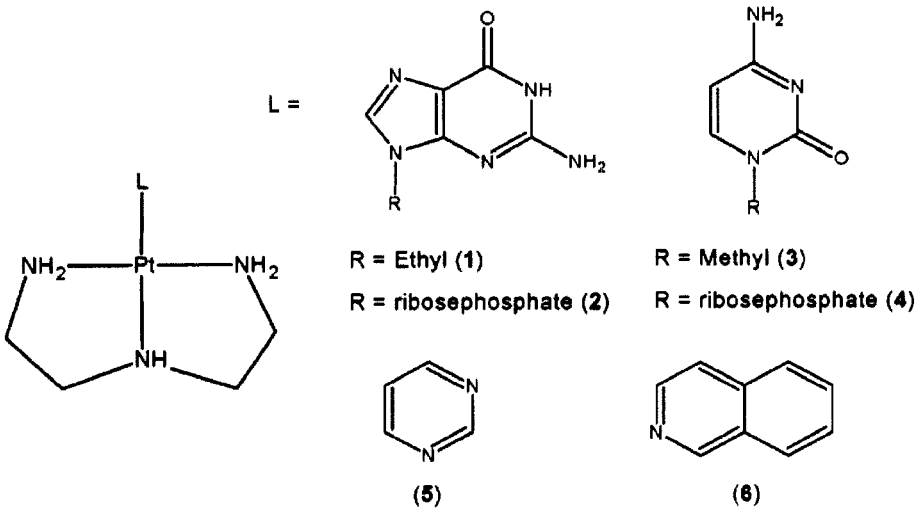

Figure 3.1. Schematic structures of complexes used in this study.

All complexes were synthesized using $[Pt(dien)(NO_3)]NO_3$ as a starting material. ^{195}Pt-NMR spectroscopy of Complex **3** gave two peaks at -2895 and -2912 ppm ($\Delta\delta$ = 17 ppm) at 20 °C coalescing to one broad peak at 80°C, indicative of the presence of rotamers in

solution due to hindered rotation about the Pt-N3 axis, Figure 3.2. The comparative values for **4** are -2901 and -2916 ppm ($\Delta\delta$ = 15 ppm) . The low field ^{1}H-NMR spectrum for **3** (9.5 – 5.5 ppm) in d^{7}-DMF shows that the unique secondary dien-NH amine proton in the dien moiety, and trans to the 1-MeCyt ligand, exhibits a broad doublet where the signals are of unequal intensity, with coalescence of the signal occurring at 40 °C. A further feature found in the 1H-NMR spectrum of 3 is the already reported chemical inequivalence among the C(4)-NH2 protons in 1-MeCyt , 8.85 and 8.42 ppm, due to hindered rotation (see section 3.3.2.).[4]

These protons also show a marked acidity in comparison to the free 1-MeCyt with a large shift ($\Delta\delta \approx 2$ ppm) exhibited upon platination. Similar shifts are observed for the 5'-CMP analog. The coupling constant ^{3}J (H5, H6) does not change significantly upon coordination; both **3** and **4** present values of 7-8 Hz. An explanation for the presence of rotamers is given from the X-ray crystal structure for the analogous complex $[Pd(dien)Cytosine]^{2+}$, where the cytosine plane is found almost perpendicular to the chelating dien ligand. [3b] The presence of rotamers is also in agreement with results reported for $[Pt(dien)adenosine]^{2+}$. In the present case the energy barrier required for coalescence of the dien-NH signal appears to be greater (25 °C vs. 40 °C for the adenosine and 1-methylcytosine respectively), probably because the amino group in the adenosine is farther from the dien-NH2 protons than in the case of Cyt. [5]

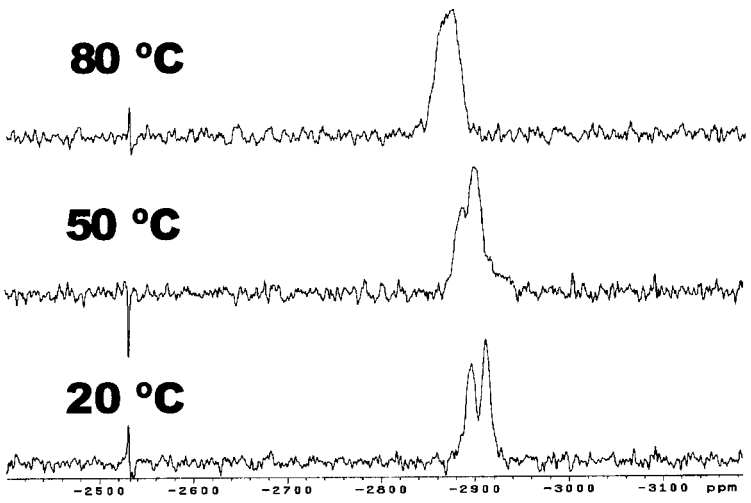

Figure 3.2. Coalescence of ^{195}Pt spectra for $[Pt(dien)(1\text{-}MeCyt)]^{2+}$.

3.3.1. Stacking Interaction by Fluorescence Spectroscopy:

Fluorescence spectroscopy can be used with high sensitivity to monitor small changes occurring on the π-cloud of the l-tryptophan indole ring due to non-covalent interactions and the degree of quenching in the Trp spectrum is an estimate of the strength of the π- π stacking interactions occurring (Fig. 3.3.).[6] Association constants (Ka) were obtained for the alkylated nucleobases (9-EtGH and 1-MeCyt) and the corresponding nucleotides (5'-GMP and 5'-CMP) with solutions of Trp. On average, the values obtained from Eadie-Hofstee plots were approximately 3.0 $x10^3$ M^{-1} for all nucleobases, except for 1-MeCyt which exhibited a significantly higher value of 6.0 $x10^3$ M^{-1}.

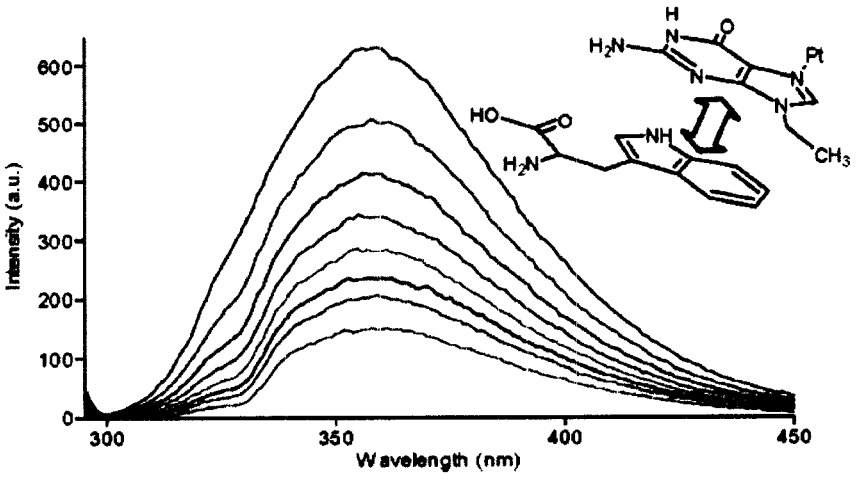

Figure 3.3. Quenching observed in Trp fluorescence spectrum upon increasing concentration of $[Pt(dien)(9\text{-EtGH})]^{2+}$.

The association constants for complexes **1** - **4** revealed significantly higher values for the platinated nucleobases in all cases, Table 3.I. In general the results obtained were very similar for complexes **1**, **2** and **4** (the average increase upon platination was $\Delta Ka = 3.7 \times 10^3$ M-1) showing that the presence of the ribose monophosphate moiety does not affect considerably the stacking interaction, at least in this simple system. These results are somewhat different to those reported for $[Pt(dien)Cl]^+$ and 9- EtGH and 5'-GMP but it is important to note that only in the 9-EtGH case was there a well-defined complex studied.[7] Complex **3** exhibited the overall highest association constant, albeit with a somewhat lower increase ($\Delta K_a = 2.7 \times 10^3\ M^{-1}$) compared to the free base. ^{1}H-NMR studies of **3**/N-acetyltryptophan (N-AcTrp) systems allowed assignments of chemical shift changes induced by the π-π stacking interactions (Fig. 3.4.). Upfield chemical shifts have been

observed for *trans*-[Cp*Rh(η^1(N3)-1-methylcytosine)(μ-OH)]$_2$(OTf)$_2$ involving both 1-MeCyt and Trp in a non-covalent interaction.[8]

The importance of the "natural" nucleic acid bases in the stacking interaction was further assessed by examination of two model compounds [Pt(dien)(pyrimidine)$^{2+}$] **5** (lacking the exocyclic substituents of cytosine) and [Pt(dien)(isoquinoline)]$^{2+}$ **6** (containing a planar heterocycle). In neither case was any significant enhancement seen over the free ligands (data not shown), even at comparatively high concentrations. Contribution to π- π stacking interactions from the cytosine functional groups C2-carbonyl and C4-amine could further decrease π –acceptor LUMO energy or play an important role by themselves in steric and H-bonding interactions.

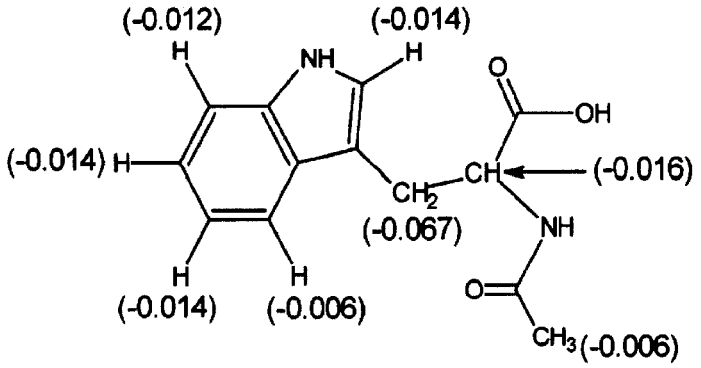

Figure 3.4. Upfield chemical shifts observed in *N*-acetyltryptophan protons after titration with complex **3** ($\Delta\delta$ = ±0.001 ppm).

The enhancement of π- π stacking interactions, and especially the high Ka associated with the 1-MeCyt system, may have interesting applications. Recently, the recognition between the viral nucleocapsid protein (NCp7) of HIV-1 to single strand RNA and DNA has been shown to involve tryptohan(phenylalanine)/guanine(cytosine) stacking

interactions.[9] The understanding of the protein/RNA(DNA) recognition is important in this case for a better understanding of how to rationally design selective Zn-finger inhibitors (usually acting through active-site Zn ejection), a target of increasing interest in antiviral therapy .[10] In parallel, the potential for simple platinum complexes to eject zinc from zinc-finger environments has been demonstrated.[11] Complexes of general formula [*SP-4-2*]-$[PtCl(nucleobase)(NH_3)(L)]^+$, where L = a planar heterocyclic ligand isoquinoline, quinoline etc.) have some anti-HIV activity and high specificity towards S-donor ligands and Zn is displaced from the NCp7 C-terminal finger.[4b] The complex [*SP-4-2*]-$[PtCl(NH_3)(9\text{-}EtGH)(quinoline)]$ gave a K_a of 12.9 x 10^3 M^{-1} (at 20 °C) and in this case the Pt(9-EtGH)/Trp interaction may be considered to serve as a template for specific recognition - sequence-selective targeting of zinc-fingers would be feasible when the platinated nucleobase is incorporated into consensus oligonucleotide strands.[12]

The applicability of complex **3** as a probe for the protein environment of l-tryptophan was studied. The 66 kDa protein Human Serum Albumin (HSA) has one Trp residue on position 214 which has been used extensively to study conformational changes in the protein upon binding events to a host of ligands including metal complexes and organic drugs.[13] The fluorescence quenching of HSA by **3** leads to a blue shift from 350 to 344 nm with a calculated association constant of 8.6 (6) x10^3 M^{-1}, very close to that for the Trp-only system. The binding constant reported for *cis*-DDP and HSA is an order of magnitude smaller, 0.85 x10^3 M^{-1}. [14] The Ka value and the instant quenching upon interaction of complex **3** with HSA suggests a direct access to the Trp residue within the hydrophobic pocket in the protein's IIA subdomain, one of the principal regions for ligand binding sites

in HSA. It is possible that small, diffusible molecules such as **3** can find further use as probes for reporter tryptophan in proteins and protein-DNA interactions.

3.3.2. Spectroscopic evidence of rotamers in complexes 3 and 4:

As can be seen in figure 3.5., a low field ^{1}H-NMR spectrum for **3** (9.5 – 5.5 ppm) in d^{7}-DMF shows the 5 amine protons in dien, specifically the proton in the central NH moiety which has a *trans* position to the 1-MeCyt and exhibits a broad doublet where the signals are not of the same intensity.

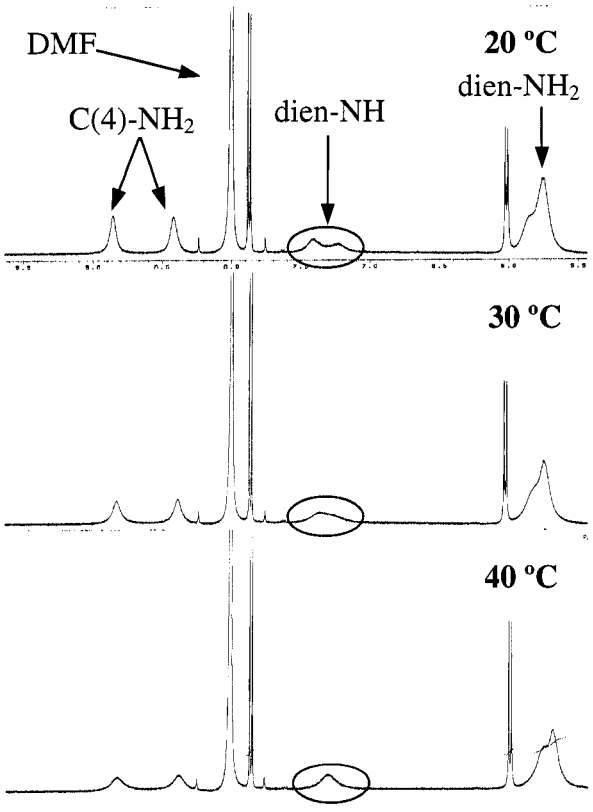

Figure 3.5. Low field ^{1}H-NMR spectrum of **3** showing the coalescence in the NH proton from diethylenetriamine (dien) as function of temperature.

The behavior of this signal was followed at higher temperatures and it could be noticed a coalescence of the signal at 40°C. The signals corresponding to the dien-NH_2 protons also exhibited changes that could suggest coalescence, though according to the spectrum maybe higher energies are required for complete coalescence.

The presence of rotamers is observed for complex **4** as well, which exhibits a similar ^{195}Pt-NMR spectrum to that of **3** (Fig. 3.6.). If a hindered rotation about the Pt-N3 axis is accepted, then two rotamers could arise due to the different functional groups present in the cytosine ligand.

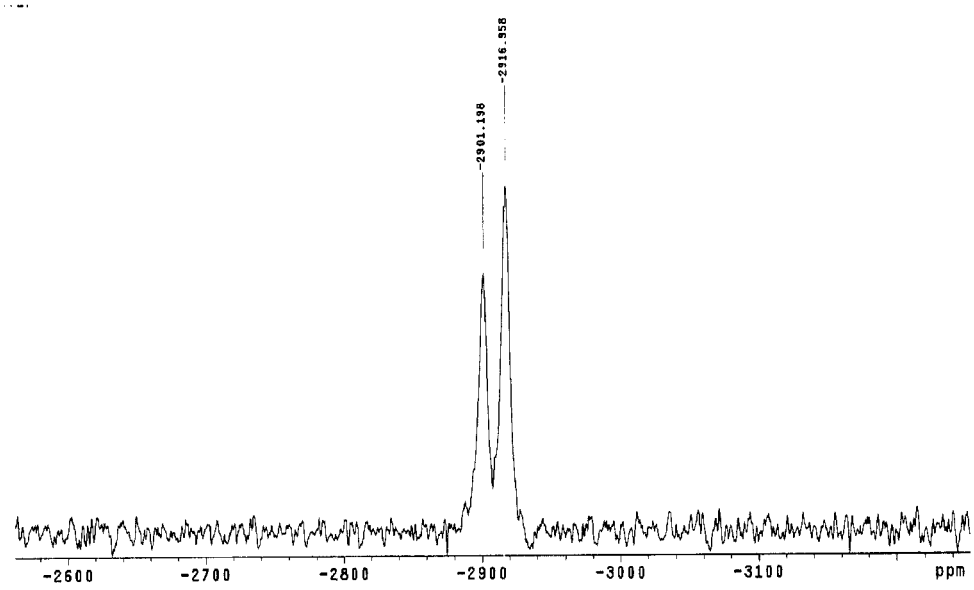

Figure 3.6. ^{195}Pt-NMR signal of **4** at 20°C.

3.4. Experimental Section:

Materials. 9-EtGH, 5'-GMP, 1-MeCyt, Iq, pyrimidine, Trp and N-AcTrp were obtained from Sigma-Aldrich Co.; complex $[Pt(dien)(NO)_3](NO_3)$ was synthesized according to reported procedures.[15]

Nuclear Magnetic Resonance experiments, ^1H NMR spectra were recorded on a Varian Inova series 400 MHz Spectrometer using a 5-mm tube; chemical shifts were referenced to the residual signal in D_2O (4.69 ppm) and DMF-d_7 (8.00 ppm). ^{195}Pt NMR spectra were recorded on a Varian Mercury series 300 MHz NMR Spectrometer using a 10 mm tube. Chemical shifts were referenced to $K_2[PtCl_6]$. The scanning frequency for ^{195}Pt nuclei was set at 64.32 MHz.

Fluorescence experiments. In a typical experiment, 3 mL of a Trp or HSA solution (5 μM) were titrated with aliquots of the corresponding quenching system (7.5 mM) in the range [Trp]/[Quencher] = 10 – 100, buffer Tris-HCl 20 mM was used in all experiments (pH = 5.2). The maximum intensity of the spectrum (ca. 357 nm for Trp and 344 nm for HSA) was measured for each addition and the association constants for each system were obtained from the analysis of Eadie-Hofstee plots[16], reported K_a's were average over a number of six different experiments. Significance of results was compared using unpaired t-test. Fluorescence spectra were recorded at a scan rate of 120 nm/min, in the range from 295 to 450 nm. All measurements were performed at 20 °C.

Electrospray Ionization Mass Spectrometry (ESI-MS). Mass Spectrometric analysis was carried out on a Micromass Q-Tof™ 2 quadrupole/time-of-flight spectrometer (TOF-MS) fitted with a dual electrospray source.

3.4.1. Synthesis and characterization of complexes 1 - 6:

[Pt(dien)(9-EtGH)]$(NO_3)_2$ (1): Complex **1** was prepared by a similar reported procedure[17] heating at 50°C equimolar quantities of [Pt(dien)$(NO)_3$](NO_3) and 9-EtGH in DMF for 24 h., then placed at 0 °C overnight and finally filtering and washing with ethanol and ether (80 % yield). Anal. Calcd for $C_{11}H_{22}O_7N_{10}Pt$: C, 21.96; H, 3.69; N, 23.29. Found: C, 22.06; H, 3.35; N, 23.34%. ESI-MS: m/z = 238.7 $[Pt(dien)(9\text{-}EtGH)]^{+2}$; ^{1}H-NMR in D_2O: δ 8.05 (s, 1 H), 4.00 (q, 2 H), 2.91 (m, 8 H), 1.30 (t, 3 H). ^{195}Pt-NMR in D_2O: δ -2847.

Pt(dien)(5'-GMP) (2): Complex **2** was synthesized according to the literature[1], washed extensively with methanol to remove any $NaNO_3$ impurity. ESI-MS: m/z = 660 [Pt(dien)(5'-GMP)] + H^+; ^{1}H-NMR in D_2O: δ 8.74 (s, 1 H), 5.92 (d, 1 H), 4.53 (t,1H), 4.39 (t, 1H), 4.25 (m, 2 H), 3.95 (m, 2H), 2.95 (m, 8 H). ^{195}Pt-NMR in D_2O: δ -2865.

[Pt(dien)(1-MeCyt)]$(NO_3)_2$ (3): Complex **3** was prepared by heating at 50°C equimolar quantities of [Pt(dien)$(NO)_3$](NO_3) and 1-MeCyt in H_2O for 4 h., then allowing to cool at r.t. and liophilized. The white precipitate was then passed through a Sephadex G-10 column and washed with methanol and ether to separate unreacted base (50 % yield). Excess of unreacted base can also be separated by extensive methanol washing improving the yield up to 80%. Anal. Calcd. for $C_9H_{20}O_7N_8Pt$: C, 19.74; H, 3.69; N, 20.47. Found: C,

19.75; H, 3.49; N, 20.20 %. ESI-MS: m/z = 211.8 $[Pt(dien)(1\text{-}MeCyt)]^{+2}$; ^{1}H-NMR in D_2O: δ 7.43 (d, 1 H), 5.85 (d, 1 H), 3.26 (s, 3 H), 2.87 (m, 8 H), ^{195}Pt-NMR in D_2O: δ -2904 (d).

Pt(dien)(5'-CMP) . $2NaNO_3$. $2H_2O$ (4): Complex **4** was synthesized analogously to complex **2**, and washed with water, ethanol and ether (70 % yield). Anal. Calcd. for $C_{13}H_{29}O_{16}N_8PPtNa_2$: C, 18.91; H, 3.55; N, 13.58. Found: C, 19.22; H, 3.85; N, 13.09 %. FAB-MS: m/z = 620.27 $[Pt(dien)(5'CMP)+H]^{+}$. ^{1}H-NMR in D_2O: δ 8.07 (dd, 1 H), 6.06 (dd, 1 H), 5.85 (s, 1 H), 4.21 (m, 2 H), 4.12 (s, 1H), 3.86 (m, 2H), 2.87 (m, 8H). ^{195}Pt-NMR in D_2O: δ -2908 (d).

[Pt(dien)(pyrimidine)]$(NO_3)_2$. H_2O (5): Complex **6** was prepared analogously to **5**. The presence of only one pyrimidine per complex molecule was confirmed by the presence of 4 signals with the ratio 1:1:1:1 in the aromatic region of the ^{1}H-NMR, whereas due to symmetry conditions only 3 signals with ratio 1:1:2 were expected in the case of {$[Pt(dien)]_2$(pyrimidine)}. The proposed composition was also confirmed by elemental analysis. Anal. Calcd. for $C_8H_{19}O_7N_7Pt$: C, 18.46; H, 3.69; N, 18.84. Found: C, 18.80; H, 3.10; N, 18.98 %. ; ^{1}H-NMR in D_2O: δ 9.27 (s, 1 H), 8.89 (d, 1 H), 8.77 (d, 1 H), 7.59 (t, 1H), 2.90 (m, 8H).

[Pt(dien)(Iq)]$(NO_3)_2$. $0.7H_2O$ (6): Complex **7** was prepared by adding Isoquinoline to a solution of $[Pt(dien)(NO)_3](NO_3)$ in water and then heating at 50 °C for 4 h. The solution was lyophilized to produce a white solid which was washed extensively with acetone and ether, then dried *in vacuo*. (70 % yield). Anal. Calcd. for $C_{13}H_{21.4}O_{6.7}N_6Pt$: C, 27.68; H,

3.82; N, 14.90. Found: C, 27.51; H, 3.67; N, 15.19 %. ; ESI-MS: m/z = 426.1 $[Pt(dien)(Iq)-H]^+$. ^{1}H-NMR in D_2O: δ 9.35 (s, 1 H), 8.35(d, 1H), 8.05 (d, 1H), 7.93 (d, 1H), 7.85 (m, 2H), 7.72 (t, 1H), 2.95 (m, 8 H); ^{195}Pt-NMR in D_2O: δ -2842.

Fluorescence quenching experiments: The association constant (K_a) for the different systems was obtained using the Eadie-Hofstee equation:

$$\Delta F = - (1/K_a) \times (\Delta F/[Quencher]) + \Delta F_c$$

Where ΔF is the difference between fluorescence intensities of Trp in the presence and absence of the quencher, and ΔFc is the difference when Trp is completely complexed with nucleic acid. From a plot of ΔF vs. (ΔF/[Quencher]) the value of Ka can be obtained from the slope of the line: m = - 1/Ka. Association constants (Ka's) between complexes 1- 4 were found as described in the experimental section, the values are compared in Figure 3.7.

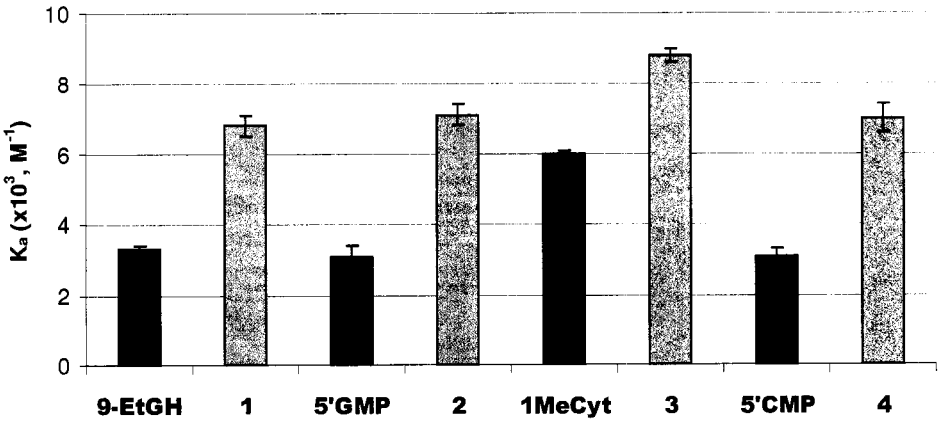

Figure 3.7. Association constants obtained for complexes **1 – 4** compared with the corresponding free nucleobases.

3.5. Conclusions.

In a broad sense, bioinorganic chemistry is the application and use of intrinsic properties of metal complexes (redox properties, substitution kinetics, ligand donor preferences and steric effects) to effect biological responses. The above results suggest further systematic manipulation of metal-ligand properties may serve as a motif for molecular recognition in protein-nucleic acid complexes.

3.6. References:

(1) (a) Hélène, C.; Lancelot, G., *Prog. Biophys. Mol. Biol.*, **1982**, 39, 1-68. (b) Hamilton, A.D.; Phillips, S.E.V.; Moras, D., *Curr. Opin. Struct. Biol.*, **1993**, 3, 11-16. (c) Nowakowski, J.; Shim, P.J.; Prasad, G.S.; Stout, C.D.; Joyce, G. F., *Nature Struct. Biol.*, **1999**, 6, 151-156. (d) Meyer, E.A.; Castellano, R.K.; Diederich, F., *Angew. Chem. Int. Ed.*, **2003**, 42, 1210 -1250.

(2) (a) Ishida, T.; Ueda, H.; Segawa, K.; Doi M.; Inoue, M., *Arch. Biochem Biophys.*, **1990**, 278, 217-227. (b) Ishida,T.; Tarui, M.; In,Y.; Ogiyama, M.; Doi, M.; Inoue, M., *FEBS Lett.*,**1993**, 333, 214 - 216. (c) Kawai, H.; Tarui, M.; Doi, M.; Ishida, T., *FEBS Lett.*,**1995**, 370, 193 -196.

(3) (a) Hitchcock, A. P.; Lock, C.J.L.; Pratt, W.M.C.; Lippert, B., In Platinum, gold and other chemotherapeutic agents: chemistry and biochemistry. Lippard, S.J. ed., A.C.S.

Washington, **1983**, p. 209. (b) Brüning,W.; Ascaso, I.; Freisinger, E.; Sabat, M.; Lippert, B., *Inorg. Chim. Acta.*, **2002**, 339, 400 - 410.

(4) Sartori, D.A.; Miller, B.; Bierbach, U.; Farrell, N., *J. Biol. Inorg. Chem.*, **2000**, 5, 575 - 583.

(5) Arpalathi, J.; Klika, K.D.; Sillampää, R.; Kivekäs, R., *J. Chem. Soc., Dalton Trans.*, **1998**, 8, 1397 - 1402.

(6) (a) Pokalsky,C.; Wick, P.; Harms, E.; Lytle, F.E.; Van Etten, R.L., *J. Biol. Chem.*, **1995**, 270, 3809 - 3815. (b) Hotopp, J.C.D.; Auchtung, T.A.; Hogan, D.A. ; Hausinger, R.P., *J. Inorg. Biochem.*, **2003**, 93, 66 - 70.

(7) Kawai, H.; Tarui, M.; Doi, M.; Ishida,T.; *FEBS Lett.*, **1995**, 370, 193 - 196.

(8) Elduque, A.; Carmona, D.; Oro, L.A.; Eisenstein, M.; Fish, R.H., *J. Organomet. Chem.*, **2003**, 668, 123 - 127.

(9) (a) De Guzman, R.N.; Wu, Z.R.; Stalling, C.C.; Pappalardo, L.; Borer, P.N.; Summers, M.F., *Science*, **1998**, 279, 384 - 388. (b) Morellet, N.; Déméné, H.; Teilleux, V.; Huynh-Dinh, T.; De Rocquigny, H.; Fournié-Zaluski, M.C.; Roques, B.P., *J. Mol. Biol.*, **1998**, 283, 419 - 434.

(10) (a) Rein, A.; Henderson, L.E.; Levin, J.G., *TIBS*, **1998**, 23, 297 - 301. (b) Stephen, A.G.; Rein, A.; Fisher, R.J.; Shoemaker, R.H., *Curr. Drug Discov.*, **2003**, Aug 33.

(11) (a) Darlix, J.L.; Gabus, C.; Nugeyre, M.T.; Clavel, F.; Barre-Sinoussi, F., *J .Mol. Biol.*,**1990**, 216, 689 - 699. (b) Volckova, E.; Evanics, F.; Yang, W.W.; Bose, R.N., *Chem Commun.*, **2003**, 10, 1128 - 1129.

(12) Louie, A. Y.; Meade, T. J., *Proc. Natl. Acad. Sci. USA.*, **1998**, 95, 6663 - 6668.

(13) Esposito, B. P.; Najjar, R. *Coord. Chem. Rev.* **2002**, *232*, 137 - 149.

(14) Neault, J. F.; Tajmir-Riahi, H. A. *Biochim. Biophys. Acta* **1998**, *1384*, 153 – 159.

(15) Pasini, A.; Fiore, C.; *Inorg. Chim. Acta.*, **1999**, 285, 249 - 253.

(16) Eadie, G.S., *J. Biol. Chem.*, **1942**, 146, 85 – 93.

(17) Frommer, G.; Schöllhorn, H.; Thewalt, U.; Lippert, B., *Inorg. Chem.*, **1990**, 29, 1417 - 1422.

CHAPTER 4 Covalent and Noncovalent Interactions for [Metal(dien)nucleobase]$^{2+}$ Complexes with l-tryptophan Derivatives: Formation of Palladium-Tryptophan Species by Nucleobase Substitution under Biologically Relevant Conditions

Atilio I. Anzellotti[a], Michal Sabat[b] and Nicholas P. Farrell[a]*

a. Department of Chemistry, Virginia Commonwealth University, 1001 W. Main St.

Richmond, VA 23284-2006, USA.

b. Department of Chemistry, University of Virginia.

Inorganic Chemistry, **2006**, 45 (4), 1638 - 1645

4.1. Abstract:

Fluorescence quenching experiments show that the stacking interaction between nucleic acid bases and l-tryptophan is enhanced significantly upon base coordination to a metal center such as Pt(II) and the biological implications of such enhancement are discussed.

4.2. Introduction:

Nucleobase coordination to platinum centers in [Pt(dien)(nucleobase/nucleotide)]$^{2+}$ complexes significantly enhances its π-π stacking interactions with l-tryptophan as measured through fluorescence quenching experiments.[1] This interaction may represent a novel motif for biomolecule targeting and molecular recognition by metal-nucleobase (nucleic acid) complexes. The study of new chemical structures may also lead to hitherto unrecognized novel biological functions and, to fully exploit the structural motif, it is necessary to explore the extent of kinetic and structural flexibility within any given system.

In the case of the $[Pt(dien)(nucleobase/nucleotide)]^{2+}$ system, the effect of metal center and kinetic lability on π-π stacking interactions may be studied using isoelectronic and isostructural palladium analogues. Palladium (II) complexes with chelating ligands such as ethylenediamine (en) or diethylenetriamine (dien) have been extensively used to model the covalent interaction of analogous platinum (II) complexes with nucleobases, nucleosides and nucleotides. The high reactivity exhibited by the palladium systems (up to 10^6 faster hydration kinetics) makes possible the study of binding equilibria which are sometimes difficult to determine for inert platinum(II) complexes.[2-6]

Palladium-peptide interactions are of relevance because of the hydrolysis of the peptide bond catalysed by palladium complexes.[7] The effect of ligand $\{Pd(en)^{2+}, Pd(terpy)^{2+}\}$ has been extensively studied for steric effects as well as peptide substrate specificity. Additionally palladium (II) and platinum (II)-tryptophan interactions are of specific significance due to the highly regioselective hydrolysis of tryptophan-containing peptides promoted by bifunctional $[M(en)]^{2+}$ (M = Pd, Pt) complexes.[8,9] More recently, the use of the $[Pd(en)]^{2+}$ moiety as a metal clip to stabilize peptide turns and short α-helices in 5-15-residue non-helical peptides is made possible by the correct combination of structure and reactivity of the palladium center – more labile complexes form transient metallopeptides whereas less inert analogues may form kinetically inert nonhelical metallopeptides.[10-12] In addition, the use of phosphine-modified peptides as ligands in palladium catalysts in order to create artificial secondary structures such as the β-turn, modulates the enantioselectivity

of allylation reactions with cyclic substrates thus extending the applications of this palladium-peptide chemistry to the fields of asymmetric catalysis and synthesis.[13]

The interactions of metal-nucleobase/nucleotide complexes, often produced and studied *in situ*, with other relevant biologic substrates, and the properties of ternary metal-nucleobase-peptide species in general, have not been extensively studied.[14-16] In this work we study the interaction between $[Pd(dien)nucleobase]^{2+}$ complexes and the aminoacid l-tryptophan and N-acetyl tryptophan (Chart 4.1.).

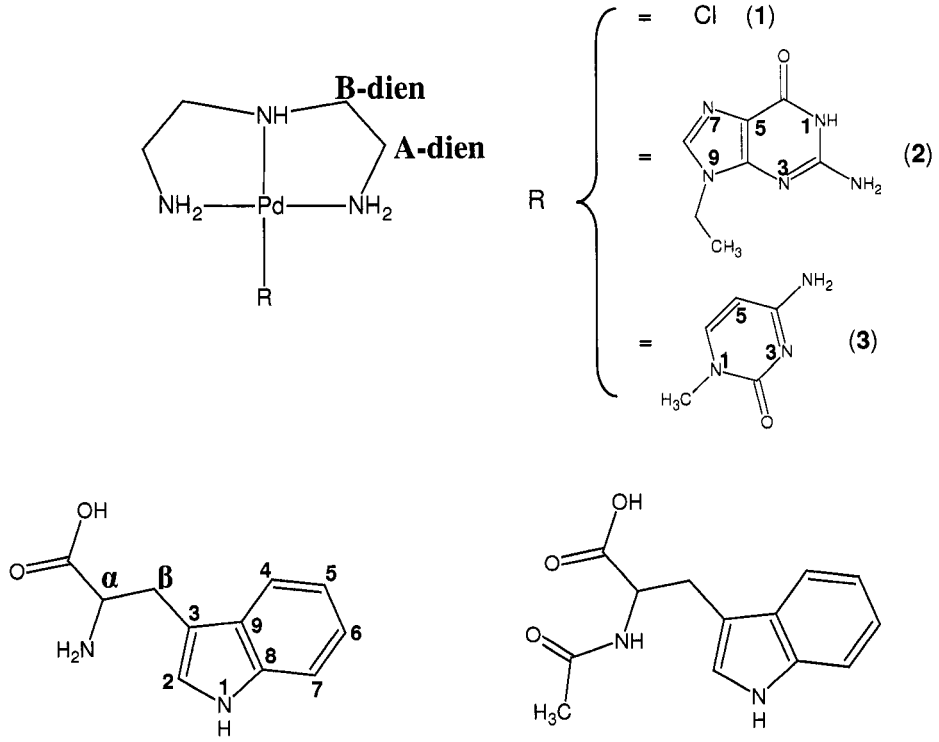

l- tryptophan N- Acetyl-tryptophan

Chart 4.1. Representation of structures for compounds used on this study with numbering scheme.

Comparison is made with their platinum analogues and evidence for a novel covalent interaction with l-tryptophan through nucleobase substitution and the structural characterization of the palladium-tryptophan moiety is reported.

4.3. Results and Discussion.

4.3.1. Crystal Structure of [Pd(dien)(1-MeCyt)]$(NO_3)_2$ (2) and [Pt(dien)(1-MeCyt)]$(NO_3)_2$ (4). The cations of complexes **2** and **4** are very similar except for the torsional angle formed between the nucleobase plane and the Pt,Pd-diethylenetriamine moiety, Figure 4.1.

The 1-MeCyt ligand is not completely perpendicular to the coordination square plane and appreciable deviations of 12.22° and 23.51° for **2** and **4** are found respectively. Reported crystal structures for the analogous complexes with cytosine ligand featured smaller deviations from perpendicularity for the nucleobase 9.14° (Pd) and 3.81° (Pt).[17] Interestingly enough these latter complexes favor the opposite rotamer observed for **2** and **4** (N4C-endo, Fig. 4.1.), which is generated due to hindered rotation in the Pd,Pt-N bond. A N-H···O interaction between the carbonyl moiety in 1-MeCyt and one of the hydrogens in the terminal amines in the dien ligand can be appreciated, this interaction appears stronger in the case of the platinum complex as indicated by a shorter distance and more linear angle compared with the palladium counterpart 2.547 Å vs. 2.955 Å and 116° vs. 131° respectively (Fig. 4.2.).

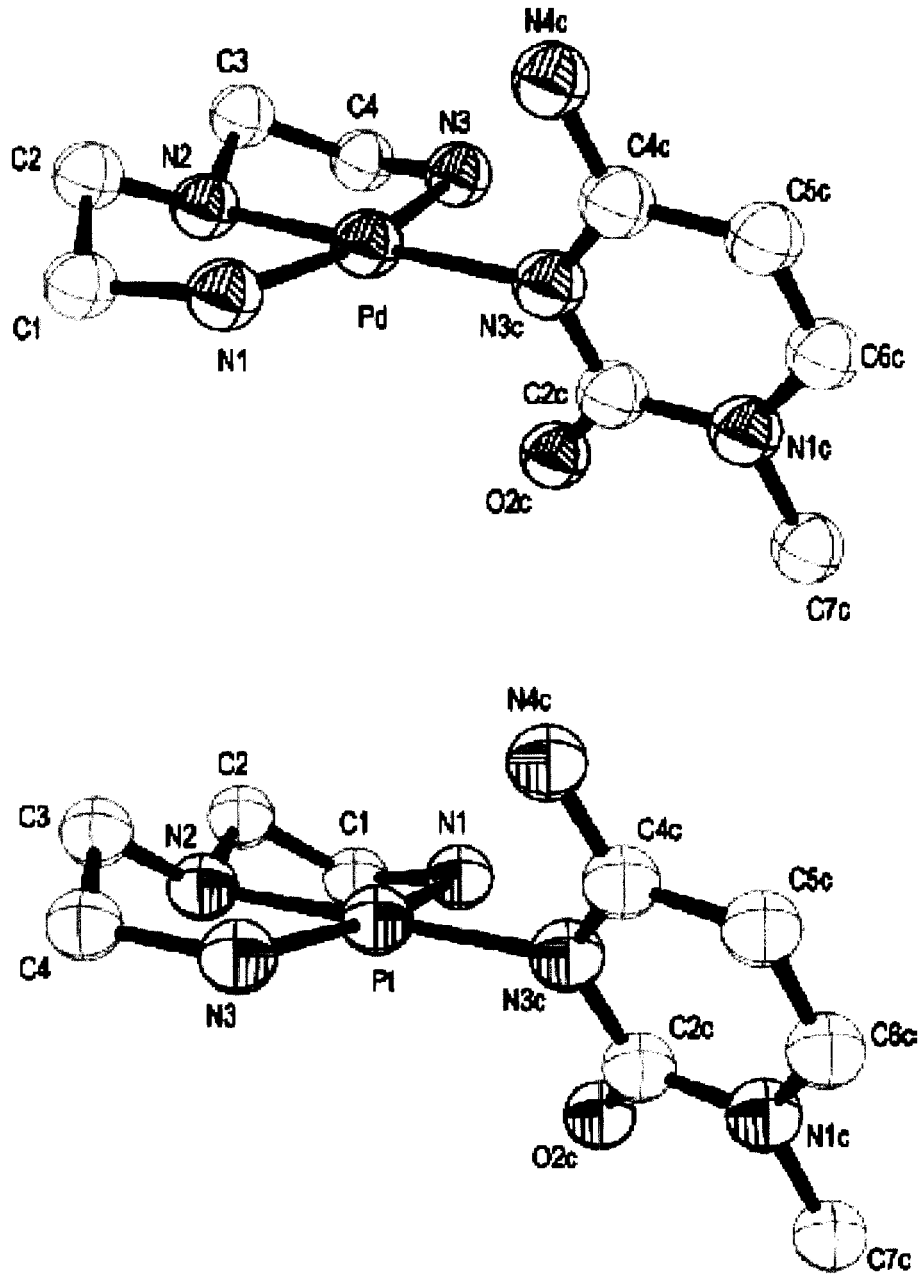

Figure 4.1. ORTEP diagram of $[Pd(dien)(1\text{-}MeCyt)]^{2+}$ (top) and $[Pt(dien)(1\text{-}MeCyt)]^{2+}$ (bottom) with numbering scheme (50% probability ellipsoids). Hydrogens atoms omitted for clarity.

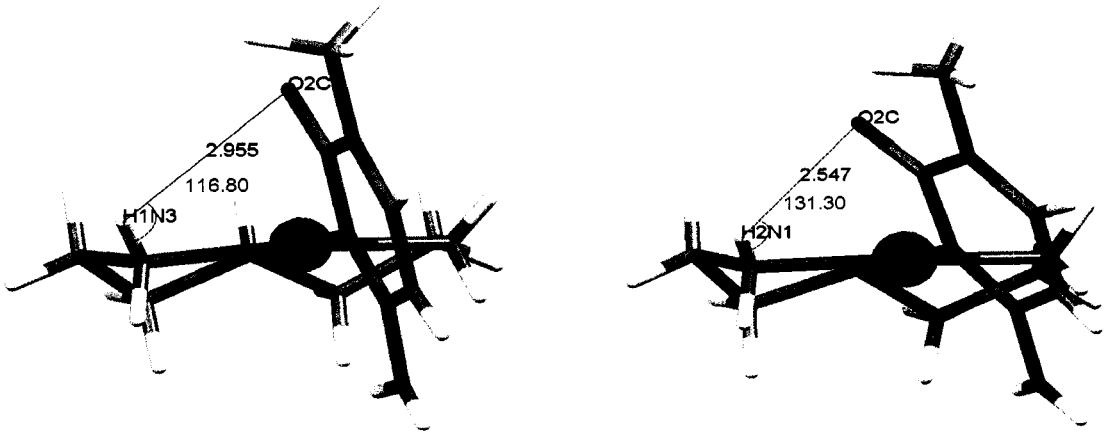

Figure 4.2. N-H···O distance (in black) and angle (in blue) for complexes [Pd(dien)(1-MeCyt)]$^{2+}$ (**2**) left and [Pt(dien)(1-MeCyt)]$^{2+}$ (**4**) rigth.

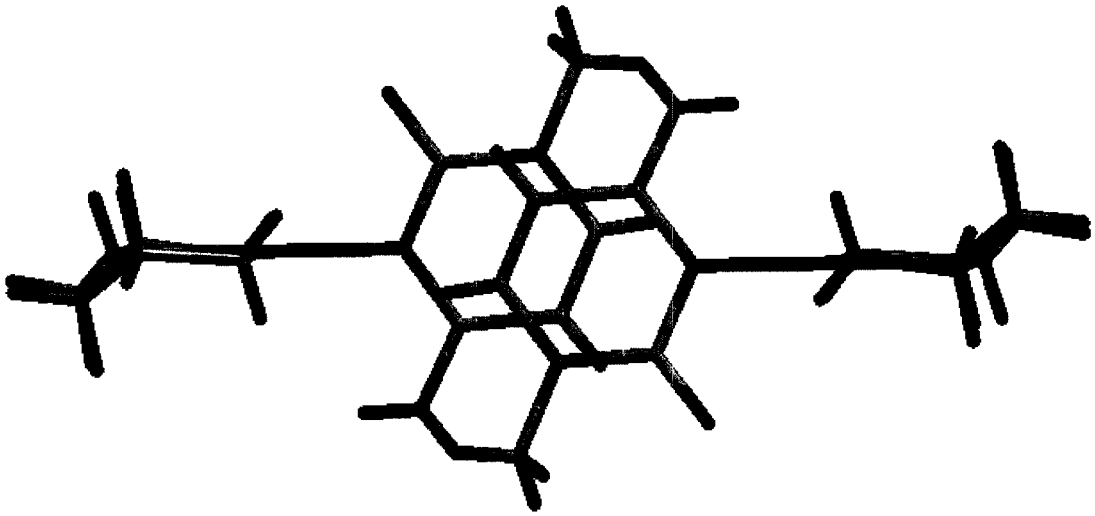

Figure 4.3. View of nucleobase stacking for complex [Pd(dien)(1-MeCyt)]$^{2+}$.

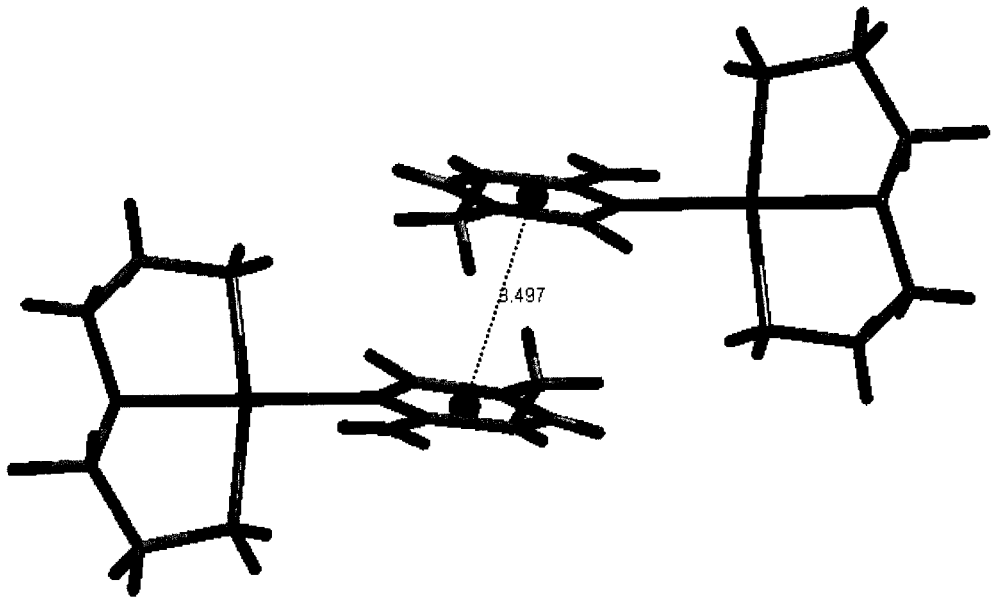

Figure 4.4. View of nucleobase stacking for complex $[Pt(dien)(1\text{-}MeCyt)]^{2+}$, showing distance between centroids on the aromatic rings.

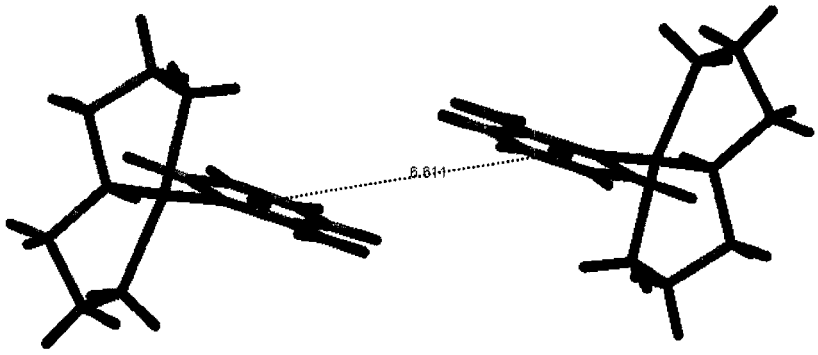

Figure 4.5. View of nucleobase interaction complex $[Pt(dien)(cytosine)]^{2+}$, showing distance between centroids on the aromatic rings and the absence of stacking, from ref. 39.

The presence of the methyl moiety modifies the intermolecular hydrogen-bonding pattern between cations in the solid state to a significant extent, since Cyt/Cyt (N1H-O2) interactions are replaced by dien/1-MeCyt (O2C-N2H) interactions. Also, the stacking interaction among 1-MeCyt's can be noticed with an approximate internucleobase distance of 3.4 Å (**2**) and 3.5 Å (**4**), which is not exhibited in the cytosine analogs (figs. 4.3.- 4.5.).

This fact could correlate with recent calculations performed at the second-order perturbation theory (MP2) level showing that the presence of substituents on an aromatic ring contribute favorably to face-to-face stacking interactions by better distributing the electrostatic potential in the surface of the nucleobase. [18]

The ring-plane overlap is appreciable since a ring overlap of less than 30% is the common feature for an offset or slipped stacking mode of interaction, according to a recent geometrical analysis on complexes with aromatic nitrogen heterocycles as ligands (7620 datasets). Contribution from π-σ attraction as stated in the Hunter-Sanders rule is not discarded since a slight offset between the nucleobase's planes is observed. [19] Bond lengths and bond angles are as expected. Table 4.I. summarizes crystallographic data and details of refinement for compounds **2** and **4** ; also selected interatomic distances and angles are shown in Table 4.II.

Table 4.I. Crystallographic data and details of refinement for compounds **2** and **4**.

	2	**4**
Formula	$C_9H_{20}N_8O_7Pd$	$C_9H_{20}N_8O_7Pd$
Formula weight	458.73	547.42
Crystal color and habit	Colorless plate	Colorless plate
Temperature (K)	153 (2)	153 (2)
Crystal size (mm)	0.31 x 0.28 x 0.12	0.28 x 0.26 x 0.08
Crystal system	triclinic	triclinic
Space group	P-1	P-1
a (Å)	9.6993 (5)	8.9086 (5)
b (Å)	9.8688 (5)	10.4677 (6)
c (Å)	10.2130 (5)	10.6379 (6)
α (°)	66.6210 (10)	61.3910 (10)
β (°)	67.1570 (10)	67.7770 (10)
γ (°)	74.0060 (10)	73.1150 (10)
Volume ($Å^3$)	818.38 (7)	798.87 (8)
Z	2	2
D_{calc} ($Mg/m^{3)}$	1.862	2.276
μ (Mo Kα) (mm^{-1})	1.188	8.838
F(000)	464	528
Theta range for data collection	2.27-32.54	2.24-32.49
Reflections collected	5398	5634
Reflections observed	4823	4289
Number of parameters refined	306	302

R_{int}	0.015	0.051
R_1 (observed data)	0.0242	0.0447
wR_2 (observed data)	0.0519	0.0754
Residual ρ_{max}, ρ_{min} (c Å^{-3})	0.851, -0.638	3.891, -2.483

Table 4.II. Selected interatomic distances (Å) and angles (°) for **2** and **4**.

	2	**4**
Pd/Pt-N1	2.0494 (16)	2.039 (5)
Pd/Pt-N2	2.0001 (14)	2.018 (5)
Pd/Pt-N3	2.0429 (15)	2.056 (5)
Pd/Pt-N3c	2.0462 (13)	2.045 (5)
N2-Pd/Pt-N3	84.16 (6)	83.4 (2)
N2-Pd/Pt-N3c	178.40 (6)	179.6 (2)
N3-Pd/Pt-N3c	94.31 (6)	97.0 (2)
N2-Pd/Pt-N1	84.17 (6)	84.4 (2)
N3-Pd/Pt-N1	167.10 (6)	167.7 (2)
N3c-Pd/Pt-N1	97.40 (6)	95.2 (2)

4.3.2. Study of the tryptophan/N-acetyltryptophan interaction with [M(dien)(nucleobase)]$(NO_3)_2$, M=Pt,Pd. The complexes [Pd(dien)Cl]Cl (**1**), [Pd(dien)(1-MeCyt)]$(NO_3)_2$ (**2**) and [Pd(dien)(9-EtGH)]$(NO_3)_2$ (**3**) were synthesized and characterized through microanalysis and spectroscopic techniques. The chloride complex

was used as control for palladium-peptide interactions in the absence of nucleobase. The chemical behavior of **1-3**, as well as **4** and **5**, toward Trp and N-AcTrp was examined over a range of pH.

4.3.2.a. Evidence for formation of the covalent [Pd(dien)(l-Tryptophan)]$^+$complex.

Mass Spectrometry.

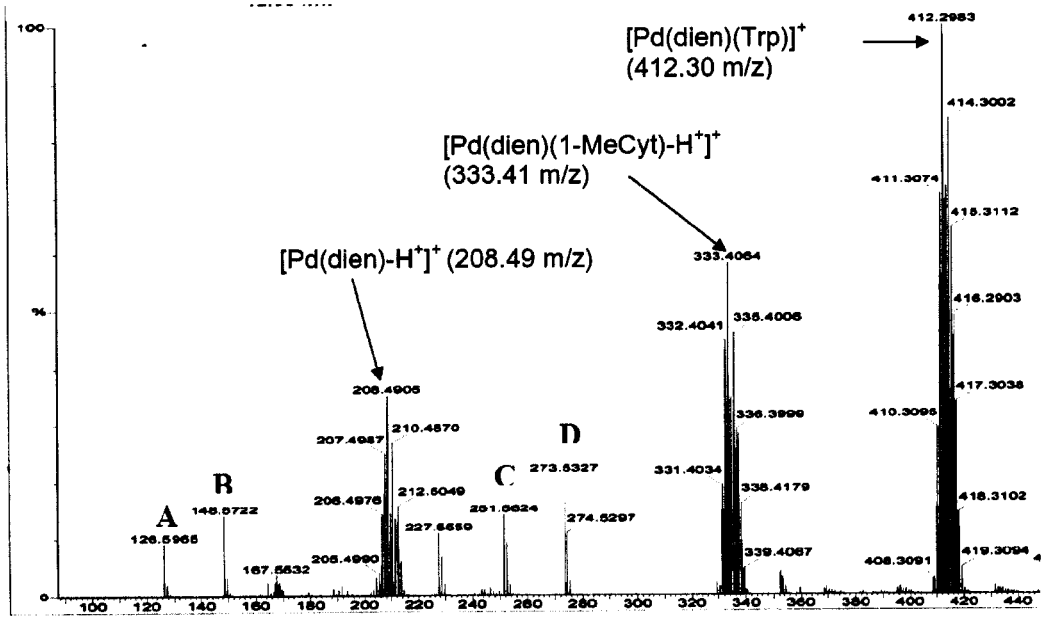

Figure 4.6. ESI-MS spectrum of a [Pd(dien)(1-MeCyt)]$^{2+}$ / Trp solution (pD = 9.0), major species are indicated, minor signals were assigned as follows: A = [1-MeCyt +H$^+$]$^+$,(126.6 m/z); B = [1-MeCyt + Na$^+$]$^+$, (148.6 m/z) ; C = [(1-MeCyt)$_2$ + H$^+$]$^+$, (251.6m/z); D = [(1-MeCyt)$_2$ + Na$^+$]$^+$, (273.6 m/z).

ESI-MS spectra of the systems **1-3**/Trp taken at pD > 9.0 (pD = pH* + 0.4[20], where pH* is the measurement of the pH meter), showed signals corresponding to the starting complexes, i.e. **1**: [Pd(dien)Cl]$^+$ (m/z = 246.0); **2**: [Pd(dien)(1-MeCyt)-H$^+$]$^+$ (m/z = 333.4) and **3**: [Pd(dien)(9-EtGH)-H$^+$]$^+$ (m/z = 387.2), along with a strong signal at m/z = 412.3(1)

which was assigned to the species $[Pd(dien)(Trp)]^+$ due (i) to the presence of the characteristic isotopic distribution for the palladium atom and (ii) a single net positive charge, determined from the average m/z value between peaks in the signal. Figure 4.6. shows the ESI-MS spectrum for the system **2**/Trp where, besides the signals due to Pd-nucleobase and Pd-Trp complexes, an additional signal also exhibiting the isotopic distribution of palladium is assigned to the species $[Pd(dien)\text{-}H^+]^+$ (m/z = 208.5). The loss of a proton from the diethylentriamine ligand was a general observation in all the palladium complexes studied here and has been reported to sometimes occur under ESI-MS conditions for other metal complexes, as well.[21]

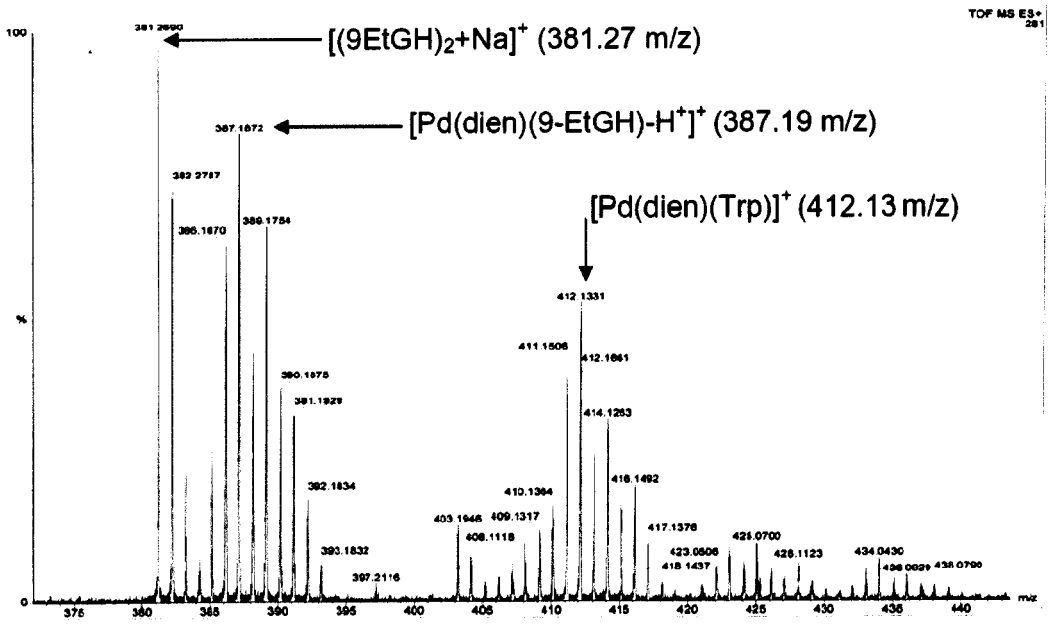

Figure 4.7. ESI-MS spectrum of a $[Pd(dien)(9\text{-}EtGH)](NO_3)_2$ / Trp solution (pD = 9.0), showing the most important species.

For complex **2**, further ESI-MS signals could be assigned to the free nucleobase forming protonated adducts such as $[1\text{-}MeCyt + H^+]^+$ (m/z = 126.6) and $[(1\text{-}MeCyt)_2 + H^+]^+$ (m/z =

251.6) . The corresponding sodium adducts [1-MeCyt + Na^+]$^+$ and [(1-MeCyt)$_2$ + Na^+]$^+$ (m/z = 148.6 and 273.6 respectively) were also observed, and are very likely due to the NaOD added in order to increase the solution pD, Figure 4.6. Signals due to nucleobase adducts with protons and sodium were also observed for system **3**/Trp with 9-EtGH: [9-EtGH + H^+]$^+$ (m/z = 180.6); [(9-EtGH)$_2$ + H^+]$^+$ (m/z = 359.4); [9-EtGH + Na^+]$^+$ (m/z = 202.5) and [(9-EtGH)$_2$+Na^+]$^+$ (m/z = 381.3), Figure 4.7.

Nuclear Magnetic Resonance Spectroscopy. Monitoring of the ^{1}H-NMR spectra of equimolar solutions of **2** and Trp also suggested the formation of the complex [Pd(dien)(Trp)]$^+$ (**6**), generated by the substitution of nucleobase ligand by the amino acid, Figure 4.8. The reaction is pH-dependent and above pH/pD = 5, new signals corresponding to free nucleobase as well as coordinated tryptophan appear with concomitant decrease in the signals of the starting complex and free peptide. The peptide signals undergo a moderate downfield shift in all the aromatic signals, as well as some significant variations in the chemical shifts for α- and β-proton signals, with the α proton signals shifted by almost 1 ppm.

These new signals were consistent upon changes in temperature (20°C – 45°C) and time (two weeks), but, as stated, the intensities exhibited a strong pD dependence. The appearance of signals corresponding to coordinated tryptophan occurs in parallel with signals corresponding to the appearance of free nucleobase.

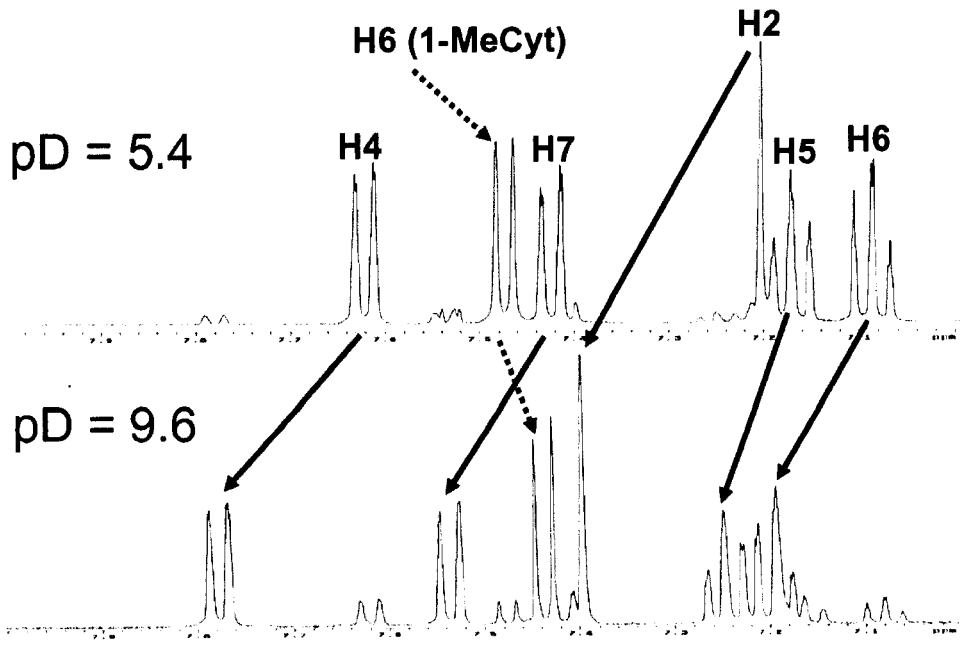

Figure 4.8. Influence of pD on ^{1}H-NMR spectrum from a $[Pd(dien)(1\text{-}MeCyt)]^{2+}$/Trp solution, arrows indicated the shift for coordinated Trp in $[Pd(dien)(Trp)]^{+}$. The peak marked with the dashed arrow corresponds to 1-methylcytosine.

Coordination of 1-MeCyt to the $[Pd(dien)]^{2+}$ group does not cause an appreciable shift of its proton signals, H6 and H5 exhibiting values of 7.47 ppm and 5.85 ppm for the coordinated nucleobase moving to 7.44 ppm and 5.84 ppm respectively for the free base, in agreement with previous results.[22] Shifts for the methyl group of 1-MeCyt were easier to follow since it appeared as a strong singlet: 3.29 ppm (coordinated) and 3.25 ppm (free). In spite of the reported stability of [Pd(dien)(nucleoside/nucleotide)] complexes even under very acidic conditions, complex **2** was found to exhibit 1-MeCyt displacement to some extent even at pD = 2.0. In this case the signals for free nucleobase corresponded to the protonated form and appeared at 7.71 (^{3}J = 7.7 Hz) and 6.03 (^{3}J= 7.7) for H6 and H5, a net downfield displacement of 0.23 and 0.17 ppm respectively. A coupling difference of

0.4 Hz was also observed for both signals (not shown). In this case, a substitution pathway involving hydrolysis through protonation of the 1-MeCyt ligand is indicated.

Table 4.III. ^{1}H-NMR - chemical shifts observed for coordinated and free Trp / N-AcTrp incomplexes **6** and **7**.

	Trp (ppm)	**Pd-Trp (ppm)**	**Δδ (ppm)**	**N-AcTrp (ppm)**	**Pd- N-AcTrp (ppm)**	**Δδ (ppm)**
H4	7.62	7.78, dd, J = 7.9 Hz	+ 0.16	7.56	7.69, dd, J = 8.1 Hz	+ 0.13
H7	7.42	7.53, dd, J = 7.9 Hz	+ 0.11	7.39	7.41, dd, J = 8.1 Hz	+ 0.02
H2	7.20	7.40, s	+ 0.20	7.14	6.97, s	- 0.17
H5	7.17	7.25, t, J = 7.5 Hz	+ 0.08	7.13	6.88, t, J = 7.4 Hz	- 0.25
H6	7.08	7.19, t, J = 7.5 Hz	+ 0.11	7.06	6.99, t, J = 7.4 Hz	- 0.07
Hα	3.88	2.87, m	- 1.01	4.40	4.32, m	- 0.08
Hβ'	3.32	3.36, m	+ 0.04	3.24	3.14, m	- 0.10
Hβ	3.16	3.36, m	+ 0.20	3.20	3.00, m	+ 0.20
CH_3	-	-	-	1.74	1.74, s	0.00

Identical spectral changes of the tryptophan moiety were seen for **1** and **3** and additionally the appearance of free nucleobase was also observed in the latter case. The initial pD values were *ca.* 4.1, 4.8 and 5.0 for **1**/Trp, **2**/Trp and **3**/Trp respectively. The singlet corresponding to the H8 proton in **3** appeared at 7.60 ppm with a downfield shift of 0.38 ppm compared to the free nucleobase. The shift of this signal is a very characteristic diagnostic tool to assess metallation/de-metallation in guanine-derived molecules such as

9-EtGH.[23] For the system **1**/Trp, no additional signals besides the ones for free and coordinated Trp were observed confirming the proposed substitution reaction and ruling out other possible side reactions.

The chemical shifts for free and coordinated Trp are compared in Table 4.III. 2D NMR COSY experiments confirmed the assignments (Figures 4.9. and 4.10.).

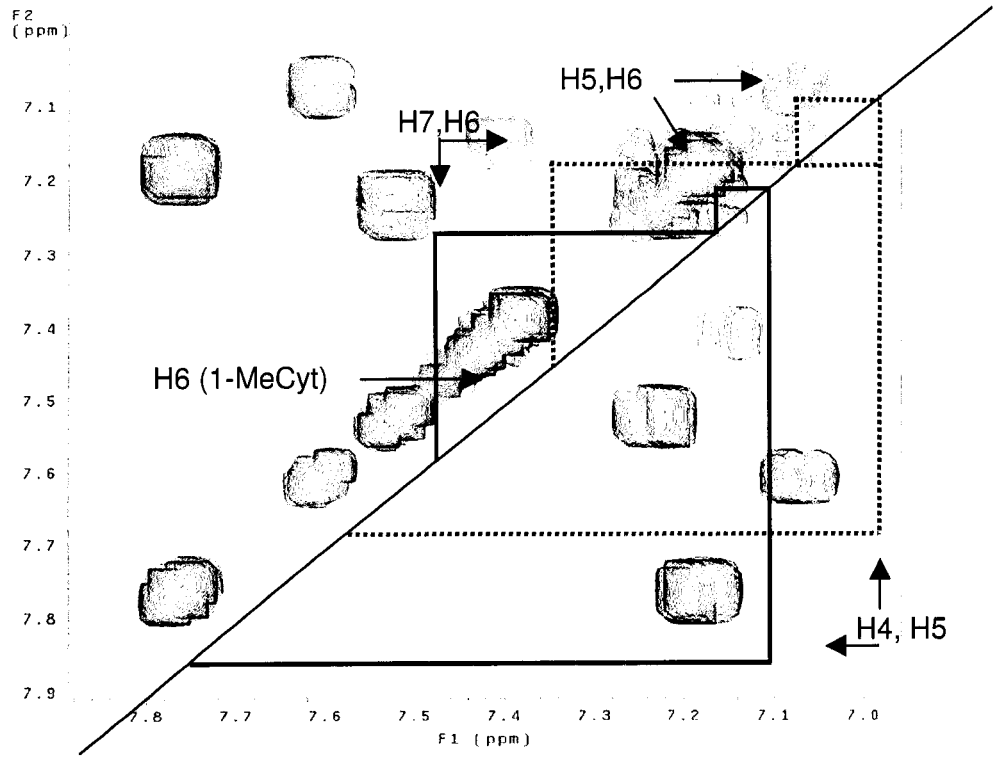

Figure 4.9. Zoom of aromatic region of a 2D NMR COSY from a $[Pd(dien)(1\text{-MeCyt})]^{2+}$ /Trp system (pD = 9.0), showing correlations for free (dashed line) and coordinated Trp (full line).

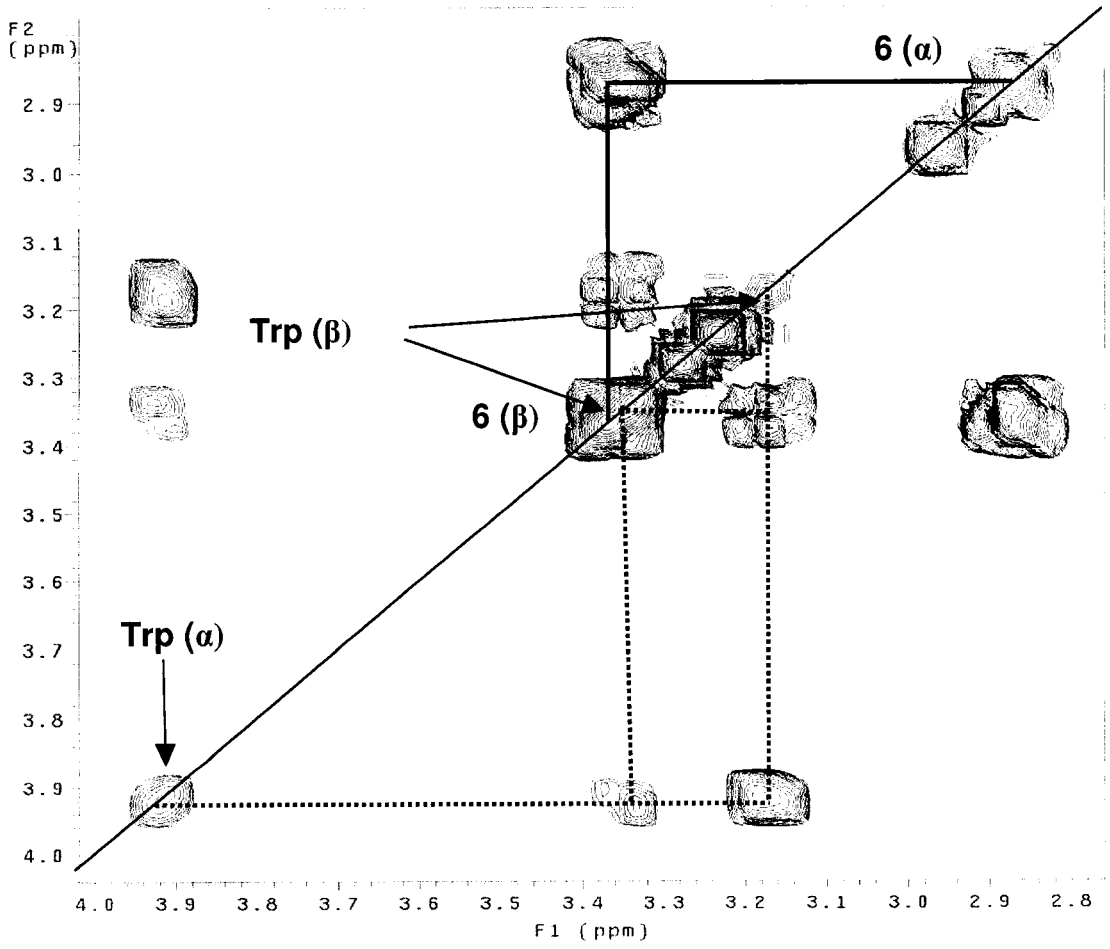

Figure 4.10. Zoom of aliphatic region of a 2D NMR COSY from a [Pd(dien)(1-MeCyt)]$^{2+}$/Trp system (pD = 9.0), showing correlations for free (dashed line) and coordinated Trp (full line).

The signal for the H4 proton in coordinated Trp was used as a good diagnostic to monitor the progress of the formation of complex **6** in the pD range tested. Using the integration for this doublet, a direct comparison between chloride and nucleobase substitution could be made. Substitution of the chloride ligand occurs at a lower pD value compared to both nucleobases suggesting a higher stability in solution for complexes **2** and **3**. It can be estimated that approximately 80 % of the starting material **1** reacted to form $[Pd(dien)(Trp)]^{2+}$, whereas 40% and 25 % is formed from **2** and **3**, respectively, around the physiological pD = 7.4, Figure 4.11. There is a consistently lower rate of $[Pd(dien)(Trp)]^{2+}$ formation from complex **3** compared with **2** at similar pD values, and beyond pD = 9 the formation of **6** is reduced considerably in the case of the **3**/Trp system.

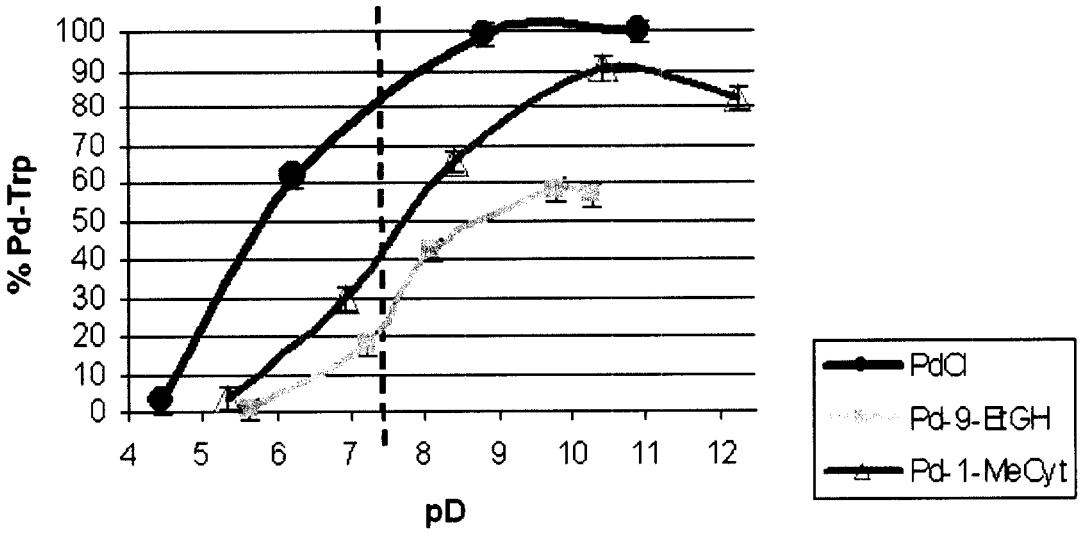

Figure 4.11. pD dependent formation of complex $[Pd(dien)(Trp)]^{+}$ from different starting complexes, physiological pH (7.4) is shown as a dashed line.

The release of the steric demands of the exocyclic groups on 1-methyl cytosine may be one feature contributing to the more efficient displacement of this ligand by tryptophan. Differences in the rate of formation of complex **6** from **2** and **3** around pD = 10 can be explained by additional equilibria in solution for 9-EtGH, involving both N1 and N7 coordination in the 9-EtGH nucleobase. The observation of an additional signal in the ^{1}H-NMR spectrum attributable to the dinuclear species {[Pd(dien)]$_2$(9-EtGH-*N1,N7*)}, previously reported for high pH values when N1 is deprotonated[16, 22, 24], supports this possibility.

4.3.2.b. Characterization of the [Pd(dien)(l-Tryptophan)]$^{2+}$complex.

The ^{13}C-NMR spectra from systems **1-3**/Trp compared to free Trp at the same pD revealed that shifts in aromatic carbons were not as pronounced as in the case of the aliphatic carbons. The principal shift changes are summarized in Table 4.IV. In the aliphatic part of the ^{13}C-NMR spectrum (data extracted from the simple system **1**/Trp) the two inequivalent sets of carbons in the diethylenetriamine ligand can be seen along with the signals for the α- and β-carbons for complex **6**, Figure 4.12.

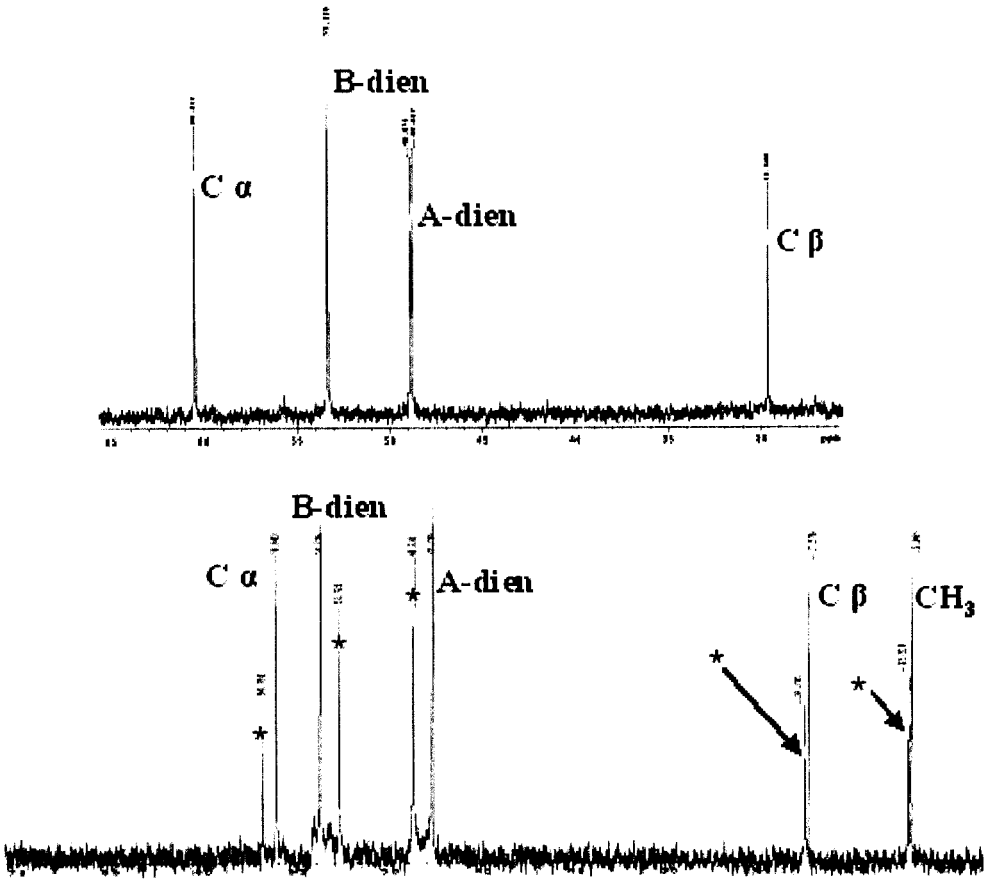

Figure 4.12. ^{13}C-NMR spectrum of $[Pd(dien)(Trp)]^+$ (top) compared to a mixture of $[Pd(dien)(N\text{-}AcTrp)]^+$ (*) and $[Pd(dien)Cl]^+$/ N-AcTrp (bottom), upfield detail showing only aliphatic signals. Spectra are in the range 65 – 20 ppm.

The α- and β-carbons suffered downfield shifts of 4.68 ppm and 2.43 ppm respectively upon coordination to palladium, and the separation of the two ^{13}C-NMR signals of the diethylenetriamine ligand was decreased to 1.5 ppm compared to free Trp, which has been correlated with displacement of chloride in the coordination sphere of the complex (*vide infra*).[25] Thus, the combined ^{1}H and ^{13}C NMR data are strongly suggestive of coordination through the amino group. This conclusion is in agreement with the reported preferences of

palladium (II) ion for ligands with *S*- or *N*- donors over *O*-donors, due mainly to thermodynamic stability factors. [26]

Table 4.IV. Summary of ^{13}C-NMR chemical shifts observed in the aliphatic region for coordinated and free Trp, N-AcTrp and diethylenetriamine (dien).

	Trp	**[Pd(dien)(Trp)]$^+$**	**Δδ (ppm)**
Cα (ppm)	56.10	60.48	+ 4.68
Cβ (ppm)	27.21	29.64	+ 2.43
	N-AcTrp	**[Pd(dien)(N-AcTrp)]$^+$**	
Cα (ppm)	54.52	56.55	+ 2.03
Cβ (ppm)	27.34	28.05	+ 0.71
	[Pd(dien)Cl]$^+$	**[Pd(dien)(Trp)]$^+$**	**[Pd(dien)(N-AcTrp)]$^+$**
dien-A CH_2 (ppm)	54.28	52.83	53.22
dien-B CH_2 (ppm)	48.28	48.35	49.23
Δδ (ppm)	6.00	4.48	3.99

The process of nucleobase (aromatic N-donor) substitution by tryptophan (aliphatic N-donor) may be correlated with the properties of the putative spectator ligand diethylenetriamine. The nature of the ligands bound to the metal ion can affect donor atom preference in substitution reactions - as an example $[Pt(terpy)Cl]^+$ was found to react selectively with the imidazole ring of histidine residues in proteins, whereas the complex was unexpectedly unreactive to methionine defying the HSAB principle.[27] In a similar manner, $[Pd(terpy)Cl]^+$ with 3 aromatic nitrogens, was reported to be unreactive towards N-acetyllysine and glycine over a range of pH, further suggesting the unfavorable

situation of simultaneous aromatic/aliphatic coordination of nitrogens around the palladium (II) center.[22] The formation of **6** from the various complexes studied here is shown in Scheme 4.1.

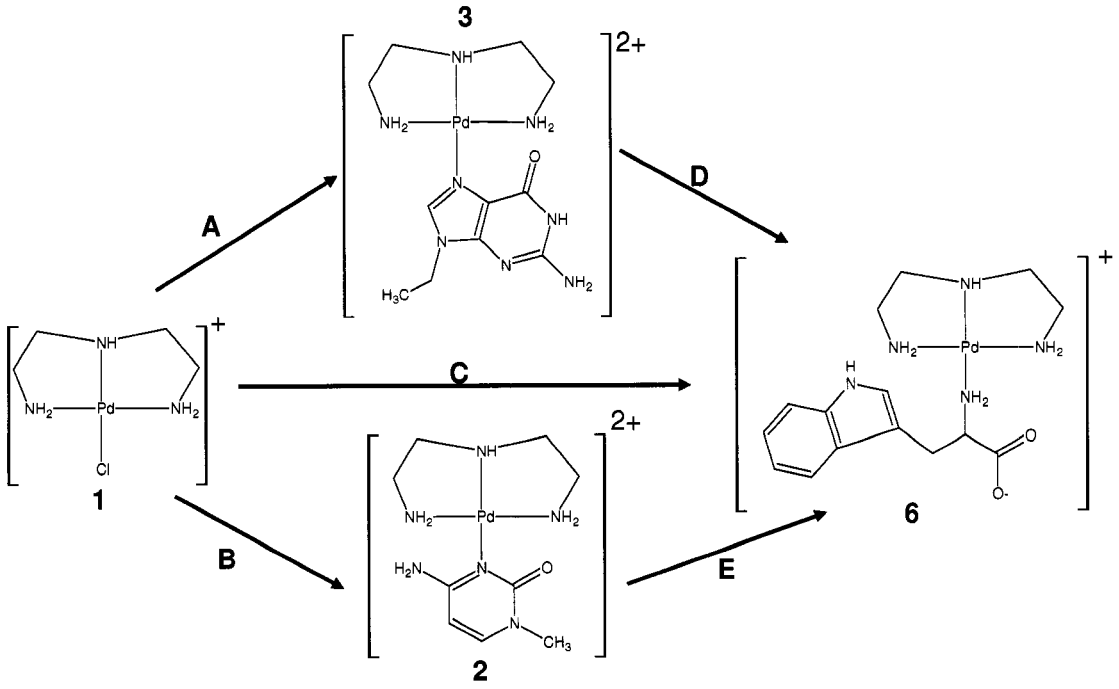

Scheme 4.1. Schematic representation of the reactions performed on this work showing the three substitution paths for the formation of complex **6. A/B**: nucleobase + $AgNO_3$; **C/D/E**: Trp + NaOH.

4.3.2.c. Formation of [Pd(dien)(N-acetyltryptophan)] complex. The reaction of complexes **1 - 3** with N-AcTrp was also followed by ESI-MS and ^{1}H-NMR Spectroscopy to evaluate the differences between an amino group and the more representative amide bond of proteins. In all cases, coordination of N-AcTrp to the palladium center was confirmed by the presence of a signal in the mass spectrum at m/z = 454.12, which was

assigned to the species $[Pd(dien)(N\text{-}AcTrp)]^+$ Figure 4.13. The protonated and/or sodium adducts of free 1-MeCyt and 9-EtGH nucleobases observed previously in the case of Trp were also observed for **2** and **3** respectively, confirming the nucleobase substitution by N-AcTrp.

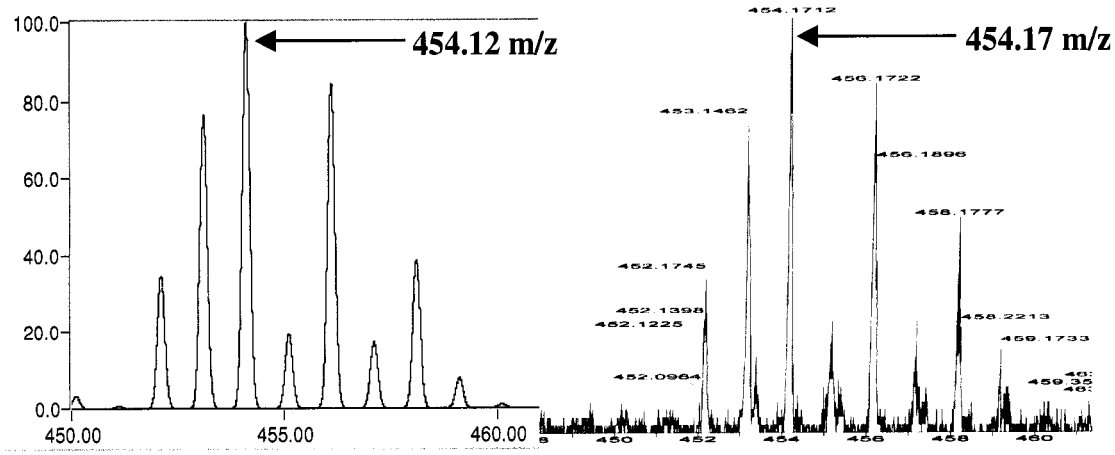

Figure 4.13. ESI-MS spectrum of $[Pd(dien)(N\text{-}AcTrp)]^+$, from a $[Pd(dien)(1\text{-}Mecyt)]^{2+}$ / N-AcTrp solution (pD = 9.2)

^{1}H-NMR spectra of systems **1-3**/N-AcTrp exhibited the presence of new signals attributed to coordination as the pD of the solution was increased above pD = 8 (Figure 4.14.). The chemical shifts for free and coordinated N-AcTrp are compared in Table 4.III. 2D NMR COSY experiments confirmed the assignments, Figure 4.15. Some differences with respect to chemical shift changes were noted in comparison to the tryptophan case, i.e. only H4 and H7 protons undergo upfield shifts and all other aromatic signals exhibited a downfield

shift indicating a different electronic influence on the indole ring upon coordination. Additionally, signals in the aliphatic part of the spectrum corresponding to protons Hα and Hβ's exhibited a smaller change in **7** compared to the **6.** The signal for the methyl group in N-AcTrp did not exhibit any appreciable change upon coordination ($\Delta\delta = 0.1$ ppm).

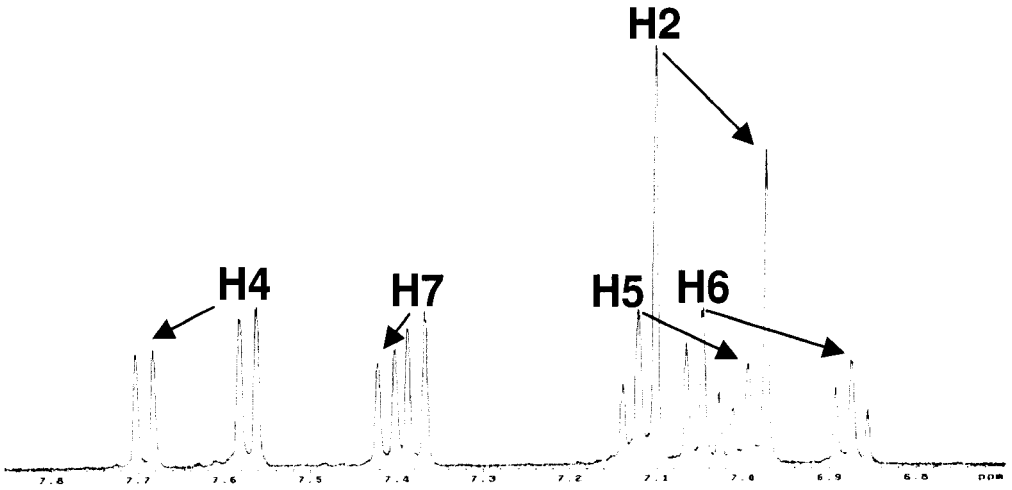

Figure 4.14. Zoom of the aromatic region in the ^{1}H-NMR spectrum of a $[Pd(dien)Cl]^+$ / N-AcTrp solution (pD = 9.2), showing the new signals corresponding to the new complex $[Pd(dien)(N\text{-}AcTrp)]^+$ at the end of the arrow.

Formation of complex **7** was monitored using the corresponding integrals for H4 in the ^{1}H-NMR spectrum. Coordination of N-AcTrp is not as favored as for the tryptophan system – the formation of **7** from **1** is approximately 50% at pD = 9.2 compared to the almost quantitative conversion of **6** at the same pD. However the trend observed for ligand displacement from the Pd(II) complex (i.e. Cl^- > 1-MeCyt > 9-EtGH) was maintained,

giving percentages for nucleobase substitution of 15% for 1-MeCyt and < 10% for 9-EtGH at pD = 10.6. Attempts to produce complex **7** in more than 50% yield by raising the pD above 11 were unsuccessful since at very high pD a more complex equilibrium is produced. Species like $[Pd(dien)(OH)]^+$ (m/z = 226.48) were detected via ^{1}H-NMR and ESI-MS suggesting a displacement of the coordinated nucleobase or chloride by the more nucleophilic hydroxyl ligand, contrasting with recent results obtained for the platinum analog under highly basic conditions.[28]

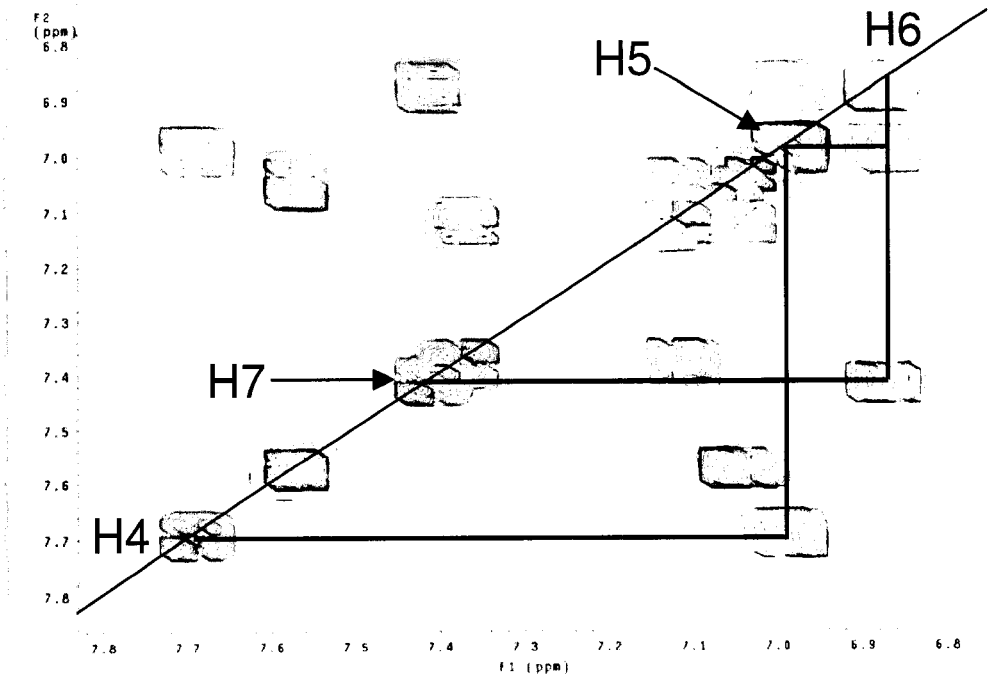

Figure 4.15. 2D COSY NMR spectrum of a [Pd(dien)Cl]Cl / N-AcTrp solution (pD = 9.2), showing only the correlations in the indole ring of coordinated N-AcTrp (full line)

4.3.2.d. Characterization of the [Pd(dien)(N-acetyltryptophan)] complex. Monitoring of the ^{13}C-NMR spectrum showed that the downfield shift experienced by alpha and beta carbons was not as large as in the case for Trp although separations of more than 2 ppm were observed (Table 4.III.), correlating well with the modest proton chemical shifts. The separation between ^{13}C-NMR signals of the diethylenetriamine ligand has been used as a diagnostic to determine the nature of L in $[Pt(dien)L]^{+n}$ complexes, for complex **1** with L = Cl^- the separation of these signals was found to be 6.00 ppm, whereas complexes **6** and **7** gave a separation ($\Delta\delta$) of 4.48 and 3.99 ppm respectively which are typical values for N-donors as nitriles or amides, Table 4.IV. Coordination through oxygen also induces similar shift differences of the dien C atoms, although in this case values close to 5 ppm and above have been observed.[25] In addition, the ^{13}C NMR shift of the C=O carbonyl moiety undergoes an upfield shift upon N-AcTrp coordination and formation of **7** – in contrast to reported downfield shifts for binding through the oxygen atom of a carbonyl moiety.[25] The combination of spectral data thus suggests the amide nitrogen as the coordination site. The coordination through the oxygen atom in any of the carbonyl moieties was further ruled out because of the weak coordination exhibited by these functionalities with a metal center. Coordination via a deprotonated amido nitrogen, in the case of N-AcTrp, can be understood given the high pD values (8 for complex **1** and > 9 for **2** or **3**) needed for formation of **7**. Glycine is reported to coordinate through *O*-coordination at low pH (3.6) but the *N*-bound species is exclusively formed at pH = 7.4 for $[Pd(dien)(H_2O)]^+$ and glycine. [26] Bifunctional binding through formation of an *N,O* chelate has been reported for other aminoacids in addition to Trp.[29] The thermodynamic tendency to form the chelate

leads even to the formation of an organometallic bond with indolyl C(3), O coordination when the model compound indole-3-acetamide is used instead of Trp.[30] The possibility of coordination via the indole N1 is also ruled out due to the small chemical shifts observed for the aromatic signals (Table 4.III.) and its high pK_a value (16.8). Interestingly, coordination through this site has been reported only after previous coordination of an organometallic (η^6 – cymene)Ru(II) fragment, which induce a drastic increase in the acidity of N1 by more than eight orders of magnitude.[31]

In summary, we propose that N-AcTrp coordinates via the deprotonated amido moiety to the Pd(II) center, and experiments aiming to obtain the solid structure of **7** and confirm the proposed structure are currently underway.

4.3.2.e. Reaction of [Pt(dien)(Nucleobase)]$(NO_3)_2$ (4,5) with l-Tryptophan and N-Acetyl Tryptophan. No covalent interaction was detected for the systems involving Pt-nucleobase complexes **4** and **5** even after 72 h. of reaction at pD = 10.2 and room temperature in terms of nucleobase displacement as followed by ^{1}H-NMR incubations. Slight chemical shifts in the range 0.01-0.07 ppm could be detected for N-AcTrp but they were attributable to stacking interactions as have been found previously.[1, 32]

4.3.3. Study of non-covalent interaction in [M(dien)(nucleobase)]$(NO_3)_2$, M = Pt,Pd complexes: The initial purpose of this study was to compare the effects of palladium and platinum in [M(dien)(nucleobase)] compounds on the enhancement of stacking interaction with tryptophan and derivatives. Experimental conditions were chosen in order to eliminate the observed covalent interactions of palladium by using a pH = (4.8) which was

low enough to limit any covalent binding, even for the more reactive Trp molecule. The degree of quenching experienced by Trp and N-AcTrp by complexes **2 - 5** was analyzed as previously through Eadie-Hofstee plots (ΔF vs. ΔF/[quencher]) which yielded the association constant value (K_a) for each system from its slope, Table 4.V. In the first place the good agreement between K_a's values obtained for N-AcTrp and Trp suggests that the N-acetyl moiety is not affecting considerably the stacking interaction with the nucleobase, and confirms the inertness of platinum-nucleobase complexes to substitution side-reactions with the Trp substrate, a result that very likely would have been compromised in the case of palladium(II) complexes.

Table 4.V. Association constants obtained from Eadie-Hofstee plots of N-AcTrp with different quenchers, values in parenthesis obtained for l-Trp from ref . 1. Eadie-Hofstee equation, where ΔF = F-F0 is the difference between fluorescence intensities of N-AcTrp in the presence (F) and absence (F0) of the quencher. ΔFc is the difference of the N-AcTrp completely complexed with the quencher.

$$\Delta F = -\frac{1}{Ka} \times \frac{\Delta F}{[\text{Quencher}]} + \Delta F_c$$

Quencher	K_a	Std. Dev.
1-MeCyt	**6.2** (6.0)	**0.3** (0.1)
$[Pt(dien)(1\text{-MeCyt})]^{2+}$	**8.8** (8.8)	**0.3** (0.2)
$[Pd(dien)(1\text{-Mecyt})]^{2+}$	**7.3**	**0.2**
9-EtGH	**3.5** (3.3)	**0.2** (0.1)
$[Pt(dien)(9\text{-EtGH})]^{2+}$	**7.0** (6.8)	**0.1** (0.3)
$[Pd(dien)(9\text{-EtGH})]^{2+}$	**5.1**	**0.3**

In a broad sense a significant enhancement of the stacking interaction was observed for metal-coordinated nucleobases in comparison to the free ones, since for both cases of platinum and palladium higher values of K_a were obtained which were statistically significant according to unpaired *t*-test. This finding is also in agreement with our previous results confirming the coordination of the nucleobase to the metal center as a definitive enhancer of π-π stacking interactions between the nucleobase and the amino acid derivative.

4.4. Experimental Section.

Reagents and Solvents. l-tryptophan, N-Acetyl-tryptophan, 1-methylcytosine, 9-ethylguanine and diethylenetriamine were obtained from Aldrich and used as received. Water was double distilled and deionized on a Barnstead ultra pure water system model NANOpure. Complexes [Pt(dien)(1-MeCyt)]$(NO_3)_2$ (**4**) and [Pt(dien)(9-EtGH)]$(NO_3)_2$ (**5**) were synthesized from [Pt(dien)Cl]Cl according to reported procedures and characterized through Elemental Analysis, ^{1}H-/^{195}Pt-NMR and ESI-MS.[1]

Instrumentation. pH measurements were performed on a Corning pHmeter model 340, equipped with an Accumet microelectrode with calomel reference, model 13-620-095. ^{1}H- and ^{13}C- NMR experiments were performed on a Varian INOVA (400 MHz). Chemical shifts were referenced to the residual peak of water at 4.69 ppm in ^{1}H-NMR and 2D NMR COSY experiments, while dioxane (67.19 ppm) was used for ^{13}C-NMR experiments. A mass spectrometer Micromas Q-Tof 2 equipped with a quadrupole/time-of-flight detector

was used for mass spectra. X-ray data were collected on a Bruker SMART APEX CCD diffractometer with area detector system.

X-ray structure determination. Colorless plates of **2** were obtained upon slow cooling (3 weeks, 0 °C) of a saturated DMF solution after addition of diethyl ether. Colorless plates of **4** were obtained by the hanging drop method in a water/2-methyl-2,4-pentanediol mixture. The structures were solved by direct method, with subsequent refinements using SHELXS-97 and SHELXL-97 programs.[33] Analysis of short contacts was performed with the Mercury 1.2.1. software from Cambridge Crystallographic Date Centre (CCDC).

Fluorescence experiments. In a typical experiment, 3 mL of a N-AcTrp (5 μM) were titrated with aliquots of the corresponding quenching compound (7.5 mM) in the range [Quencher]/[N-AcTrp] = 10 – 100; buffer Tris-HCl 20 mM adjusted with a few drops of HNO_3 was used in all experiments (pH = 4.8). The maximum intensity of the spectrum (ca. 362.9 nm) was measured for each addition and the association constants for each system were obtained from the analysis of Eadie-Hofstee plots[34]. Measurements were made at 20 °C and reported association constants (K_a) were averaged over a number of six different experiments, significance of results was compared using unpaired t-test. Fluorescence spectra were recorded in the range of 295 to 450 nm. with a scan rate of 120 nm/min.

4.4.1. Synthesis of complexes.

[Pd(dien)Cl]Cl (1): Complex (**1**) was synthesized by a modification of the reported procedure.[35] $PdCl_2$ was suspended in 2 mL of water and reacted with dien in a 1:2 molar ratio at 90 °C until a yellow solution resulted (aprox. 15 min.). The pH of this solution was then decreased from 6.9 to 4.8 by addition of concentrated HCl and half of the solvent evaporated. After this a few drops of ethanol was added and yellow crystals appeared, which were filtrated, washed with cold ethanol/ether and dried in vacuo (Yield 60%). Anal. Calcd. for $C_4H_{13}N_3Cl_2Pd$: C, 17.13; H, 4.68; N, 14.98. Found: C, 17.26; H, 4.40; N, 14.71 %.^{1}H-NMR in D_2O: δ 2.90 (8 H, m).

[Pd(dien)(1-MeCyt)]$(NO_3)_2$ (2): To a solution of (**1**) in water two equivalents of $AgNO_3$ were added and stirred overnight to remove the chloride ligands and produce the complex $[Pd(dien)NO_3]NO_3$ *in situ*. The solution was then filtered and 1-MeCyt was added in equimolar amounts and stirred at room temperature for 24 h. The off-white solid was obtained upon solvent evaporation and the powder was then washed with methanol and ether to remove unreacted 1-MeCyt (Yield 80%). Anal. Calcd. for $C_9H_{20}O_7N_8Pd$: C, 23.55; H, 4.40; N, 24.43. Found: C, 23.69; H, 4.05; N, 24.28 %. ; ^{1}H-NMR in D_2O: δ 7.45 (1H, d, J = 7.3 Hz), 5.82 (1H, d, J = 7.3 Hz), 3.27 (3H, s), 2.95 (8H, m); ESI-MS: m/z = 333.41 $[Pd(dien)(1\text{-}MeCyt) - H^+]^+$.

[Pd(dien)(9-EtGH)]$(NO_3)_2$ (3): Complex (**3**) was prepared in a similar way to (**2**) using 9-EtGH as a nucleobase, the white product was then recrystallized in a water/methanol solution to obtain the final complex (Yield 60%). Anal. Calcd. for $C_{11}H_{22}O_7N_{10}Pd$: C, 25.76; H, 4.33; N, 27.32. Found: C, 24.69; H, 4.05; N, 27.28 %. ; ^{1}H-NMR in D_2O: δ 7.98

(1 H, s), 3.97 (2H, q, J = 7.3 Hz), 3.02 (8H, m), 1.29 (3H, t, J = 7.3 Hz); ESI-MS: m/z = 387.31 $[Pd(dien)(9\text{-}EtGH) - H^+]^+$.

Incubation experiments (NMR Spectroscopy). In a typical experiment, 7-10 mM solutions of the complexes (**1-5**) were incubated with Trp or N-AcTrp, at room temperature for 30 min (Pd) or overnight (Pt). pD was adjusted by addition of NaOD solution, NMR spectra were referenced to the residual signal of D_2O (^{1}H-4.69 ppm) or dioxane (^{13}C-67.19 ppm).

Structures were visualized with software Mercury 1.2.1. from Cambridge Crystallographic Date Centre (CCDC). Structures of cytosine complexes were downloaded from the database CCDC N° 175000, 175001.[36]

4.5. Conclusions.

The kinetic lability of the Pd(II) center compared to Pt(II) resulted in a novel nucleobase substitution and Pd-aminoacid complex formation. The increased steric hindrance inherent in metal-cytosine compounds suggests that the 1-MeCyt compound should be *less susceptible* to nucleophilic substitution by hindering (in the classic explanation) the approach of the incoming nucleophile. It is possible that the substitution is favored by the correct orientation of the amino acid through the enhanced stacking interaction – the higher association constants observed for cytosine over guanine derivatives is in agreement with this possibility. Palladium-peptide conjugates are proposed intermediates in the catalytic cycle involving peptide bond hydrolysis catalyzed by species such as $[Pd(en)(H_2O)_2]^{2+}$.

The results presented here also support the mechanism of cleavage reported by confirming the ability of Pd to form a bond with the amido group of the peptide linkage.[37, 38] The application of the chemistry reported here to tryptophan-containing peptides and proteins is ongoing.

4.6. References.

(1) Anzellotti, A.I.; Ma, E; Farrell, N.P., *Inorg. Chem.*, **2005**, 44, 483-485.

(2) Ericson, A.; Iljina, Y.; McCary, J.L.; Coleman, R.S.; Elmroth, S.K.C., *Inorg. Chim. Acta.*, **2000**, 297, 56-63.

(3) Sheldrick, W.S.; Neumann, D., *Inorg. Chim. Acta*, **1994**, 223, 131-137.

(4) Breet, E.L.J.; van Eldik, R., *Inorg. Chem.*, **1987**, 26, 2517-2524.

(5) Laussac, J.P.; Pasdeloup, M.; Hadjiliadis, N.; *J. Inorg. Biochem.*, **1987**, 30, 227-238.

(6) Tercero-Moreno, J.M.; Matilla-Hernandez, A.; Gonzalez-Garcia, S.; Niclos-Gutierrez, J., *Inorg. Chim. Acta.*, **1996**, 253, 23-29.

(7) Milović, N.M.; Dutcă, L.-M.; Kostić, N.M., *Inorg. Chem.*, **2003**, 42, 4036-4045.

(8) Kaminskaia, N.V.; Kostić, N.M., *Inorg. Chem.*, **2001**, 40, 2368-2377.

(9) Kaminskaia, N.V.; Johnson, T.W.; Kostić, N.M., *J. Am. Chem. Soc.*, **1999**, 121, 8663-8664.

(10) Kelso, M.J.; Beyer, R.L.; Hoang, H.N.; Lakdawata, A.S.; Snyder, J.P.; Oliver, W.V.; Robertson, T.A., Appleton, T.G.; Fairlie, D.P., *J. Am. Chem. Soc.*, **2004**, 126, 4828-4862.

(11) Kelso, M.J.; Hoang, H.N.; Oliver, W.V.; Sokolenko, N.; March, D.R.; Appleton, T.G.; Fairlie, D.P., *Angew. Chem. Int. Ed.*, **2003**, 42, 421-424.

(12) Kelso, M.J.; Hoang, H.N.; Appleton, T.G.; Fairlie, D.P., *J. Am. Chem. Soc.*, **2000**, 122, 10488-10489.

(13) Agarov, A.; Greenfield, S.J.; Ohishi, T.; Collibee, S.E.; Gilberston, S.R., *J. Org. Chem.*, **2004**, 69, 8077-8085.

(14) Rombeck, I.; Lippert, B., *Inorg. Chim. Acta.*, **1998**, 273, 31- 40.

(15) Wienken, M.; Kiss, A.; Sóvágó, I.; Fusch, E. C.; Lippert, B., *J. Chem. Soc., Dalton Trans.*, **1997**, 4, 563 – 568.

(16) Pesch, F.J.; Preut, H.; Lippert, B., *Inorg. Chim. Acta*, **1990**, 169, 195-200.

(17) Brüning, W.; Ascaso, I.; Freisinger, E.; Sabat, M.; Lippert, B., *Inorg. Chim. Acta*, **2002**, 339, 400-410.

(18) Sinnokrot, M.O.; Sherrill, C.D., *J. Phys. Chem. A* , **2003**, 107, 8377-8379.

(19) Janiak, C., *J. Chem. Soc., Dalton Trans.*, **2000**, 21, 3885-3896

(20) Glasoe, P.K.; Long, F.A., *J. Phys. Chem.*, **1960**, 64, 188-190.

(21) Reid, G.E.; O'Hair, R.A.J.; Styles, M.L.; McFadyen, W.D.; Simpson, R.J., *Rapid. Commun. Mass Spectrom.*, **1998**, 12, 1701-1708.

(22) Kiss, A.; Farkas, E.; Sóvágó, I.; Thormann, B.; Lippert, B., *J. Inorg. Biochem.*, **1997**, 68, 85-92.

(23) Miller, S.K.; Marzilli, L. G., *Inorg. Chem.*, **1985**, 24, 2421-2425.

(24) Griesser, R.; Kampf, G.; Kapinos, L.E.; Komeda, S.; Lippert, B.; Reedijk, J.; Sigel, H., *Inorg. Chem.*, **2003**, 42, 32-41.

(25) Woon, T.C.; Fairlie, D.P., *Inorg. Chem.*, **1992**, 31, 4069-4074.

(26) Appleton, T.G., *Coord. Chem. Rev.*, **1997**, 166, 313-359.

(27) Ratilla, E. M. A.; Brothers, H.M.; Kostić, N.M., *J. Am. Chem. Soc.*, **1987**, 109, 4592-4599.

(28) Šponer, J.E.; Miguel, P.J.S.; Rodriguez-Santiago, L.; Erxleben, A.: Krumm, M.; Sodupe, M.: Šponer, J.; Lippert, B., *Angew Chem Int. Ed.* , **2004**, 43, 5396-5399.

(29) Staubach, B.; Buddrus, J., *Angew. Chem. Int. Ed. Engl.*, **1996**, 35, 1344-1346.

(30) Kaminskaia, N.V.; Ullmann, G.M.; Fulton, D.B.; Kostić, N.M., *Inorg. Chem.*, **2000**, 39, 5004-5013.

(31) Schlüter, A.; Bieber, K.; Sheldrick, W.S., *Inorg. Chim. Acta.*, **2002**, 340, 35-43.

(32) Elduque, A.; Carmona, D.; Oro, L.A.; Eisenstein, M.; Fish, R.H., *J. Organomet. Chem.*, **2003**, 668, 123-127.

(33) Sheldrick, G. M. SHELX-97 Programs for Crystal Structure Analysis; Institut für Anorganische Chemie der Universität: Göttingen, Germany, 1998.

(34) G.S. Eadie, *J. Biol. Chem.*, **1942**, 146, 85-93.

(35) Baddley, W.H.; Basolo, F., *J. Am. Chem. Soc.*, **1966**, 88, 2944-2950.

(36) F. H. Allen, *Acta Crystallogr.*, **2002**, B58, 380-388.

(37) Milović, N.M.; Kostić, N.M., *J. Am. Chem. Soc.*, **2002**, 124, 4759-4769.

(38) Milović, N.M.; Dutcă, L.-M.; Kostić, N.M., *Chem. Eur. J.*, **2003**, 9, 5097-5106.

(39) Brüning, W.; Ascaso, I.; Freisinger, E.; Sabat, M.; Lippert, B., *Inorg. Chim. Acta*, **2002**, 339, 400-410.

CHAPTER 5 Targeting the Retroviral Zinc Finger-DNA Interaction. A small molecule approach utilizing the electrophilic nature of trans-Platinum-Nucleobase Compounds.

Atilio I. Anzellotti[a], Qin Liu[a], Marieke J. Bloemink[a], J. Neel Scarsdale[b, c] and Nicholas P. Farrell[a*]

a. Department of Chemistry, Virginia Commonwealth University, 1001 W. Main St. Richmond, VA 23284-2006, USA.

b. Institute for Structural Biology & Drug Discovery, PO Box 980133, Richmond, VA 23298-0133.

c. Department of Biochemistry, PO Box 980614, Richmond, VA 23298-0614.

Chemistry & Biology, **2006**, 13 (5), 539 - 548

5.1. Abstract.

Non-covalent interactions are ubiquitous in ternary systems involving metal ions, DNA/RNA and proteins and represent a structural motif for design of selective inhibitors of biological function. This contribution shows that small molecules containing platinated purine nucleobases mimic the natural DNA(RNA)-tryptophan recognition interaction of zinc finger peptides, specifically the C-terminal finger of HIV NCp7 protein. Interaction with platinum results in Zn ejection from the peptide accompanied by loss of tertiary

structure. Targeting the NCp7-DNA interaction for drug design represents a conceptual advance over electrophiles designed for chemical attack on the zinc finger alone. These results demonstrate examples of a new platinum structural class targeting specific biological processes, distinct from the bifunctional DNA-DNA binding of cytotoxic agents like cisplatin. The results confirm the validity of a chemical biological approach for metallodrug design for selective ternary DNA(RNA)-protein interactions.

5.2. Introduction

The nucleocapsid NCp7 protein is an attractive target for antiviral drug design. Retroviral nucleocapsid proteins (NCps) from all strains of known retroviruses contain one or more copies of the conserved CCHC zinc finger or "knuckle" sequence Cys-X_2-Cys-X_4-His-X_4-Cys (X=variable)[1]. The nucleocapsid protein NCp7 of human immuno deficiency virus type I (HIV-I) contains two of these highly conserved zinc finger domains which are necessary for viral replication.[2,3] NCps contribute to multiple steps of the viral life cycle, all of which seem to involve binding to single-stranded nucleic acids. [4, 5] NCp7 is known to have a high affinity for single-stranded nucleic acids[6] and has been shown to be a potent chaperone for general nucleic acid folding and unfolding[7]. The protein is required for correct encapsidation and packaging of viral RNA[8, 9] and in the virion, NCp7 is thought to stabilize the dimeric RNA genome through formation of a ribonucleoprotein complex. [10]

Studies *in vitro* show that NCp7 can activate the retroviral RNA dimerization and also enhances the annealing of the $tRNA_3^{Lys}$ primer to the initiation site of reverse transcription suggesting that correct genomic RNA packaging and reverse transcription depend upon NCp7.[11, 12] The participation of the nucleocapsid protein in multiple steps in the virus life cycle and the relative rarity of the CCHC motif in cellular proteins, make NCp7 an attractive target for antiviral drug design. Such an approach would be complementary to drugs such as protease inhibitors and nucleoside analogs aimed at other targets of the viral life cycle. Zinc fingers are estimated to represent 3% of the human genome - a total of 4500 C_2H_2 zinc finger domains from 564 proteins are recognized, whereas only 17 domains from 9 proteins contain the CCHC zinc knuckle motif .[13, 14]

The molecular details of the interaction of the entire HIV nucleocapsid protein NCp7 (See Figure 5.1.) bound to the 20-bp SL3 Ψ-RNA recognition element have been elucidated by NMR spectroscopy.[15] The structure showed interactions between the guanine bases of the single-stranded G_6 -G_7-A_8-G_9 tetraloop involving stacking and H-bonding interactions of the exposed G_7 and G_9 residues with Phe and Trp, respectively .[15] The complex formed between the (12 - 53) NCp7 fragment, encompassing the two Zn knuckles and the short linking region, and d(ACGCC), a single-stranded deoxynucleotide sequence corresponding to the shortest NCp7 binding site, showed similar features .[16] The indole ring of the W37 tryptophan residue is inserted between adjacent C and G bases and stacked on the latter .[16] An important recognition motif in both structures is thus the presence of guanine/tryptophan (and/or phenylalanine) stacking interactions. The presence of the W37 residue has been revealed as a key feature for molecular recognition from the zinc finger toward oligonucleotides, as surface plasmon resonance and other experiments have confirmed.[17, 18] The non-covalent interaction is conserved even for the more complex SL2 and SL3 domains in the Ψ-recognition element of the viral genome.[15, 19]

In terms of drug development, covalent modification of the nucleocapsid protein has been achieved by use of electrophiles.[20] The electrophiles covalently modify the zinc binding site through cysteine oxidation or alkylation to thioether resulting in eventual cleavage of the Zn-S bond and zinc ejection. Loss of tertiary structure and nucleic acid binding ability leads to inhibition of function and prevention of infectivity. An inherent challenge for all small molecule electrophiles is selectivity. Some anti-HIV agents have been described which target the NCp7 protein without affecting cellular zinc finger

proteins.[21] In general, there is little intrinsic selectivity in anti-HIV, Zn-ejecting drugs. Thus a worthwhile approach is to search for antagonists of the RNA(DNA)-protein interaction .[22] In this latter respect, the recognition motif of guanine/tryptophan stacking is worthy of exploitation in design of NCp7 selective agents. Small molecules containing dual properties of protein-DNA recognition as well as zinc ejection capacity would represent a building block for more selective interaction and therapeutic intervention.

Recently, we have proposed analogies between platinum and alkylating electrophiles and possible biological implications thereof. Fluorescence quenching experiments showed that the stacking interaction between nucleic acid bases and l-tryptophan is significantly enhanced upon nucleobase coordination to a Pt(II) center in $[Pt(dien)(L)]^{2+}$ (where L = 9-Ethylguanine (9-EtGH), 1-MethylCytosine (1-MeCyt) or their nucleotide monophosphate analogs 5'GMP and 5'-CMP).[23, 24] In the absence of a reactive leaving group, only non-covalent hydrogen-bonding and stacking interactions need to be taken into account. The effect mimics the enhancement of π-π stacking interactions to l-tryptophan upon methylation of purine and pyrimidine nucleic acid bases, attributable to a lowering in energy for the π-acceptor LUMO in the methylated nucleobase, thus improving the acceptor properties toward the π-donor HOMO of the amino acid .[25] In parallel studies the interaction of *trans*-$[PtCl(9\text{-}EtGH)(py)_2]^+$ and the model zinc chelate $[Zn(bme\text{-}dach)]_2$ results in Zn ejection and eventual incorporation of Pt into the macrocycle. [26] Intermediate heterodinuclear thiolate bridged Pt-S-Zn species are formed. The thiolate ligand binding sites of $[Zn(bme\text{-}dach)]_2$ present a precedent for S-alkylation reactions in nature, being sufficiently nucleophilic to be readily alkylated.[27]

We therefore wished to extend these findings to a biologically relevant system. This paper reports on model studies for recognition and fixation of platinum-nucleobase complexes on the C-terminal peptide (F2) of the HIVNCp7 zinc knuckle. Figure 5.1. shows the structure of the nucleocapsid protein and the platinum compounds studied. The C-terminal peptide was chosen as proof of principle for a number of reasons: the knuckle contains the tryptophan moiety and many observations indicate that the C-terminal Zn site is more reactive than the N-terminal sequence. The chemical composition of a zinc finger core as well as the local protein environment determines the reactivity of the zinc finger. Analysis through protein packing and electrostatic screening of 207 zinc fingers indicated that the C-terminal finger was one of the most reactive sites. [28] Experimentally, Cys^{49} is the most reactive cysteine and theoretically S^{49} is predicted to be the most nucleophilic site. [28] The complexes chosen for extensive study were $[Pt(dien)(9\text{-}EtGH)]^{2+}$ (**Ia**), Pt(dien)5'GMP (**Ib**) and *cis*-$[Pt(NH_3)_2(Guanosine)_2]^{2+}$ (**III**) capable of only non-covalent interactions, and in addition the *trans*-$[PtCl(9\text{-}EtGH)(pyr)_2]^{+}$ (**II**), containing one substitution-labile Pt-Cl bond suitable for covalent interactions. This paper shows that modulation of the $[PtCl(L)(L')(Nucleobase)]^{+}$ (L = NH_3, L'= pyr, quin etc. or L = L' = pyr etc.) structural motif is a viable approach to more effective and selective inhibitors of the zinc-finger-nucleic acid interaction and subsequent zinc ejection. Circular dichroism, fluorescence quenching and Electrospray Ionization Mass Spectrometry (ESI-MS) were used to examine both non-covalent and covalent interaction of the platinum electrophiles with the 18-residue sequence corresponding to the C-terminal finger of HIVNCp7. 1-D and 2-D

NMR studies were used to confirm the nature of the interaction between the peptide and a model oligonucleotide d(TACGCC).

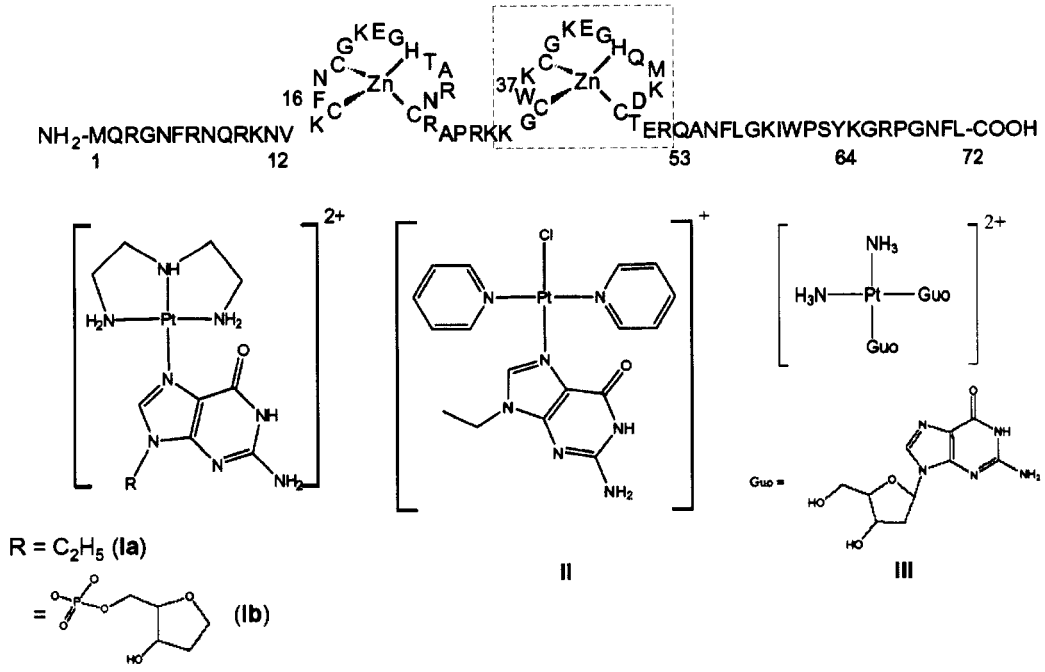

Figure 5.1. Structure of the entire HIV nucleocapsid protein and platinum compounds used on this study.

5.3. Results and Discussion.

The Zinc Finger-DNA Interaction

The formation of the zinc finger can be monitored by Circular Dichroism, ESI-Mass Spectrometry and ^{1}HNMR Spectroscopy, Figure 5.2. The mass spectrum shows peaks corresponding to the 2+ to 5+ states of the metallopeptide at m/z = 1144.1, 763.1, 572.8 and 458.6 amu respectively, Figure 5.2.A. The CD spectrum confirms the metallation with a red shift of the ellipticity minimum, typical of zinc-peptide formation, Figure 5.2.B.[29-31]

The ^{1}H NMR spectrum in H_2O of the F2 zinc finger shows a downfield shift of the histidine protons and sharp signals at room temperature, indicating a conformationally stable structure (Figure 5.2.C). Previous reports on the C-terminal domain had given spectra indicative of conformational lability.[32] The reasons for the discrepancy are unclear.

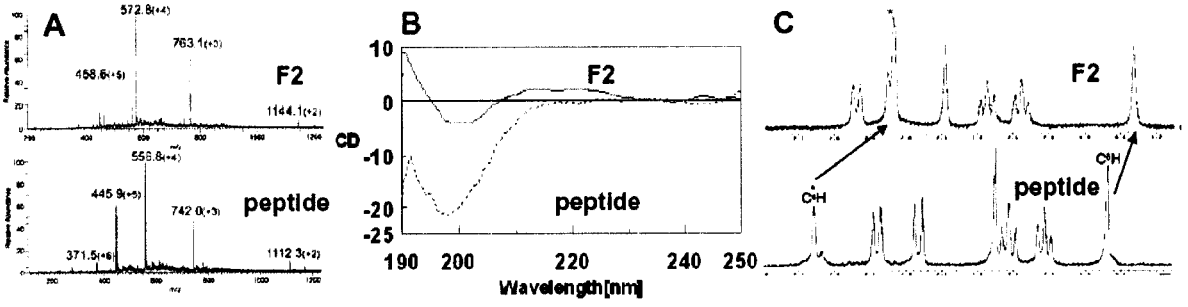

Figure 5.2. Spectroscopic characterization of F2 formation showing the changes that can be monitor using ESI-MS (A), Circular dichroism (B) and ^{1}H-NMR (C) for the free peptide (bottom) upon coordination to Zn^{2+}. The chemical shifts for histidine (H44) protons are highlighted in C with the arrows.

The interactions of the 18-residue sequence corresponding to the N-terminal sequence of HIVNCp7 with oligonucleotides d(ACGCC) and d(TTTGGTTT) have been studied by NMR methods.[33, 34] In the former case the affinity is significantly less than for the intact finger.[16] The complementary study of the C-terminal F2 alone with a suitable oligonucleotide has not been reported. To confirm the basic features of the C-terminal finger-RNA(DNA) interaction, the binding to the hexanucleotide d(TACGCC) was studied.

Table 5.I. ^{1}H NMR protein chemical shift assignments for d(TACGCC)-NCp7(F2)

residue	NH	Hα	Hβ	others
K(1)	-	3.84	1.82/1.75	γCH$_2$ 1.42; δCH$_2$ 1.66 εCH$_2$ 2.93
G(2)	-	3.88/3.33		
C(3)	7.63	4.74	3.85/3.37	
W(4)	8.85	4.49	3.21/3.18	H$^{\zeta 3}$ 6.71; H$^{\delta 1}$ 7.04 H$^{\eta 2}$ 6.78; H$^{\zeta 2}$ 7.12 H$^{\varepsilon 3}$ 6.99; NH$^{\varepsilon 1}$ 9.78
K(5)	9.61	4.29	1.77/1.64	γCH$_2$ 1.30; δCH$_2$ 2.72 εCH$_2$ 2.91
C(6)	8.54	4.90	3.19/2.50	
G(7)	8.04	4.11/3.81		
K(8)	8.41	4.27	1.77/1.68	γCH$_2$ 1.38; δCH$_2$ 1.56; εCH$_2$ 2.96
E(9)	8.24	4.07	1.93	γCH$_2$ 2.79
G(10)	8.51	4.30/3.60		
H(11)	9.09	4.67	3.24/3.12	H$^{\delta 2}$ 6.81; H$^{\varepsilon 1}$ 7.40
Q(12)	8.38	4.10	1.92	γCH$_2$ 2.22/2.13; εNH$_2$ 8.09/8.15
M(13)	8.77	4.33	1.68	γCH$_2$ 2.01 εCH$_3$ 1.86
K(14)	8.75	4.12	1.82/1.74	γCH$_2$ 1.27/1.21; δCH$_2$ 1.60; εCH$_2$ 2.94/2.89
D(15)	7.89	4.82	2.87/2.46	
C(16)	7.60	3.64	3.21/2.84	
T(17)	8.13	3.72	4.39	γCH$_3$ 1.04
E(18)	8.49	4.00	2.04/1.79	γCH$_2$ 2.30/2.13

The sequence was chosen to compare with previous studies and the extra thymine was added to contribute additional stability to the peptide-oligonucleotide complex, especially given the presence of a number of lysine residues in the peptide. Addition of d(TACGCG) to the peptide resulted in a progressive shift of the protein resonances, indicative of fast exchange. The resonances were assigned from 2D NOESY and COSY data sets. The full list of assigned chemical shifts is given in Table 5.I.

For the protein, three stretches of NH-NH connectivities are present: from Lys(5) - Glu(9), from Lys(14) - Cys(16) and from Thr(17) - Glu(18). The $d_{\alpha N}$ sequential assignment is present from Lys(5) - Glu(9) and from Met(13) - Glu(18). Comparison of the NOESY spectra in H_2O and D_2O allowed unambiguous assignment of the non-exchangeable aromatic H's of the His and Trp residues and long-range NOEs between these two aromatic residues are observed. The aromatic proton resonances of the tryptophan residue all show an upfield shift during the titration ($\delta H^{\delta 1}$ 0.34 ppm, $\delta H^{\varepsilon 1}$ 0.33 ppm, $\delta H^{\zeta 2}$ 0.38 ppm, $\delta H^{\eta 2}$ 0.03 ppm, $\delta H^{\zeta 3}$ 1.20 ppm and $\delta H^{\varepsilon 3}$ 0.64 ppm), indicating electrostatic interactions between the nucleobases and the tryptophan ring. Another indication for strong interactions between the oligonucleotide and the protein is the appearance of new NH resonances during the titration which can be assigned to oligonucleotide NH's (see below) and the progressive sharpening of the original broad water signal upon addition of d(TACGCC). This reduced exchange broadening of NH with the solvent can be ascribed to protein-oligonucleotide interactions (i.e. shielding the exchangeable H's from the solvent and/or the presence of H- bonding interactions between the oligonucleotide and the protein).

The 2D NMR data gave a more detailed picture of the DNA-protein interactions. The full set of NOE restraints did not allow an unambiguous structure determination but the main features of the interaction may be deduced. Figure 5.3.A shows the region from a NOESY data set containing contacts between base protons from the DNA hexamer and aromatic protons from the F2 peptide. In this region weak crosspeaks are observed between C_3H5 and both W4-Hζ3 and W4-Hε3 while stronger crosspeaks are observed between one of the exoyclic NH2 protons of G_4 and W4-Hζ3. In Figure 5.3.B, crosspeaks are noted between T_1H6 and K14-Hε2 and between A_2H2 and K14-Hγ1 which clearly indicate that the K14 sidechain is also involved in intermolecular interactions. Note the presence of close contacts between the thymine and lysine residues seen from the NMR data. As a result of intermolecular interactions involving C_3 and G_4, the sequential assignment is interrupted between C_3 and G_4. These results are consistent with destacking of the cytosine from the nucleic acid single strand, as indicated by the break in connectivity between C_3 and G_4, rather than a formal intercalation of the tryptophan ring between the adjacent C_3 and G_4 bases. The structure of the complex formed between NCp10 from Moloney Murine Leukemia Virus and the pentanucleotide d(ACGCC) studied by NMR methods showed insertion of Trp between two successive bases and its stacking to dG. [35]

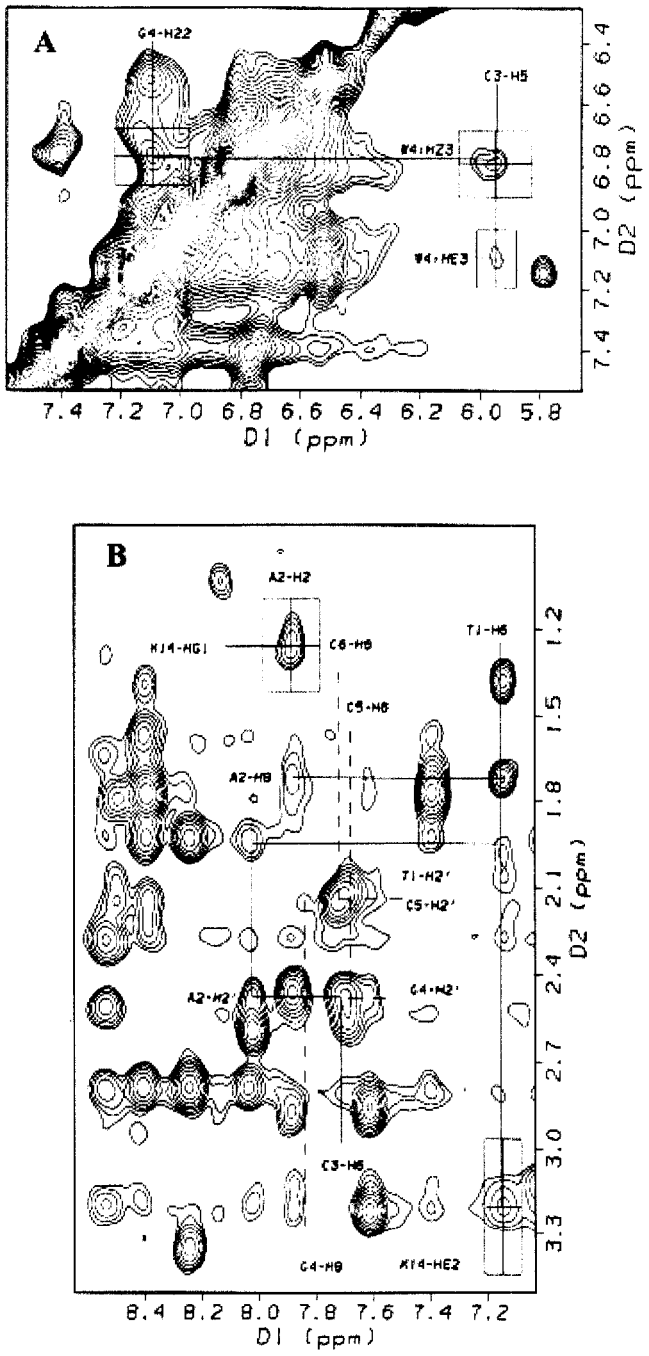

Figure 5.3. Expanded regions from a 200 ms NOESY data set obtained on d(TACGCC)-NCp7-F2(Zn) (in H_2O,D_2O (90:10), 298K) showing: (A) Intermolecular NOE contacts between the aromatic protons of the TRP residue and C_3H5 and G_4NH22 of the oligonucleotide. (B) H_{base} -H2'/H2" connectivities of d(TACGCC). Note the sequential 'break' between C_3 and G_4, caused by the interaction with the Trp residue. Sequential H6/H8,H2'/H2" connectivities are observed for T_1, G_2 and C_3; however no connectivities are observed from either C_3H2' or $C_3H2"$ to G_4H8. The sequential walk resumes for C_5 as H2'/H2", H6 connectivities are observed for C_5 and C_6. In addition, intermolecular connectivities between protons on the K14 sidechain and T_1 and A_2 are shown.

Zinc Finger Interaction with Platinated Nucleobases. Non-Covalent Interactions.

Once the essential nature of the F2-DNA interaction had been determined we aimed to mimic this interaction with small molecules. Addition of the hexanucleotide to F2 caused the quenching of the tryptophan fluorescence to a large degree, in agreement with previous studies.[36, 37] Upon incubation of F2 with $[Pt(dien)(9\text{-EtGH})]^{2+}$, **Ia**, the fluorescence intensity also decreased and the fluorescence quenching is more effective than for free nucleobase, as observed previously.

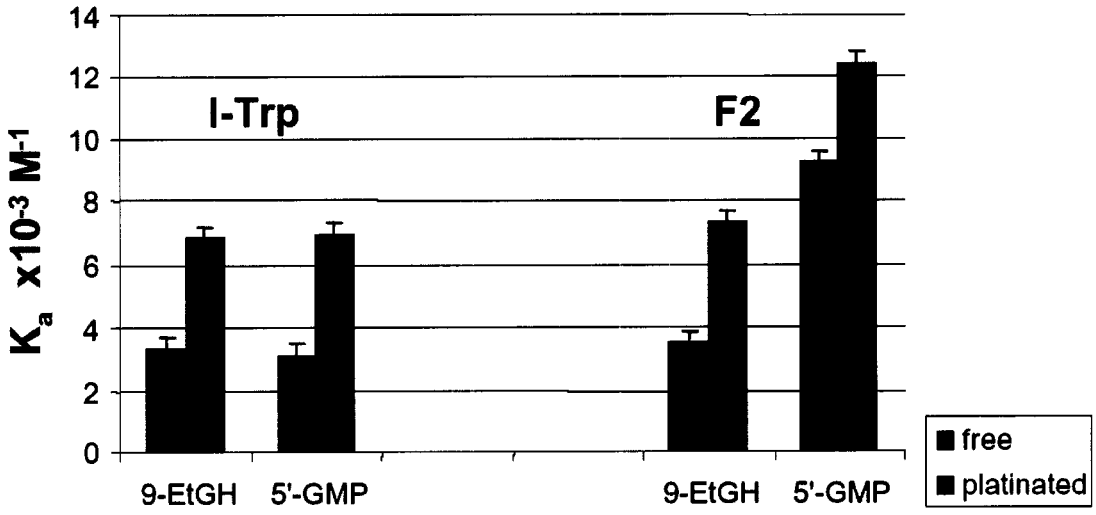

Figure 5.4. Comparison between association constants determined for Pt-nucleobase/nucleotide complexes with N-Acetyl tryptophan (left) and F2 (right).

Similar enhancement is also found for platinated 5'-GMP, (**Ib**, [Pt(dien)(5'GMP)]). The association constant values found using Eadie-Hofstee analysis are 7.5 x 10^3, 12.4 x10^3 and 60.0 x 10^3 M^{-1} for **Ia**, **Ib** and d(TACGCC) respectively. Interestingly, while there

is little difference in tryptophan binding between the 9-EtGH and 5'-GMP species, the extra phosphate group enhances binding to the zinc finger, Figure 5.4. The ribose monophosphate moiety could be involved in extra recognition features of the type Lys-phosphate previously reported for the complex NCp7/ACGCC.[16] While binding is predictably not as high as for free hexanucleotide the results indicate that further incremental increases can be achieved by extending the length of the oligonucleotide chain bound to Pt.

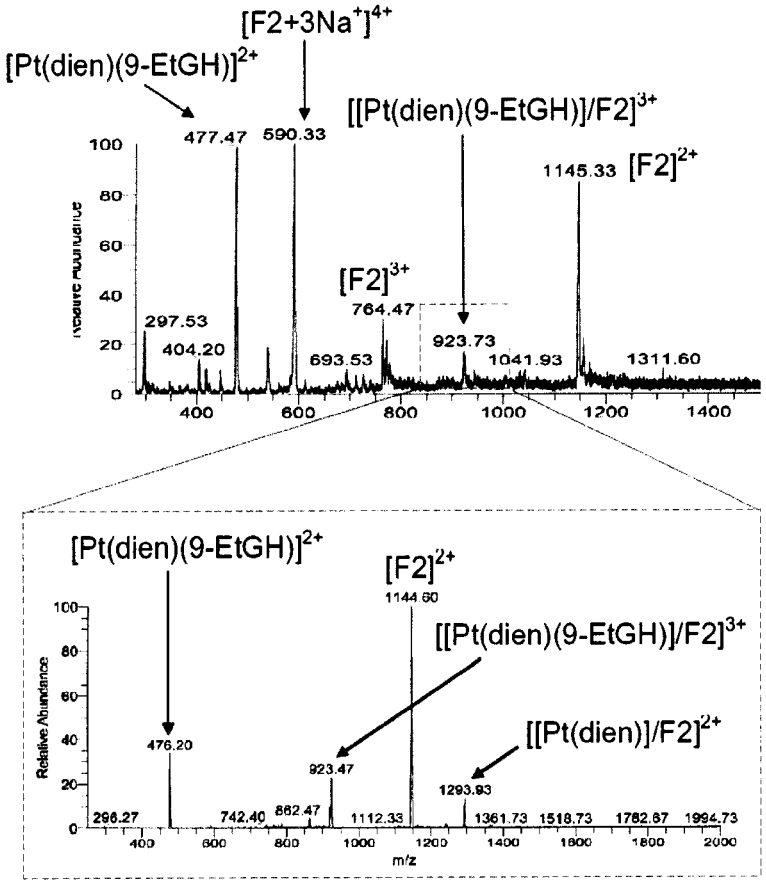

Figure 5.5. Full ESI-MS spectrum of the 1:1 incubation for Pt(dien)9-EtGH with F2 (A), MS2 from the species at 923.73 *m/z* confirming the assignation of the signal to the 1:1 adduct $[[Pt(dien)(9\text{-}EtGH)]/F2]^{3+}$.

The zinc finger-DNA interaction is amenable to study by mass spectrometry .[38] The ESI-MS spectrum of F2 in the presence of a 1:1 ratio of $[Pt(dien)(9\text{-EtGH})]^{2+}$ shows a new peak at m/z = 923.47 corresponding to the 3+ state of the 1:1 adduct between the peptide and Pt complex, Figure 5.5.A. MS-MS experiments on the peak at m/z 923.47 shows dissociation to reactants and a minor peak at m/z = 1293.93 corresponding to the 2+ state of a F2/[Pt(dien)] adduct implying loss of 9-EtGH, Figure 5.5.B.

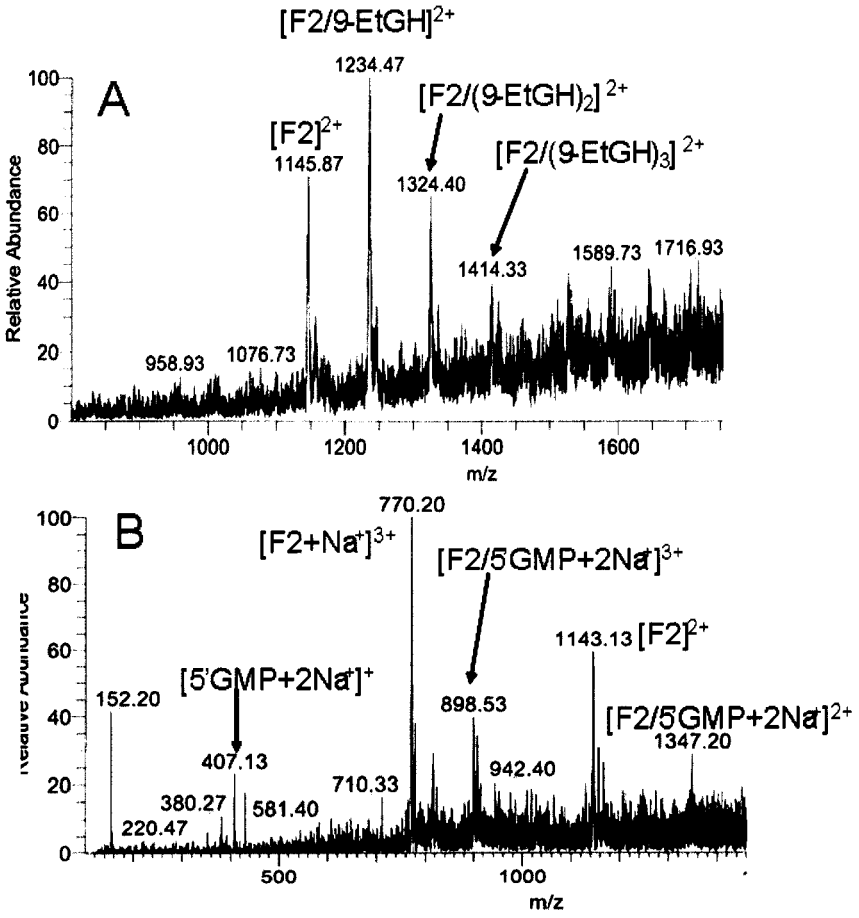

Figure 5.6. ESI-MS spectra from the incubation of F2 with 9-ethylguanine (A) and 5'-guanine monophosphate (B) showing the assignation of more important species.

Interestingly, the ESI-MS of F2 in the presence of free 9-Ethylguanine itself shows the presence of multiple adducts with more than one purine associated with the peptide, Figure 5.6.A. The predominant adducts are the 1:1 (m/z = 1234.47) and 2:1 (m/z = 1324.40) but higher stoichiometries of 3:1 are also observed. Since only one aromatic residue (W37) is available for stacking, the presence of 1:2 and higher ratio adducts suggests additional extra non-covalent cation-π interactions given the positively charged lysines (4) and arginine (1) residues present in F2 .[39] In this regard, cation - π interactions have been found to occur with a higher frequency than π-π stacking interactions in protein/nucleic acid base systems.[40] Cooordinate bond formation between the Zn and 9-EtGH forming a 5-coordinate complex is also possible since the F2/9-EtGH specie was observed when *trans*-$[PtCl(py)_2(9\text{-EtGH})]^+$ was used (see below). The observation of multiple adducts may be due to the gas phase nature of the reactions – in solution the platinated 9-Ethylguanine interacts more strongly than the free base with both simple tryptophan and F2 (Figure 5.4.).

In the case of the F2/5'GMP system only the 1:1 adduct was observed (Figure 5.6.B.). The presence of 1:1 adducts between N-AcTrp, as a model of W37 in F2, and the complex Pt(dien)(5'GMP) have also been detected *via* ESI-MS (Figure 5.7.) but mass spectra with the hexanucleotide d(TACGCC) were very noisy and were not pursued at this time.

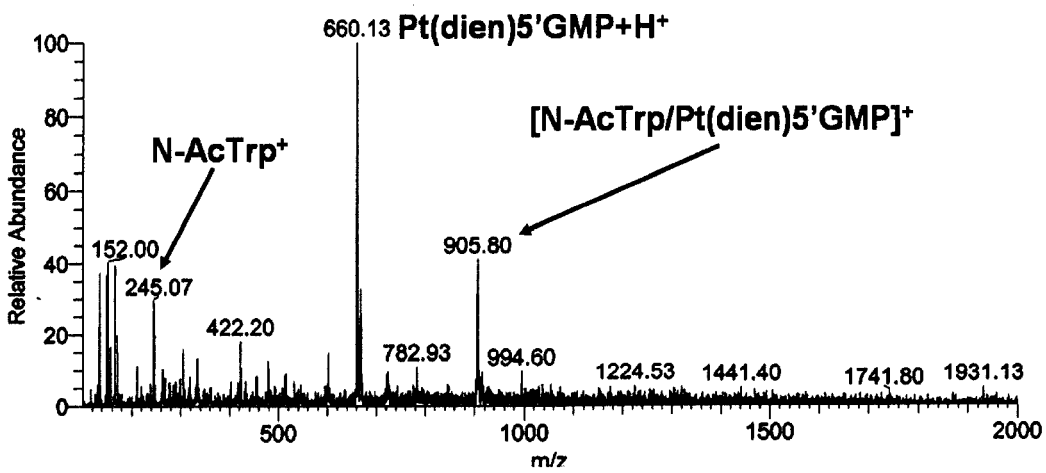

Figure 5.7. ESI-MS spectrum of a 1:1 solution of N-acetyltryptophan(N-Actrp) with Pt(dien)5'GMP, showing the presence of the 1:1 adduct at 905.80 *m/z*.

The CD spectrum of F2 in presence of $[Pt(dien)(9\text{-}EtGH)]^{2+}$ shows little perturbation of the secondary metallopeptide structure (data not shown). A reasonable interpretation of the results then is that adduct formation has occurred between the F2 and $[Pt(dien)(9\text{-}EtGH)]^{+}$ facilitated by the π-π stacking between tryptophan and the platinated purine nucleobase, but this association does not disrupt the three-dimensional structure of F2 to a significant degree. Covalent interaction on the other hand prove to have significantly different consequences (*vide infra*).

The incubation of *cis*-$[Pt(NH_3)_2(Guo)_2]^{2+}$ (Guo = Guanosine, **III**) with F2 showed a very small peak at *m/z* = 1029.40 amu corresponding to association to the 1:1 adduct $[Pt(NH_3)(Guo)_2/F2]^{3+}$. The peak assignment was supported by comparison of the calculated isotopic distribution. An MS2 experiment on the peak clearly revealed signals assignable to the free F2 and the platinum complex indicating dissociation (Figure 5.8.).

The presence of these species again implies a chemical model for DNA recognition. The binding is much weaker than that of $[Pt(dien)(9\text{-}EtGH)]^{2+}$ and thus there are distinctions between platinum complex structures in their interactions with zinc fingers. In this case steric hinderance of the two *cis*-oriented purine nucleosides may account for the weaker binding. Studies of this compound are also of interest because of its previously reported anti-viral activity.[41, 42]

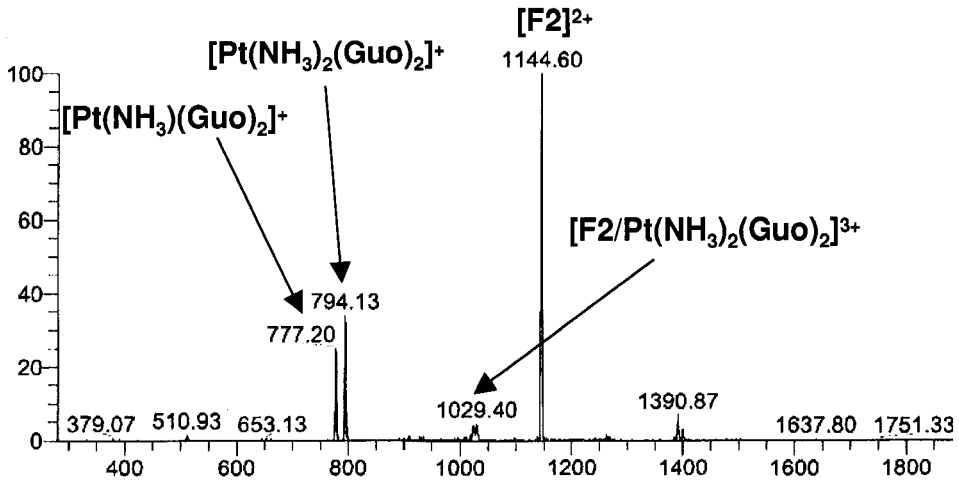

Figure 5.8. Tandem MS of the peak at 1029.4 *m/z* showing confirmation for this specie as the 1:1 adduct between the platinum complex and the F2 zinc finger.

Zinc Finger Interaction with Platinated Nucleobases. Covalent Interaction and Zinc Ejection. To examine the possible covalent attachment of Pt to the Zn finger the interaction was studied with *trans*-$[PtCl(9\text{-}EtGH)(py)_2]^+$, **II**. This complex has previously been shown to have a high kinetic preference for sulfur (methionine) over nitrogen (5'-GMP) binding .[43] Further, Zn was shown to be ejected from model chelates in the presence of the complex

.[26] In the presence of a 1:1 stoichiometric ratio of **II**, the ESI-MS spectrum of F2 after 24h now shows a number of peaks, Figure 5.9. Free 9-EtGH is observed and, again, a 1:1 adduct of F2 and 9-EtGH is seen with a peak at 1233.5 (2+ state). Interestingly a peak corresponding to *trans*-$[Pt(py)_2(9\text{-}EtGH)_2]^{2+}$ is also seen at *m/z* of 355.7. A reasonable interpretation of these results is that formation of a Zn-S-Pt intermediate will labilize the *trans* 9-EtGH ligand due to the strong *trans* influence of thiolate. Free 9-EtGH may then form the 5-coordinate species with Zn and substitute Cl in **II**. The species of interest in the mass spectrum is firstly, that assigned to F2 + $[Pt(py)_2]$: m/z = 1320.1 (2+); 880.5 (+3) and , 655.3(+4). The isotopic distribution is consistent with a Pt,Zn species (data not shown). As observed previously, the presence of multiple isotopes in transition metals makes analysis of isotopic distribution a very useful asset in assigning stoichiometry.[26] The second major species of interest is that with m/z values for a 2+, 3+ and 4+ state of 1464.1, 976.5 and 733.3 respectively. This species corresponds to an adduct $\{F2[[Pt(py)_2]_2\text{-}Zn\}$. That is, two $[Pt(py)]_2$ units are bound to the protein with resultant loss of the zinc atom. The isotopic distribution of this peak is also consistent with only 2 Pt atoms and no Zn.

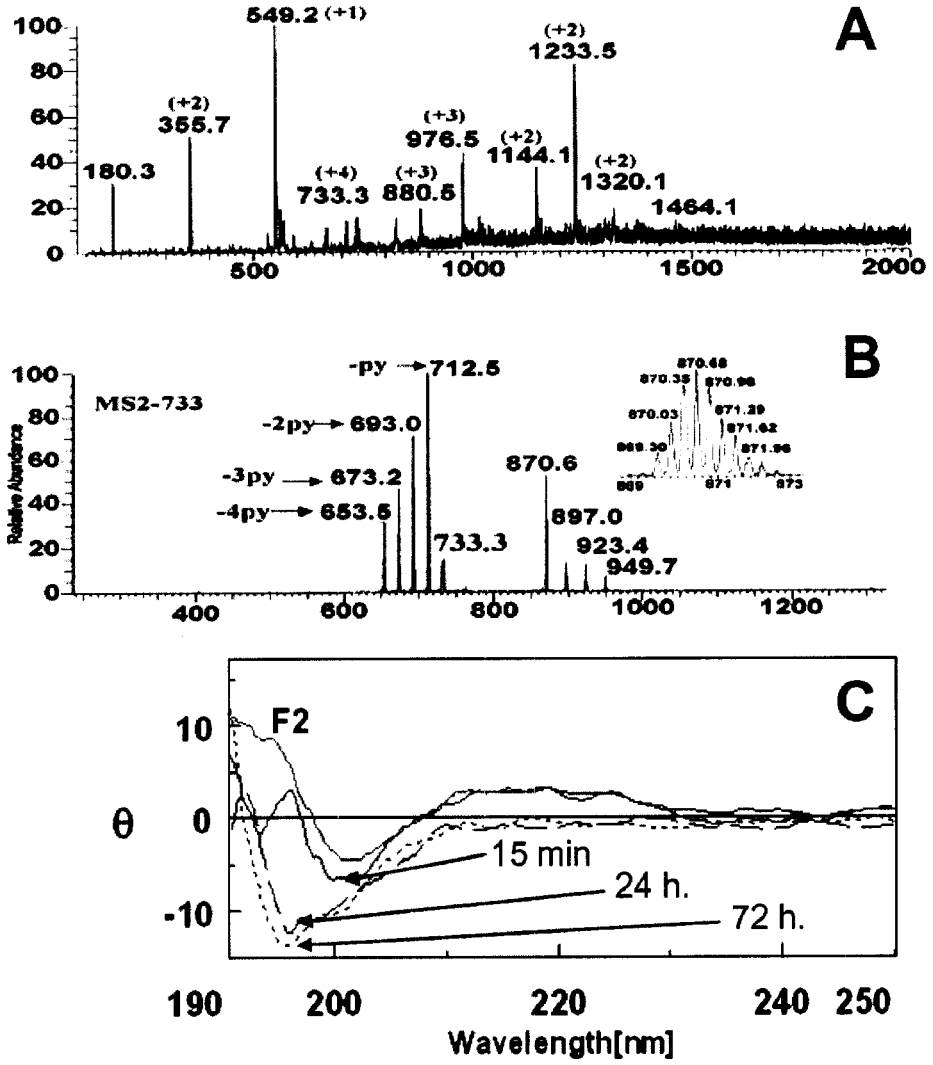

Figure 5.9. Covalent interaction between F2 and *trans*-$[PtCl(py)_2(9\text{-}EtGH)]^+$: (A) ESI-MS spectrum after 24 h. incubation shows 1:1 adducts of the platinum complex and F2 (*m/z* = 1320.1, 880.5 and 655.3), also signals corresponding to two $Pt(py)_2$ units with the free peptide (*m/z* = 1464.1, 976.5 and 733.3) indicating loss of the zinc ion; (B) Tandem MS/MS experiments and isotopic distribution of the signals confirmed the assignation; (C) CD spectra of F2 undergo a blueshift of the elipticity minimum after incubation with 2 eq. *trans*-$[PtCl(py)_2(9\text{-}EtGH)]^+$, after 72 h. the spectrum is very similar to the free peptide. Intact F2 is shown in red as a reference.

Tandem MS/MS of the 733.3 (4+) state showed sequential loss of 4 pyridine ligands leading to the observation of + 4 state fragments with *m/z* of 712.5, 693.0, 673.2 and 653.5. The corresponding +3 state peaks at *m/z* of 949.7, 923.4, 897.0 and 870.6 were observed as well, and the isotopic distribution of the latter peak (*m/z* of 870.6) was also consistent with the presence of 2 Pt atoms, Figure 5.9.B. Essentially identical behavior was observed with *[SP-4-2]*-[PtCl(9-EtGH)(NH_3)(quin)]$^+$ (data not shown) indicating that this chemistry is a general feature of this class of compounds. After 7 days incubation the major species observed were *trans*-[Pt(py_2)(9-EtGH)$_2$]$^{2+}$ (m/z = 355.7), {F2 + [Pt(py_2)]$_2$}$^{3+}$ (m/z = 880.5), {F2 + 2[Pt(py_2)] - Zn}$^{3+}$ (m/z = 976.5) and {F2 + 9-EtGH}$^{2+}$ (m/z = 1233.5) (see Figure 5.10.).

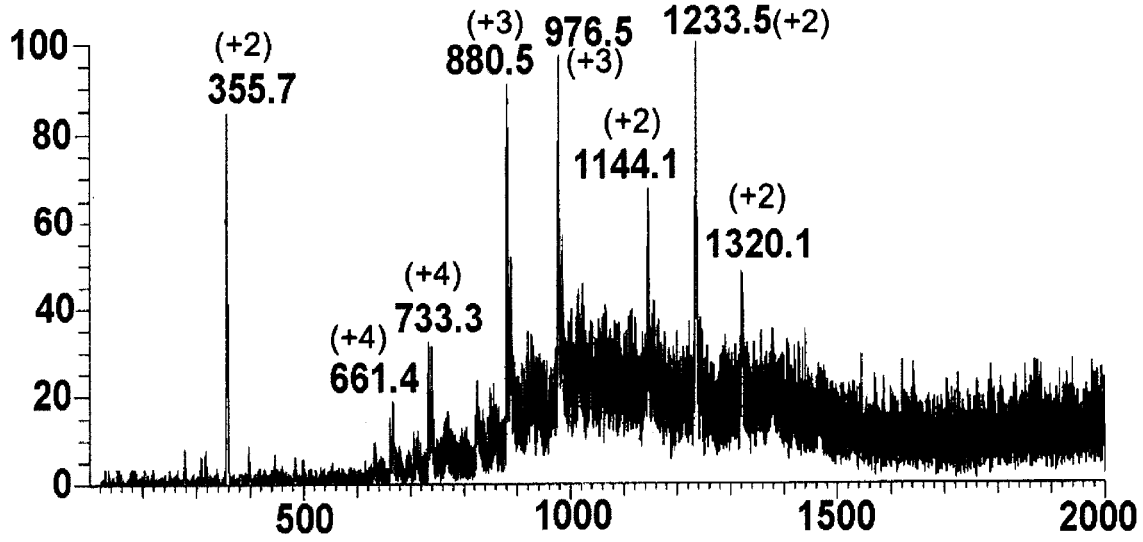

Figure 5.10. ESI-MS results of the reaction between trans-[PtCl(9-EtGH)(py_2)]+ and F2 recorded after 7 days of incubation at 37 °C .

The CD spectra of F2 in presence of *trans*-$[PtCl(9\text{-}EtGH)(py)_2]^+$ is shown in Figure 5.9.C. Monitoring of the spectrum through time revealed important changes in the three-dimensional structure of F2 within the first 24 h. It is clear that the loss of structural feature is consistent with loss of tertiary structure due to Zn elimination

The results presented here suggest that modulation of the basic $[PtCl(L)(L')(Nucleobase)]^+$ (L = NH_3, L'= pyr, quin etc. or L = L' = pyr etc.) structural motif is a viable approach to more effective and selective inhibitors of the zinc-finger-nucleic acid interaction. The concept mechanism involving a classic two-step approach (i) target recognition through tryptophan interaction and (ii) target fixation or inhibition involving platinum-protein complexation followed by zinc ejection is shown in Figure 5.11.. The proposed chemical mechanism shown in Figure 5.11. is reasonable based on previous results with zinc fingers and with model zinc chelates.[26, 28, 46] Subsequent reactions including incorporation of platinum into the finger are possible.

The results are of interest for two main reasons. Firstly, study of metal displacement of zinc from zinc-finger or zinc-based proteins has probed the potential biomedical implications involved in incorporation of metals such as Cd, Hg, Pb and Ni (usually studied as aquated 2+ cations).[30, 44] The reactions of gold thiomalate with the Sp1 zinc finger[31] and the use of oligonucleotide-tethered cobalt(salen) as a sequence-specific recognition probe[45] are, in principle, examples of zinc finger interaction using *functionalized* metal complexes. The results presented here indicate that functionalized platinum complexes (in this case the presence of purine nucleobases and the absence or

presence of substitution-labile binding site) display a variety of chemical reactivity on the Zn-finger site. While the present study demonstrates the use of Cys_3His finger, it would be expected that the different limiting Zn-finger coordination sites would also display different chemical reactivity. [28] In this context, the reaction between cisplatin and a 31-amino acid zinc finger sequence (zpp) N-I $\mathbf{C_1}$ E E P T $\mathbf{C_1}$ R N R T R H L P L Q F S R T G P L $\mathbf{C_2}$ P A $\mathbf{C_2}$ M K A is noteworthy. [46] The reaction proceeds in a stepwise manner and complete deligation of Zn(II) was only observed with two equivalent of *cis*-DDP. [46] The subscripted residues represent the four Zn ligands and the sites of the first and second attachment of platinum, respectively. These results have been discussed with respect to apoptosis initiated by direct interaction of the platinum antitumor agent with zinc finger transcription factors but it is of interest to note that 2 Pt atoms appear necessary before zinc is lost from the peptide. In the case of F2 the possible sulfur binding sites on F2 include the methionine and the three Zn-bound cysteines. It is possible that the first platination occurs at the methionine site and this may not disturb the zinc coordination sphere. The second platination would then involve a ligand intimately involved in maintaining the tetrahedral zinc geometry and loss of Zn could then occur, as seen in model systems. Evidence for competitive binding of methionine in proteins rather than cysteine has come from studies of cisplatin with Human Serum Albumin. [47] The use of *trans*-DDP to cross-link the zinc-finger nucleocapsid protein to HIV-1 RNA has been reported[48] and the specific interactions are likely to be similar to those described here.

Secondly, these results suggest novel approaches to targeting the nucleic acid-zinc finger interaction. Most approaches to NCp7 inhibition have involved alkylation or

oxidation of the cysteine residues resulting in reduced ability to bind zinc, and subsequent loss of conformation thereby diminishing or eliminating infectivity.[20] The small organic molecules designed for electrophilic attack have little or no DNA selectivity, therefore precluding attack on the protein-DNA interaction.

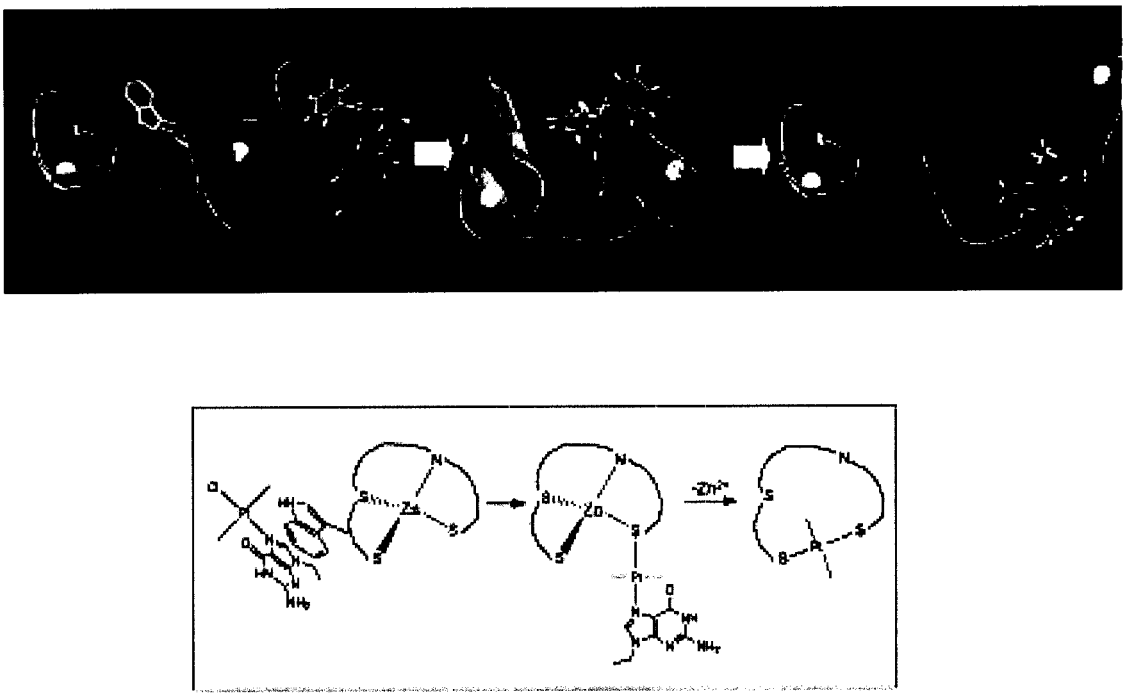

Figure 5.11. (top) Proposed concept mechanism of zinc ejection from F2 involving an initial recognition process through noncovalent interactions and a further covalent interaction that eventually disrupts the secondary structure in the protein. (bottom) A chemical mechanism for zinc ejection using platinum-nucleobase electrophiles. The specific nature of the coordination site for the $[Pt(py)_2]$ unit remains to be determined

The presence of an aromatic residue – tryptophan, phenylalanine and tyrosine – as a recognition motif for single-stranded DNA and RNA is a structural handle one can use in inhibitor design. A study of oligonucleotide affinity for HIV nucleocapsid protein showed

that small GT sequences such as $d(GT)_4$ had high binding affinity and indeed this property has been used as a screen for nucleic acid antagonists of NCp7. [49] The incipient and moderately selective antiviral activity of *trans*-[PtCl(Nucleobase)(L)(L')]$^+$ is worthy of further rational study based on the concept hypothesis.[50]

5.4. Experimental Section

Starting Materials. Preparation of F2: Coordination of the zinc ion to the peptide (34-52) and secondary structure characterization of the F2 zinc finger were monitored using ^{1}H-NMR, ESI-MS and CD spectroscopy, the data obtained were in agreement with reported values in the literature.[30, 45]

The C-terminal zinc finger from the retroviral HIV-1 p7 nucleocapsid protein (F2, sequence Lys-Gly-Cys-Trp-Lys-Cys-Gly-Lys-Glu-Gly-His-Gln-Met-Lys-Asp-Cys-Thr-Glu) was purchased from the Macromolecular Structure Facility of the University of Arizona (Division of Biotechnology). The peptide was dissolved in degassed H_2O-solution (HPLC-grade, J.T. Baker) and $ZnCl_2$ (1.2 equimolar) was added in slight excess with respect to the concentration of the zinc finger. The pH was adjusted to 6.4 and the sample was lyophilized. The oligonucleotide d(TACGCC) was synthesized with an Expedite 8909 DNA synthesizer (Perseptive Biosystems) using the cyanoethyl phosphoramidite method (reagents were from Glen Research, Sterling, VA).

NMR Spectroscopy. All NMR spectra were acquired at 298 K and pH 6.4 on a Varian UNITY 500 MHZ spectrometer at 2.9 mM concentration. ^{1}H NMR chemical shifts were

referenced to internal H_2O (4.72 ppm at 298 K) and ^{31}P NMR data are referenced to Trimethyl phosphate (TMP). 2D NMR data were collected without sample spinning. 2D NOESY data were recorded in 90% H_2O/10% D_2O (t_{mix} 100, 200 and 400 msec) and in D_2O (99.99%, t_{mix} 300 msec). The non-exchangeable NOESY spectrum was recorded using the States/TPPI technique with 512 t_1 increments and a sweep width of 6802.72 Hz. Solvent suppression for the homonuclear 2D measurements in H_2O was achieved using the WATERGATE technique. 512 t_1 increments, each with 1024 t_2 complex points, were collected with a SW of 6802.72 Hz. For the TOCSY experiment a t_{mix} of 80 msec was used. The 2QF-COSY was measured according to literature procedures.[51] The 2D heteronuclear ^{31}P-^{1}H correlation spectra were recorded using the method described.[52] The data were processed using the Felix 2.10 software (BioSym Technologies) with a cosine-bell function before Fourier transformation.

Assignment of proteinand oligonucleotide resonances. The protein resonances of the d(TACGCC)-hivf2 complex were assigned according to established procedures.[53] A summary of the protein assignments is listed in Supplementary Table S5.1A. Interesidual NOEs between the four residues coordinated to the zinc confirm their spatial proximity. The NH^{ε} protons of Gln(12) can be observed in the TOCSY from a long-range coupling towards the H^{γ}(12). The chemical shifts of the oligonucleotide moiety are summarized in Supplementary Table 5.II

Table 5.II. ^{1}H NMR oligonucleotide chemical shift assignments for d(TACGCC)NCp7(F2).

Residue	H8/H2/H6	H5/CH_3	H1'	H2'/H2"	H3'	H4'	H5'/H5"	NH
dT1	7.14	1.73	5.79	1.36/1.97	4.46	3.89	3.52	-
dA2	8.02/8.01	-	5.76	2.59/2.46	4.87	4.23	3.95/3.87	6.41
dC3	7.70	5.89	6.21	2.10/2.46	4.84	4.34	4.10	6.30;6.00
dG4	7.82	-	5.95	2.45/2.56	4.82	4.31	4.10/4.06	6.50;10.2
dC5	7.68	5.91	6.15	2.28/2.15	4.43	4.04	3.98	6.63
dC6	7.75	5.94	6.18	2.16/2.48	4.72	4.26	4.03	-

5.6.1. Electrospray Ionization Mass Spectrometry (ESI-MS) Method: Electrospray ionization mass spectra were recorded by Finnigan LCQ ion-trap electrospray meter (LCQ-MS) in positive mode. The employed voltage at the electrospray needles was 2.5 kV. The capillary was heated to 150 ^{0}C. The solutions were injected into the Nano-ESI source directly at the flow rate of 1.0 μL/min. Tandem mass and zoom scan were used to analyze the structure of the product. Helium gas was admitted directly into the ion trapping efficiency and as collision gas in the Collision-Induced Dissociation (CID) experiment. A maximum ion injection time of 500 ms along with 10 scans was set. To induce collision activation, the relative collision energy was controlled to 10-30% of maximum, depending on the precursor ions and the MS^{n}. In MS/MS experiments, 6-12 isolation width for the precursor ions were used to allow the Pt isotopic signature to be observed.

5.6.2. Circular Dichroism (CD) Spectropolarimetry: The CD spectra were recorded in a JASCO J-600 Spectropolarimeter (Jasco, Corp., Tokyo, Japan). The pH of the solutions was maintained in the range 6.9 – 7.4 by addition of NaOH solution. Each spectrum was recorded at a wavelength range 190 – 250 nm in a 0.1-cm cuvette path length at room temperature under N_2. Spectra were baseline-corrected and noise-reduced using the Jasco software.

5.6.3. Fluorescence Spectrophotometry: The fluorescence spectra were recorded in a VARIAN Cary Eclipse fluorescence spectrophotometer equipped with a single cell Peltier accessory. Fluorescence spectra were recorded in the range of 295 to 450 nm. with a scan rate of 120 nm/min. The maximum intensity of the spectrum (at ca. 362.9 and 358.9 nm for N-AcTrp and F2 respectively) was measured for each addition and the association constants for each system were obtained from the analysis of Eadie-Hofstee plots. [54] Measurements were made at 20 °C and reported association constants (K_a) were averaged over a number of six different experiments, with the significance of results compared using the unpaired t-test.

5.5. Conclusions. This contribution shows that the interaction of small molecules such as *trans*-[PtCl(9-EtGua)$(pyr)_2]^+$ with the C-terminal zinc finger of HIV NCp7 protein results in Zn ejection from the peptide accompanied by loss of tertiary structure. The nature of the protein-DNA interaction on the C-terminal finger alone with the hexanucleotide d(TACGCT) was examined. The results confirm the tryptophan-guanine/cytosine recognition motif for zinc finger-single stranded DNA/RNA interactions and may be placed in context with structural

examinations of the N-terminal finger and the intact 2-zinc finger peptide with similar DNA sequences. The platinated nucleobase motif of Complexes **I** and **II** mimics the DNA-protein stacking interaction. Targeting the NCp7-DNA interaction for drug design represents a conceptual advance over electrophiles designed for chemical attack on the zinc finger alone. Thus, Complex **II** is a first example of a new chemotype capable of selective zinc finger attack through targeting of the tryptophan/guanine recognition. In a broader sense, these results demonstrate examples of a new platinum structural class targeting specific biological processes, distinct from the bifunctional DNA-DNA binding of cytotoxic agents like cisplatin.

Extension of this analogy between Me^{+} and Pt^{2+} can suggest further novel structural motifs capable of expanding the role of platinum in biology beyond the current paradigm. An important goal for medicinal inorganic chemists is to manipulate the many intrinsic features of transition metal complexes – the number and type of exchangeable ligands, oxidation state of the central metal ion, coordination number and stereochemistry as well as rate of reaction – to design more selective agents capable of targeting specific biomolecules and thus eventually capable of exerting a more specific biological response.

5.6. References.

(1) Summers, M.F.; Henderson, L.E.; Chance, M.R.; Bess, J.W.; South, T.L.; Blake, P.R.; Sagi, I.; Perez-Alvarado, G.; Sowder, R.C.; Hare, D.R.; Arthur, L.O. *Protein Sci.*, **1992**, 1, 563-574.

(2) Bess, J.W.Jr.; Powell, P.J.; Issaq, H.J.; Schumack, L.J.; Grimes, M.K.; Henderson, L.E.; Arthur, L.O. *J. Virol.*, **1992**, 66, 840 - 847.

(3) Gorelick, R.J.; Nigida, S.M., Jr., Bess, J.W.Jr., Aurthor, L.O.,Henderson, L.E., Rein, A. J. Virol., 1990, 64, 3207 - 3211.

(4) Mely, Y., de Rocquigny, H., Sorinas-Jimeno, M., Keith, G., Roques, B.P., Marquet, R.; Gerard, D. *J. Biol. Chem.*, **1995**, 270, 1650 - 1656.

(5) Khan, R.; Giedroc, D. P. *J. Biol. Chem.*, **1994**, 269, 22538 - 22546.

(6) Surovoy, A., Dannull, J., Moelling, K.; Jung, G. *J. Mol. Biol.*, **1993**, 229, 94 -104.

(7) Herschlag, D.J. *J. Biol. Chem.*, **1995**, 270, 20871-20873.

(8) Gorelick, R. J., Nigida, S. M., Jr., Bess, J. W., Jr., Arthur, L. O., Henderson, L. E.; Rein, A. *J. Virol.*, **1990**, 64, 3207-3211.

(9) Sakaguchi, K., Zambrano, N., Baldwin, E. T., Shapiro, B. A., Erickson, J. W., Omichinski, J. G., Clore, G. M., Gronenborn, A. M.; Appella, E. *Proc. Natl. Acad.* USA, **1993**, 90, 5219 - 5223.

(10) Darlix, J. L., Gabus, C., Nugeyre, M T., Clavel, F.; Barre-Sinoussi, F. *J. Mol. Biol.*, **1990**, 216, 689 - 699.

(11) Barat, C., Lullien, V., Schatz, O., Keith, G., Nugeyre, M. T., Gruninger-Leitch, F., Barre-Sinoussi, F., LeGrice, S. F.; Darlix, J. L., *EMBO J.*, **1989**, 8, 3279 - 3285.

(12) Barat, C., Le Grice, S. F.; Darlix, J. L. *Nucleic Acids Res.*, **1991**, 19, 751 - 757.

(13) Venter, J.C., Adams, M.D., et al., *Science*, **2001**, 291, 1304 -1313.

(14) Hoovers, J. M.N., Mannens, M., John, R., Bliek, J., van Heyningen, V., Porteous, D.J., Leschot, N.J., Westerveld, A.; Little, P.F.R. *Genomics* , **1992**, 12, 254-263.

(15) De Guzman, R. N., Wu, Z. R., Stalling, C. C., Pappalardo, L., Borer, P. N.; Summers, M. F. *Science*, **1998**, 279, 384-388.

(16) Morellet, N.; Déméné, H.; Teilleux, V.; Huynh-Dinh, T.; de Rocquigny, H.; Fournié-Zaluski, M.C.; Roques, B.P. *J. Mol. Biol.*, **1998**, 283, 419 - 434.

(17) de Rocquigny, H.; Delaunay, T.; Petitjean, P.; Fournié-Zaluski, M.C.; Roques, B.P. *Reg. Biochimie*, **1998**, 2, 44 - 50.

(18) Remy, E., de Rocquigny, H., Petitjean, P., Muriaux, D., Theilleux, V., Paoletti, J. and Roques, B. P. *J. Biol. Chem.*, **1998**, 273, 4819 - 4822.

(19) Amarasinghe, G.K., de Guzman, R.N., Turner, R.B., Chancellor, K.J., Wu, Z.R. and Summers, M.F. *J. Mol. Biol.*, **2000**, 301, 491 - 511.

(20) Musah, R.A. *Curr. Top. Med. Chem.*, **2004**, 4, 1605 - 1622.

(21) Stephen, A.G., Worthy, K.M. et al. *Biochem. Biophys. Res. Comm.*, **2002**, 296, 1228 - 1237.

(22) Huang, M., Maynard, A., Turpin, J.A., Graham, L., Janini, G.M., Covell, D.G. and Rice, W.G. *J. Med. Chem.*, **1998**, 41, 1371-1381.

(23) Anzellotti, A.I.; Ma, E.S.; Farrell, N. *Inorg. Chem.*, **2005**, 44, 483 – 485.

(24) Anzellotti, A.I.; Sabat, M.; Farrell, N. *Inorg. Chem.*, **2006**, 45, 1638 – 1645.

(25) Ishida, T., Ueda, H., Segawa, K., Doi, M.; Inoue, M., *Arch. Biochem Biophys.*, **1990**, 278, 217 – 227.

(26) Liu, Q., Golden, M., Darensbourg, M.Y.; Farrell, N. *Chem. Commun.*, **2005**, 34, 4360 – 4362.

(27) Wilker, J.J.; Lippard, S.J. *Inorg. Chem.*, **1997**, 36, 969 – 978.

(28) Maynard, A. T.; Covell, D. G. *J. Am. Chem. Soc.*, **2001**, 123, 1047-1058.

(29) Nomura, A.; Sugiura, Y. *Inorg. Chem.*, **2002**, 41, 3693 – 3698.

(30) Kopera, E., Schwerdtle, T., Hartwig,A., Bal, W. *Chem. Res. Toxicol.*, **2004**, 17, 1452 – 1458.

(31) Larabee, J.L., Hocker, J.R. and Hanas, J.S. *Chem. Res. Toxicol.*, **2005**, 18, 1943 - 1954.

(32) South, T. L., Blake, P. R., Hare, D. R.; Summers, M. F. *Biochemistry*, **1991**, 30, 6342 – 6349.

(33) Delahunty, M.D., South, T. L., Summers, M. F.; Karpel R. L. *Biochemistry*, **1992**, 31, 6461 – 6469.

(34) Summers, M. F., Henderson, L. E., Chance, M. R., Bess, J. W., Jr., South, T. L., Blake, P. R., Sagi, I., Perez-Alvarado, G., Sowder, R. C., III, et al. *Prot. Sci.*, **1992**, 1, 563 - 574.

(35) Schuler, W., Dong, C-Z, Wecker, K.; Roques, B.P. *Biochemistry*, **1999**, 38,12984-12994.

(36) Vuilleumier, C., Bombarda, E., Morellet, N. Gerard, D.; Roques, B.P. *Biochemistry*, **1999**, 38, 16816-16825.

(37) Bombarda, E., Ababou, A., Vuilleumier, C., Gérard, D., Roques, B. P., Piémont, E. Mély Y. *Biophys J.*,**1999**, 76, 1561-1570.

(38) Loo, J.A. *Mass Spectrom. Rev.*, **1997**, 16, 1 - 23.

(39) Ma, J.C.; Dougherty, D.A. *Chem. Rev.*, **1997**, 97, 1303-1324.

(40) Biot, C.; Buisine, E.; Kwasigroch, J-.M.; Wintjens, R.; Rooman, M. *J. Biol. Chem.*, **2002**, 277, 40816 - 40822.

(41) Snyder, M.B., Saravolatz, L.D., Markowitz, N., Pohlod, D., Taylor, R.C;. Ward, S. *J. Antimicrob. Chemother.*, **1987**, 19, 815 - 822.

(42) Pommier, Y., Johnson, A.A.; Marchand, C. *Nature Rev. Drug. Discov.*, **2005**, 4, 236-248.

(43) Anzellotti, A.; Stefan, S.; Gibson, D.; Farrell, N. *Inorg. Chim. Acta*, **2006**, 359, 3014 - 3019.

(44) Godwin, H. A., Payne, J.C.; ter Horst, M.A. *J. Am. Chem. Soc.*, **1999**, 121, 6850-6855.

(45) Louie, A.Y.; Meade, T.J. *Proc.Natl. Acad. USA*, **1998**, 95, 6663 – 6668.

(46) Bose, R.N., Wei, W. Yang, W.; Evanics, F. *Inorg. Chim. Acta*, **2005**, 358, 2844 - 2854.

(47) Ivanov, A I., Christodoulou, J., Parkinson, J A., Barnham, K J., Tucker, A., Woodrow, J.; Sadler, P. J. *J. Biol. Chem.*, **1998**, 273, 14721-14730.

(48) Darlix, J.L., Gabus, C., Nugeyre, M.T., Clavel, F.; Barre-Sinoussi, F. *J. Mol. Biol.*, **1990**, 216, 689-699.

(49) Stephen A.G., Worthy, K.M., Towler, E., Mikovits, J.A., Sei, S., Roberts, P., Yang, Q., Akee, R.K., Klausmeyer, P., McCloud, T.G., Henderson, L., Rein, A., Covell, D.G., Currens, M., Shoemaker, R.H.; Fisher, R.J. *Biochem. Biophys. Res. Comm.*, **2002**, 296, 1228-1237.

(50) Sartori, D.A., Miller, B., Bierbach, U.; Farrell, N. *J. Biol. Inorg. Chem.*, **2000**, 5, 575-583.

(51) Rance, M., Sorenson, O.W., Bodenhausen, G., Wagner, G., Ernst, R.R., Wuthrich, K. *Biochem. Biophy. Res. Commun.*, **1983**, 117, 479 - 485.

(52) Keniry, M.A. *Magn. Reson. Chem.*, **1996**, 34, 33 - 35.

(53) Wütrich, K. (1986), NMR of Proteins and Nucleic Acids. (New York : John Wiley & Sons)

(54) Eadie, G. S. *J. Biol. Chem.*, **1942**, 146, 85-93

CHAPTER 6 Effects of Nucleobase Metallation on Frontier Molecular Orbitals: Potential Implications for π-stacking Interaction with Tryptophan.

Atilio I. Anzellotti[a], Craig A. Bayse [b] and Nicholas P. Farrell[a*]

a. Department of Chemistry, Virginia Commonwealth University, 1001 W. Main St. Richmond, VA 23284-2006, USA.

b. Chemistry Department, Old Dominion University, Norfolk, VA.

In Preparation for Journal of the American Chemical Society

6.1. Abstract.

This work shows that protonation, alkylation or coordination to a metal ion such as Pt(II) or Pd(II) of a nucleobase generally decreases the energy of its lowest unoccupied molecular orbital (LUMO), thereby improving the potential for π-stacking interactions with the highest occupied molecular orbital (HOMO) in N-Acetyl tryptophan. The change in the resulting energy difference between the frontier orbitals for nucleobase/tryptophan can be used as a predictive tool for the π-stacking interaction on these systems. For metal-nucleobase complexes an adequate LUMO localization in the nucleobase together with a proper orbital symmetry is also necessary for the constructive overlap of molecular orbitals. The analysis of frontier molecular orbitals correlates to a good degree with

previous experimental results involving Pt(II)-, Pd(II)-nucleobase complexes and alkylated nucleobases with tryptophan where higher association constants have been measured (by fluorescence experiments) in comparison to the free nucleobases.

6.2. Introduction.

Non-covalent π-π stacking interactions occurring between parallel aromatic rings are important for molecular recognition processes relevant to biological systems, such as DNA transcription, protein folding and gene regulation.[1-3] They can also direct the architecture and self-assembly of extended supramolecular systems with high relevance to material science or nanotechnology.[4-8] However, the exact nature of this interaction is still a matter of debate. A combination of electrostatic, hydrophobic, solvation, charge-transfer and frontier orbital interactions has been used to account for the three-dimensional arrangements observed in molecules exhibiting such motifs.[9] While simple systems such as the neutral benzene dimer adopts a different type of non-covalent interaction (i.e. T-shape or edge-to-face),[10, 11] the π-stacking interaction commonly found for larger systems and specifically aromatic residues in proteins and nucleic acids, is the off-centered, slipped or parallel displaced stacking (Chart 6.I.).[12, 13] The Hunter-Sanders rules based on electrostatic considerations have greatly contributed to explain qualitatively this kind of interaction. [9, 14] According to these rules a separation can be made in an aromatic system between a formally positive σ framework and the π-electrons, and the resulting geometry can then be evaluated in terms of π-π repulsions and π-σ attractions. However, other

important effects for π-stacking interaction, such as induction or short-range repulsions, are ignored with this model.

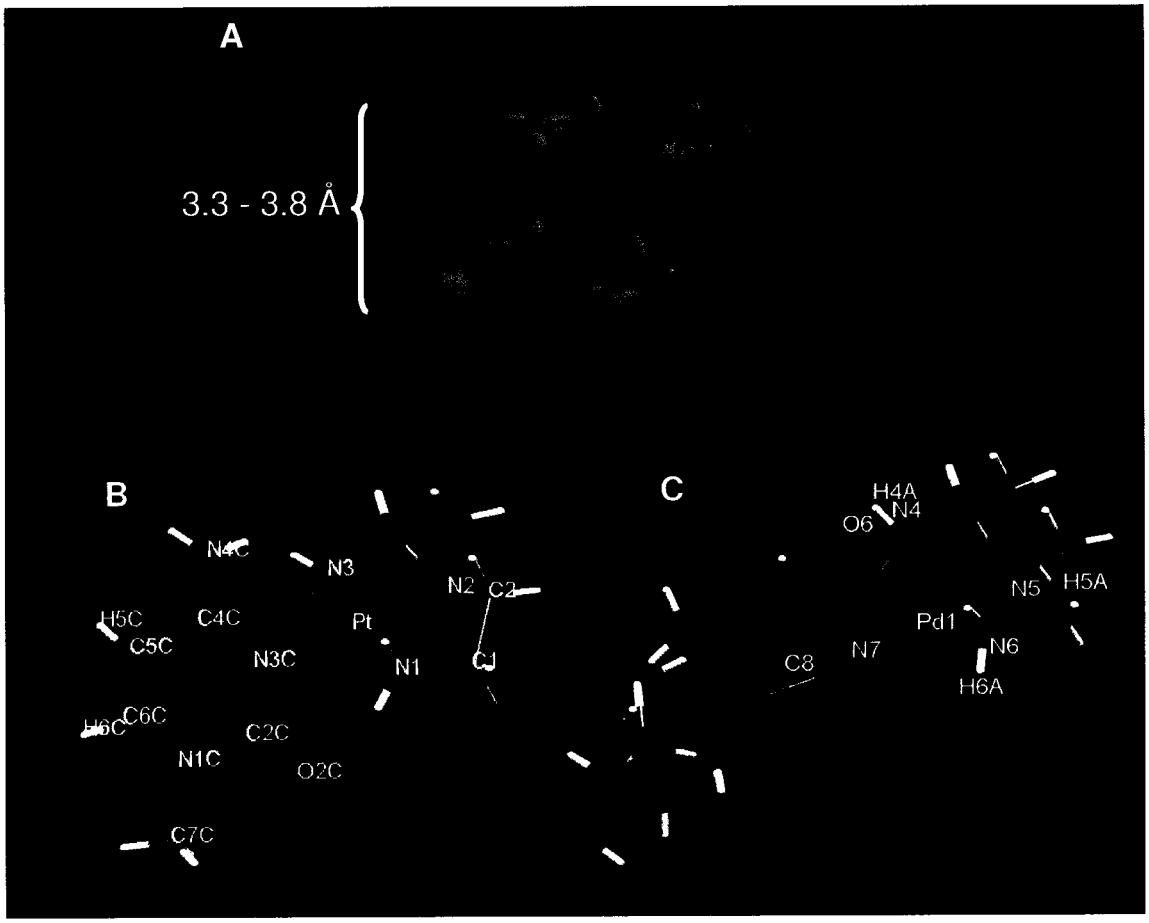

Chart 6.1. Schematic representation of a parallel displaced or off-centered π-stacking interaction, showing the common interplanar distance (A), numbering scheme for [metal(dien)1-MeCyt]$^{2+}$ (B) and [metal(dien)guanosine]$^{2+}$ complexes studied (C)

An alternative way to study the nature of π-stacking interactions takes into consideration the role of the frontier molecular orbitals: the highest occupied molecular orbital (HOMO)

and lowest unoccupied molecular orbital (LUMO) for the interacting molecules. It is accepted that a π-electron donor-acceptor complex can be formed from the HOMO of an appropriate donor system, to the LUMO of an acceptor.[15] This approach has been used to explain the main features of π-stacking interactions in relevant aromatic systems,[16, 17] in particular the interaction of alkylated nucleobases with tryptophan. Donation from the HOMO of the electronic-rich indole moiety in tryptophan is enhanced by a decrease in LUMO energy in the nucleobase due to N7 alkylation.[18-22] Several experimental studies regarding structural characterization of this binary system in the solid state, as well as in solution, have been performed. The system has relevance in eukaryotic protein translation mechanisms (i.e. mRNAcap - eukaryotic initiation factor (eIF) 4E interaction).[23-26] Molecular recognition from tryptophan residues based on a stacking interaction with a N7-methylated nucleobase has also been found in viruses, such as the viral cap-binding protein in vaccinia VP39 [27, 28] , confirming the motif as important for RNA-protein interactions.[29]

From the bioinorganic point of view, the off-centered π-stacking interaction is also a commonly observed motif.[9, 30] An enhanced understanding of the role of π-stacking in the recognition of DNA/RNA or proteins by appropriate ligands in metal complexes could result in the design of more specific chemotherapeutic agents.[31] Metal ions such as Pd(II) and Pt(II) have been shown to enhance intra- and inter-molecular π-π interactions by decreasing the π-electron density in aromatic nitrogen heterocycles.[32-34] Our recent fluorescence experiments have shown enhancement in the association constant between metallated nucleobases / nucleotides and l-tryptophan, when compared to the corresponding free nucleobases / nucleotides. The degree of enhancement for association

constant was dependent on the nature of the metal ion and nucleobase studied, favoring Pt(II) over Pd(II) and cytosine over guanine respectively.[35, 36]

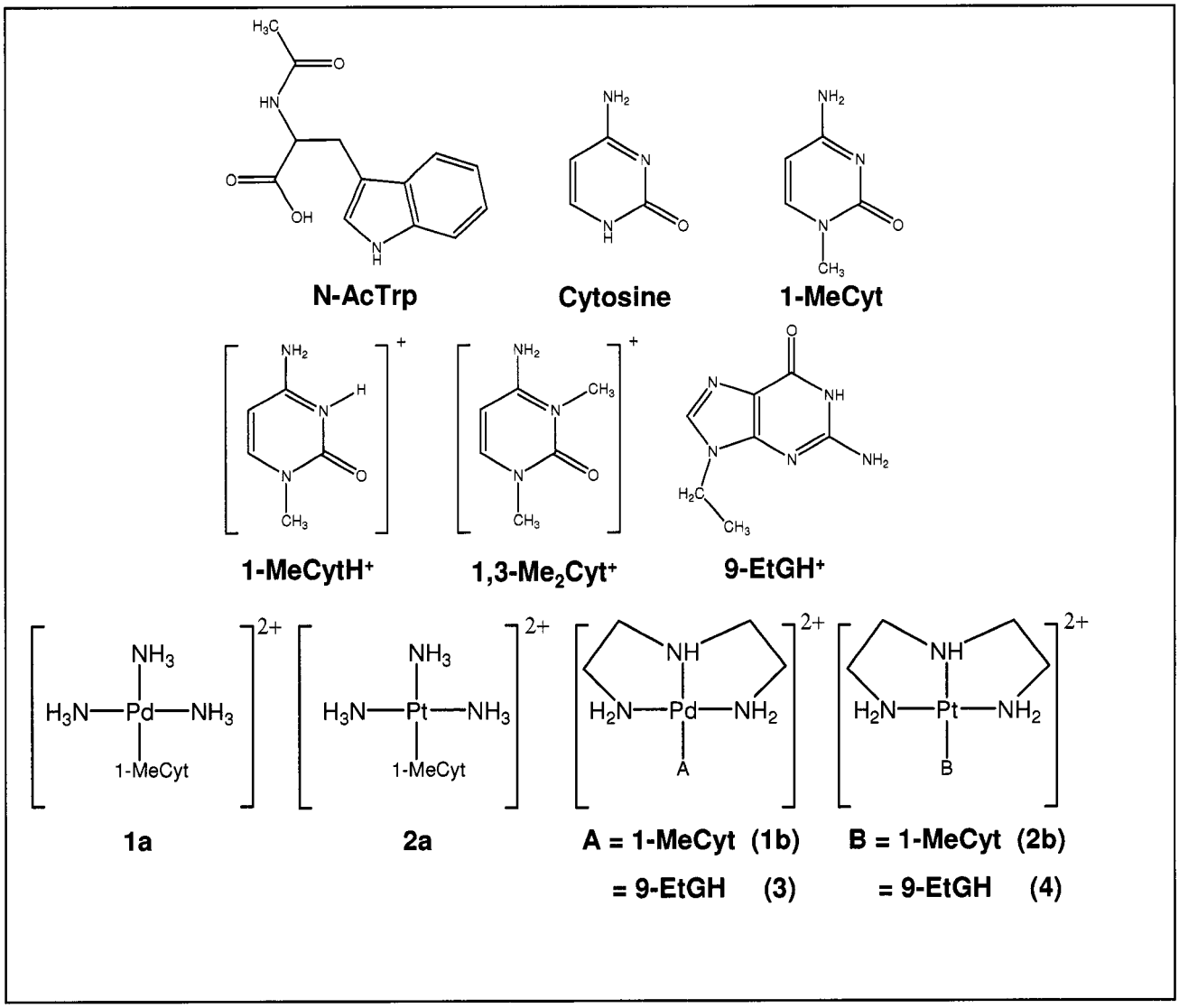

Chart 6.2. Structures of organic compounds and metal complexes studied.

Non-covalent interactions between tryptophan and metallated nucleobases have been studied subsequently in more complex systems such as the C-terminal zinc finger (F2) from the HIV nucleocapsid protein (NCp7). The complexes $[Pt(dien)(9\text{-EtGH})]^{2+}$ and cis-$[Pt(NH_3)_2(Guo)_2]^{2+}$ (9-EtGH = 9-ethylguanine, Guo = guanosine), exhibiting kinetically inert N4 coordination spheres capable only of non-covalent interactions (Chart 6.2.), were found to associate with the F2 zinc finger in solution. The formation of 1:1 adducts was detected by ESI-MS and further confirmed through MS-MS experiments.[37] These observations suggest an important π-stacking interaction between the amino acid and the metallated nucleobase.

Theoretical studies focused on HOMO-LUMO interactions have been restricted to the nucleobase LUMO, using semi-empirical methods (MNDO).[18] In this respect, the intercalation into DNA of charge-neutral molecules such as naphthopyranone epoxide is considered to be a HOMO-controlled process. [38, 39] Further, the site-selective binding of metal ions to G-rich sequences correlates well with the calculated HOMO distribution of the bases. In order to better understand and complement the experimental findings regarding π-stacking interactions between modified nucleobases and tryptophan, we have used Density Functional Theory (DFT) calculations with hybrid functionals (mPW1PW91) to compare and analyze the relevant HOMO/LUMO energies. The systems studied included also N3- and N7-protonated and alkylated 1-methylcytosine (1-MeCyt) and 9-ethylguanine (9-EtGH) respectively, as representative examples of quaternized nucleobases used for comparison to the metallated (Pt and Pd) systems. The decrease in

energy for the nucleobase LUMO upon modification (protonation, alkylation or metallation) results in a concomitant decrease of the energy difference toward the HOMO of the N-acetylytrptophan, thus favoring frontier orbital π-stacking interactions. The results correlate to a good degree with experimental results from fluorescence experiments involving Pt(II)-, Pd(II)-nucleobase complexes and alkylated nucleobases with tryptophan.

6.3. Results and Discussion.

6.3.1. Structure optimization.

6.3.1.a. Metallated nucleobases: $[Pd(NH_3)_3(1\text{-MeCyt})]^{2+}$ (**1a**) and $[Pt(NH_3)_3(1\text{-MeCyt})]^{2+}$ (**2a**) were used as initial models for the metallated 1-MeCyt complexes $[Pd(dien)(1\text{-MeCyt})](NO_3)_2$ (**1**) and $[Pt(dien)(1\text{-MeCyt})](NO_3)_2$ (**2**) whose crystal structures are known[36] (Chart 6.2.). The structures obtained for **1a** and **2a** using the monodentate ammine NH_3 ligand were close to those of an ideal square planar geometry (≈90°) and did not replicate the bite-angle from the chelating dien ligand, a consequence of the lack of steric constraints of the NH_3 groups in comparison to that of the chelating dien. Deviations in NH-Pt-NH2 bond angles of up to 7° were calculated for $[Pd(dien)(1\text{-MeCyt})]^{2+}$ (**1b**) and $[Pt(dien)(1\text{-MeCyt})]^{2+}$ (**2b**) with the dien ligand (Fig. 6.1., Table 6.I.) consistent with the crystal structures of **1** and **2**.

Differences in bond distance for atoms in the first sphere of coordination were rather small (≈ 0.1 Å). For 1b and 2b, the expected "sting ray" structure of the dien ligand was obtained (Fig. 6.2.).

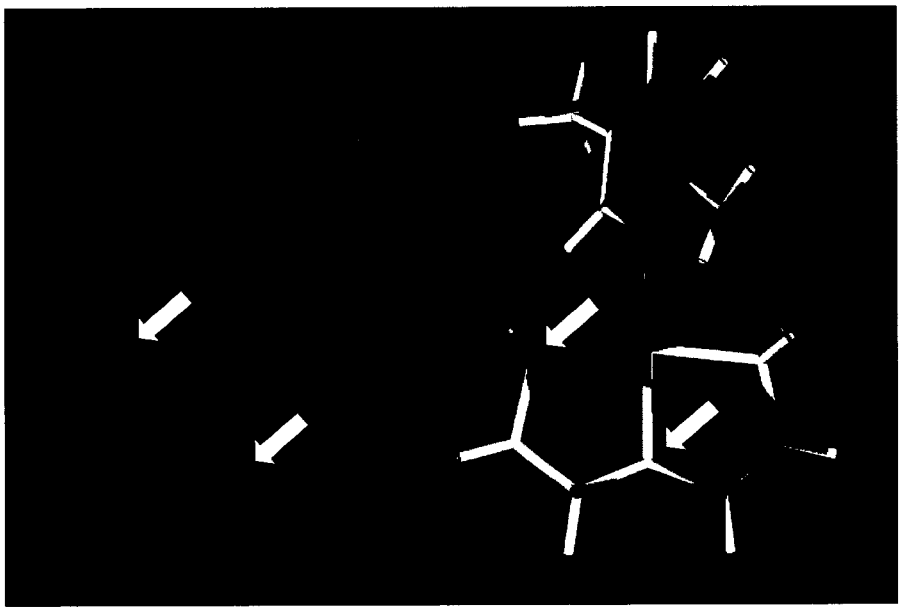

Figure. 6.1. Overlap of crystal structure of $[Pd(dien)(1\text{-}MeCyt)]^{2+}$ (in green) with calculated cations **1a** (left) and **1b** (right), showing critical distances and angles (white arrows).

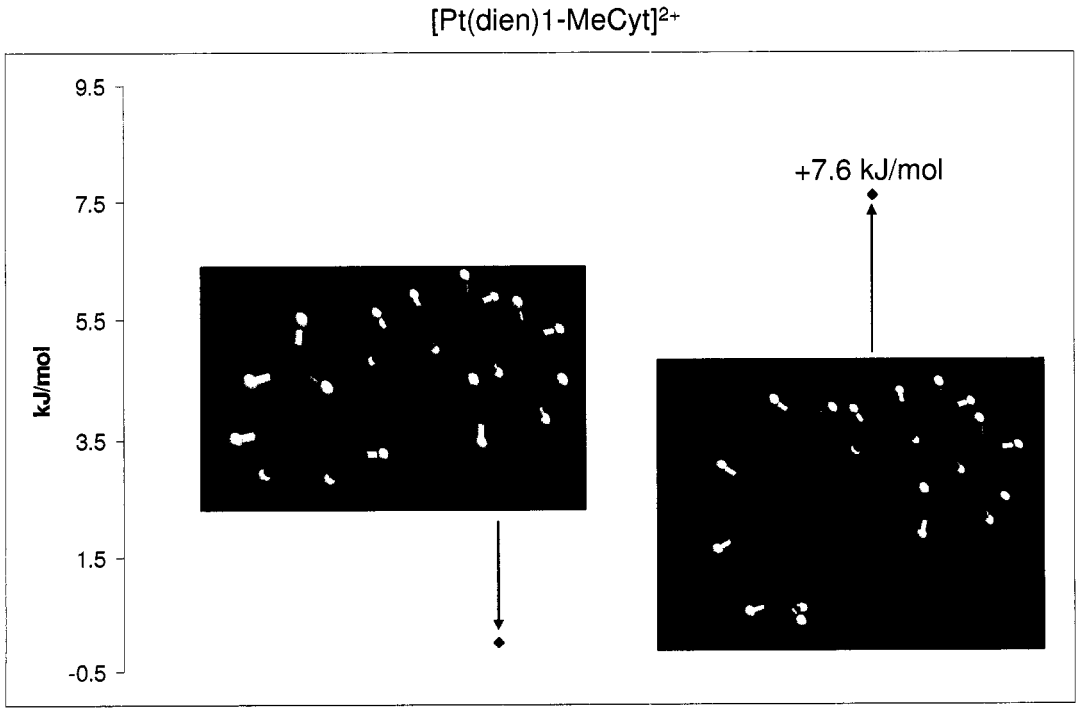

Figure 6.2. Calculated rotamers of $[Pt(dien)(1\text{-}MeCyt)]^{2+}$.

In this conformation, the methylene groups C2 and C3 are above the plane of the metal coordination sphere in a symmetric way, in agreement with the reported crystal structures **1** and **2** (Fig. 6.1.).

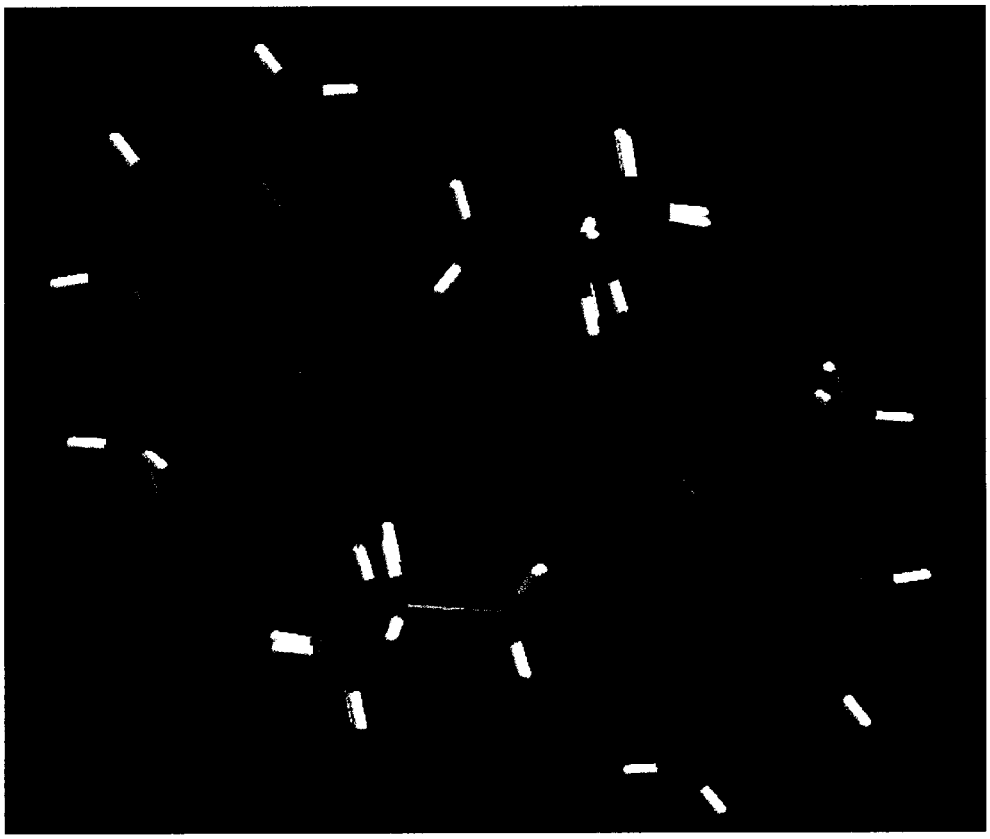

Figure 6.3. Inter-molecular H-bond found in **1** originates differences with the calculated structure **1b** in terms of nucleobase torsional angles.

An important feature exhibited by **1** and **2** is the tilt of the nucleobase plane with respect to the $[Pt,Pd(dien)]^{2+}$ moiety typical for these kind of complexes.[40] For the calculated structures, the torsional angle between the nucleobase and the $[M(dien)]^{2+}$ moiety was small enough to allow an intramolecular H-bond between the 1-MeCyt carbonyl and the

dien ligand (O2C...H2N1). A significantly larger torsional angle can be noticed for 1 compared to 2 (72° vs. 65°), originating longer O2C...H2N1 distances in the case of the palladium complex (Table I). These intra-molecular H-bonding interactions are replaced by inter-molecular interactions in the crystal structure, where the 1-MeCyt carbonyl in one cation complex interacts with the dien ligand of another independent cation, figure 6.3. and 6.4. In addition H-bond distances in calculated complexes followed the trend observed in solid state being longer for palladium compared to the platinum complexes (Table 6.I.).

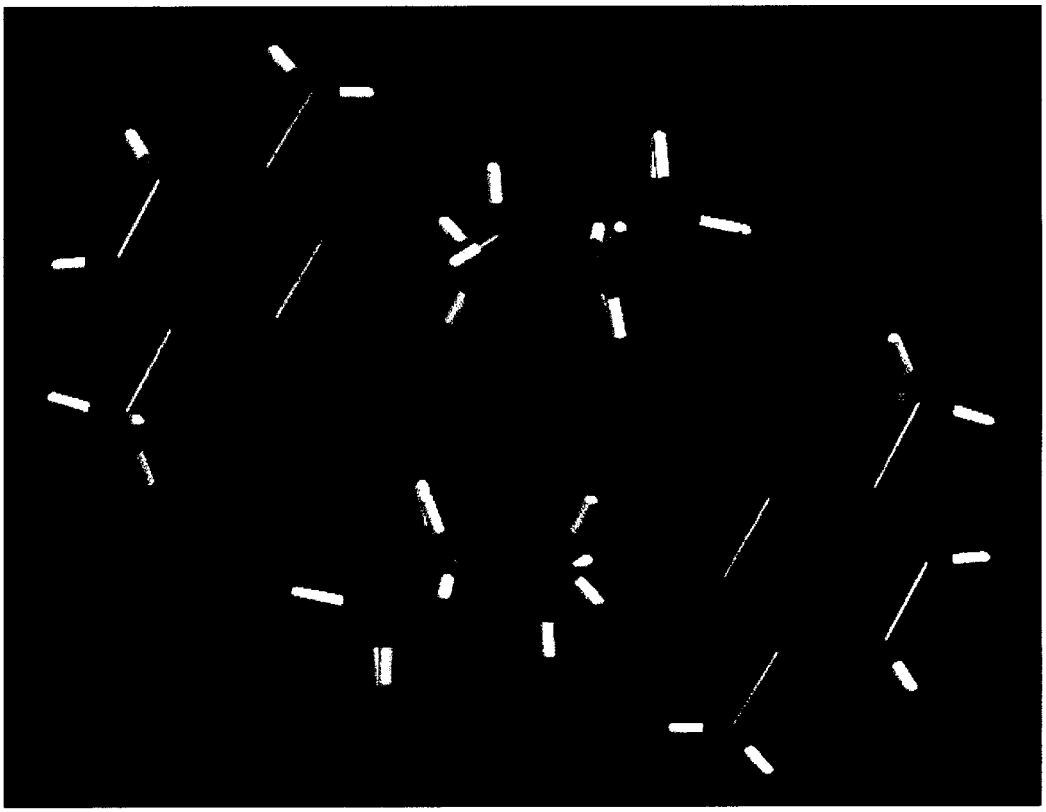

Figure 6.4. Inter-molecular bond for **2**, originates differences with the calculated structure **2b** in terms of nucleobase torsional angles.

Table 6.I. Summary of bond distances and angles for the calculated and crystal structures of metal complexes of 1-MeCyt. {[Pd(dien)1-MeCyt]$(NO_3)_2$ crystal struct. (**1**); $[Pd(NH_3)_3$1-MeCyt$]^{2+}$ calc.(**1a**); [Pd(dien)1-MeCyt] $^{2+}$ calc. (**1b**); [Pd(dien)1-MeCyt] $^{2+}$ calc. endo rotamer (**endo 1b**); [Pt(dien)1-MeCyt]$(NO_3)_2$ crystal struct. (**2**); $[Pt(NH_3)_3$1-MeCyt$]^{2+}$ calc.(**2a**); [Pt(dien)1-MeCyt] $^{2+}$ calc. (**2b**); [Pt(dien)1-MeCyt] $^{2+}$ calc. endo rotamer (**endo 2b**)}.

	1	**1a**	**1b**	***endo* 1b**
Pd-N1	2.0494 (16)	2.096	2.082	2.077
Pd-N2	2.0001 (14)	2.112	2.030	2.036
Pd-N3	2.0429 (15)	2.083	2.060	2.060
Pd-N3C	2.0462 (13)	2.069	2.067	2.065
N2-Pd-N3	84.16 (6)	90.87	84.01	84.13
N2-Pd-N3C	178.40 (6)	177.56	176.70	175.03
N3-Pd-N3C	94.31 (6)	88.13	95.25	94.64
N2-Pd-N1	84.17 (6)	91.52	83.88	84.25
N3-Pd-N1	167.10 (6)	175.00	167.67	165.65
N3C-Pd-N1	97.40 (6)	89.30	96.97	96.21
N1-Pd-N3C-C2C	72.37	71.97	61.56	-107.7
O2C...H2N1	2.955	2.207	2.224	2.198[a]
	2	**2a**	**2b**	***endo* 2b**
Pt-N1	2.039 (5)	2.082	2.077	2.075
Pt-N2	2.018 (5)	2.110	2.036	2.040
Pt-N3	2.056 (5)	2.094	2.057	2.058
Pt-N3C	2.045 (5)	2.067	2.066	2.064
N2-Pt-N3	83.4 (2)	91.51	84.26	84.31
N2-Pt-N3C	179.6 (2)	178.2	177.3	176.3
N3- Pt-N3C	97.0 (2)	89.3	95.0	94.6
N2-Pt-N1	84.4 (2)	91.0	84.0	84.4
N3-Pt-N1	167.7 (2)	174.8	168.2	166.3
N3c-Pt-N1	95.2 (2)	88.1	96.8	96.2
N1-Pt-N3C-C2C	65.12	64.17	57.91	-114.5
O2C...H2N1	2.547	2.139	2.168	2.134[a]

[a] O2C...H1N1

The presence of rotamers in platinum and palladium complexes of 1-MeCyt due to hindered rotation about the Pt,Pd-N3C axis has been observed in solution.[35, 41] The orientation of 1-MeCyt with respect to the central nitrogen N(2)H proton of the dien ligand (See Chart 2) serves to distinguish between the two possible rotamers.

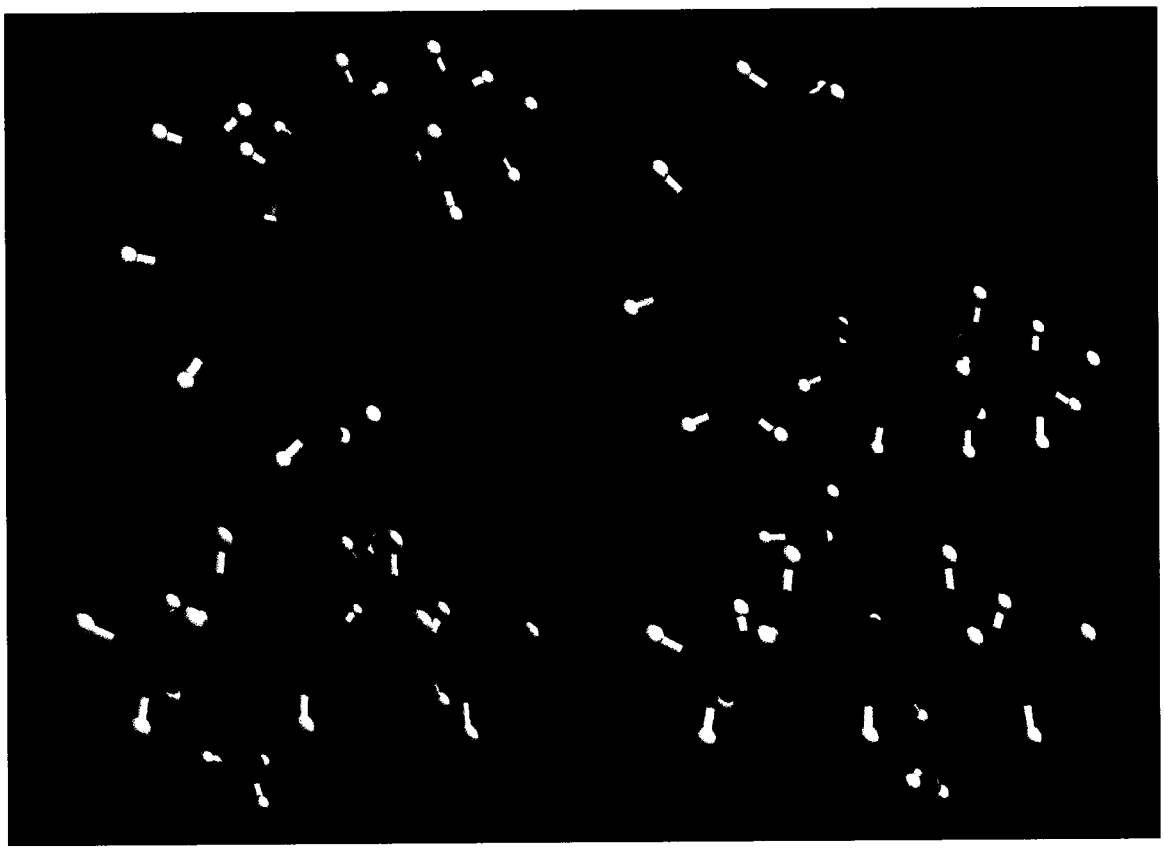

Figure 6.5. View of the *exo-* (left) and *endo-* rotamers (right) from cation **2b**, showing the hydrogen bond formed by the exocyclic oxygen with dien (top) and the obtained "sting ray" conformation for the dien ligand (bottom).

The reported crystal structure has the exocyclic amine group of 1-MeCyt on the opposite side (exo) of N(2)H for both **1** and **2**. A recent computational study reported that the opposite rotamer (endo) was lower in energy by 14.8 kJ/mol^{-1} and attributed this

discrepancy to crystal packing effects.[42] In our calculations we also found that the endo structure was more stable than the exo (8.2 kJ/mol^{-1} for **1b** and 7.6 kJ/mol^{-1} for **2b** (Figs. 6.2. and 6.5.).

These small energies calculated for different rotamers don't explain alone the relative high temperatures needed for coalescence of ^{195}Pt-NMR signals as observed previously, this fact is very likely due to the afore mentioned inter-molecular and stacking associations present in solution. Calculated distances between the exocyclic oxygen in the 1-MeCyt carbonyl group with the appropriate amino group in dien (H1 N1) for endo **1b** and endo **2b** were smaller compared to the exo rotamers and maintained the trend of a longer distance for Pd(II). No significant differences in terms of bond distances and angles were observed between the rotamers (Table I).

A similar conformational analysis was made for the cations [Pd(dien)(9-EtGH)]$^{2+}$ (**3**) and [Pt(dien)(9-EtGH)]$^{2+}$ (**4**). A difference of about 4.5 kJ/mol was calculated for complexes of both metal ions with the exo conformation of the exocyclic 9-EtGH carbonyl relative to the dien N(2)H more stable. This conformation, in contrast to the 1-MeCyt complexes, corresponds to the known crystal structure of [Pd(dien)(guanosine)]$^{2+}$.[43] The crystal structure of [Pd(dien)(guanosine)]$^{2+}$ exhibits a borderline intramolecular H-bond (2.479 Å) between the oxygen atom (O8 in Chart 1) in the carbonyl moiety of the guanosine and an appropriate amine proton in the dien ligand (H6B); moreover a stronger inter-molecular H-bond is exhibited with the exocyclic amine from another guanosine moiety (2.169 Å, not shown). This case is similar to the one observed for complexes **1b** and **2b**. For the calculated complexes **3** and **4**, the intra-molecular H-bond is stronger due to the absence of

additional complexes in the extended array. This H-bond (O6...H6B) was consistently longer for palladium compared to platinum complexes (1.826 vs. 1.803 Å, **3** and **4** respectively) in agreement to the results with 1-MeCyt (**1b**, **2b**).[44] Rotation of the ethyl moiety gave a difference of only 0.5-0.6 kJ/mol between conformers indicating the free rotation of this moiety in solution (Fig. 6.6).

Table 6.II. Summary of bond distances and angles for the calculated and crystal structures of metal complexes of 9-EtGH. {[Pd(dien)9-EtGH] $^{2+}$ calc. (**3**); [Pt(dien)9-EtGH] $^{2+}$ calc.(**4**) }.

	[Pd(dien)(Guanosine)]$^{2+}$ (42)	**3**	**4**
Pd,Pt-N4	2.029 (16)	2.051	2.051
Pd,Pt-N5	1.988 (14)	2.034	2.037
Pd,Pt-N6	2.019 (15)	2.086	2.079
Pd,Pt-N7	2.013 (13)	2.048	2.044
N4-Pd,Pt-N5	84.16 (6)	84.08	84.33
N5-Pd,Pt-N6	83.68 (6)	84.10	84.24
N4-Pd,Pt-N7	98.55 (6)	94.40	94.22
N4-Pd,Pt-N6	167.11 (6)	165.95	166.58
N5-Pd,Pt-N7	177.25 (6)	176.40	177.23
N7-Pd,Pt-N6	93.58 (6)	96.96	96.90
N6-Pd,Pt-N7-C8	-115.95	-57.24	-54.60

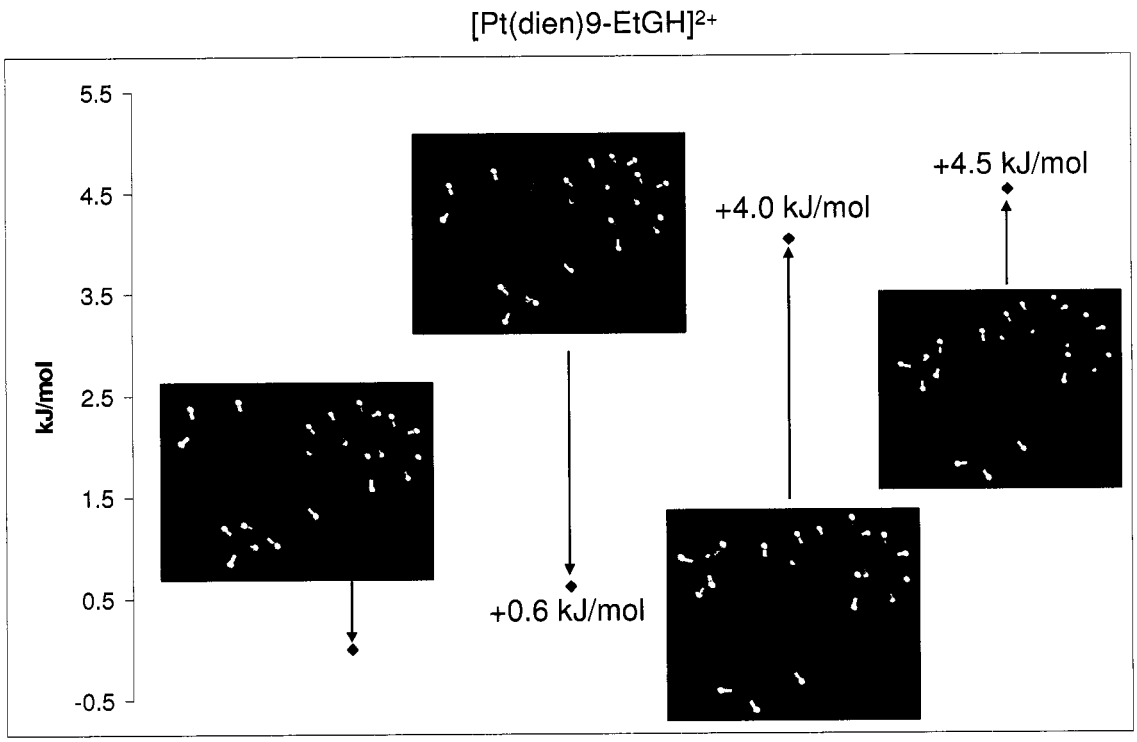

Figure 6.6. Calculated rotamers of $[Pt(dien)(9\text{-}EtGH)]^{2+}$.

6.3.1b. N-acetyl Tryptophan: The optimized geometry for N-AcTrp had the methyl group of the acetyl moiety facing the aromatic ring of the indole with an approximate distance of 3 Å between the five-membered ring and the protons. This structure was 6.6 kJ/mol more stable than when the methyl group was oriented away from the aromatic ring. The energy difference could suggest a dynamic equilibrium where the cation/π interaction slightly favors the former conformation (Fig. 6.7.). A very similar structure has been reported for the Ala-Trp dipeptide with the methyl group in alanine facing the indole ring in the tryptophan residue.[45]

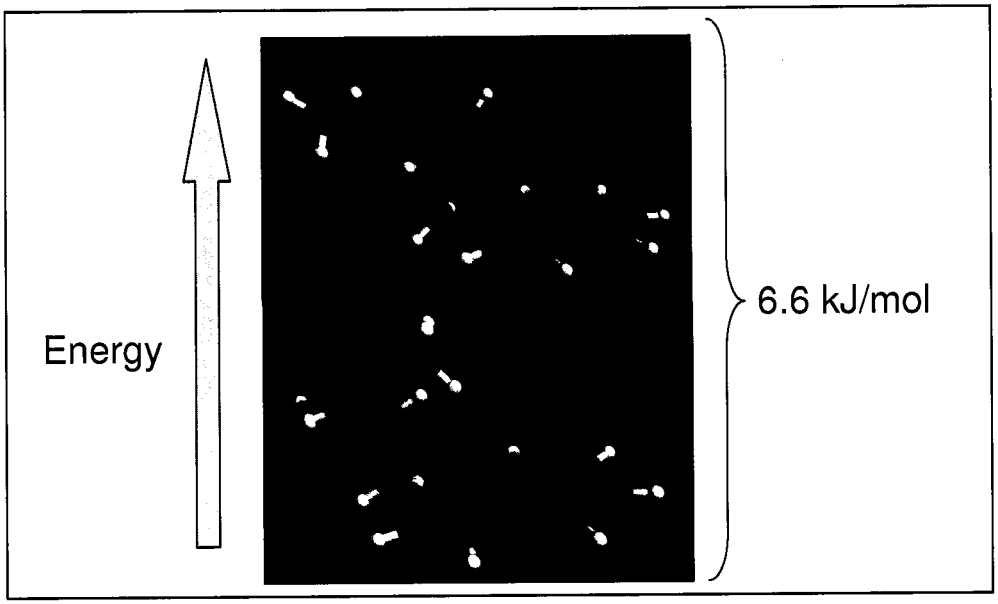

Figure 6.7. Calculated rotamers of N-AcTrp.

6.3.2. HOMO / LUMO analysis.

In order to obtain a qualitative measure of the strength of the potential π–stacking interaction between N-AcTrp and nucleobases quaternized by protonation, alkylation or metallation, we examined the properties of the HOMOs and LUMOs of N-AcTrp and the quaternized nucleobases respectively. Frontier molecular orbitals control numerous reactions and the smaller the energetic difference, the better the orbitals will be suited for interaction or mixing. By perturbation theory, the strength of these interactions is expected to be inversely proportional to the absolute value of the difference of εHOMO of the nucleobase and εLUMO of the N-AcTrp assuming there is proper character between these orbitals to allow overlap. Specifically for the systems studied in this work N-AcTrp exhibits a suitable π-donor ring system (indole), and the nucleobase a suitable π-acceptor ring system.

The energy difference in absolute values (eV) between the HOMO in N-AcTrp and the LUMO for the nucleobase systems considered was compared, Table III. This quantity is denoted as $\Delta\varepsilon$ in the following discussion to differentiate it from the HOMO/LUMO gap within a given molecule.

6.3.2.a. Free nucleobases and N-acetyl tryptophan: HOMO/LUMO energies calculated for the optimized structures of cytosine and 1-MeCyt, as representative pyrimidine nucleobases, were very similar and only minor increases in energy (0.156 eV HOMO and 0.098 eV LUMO) were observed in 1-MeCyt compared to cytosine (Fig. 6.8.). This resulted in a very similar HOMO/LUMO gap obtained for these two molecules, 5.739 and 5.797 eV respectively (Table IV).

Table 6.III. Summary of kappa ($\Delta\varepsilon$) values calculated for stacking interactions of different chemical species with N-acetyltryptophan.

Compound	$\Delta\varepsilon$ (abs. value, eV)*
N-Acetyl tryptophan	-
Cytosine	5.134
1-methyl cytosine (1-MeCyt)	5.232
$[1\text{-MeCytH}]^+$	0.154
$[1,3\text{-Me}_2\text{Cyt}]^+$	0.099
$[Pt(dien)1\text{-MeCyt}]^{2+}$ (*exo*)	1.838
$[Pd(dien)1\text{-MeCyt}]^{2+}$(*exo*)	2.777
$[Pt(dien)1\text{-MeCyt}]^{2+}$(*endo*)	1.786
$[Pd(dien)1\text{-MeCyt}]^{2+}$(*endo*)	2.768
$[Pt(NH_3)_3 1\text{-MeCyt}]^{2+}$	2.255
$[Pd(NH_3)_3 1\text{-MeCyt}]^{2+}$	3.046
9-ethylguanine (9-EtGH)	5.907
$[9\text{-EtGH-H}]^+$	1.307
$[9,7\text{-Et,meGH}]^+$	1.716
$[Pt(dien)9\text{-EtGH}]^{2+}$	1.187
$[Pd(dien)9\text{-EtGH}]^{2+}$	2.366

Table 6.IV. Summary of HOMO/LUMO gap for the chemical species calculated on this study.

Compound	HOMO/LUMO gap (eV)
N-Acetyl tryptophan	5.507
Cytosine	5.797
1-methyl cytosine (1-MeCyt)	5.739
$[1\text{-MeCytH}]^+$	5.485
$[1,3\text{-Me}_2\text{Cyt}]^+$	5.526
$[\text{Pt(dien)1-MeCyt}]^{2+}$ (*exo*)	5.438
$[\text{Pd(dien)1-MeCyt}]^{2+}$(*exo*)	4.503
$[\text{Pt(dien)1-MeCyt}]^{2+}$(*endo*)	5.480
$[\text{Pd(dien)1-MeCyt}]^{2+}$(*endo*)	4.500
$[\text{Pt(NH}_3)_3\text{1-MeCyt}]^{2+}$	5.378
$[\text{Pd(NH}_3)_3\text{1-MeCyt}]^{2+}$	4.245
9-ethylguanine (9-EtGH)	5.901
$[9\text{-EtGH-H}]^+$	5.208
$[9,7\text{-Et,meGH}]^+$	5.356
$[\text{Pt(dien)9-EtGH}]^{2+}$	4.965
$[\text{Pd(dien)9-EtGH}]^{2+}$	3.786

9-EtGH as a representative purine exhibited higher energy values for both HOMO and LUMO compared to 1-MeCyt, however the degree of energy increase was not the same extent for both frontier orbitals, i.e. 0.514 eV (HOMO) and 0.675 eV (LUMO) vs. 1-MeCyt (Fig. 6.8). Consequently the calculated HOMO/LUMO gap was slightly higher for 9-EtGH (5.901 eV). The resulting energy for frontier orbitals in N-AcTrp was close to the value obtained for the corresponding orbitals in the free nucleobases: LUMO, -0.560 eV and HOMO, -6.067 eV (Fig. 6.8). These orbitals were considered as a reference for the comparison with the different nucleobase systems (Fig. 6.8).

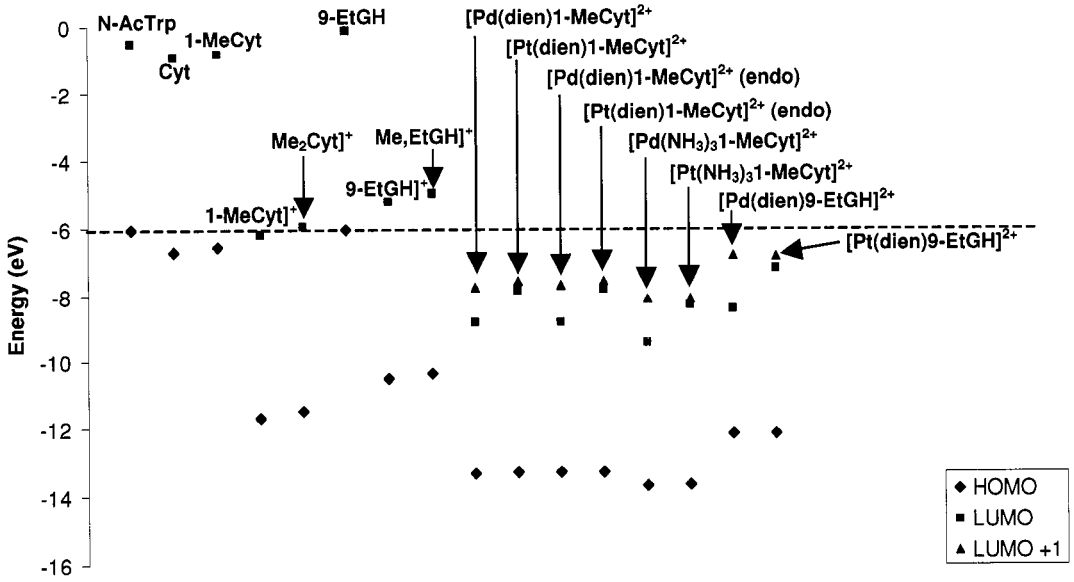

Figure 6.8. Comparison of HOMO\LUMO energies found for the different organic compounds and metal complexes studied, the energy of the HOMO in N-AcTrp is taken as a reference for the value $\Delta\varepsilon$ (dashed line).

The $\Delta\varepsilon$ found for the potential π–stacking interaction between cytosine and 1-MeCyt and N-AcTrp were therefore similar due to the similarities in the electronic structures of the pyrimidine bases (5.134 and 5.232 eV, respectively (Table III). The donor-acceptor ineraction is predicted to be less favorable (5.907 eV) for for 9-EtGH given its higher energy LUMO. These $\Delta\varepsilon$ values are consistent with experimentally-determined association constants (Ka) which indicate a stronger interaction for 1-MeCyt/N-AcTrp over 9-EtGH/N-AcTrp.[35,36] It has been shown for the benzene dimer, using MP2 level calculations, that the presence of substituents in the aromatic ring could favor to a significant degree the π-stacking interaction over the T-shaped alternative, due to electrostatic and dispersion contributions.[46, 47] This effect however was not evident in the HOMO-LUMO energetic profile comparison found for cytosine/1-MeCyt and N-AcTrp, since the LUMO energy did not vary significantly in both cases.

6.3.2.b. Protonated/alkylated nucleobases: Protonation or methylation at the N3 position for 1-methylcytosine and at the N7 position for 9-ethylguanine reduced the frontier orbital energies by ca. 4-5 eV (Fig 6.8.). This decrease was slightly larger for the LUMO than for the HOMO in any given nucleobase. The decrease in energy was also consistently larger by approximately 0.25 eV for protonated vs. alkylated nucleobases, and larger for 1-MeCyt vs. 9-EtGH systems to a similar degree (0.28 eV). The HOMO/LUMO gap for the quaternized systems decreased in the range 0.3 - 0.6 eV compared to neutral nucleobases. These results are consistent with the shift to lower wavelengths observed in the electronic

spectrum of N3-protonated 1-MeCyt and N7-protonated 9-EtGH compared to the neutral nucleobase (Fig. 6.9.).

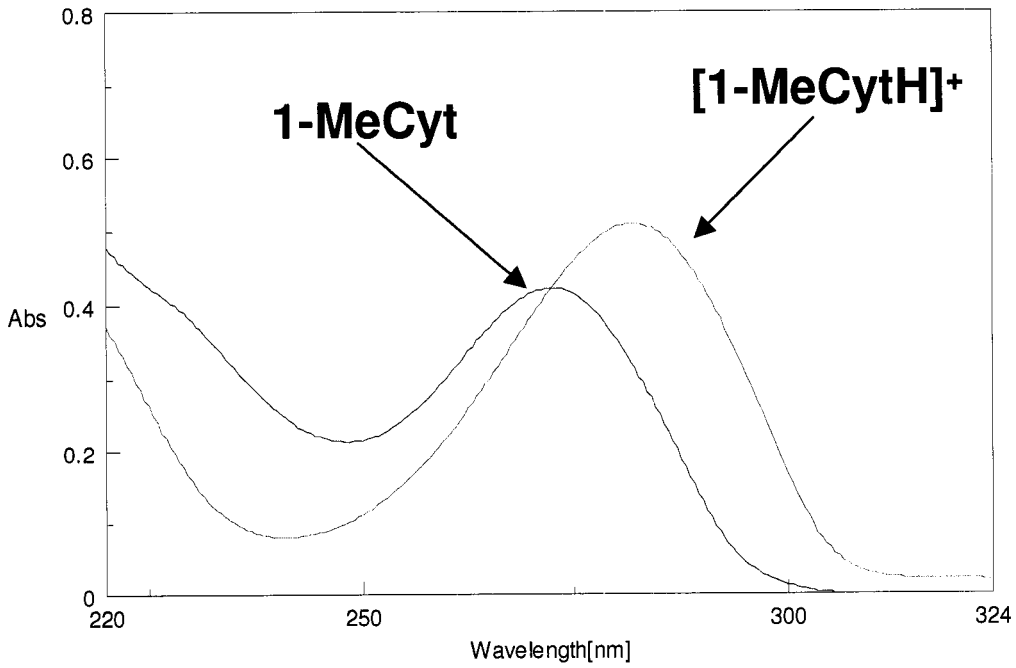

Figure 6.9. UV-vis spectrum of neutral and protonated 1-MeCyt showing the shift in absorption maxima predicted according to HOMO/LUMO gap calculated.

The lower LUMO energies obtained for protonated- and alkylated-nucleobases therefore resulted in much lower $\Delta\varepsilon$ values in comparison to the free neutral nucleobases (Table III).

As shown in fig. 6.8., LUMOs in quaternized nucleobases exhibited comparable energies to HOMOs in neutral nucleobases and N-AcTrp, favoring a potential interaction between the aminoacid and the quaternized nucleobases. Visualization of the frontier orbitals for the interacting species showed that the HOMO (N-AcTrp) and LUMOs (quaternized nucleobases) were π-type localized in the aromatic rings supporting a π-stacking

interaction (Fig. 6.10). The prediction of a stronger interaction is consistent with recent calculations at the MP2 level which show an increase in π-stacking interaction between methylated adenine and different aromatic aminoacids compared with the free nucleobase.[48]

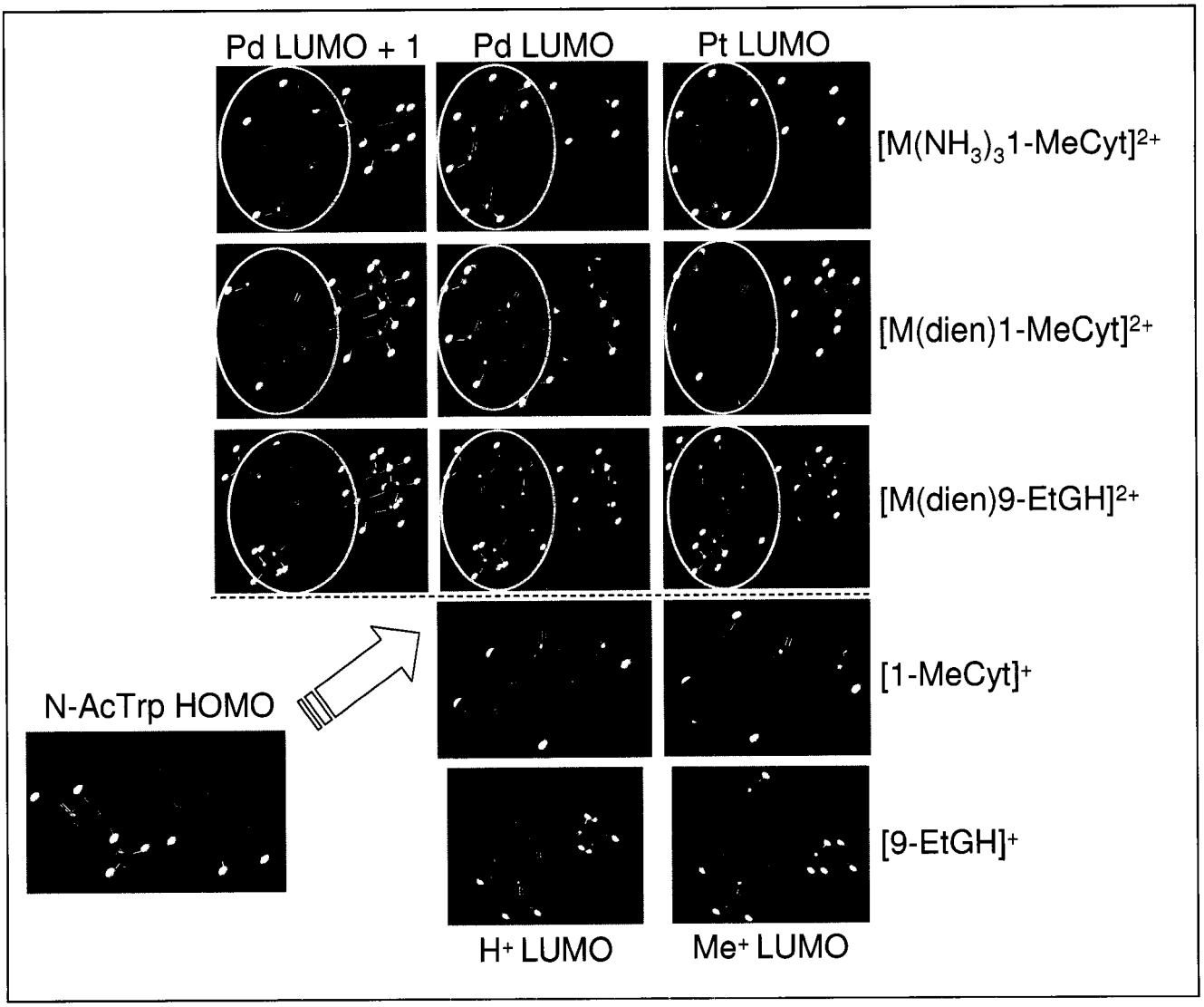

Figure 6.10. Orbital Contour Plot of the HOMO in N-AcTrp along with different LUMOs for systems studied. The nucleobase is highlighted inside a yellow circle to facilitate identification.

6.3.2.c. Metallated nucleobases: Coordination of the nucleobases to $M(dien)^{2+}$ produces complexes with higher net charge compared to alkylation (+2 vs. +1). HOMO and LUMO frontier orbitals in Pt(II)- and Pd(II)-nucleobase complexes exhibited a general decrease in energy compared to the corresponding neutral nucleobase in the range 7 – 8 eV, which was even larger than for alkylated/protonated nucleobases. This decrease as observed in the previous case was consistently larger (ca. 1 eV) for the LUMO in comparison to the HOMO in all complexes. In terms of nucleobase influence on the energy profile, 9-EtGH complexes exhibited higher frontier orbital energy values compared to 1-MeCyt complexes in agreement with the results found for the neutral and protonated/alkylated nucleobases.[18] Moreover, the LUMO energy for Pt(II)-nucleobase complexes was consistently higher than the Pd(II)-nucleobase analogue by ca. 1 eV. The use of different witness ligands, i.e. the monodentate NH_3 vs. the chelating dien produced variations in energy of 0.4 eV among the metallated complexes. The dien complexes were lower in energy for both HOMO and LUMO (Fig. 6.8). Energy differences between rotamers in complexes **1a** and **2b** were almost negligible.

When LUMOs for Pt(II), Pd(II)-nucleobase complexes were compared with the HOMO in N-AcTrp it was found that quaternization of the nucleobases by metallation involved additional features in comparison to protonation and alkylation. Firstly, although metallation also decreased the LUMO energy in the resulting metal-nucleobase complexes, the $\Delta\varepsilon$ values were not as favorable as in the case of protonation/alkylation, since the decrease in energy led to an increased energy separation from the HOMO in N-AcTrp (Fig. 6.8 and Table 6.III). $\Delta\varepsilon$ values were still ca. 55% smaller than free nucleobases,

suggesting a better interaction between the frontier orbitals when the nucleobase is coordinated to the metal ion, in good agreement with experimental results obtained previously.[35, 36]

Secondly, the character of the LUMOs in the metal-nucleobase complexes varied depending upon the nature of the metal and the nucleobase. This feature explained a trend previously observed in fluorescence experiments where a consistently higher Ka was observed for Pt(II)- vs. Pd(II)-nucleobase complexes. Comparison of data for the metal-nucleobase complexes showed that $\Delta\varepsilon$ values were smaller for Pt(II)- vs. Pd(II), implying a more favorable π-interaction with the HOMO in N-AcTrp. For 1-MeCyt, an inverse correlation can be shown between the $\Delta\varepsilon$ value and the experimental Ka found for free and metallated nucleobase (Figure 6.11.).

Analysis of the LUMOs showed that those of the Pt(II)-MeCyt complexes (2a, 2b) π-type orbitals localized in the nucleobase ring, whereas those of the Pd(II) complexes (**1a**, **1b**) were localized on the metal-dien fragment. These data could explain the diminished Ka measured experimentally in the latter case. For 9-EtGH complexes the correct trend for association with N-AcTrp Pt(II) > Pd(II), and a very good inverse correlation Ka vs. $\Delta\varepsilon$ (Figure 6.11) between the free and metallated nucleobases was again observed However, the position of LUMO in metallated 9-EtGH suggested a better interaction for this complexes vs. metallated 1-MeCyt Again the visualization of LUMOs in the corresponding metal-9-EtGH complexes (**3**, **4**) showed that the orbital was localized in the metal-dien fragment possibly attenuating the advantageous energy position for the LUMO in these complexes (Fig. 6.10).

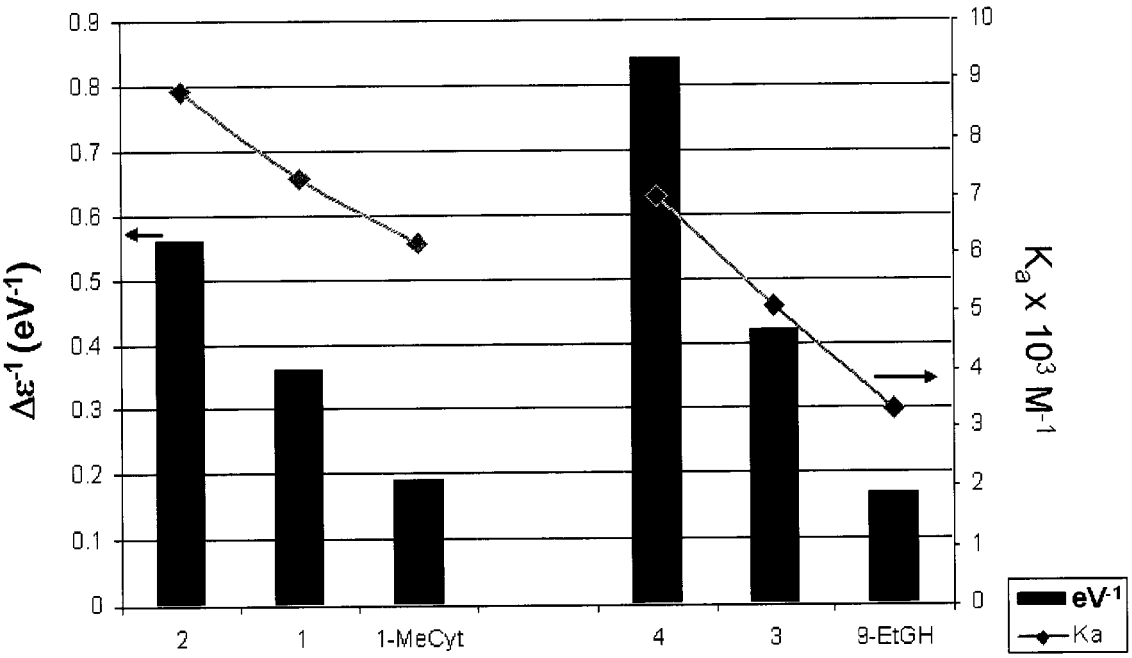

Figure 6.11. Correlation between association constants, determined for free 1-MeCyt and Pt/Pt-1-MeCyt complexes, with the Δε value. $[Pd(dien)1\text{-}MeCyt]^{2+}$(**1**); $[Pt(dien)1\text{-}MeCyt]^{2+}$(**2**); $[Pd(dien)9\text{-}EtGH]^{2+}$ (**3**); $[Pt(dien)9\text{-}EtGH]^{2+}$ (**4**) .

The localization of the LUMO in the metal fragment for complexes 1a and 1b could actually favor an alternative pathway for interaction, i.e. ligand substitution via an associated mechanism. In agreement, 1-MeCyt substitution by N-AcTrp in complex 11 under basic conditions has been observed in solution.[36] In an additional step of analysis we visualized the LUMO+1 for the metal complexes considered in this study and compared their energy (Fig. 6.8) and symmetry (Fig. 6.10). It was found that in general LUMO+1 is mainly centered on the nucleobase and this could suggest that for the palladium-1-MeCyt complexes **1a** and **1b**, as well as, for **3** and **4** these orbitals will exhibit an improved

symmetry and also energy to interact via π-stacking. In general, the difference between LUMO and LUMO+1 is bigger for palladium-nucleobase complexes compared to platinum-nucleobases (Fig. 6.8). The LUMO+1 exhibited smaller Δε values compared to the LUMO. A partial contribution from the LUMO+1 could be important for the π-stacking interaction in these systems.

6.4. Computational Methods.

Calculations were carried out at the DFT/mPW1PW91 level[49] with the Gaussian03 suite of programs.[50] Palladium and platinum were represented by the Ermler-Christiansen relativistic effective core potential basis set[51, 52] modified with the Couty-Hall contraction of the (n+1)p functions.[53] Basis sets for nitrogen and oxygen were split valence triple-ζ quality augmented with polarization functions.[54] Carbon and hydrogen were represented by Dunning double-ζ basis sets;[55] polarization functions were added to carbon. Optimized geometries were characterized as minima through calculation of their vibrational frequencies. Results were visualized using ArgusLab,[56] Mercury 1.4.1.[57] and Swiss-PDB viewer software.[58]

6.5. Conclusions.

There is an incomplete understanding of π-stacking interactions, and in this work we explore one of the factors potentially involved in the recognition process between a metallated-nucleobase with an aromatic residue. For more complex systems found in vivo it is reasonable to expect contributions from other van der Waals interactions, notably H-bonds. In addition, the agreement between DFT calculations (gas phase) and association constants obtained experimentally could be due to a cancellation of effects present in

solution, (such as solvent rearrangement upon stacking) as a result of the comparison between the different systems.

Several results on non-covalent interactions, especially π-stacking, for metal complexes with biological ligands have demonstrated its significance, i.e. the role of the phenylalanine residue from the protein HMG1 in the recognition of platinated DNA [59, 60], the potential chemotherapeutic use of DNA-intercalator complexes[61 - 63] and the use of monofunctional platinum-nucleobase compounds to mimic DNA(RNA)-zinc finger interactions.[37] The lack of a description of van der Waals interactions is considered a general deficiency of DFT, [64, 65] thus hindering its application to study of π-stacking interactions. However the approach taken for comparing the frontier orbitals in donor-acceptor complexes allowed us to use DFT to indirectly fulfill this task. The analogies concerning the biochemistry of Pt^{2+} and CH_3^+ can be made by isolobal analogy and are exemplified by the similar mechanism of action of anticancer alkylating agents and cisplatin derivatives – both covalently modifying target DNA. The current findings indicate an additional similar mode of molecular interaction for these chemical species based on lowering of LUMO energies.

The geometry of the different compounds in this study were optimized and the possible rotamers were compared using mPW1PW91 hybrid functionals. Calculated structures for Pt(II) and Pd(II) complexes were in excellent agreement with the reported x-ray crystal structures. An important decrease in LUMO energy was found for all quaternized nucleobases considered in comparison with the free nucleobases. The energy minimization between the quaternized LUMOs and the HOMO in N-AcTrp suggests a better interaction

for these orbitals and could explain the reported higher stacking interaction observed previously in experimental conditions.

The extent of energy decrease in the quaternized LUMOs was larger in the case of nucleobases coordinated to Pt(II) and Pd(II) ions than for protonation or alkylation, however the final net energy difference with the HOMO in N-AcTrp ($\Delta\varepsilon$) was smaller for protonation/alkylation. In general, $\Delta\varepsilon$ values correlated well with previous experimental observations confirming an enhanced π-stacking interaction for 1-MeCyt vs. 9-EtGH, and for metallated nucleobases in general. However $\Delta\varepsilon$ values alone cannot explain the consistently lower Ka found for Pd(II)- compared to Pt(II)-complexes or for metallated 9-EtGH compared to metallated 1-MeCyt. In this regard it was found that the character of the LUMO constitutes an additional variable to take into account to predict interaction trends. Analysis of the LUMO symmetry for the systems studied revealed that LUMOs in palladium-nucleobase complexes, as well as metallated 9-EtGH, were not completely localized on the nucleobase ring. This feature can contribute negatively to π-stacking interactions in these systems and would help to explain more completely the solution trends observed.

Coordination of nucleobase to metal ions (specifically Pt(II)) is known to affect the acidity of -NH and -NH2 groups (depending on factors such as coordination site and hydrogen bond stabilization). [66, 67] This change can modulate the strength of H-bonding between nucleic acids bases, as exemplified by an enhanced Watson-Crick interaction in N7-platinated guanines towards a corresponding cytosine. [68, 69] This study demonstrates that modulation of π-stacking interactions is a further consequence of general nucleobase

quaternization. Understanding such intricate details of nucleobase properties upon alkylation and/or metallation may lead to understanding and design of more specific modified-nucleobase-biomolecule interactions of potential biological significance.

6.6. References.

(1) Bhosale, S.; Sisson, A.L.; Talukdar, P.; Fürstenberg, A.; Banerji, N.; Vauthey, E.; Bollot, G.; Mareda, J.; Röger, C.; Würthner, F.; Sakai, N.; Matile, S. *Science*, **2006**, 313, 84 - 86.

(2) Meyer, E.A.; Castellano, R.K.; Diederich, F. *Angew. Chem. Int. Ed.*, **2003**, 42, 1210 - 1250.

(3) Williamson, J.R. *Nat. Struct. Biol.*, **2000**, 7, 834 - 837.

(4) de la Escosura, A.; Martinez-Diaz, M.V.; Guldi, D.M.; Torres, T. *J. Am. Chem. Soc.*, **2006**, 128, 4112 - 4118.

(5) Ajayaghosh, A.; Vijayakumar, C.; Varghese, R.; George, S.J. *Angew. Chem. Int. Ed.*, **2006**, 45, 456 - 460.

(6) Reczek, J.J.; Iverson, B.L., *Macromol.*, **2006**, 39, 5601 – 5603.

(7) Hoeben, F.J.M.; Jonkheijm, P.; Meijer, E.W.; Schenning, P.H.J., *Chem. Rev.*, **2005**, 105, 1491 – 1546.

(8) Schenning, A.P.H.J.; Meijer, E.W. *Chem. Commun.*, **2005**, 26, 3245 - 3258.

(9) Janiak, C. *J. Chem. Soc., Dalton Trans.*, **2000**, 21, 3885 – 3896.

(10) Muller-Dethlefs, K.; Hobza, P. *Chem. Rev.*, **2000**, 100, 143 -167.

(11) Tauer, T.P.; Sherrill, C.D. *J. Phys. Chem. A*, **2005,** 109, 10475 – 10478.

(12) McGaughey, G.B.; Gagné, M.; Rappé, A.K. *J. Biol. Chem.*, **1998**, 273, 15458 – 15463.

(13) Chelli, R.; Gervasio, F.L.; Procacci, P.; Schettino, V. *J. Am. Chem. Soc.*, **2002**, 124, 6133 -6143.

(14) Hunter, C.A.; Sanders, J.K.M. *J. Am. Chem. Soc.*, **1990**, 112, 5525- 5534.

(15) Fukui, K. *Acc. Chem. Res.*, **1981**, 14, 363 – 368.

(16) Schmidt, A.; Lindner, A.; Nieger, M.; Ruiz-Delgado, M.C.; Ramirez, F.*J. Org. Biomol. Chem.*, **2006**, 4, 3056 – 3066.

(17) Iijima, T.; Vignon, S.A.; Tseng, H-.R.; Jarrosson, T.; Sanders, J.K. M.; Marchioni, F.; Venturi, M.; Apostoli, E.; Balzani, V.; Stoddart, J.F. *Chem. Eur. J.*, **2004**, 10, 6375 – 6392.

(18) Ishida, T.; Ueda, H.; Segawa, K.; Doi, M.; Inoue, M. *Arch. Biochem. Biophys.*, **1990**, 278, 217 - 227.

(19) Ishida, T.; Iyo, H.; Ueda, H.; Doi, M.; Inoue, M. *J. Chem. Soc., Chem. Commun.*, **1990**, 3, 217-218.

(20) Ishida, T.; Tarui, M.; In, Y.; Ogiyama, M.; Doi, M.; Inoue, M. *FEBS Lett.*, **1993**, 333, 214 - 216.

(21) Ishida, T.; Toda, Y.; Tarui, M.; Doi, M.; Inoue, M. *Chem & Pharm. Bull.*, **1994**, 42, 674 – 676.

(22) Doi, M.; Tarui, M.; Ogata, M.; Asano, A.; Ishida, T. *Acta Cryst.*, **1998**, C54, 1941 – 1943.

(23) Tomoo, K.; Matsushita, Y.; Fujisaki, H.; Abiko, F.; Shen, X.; Taniguchi, T.; Miyagawa, H.; Kitamura, K.; Miura, K.; Ishida, T. *Biochem. Biophys. Acta*, **2005**, 1753, 191 – 208.

(24) Niedzwiecka, A.; Stepinski, J.; Balaspiri, L.; Darzynkiewicz, E.; Stolarski, R. *Nucleos. Nucleot. & Nucl. Acids*, **2003**, 22, 1557-1561.

(25) Quiocho, F.A.; Hu, G.; Gershon, P.D. *Curr. Op. Struct. Biol.*, **2000**, 10, 78 -86.

(26) Wieczorek, Z.; Zdanowski, K.; Chlebicka, L.; Stepiński, J.; Jankowska, M.; Kierdaszuk, B.; Temeriusz, A.; Darzynkiewicz, E.; Stolarski, R. *Biochim. Biophys. Acta*, **1997**, 1354, 145 – 152.

(27) Hodel, A.E.; Gershon, P.D.; Shi, X.; Wang, S.M.; Quiocho, F.A. *Nat. Struct. Biol.*, **1997**, 4, 350 – 354.

(28) Hodel, A.E.; Gershon, P.D.; Quiocho, F.A. *Mol. Cell.*, **1998**, 1, 443 – 447.

(29) Hsu, P-.C.; Hodel, M.R.; Thomas, J.W.; Taylor, L.J.; Hagedorn, C.H.; Hodel, A.E. *Biochemistry*, **2000**, 39, 13730 – 13736.

(30) Tomić, Z.D.; Sredojević, D.; Zarić, S. D. *Cryst. Growth Design*, **2006**, 6, 29 - 31.

(31) Yamauchi, O.; Odani, A.; Takani, M. *J. Chem. Soc., Dalton Trans.*, **2002**, 18, 3411 - 3421.

(32) Magistrato, A.; Pregosin, P.S.; Albinati, A.; Rothlisberger, U. *Organomet.*, **2001**, 20, 4178 – 4184.

(33) Crowley, J.D.; Bosnich, B. *Eur. J. Inorg. Chem.*, **2005**, 11, 2015 – 2025.

(34) Ye, B-.H.; Tong, M-.L.; Chen, X-.M. *Coord. Chem. Rev.*, **2005**, 249, 545 – 565.

(35) Anzellotti, A.; Ma, E.; Farrell, N. *Inorg. Chem.*, **2005**, 44, 483-485.

(36) Anzellotti, A.; Sabat, M.; Farrell, N. *Inorg. Chem.*, **2006**, 45, 1638-1645.

(37) Anzellotti, A.I.; Liu, Q.; Bloemink, M.J.; Scarsdale, J.N.; Farrell, N. *Chem & Biol.*, **2006**, 13, 539-548.

(38) Okamoto, A.; Kanatani, K.; Taiji, T.; Saito, I. *J. Am. Chem. Soc.*, **2003**, 125, 1172 – 1173.

(39) Nakatani, K.; Matsuno, T.; Adachi, K.; Hagihara, S.; Saito, I. *J. Am. Chem. Soc.*, **2001**, 123, 5695 – 5702.

(40) Zangrando, E.; Picherri, F.; Randaccio, L.; Lippert, B. *Coord. Chem. Rev.*, **1996**, 156, 275- 332.

(41) Brüning, W.; Ascaso, I.; Freisinger, E.; Sabat, M.;Lippert, B. *Inorg. Chim. Acta*, **2002**, 339, 400 – 410.

(42) Miguel, P.J.S. ; Lax, P. ; Lippert, B. *J. Inorg. Biochem.*, **2006**, 100, 980 - 991.

(43) Rochon, F.D.; Kong, P.C.; Coulombe, B.; Melanson, R. *Can. J. Chem.*, **1980**, 58, 381 - 386.

(44) It is interesting to note that for the complex [Pd(dien)(adenosine)]2+ were there are no possibilities of H-bond formation from the nucleobase towards the dien ligand, the tilt of the nucleobase is remarkably diminished. (Arpalahti, J.; Klika, K.D.; Sillanpää, R.; Kivekäs, R. *J. Chem. Soc., Dalton Trans.*, **1998**, 8, 1397 – 1402)

(45) Emge, T.J.; Agrawal, A.; Dalessio, J.P.; Dukovic, G.; Inghrim, J.A.; Janjua, K.; Macaluso, M.; Robertson, L.L.; Stiglic, T.J.; Volovik, Y.; Georgiadis, M.M. *Acta Cryst.*, **2000**, C56, e469-e471.

(46) Ringer, A.L.; Sonnokrot, M.O.; Lively, R.P.; Sherrill, C.D. *Chem. Eur. J.*, **2006**, 12, 3821 - 3828.

(47) Sherrill, C.D.; Sinnokrot, M.O. *J. Am. Chem. Soc.*, **2004**, 126, 7690 - 7697.

(48) Rutledge, L.R.; Campbell-Verduyn, L.S.; Hunter, K.C;.Wetmore, S.D. *J. Phys. Chem. B*, **2006**, 110, 19652 - 19663.

(49) Adamo, C.; Barone, V. *J. Chem. Phys.*, **1998**, 108, 664 – 675.

(50) Gaussian 03, Revision C.02, Frisch, M. J.; Trucks, G. W.; Schlegel, H. B.; Scuseria, G. E.; Robb, M. A.; Cheeseman, J. R.; Montgomery, Jr., J. A.; Vreven, T.; Kudin, K. N.; Burant, J. C.; Millam, J. M.; Iyengar, S. S.; Tomasi, J.; Barone, V.; Mennucci, B.; Cossi, M.; Scalmani, G.; Rega, N.; Petersson, G. A.; Nakatsuji, H.; Hada, M.; Ehara, M.; Toyota, K.; Fukuda, R.; Hasegawa, J.; Ishida, M.; Nakajima, T.; Honda, Y.; Kitao, O.; Nakai, H.; Klene, M.; Li, X.; Knox, J. E.; Hratchian, H. P.; Cross, J. B.; Bakken, V.; Adamo, C.; Jaramillo, J.; Gomperts, R.; Stratmann, R. E.; Yazyev, O.; Austin, A. J.; Cammi, R.; Pomelli, C.; Ochterski, J. W.; Ayala, P. Y.; Morokuma, K.; Voth, G. A.; Salvador, P.; Dannenberg, J. J.; Zakrzewski, V. G.; Dapprich, S.; Daniels, A. D.; Strain, M. C.; Farkas, O.; Malick, D. K.; Rabuck, A. D.; Raghavachari, K.; Foresman, J. B.; Ortiz, J. V.; Cui, Q.; Baboul, A. G.; Clifford, S.; Cioslowski, J.; Stefanov, B. B.; Liu, G.; Liashenko, A.; Piskorz, P.; Komaromi, I.; Martin, R. L.; Fox, D. J.; Keith, T.; Al-Laham, M. A.; Peng, C. Y.; Nanayakkara, A.; Challacombe, M.; Gill, P. M. W.; Johnson, B.; Chen, W.; Wong, M. W.; Gonzalez, C.; and Pople, J. A.; Gaussian, Inc., Wallingford CT, 2004.

(51) Lajohn, L.A.; Christiansen, P.A.; Ross, R.B.; Atashroo, T.; Ermler, W.C. *J. Chem. Phys.*, **1987**, 87, 2812-2824.

(52) Ross, R.B.; Powers, J.M.; Atashroo, T.; Ermler, W.C.; Lajohn, L.A.; Christiansen, P.A. *J. Chem. Phys.*, **1990**, 93, 6654 - 6670.

(53) Couty, M.; Hall, M.B. *J. Comput. Chem.*, **1996**, 17, 1359 - 1370.

(54) Dunning, T.H. *J. Chem. Phys.*, **1971**, 55, 716 - 723.

(55) Dunning, T.H.; Hay, P.J. in Modern Theoretical Chemistry, ed. H.F. Schaefer, vol 3., Plenum, new York: 1976. p 1-28.

(56) Thompson, M.A. 2004, ArgusLab 4.0.1 Seattle, WA Planaria Software LLC. http://www.arguslab.com

(57) Macrae, C.F.; Edgington, P.R.; McCabe, P.; Pidcock, E.; Shields, G.P.; Taylor, R.; Towler, M.; van de Streek, J. *J. Appl. Cryst.*, **2006**, 39, 453 - 457.

(58) Guex, N.; Peitsch, M.C. *Electrophoresis*, **1997**, 18, 2714 - 2723.

(59) Ohndorf, U.M.; Rould, M.A.; He, Q.; Pabo, C.O.; Lippard, S.J. *Nature*, **1999**, 399, 708 - 712.

(60) Burdette, S. *Chem. & Biol.*, **2006**, 13, 465 - 467.

(61) Müller, J.; Lippert, B. *Angew. Chem. Int. Ed.*, **2006**, 45, 2503 - 2505.

(62) Lu, W.; Vicic, D.A.; Barton, J.K. *Inorg. Chem.*, **2005**, 44, 7970 - 7980.

(63) Baruah, H.; Right, M.W.; Bierbach, U. *Biochemistry*, **2005**, 44, 6059 - 6070.

(64) Neese, F. *J. Biol. Inorg. Chem.*, **2006**, 11, 702 - 711.

(65) Siegbahn, P.E.M. *J. Biol. Inorg. Chem.*, **2006**, 11, 695 - 701.

(66) Roitzsch, M. ; Añorbe, M.G. ; Miguel, P.J.S.; Müller, B. ; Lippert, B. *J. Biol. Inorg. Chem.*, **2005**, 10, 800 - 812.

(67) Añorbe, M.G. ; Lüth, M.S. ; Roitzsch, M. ; Cerdà, M.M. ; Lax, P. ; Kampf, G. ; Sigel, H. ; Lippert, B. *Chem. Eur. J.*, **2004**, 10, 1046 - 1057.

(68) Sigel, R.K.O.; Lippert, B. *Chem. Commun.*, **1999**, 21, 2167 - 2168.

(69) Burda, J.V.; Šponer, J. ; Leszcynski, *J. Phys. Chem. Chem. Phys.*, **2001**, 3, 4404 - 4411.

CHAPTER 7 Donor Atom Preferences in Substitution Reactions of trans-Platinum Mononucleobase Compounds. Implications for DNA-Protein Selectivity

A. Anzellotti[a], S. Stefan[a], D. Gibson [b] and Nicholas P. Farrell[a*]

a. Department of Chemistry, Virginia Commonwealth University, 1001 W. Main St. Richmond, VA 23284-2006, USA.

b. Department of Medicinal Chemistry and Natural Products, School of Pharmacy, P.O.Box 12065, The Hebrew University of Jerusalem, 91120, Israel.

Inorganica Chimica Acta, **2006**, 359 (9), 3014 - 3019

7.1. Abstract

The competitive reactions of mononucleobase cations *SP*-4-2-[PtCl(9-EtGua)(NH_3)(quinoline)]$^+$, **1**, and *trans*-[PtCl(9-EtGua)(pyridine)$_2$]$^+$, **2**, with 5'-guanosine monophosphate (5'-GMP) and N-Acetylmethionine (NAcMet) were studied by ^{1}H NMR Spectroscopy. The results confirmed the previously observed kinetic selectivity for sulfur over nitrogen binding. The symmetric bis(pyridine) complex reacted faster than the ammine/quinoline moiety – the estimated half-times for reaction with 5'-GMP and N-AcMet were, respectively, 7.4 and 2.3 h for **1** and 4.90 and < 0.75 h for **2**. Thus modification of the planar amine can enhance sulfur selectivity – based on the observed rates a S/N selectivity ratio of 3.2 is obtained for **1** but > 6.5 for **2**. Applications of these findings were extended to study the reaction of **1** and **2** with Ubiquitin. One principal

adduct corresponding to chloride displacement is observed for both species and in this case little difference in rate is observed. The likely binding site is the unique methionine residue. The percentage of platinum-bound ubiquitin is higher for **1** and **2** than the parent dichlorides *trans*-[$PtCl_2(NH_3)$(quinoline)] and *trans*-[$PtCl_2$(pyridine)$_2$]. The results suggest that systematic ligand modification can modulate sulfur donor specificity and suggest possible structural features for design of platinum-based bifunctional DNA-protein crosslinking agents, rather than the DNA-DNA crosslinking principally adopted by the anticancer drug cisplatin and congeners.

7.2. Introduction.

Transplatin complexes containing planar amines *trans*-[$PtCl_2$(L)(L')], where L = L' = py or tz; L = NH_3, L' = py, quin, tz, etc.exhibit *in vitro* cytotoxicity equivalent to cisplatin in many human tumor cell lines.[1,2] This class of **trans**-**pl**anar**a**mine (TPA) compounds also displays an unusual biological profile including activity in cells resistant to cisplatin and oxaliplatin.[3] The most striking feature of the biological activity of these transplanar amine (TPA) compounds is the production of single-stranded protein-associated DNA strand breaks and induction of topoisomerase I-DNA complexes in human tumor cells.[4] An attractive explanation for these findings is the formation of ternary Pt-DNA-protein adducts rather than the bifunctional Pt-DNA adducts which are the predominant lesion of cisplatin and its structural analogues. Cellular studies have further confirmed intracellular production of a higher percentage of DNA-protein crosslinks in comparison to cisplatin.[4] Studies on isolated DNA for a typical TPA complex, *trans*-

$[PtCl_2(NH_3)(thiazole)]$, showed the presence of over 30% of monofunctional long-lived adducts which, in principle, could give rise to DNA-protein crosslinking .[5,6] DNA-protein, rather than DNA-DNA cross-linking may be a dominant feature of *trans*platinum chemistry. The use of *trans*-DDP to cross-link the zinc-finger nucleocapsid protein to HIV-1 [7] and the role of the monofunctional DNA adduct of *trans*-DDP in cross-linking ribosome from *E. coli* and an aminoacyl-tRNA synthetase/tRNA complex, showing contact points between RNA and protein ,[8] support this view.

The nucleobase cations, $[PtCl(9\text{-}EtGua)(L)(L')]^+$ are convenient models for the monofunctional adduct on DNA. The 1:1 reactions of *SP*-4-2-$[PtCl(9\text{-}EtGua)(NH_3)(L)]^+$ (L = NH_3, quin) with 5'-guanosine monophosphate (5'-GMP) and N-acetylmethionine (N-AcMet) showed a clear kinetic preference for sulfur binding.[9] These monofunctional nucleobase cations show some indications of selective antiviral activity and an attractive possibility is that the antiviral activity is mediated through protein zinc finger targeting, as a consequence of the high sulfur selectivity.[10] In agreement the complex *trans*-$[PtCl(9\text{-}EtGua)(py)_2]^+$ may displace Zn in model Zn chelates initially through formation of a thiolate bridged heterodinuclear Zn-S-Pt species.[11] It is therefore of interest to examine the effects of the planar amine on this sulfur selectivity and how this may aid design of agents capable of specific DNA-protein crosslinking. In this paper the competitive reactions of two representative transplatinum complexes containing 9-Ethyl guanine with a nucleotide and an aminoacid residue were studied to examine trends in sulfur selectivity. Binding to a model protein, ubiquitin, was also examined and the results compared with the parent dichlorides *trans*-$[PtCl_2(L)(L')]$.

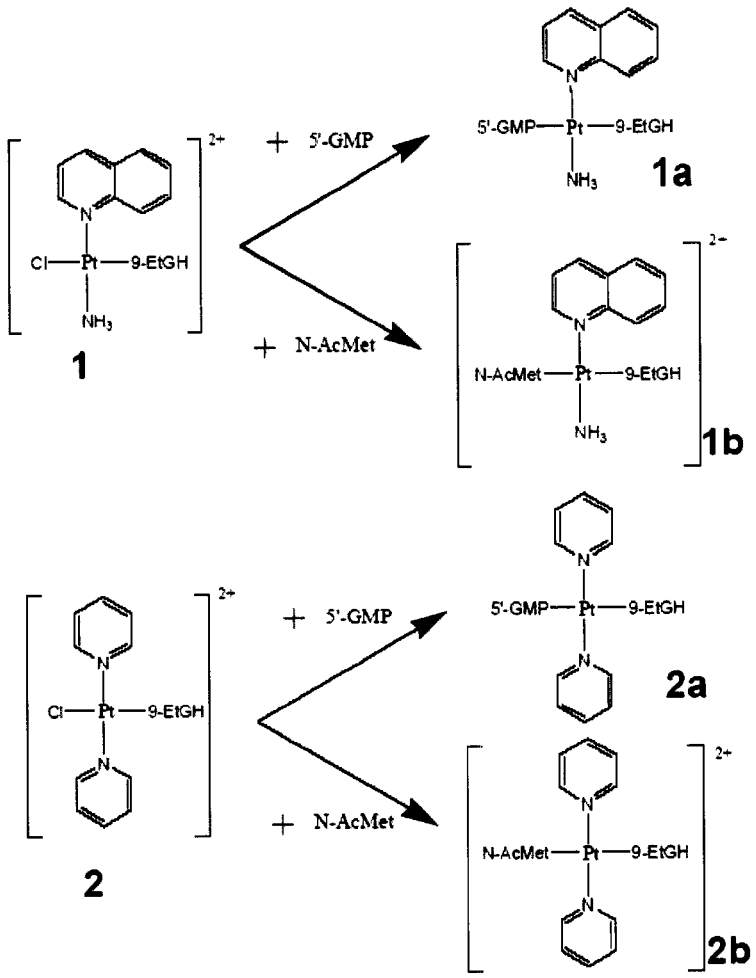

Scheme 7.1. Reactions studied on this work with numbering.

7.3. Results and discussion.

The kinetics of nucleotide binding for **1** and **2** was monitored by following the changes in the ^{1}H NMR spectra in the presence of one equivalent of 5'-GMP. Complex **1**, *SP*-4-2-[PtCl(9-EtGua)(NH_3)(quin]$^+$ has been examined previously and will not be

discussed in detail. The results are consistent with previous reports.[10,13] The signal for the H(8) of the free ligand moves downfield upon coordination and the signal is split into a doublet and a slight upfield shift is also seen for the H1' of the sugar, Figure 7.1.

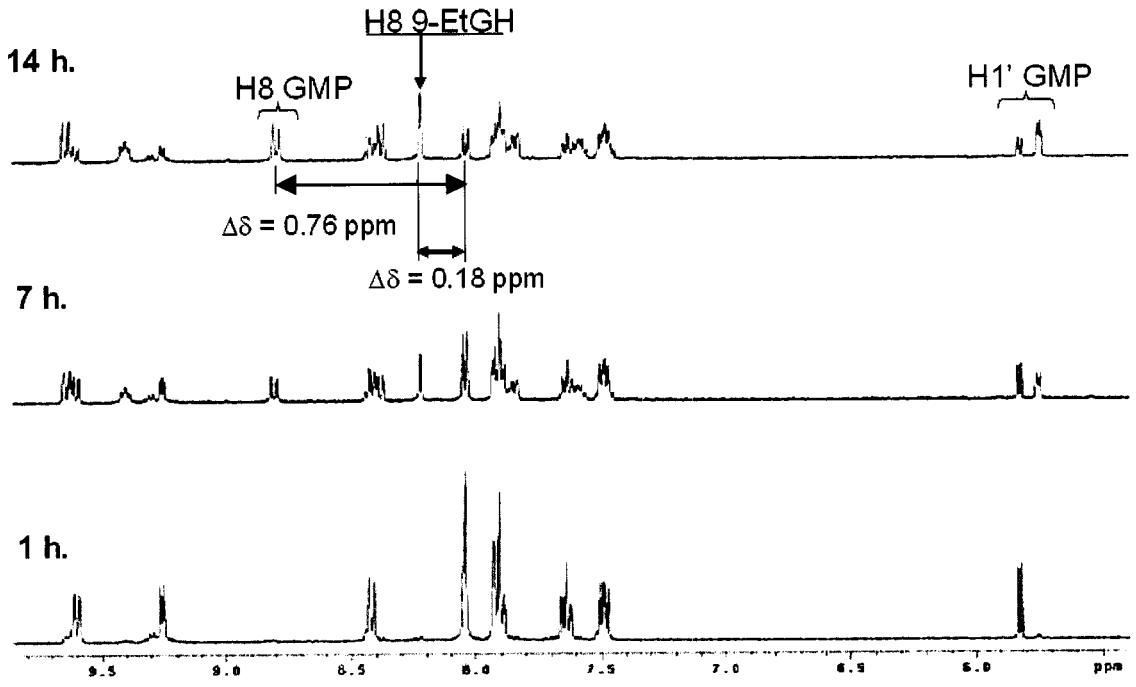

Figure 7.1. Time dependent changes in the ^{1}H-NMR spectrum from a 1:1 solution of [*SP-4-2*]-[PtCl(9-EtGua)(NH_3)(Quin)]$^+$ / 5'GMP, showing the new signals appearing in the aromatic region due to formation of **1a**.

A concomitant smaller shift for the coordinated 9-EtGua is also observed upon displacement of the trans chloride by the guanine N7 of 5'-GMP. The splitting of the H(8) signal of 5'-GMP is best explained by considering the unsymmetric environment of the platinum and the chirality of the sugar residue – hindered rotation will give rise to pairs of diastereomers observable on the NMR timescale. The results for Complex 2, trans-[PtCl(9-EtGua)(py)2]+ are shown in Figure 7.2.

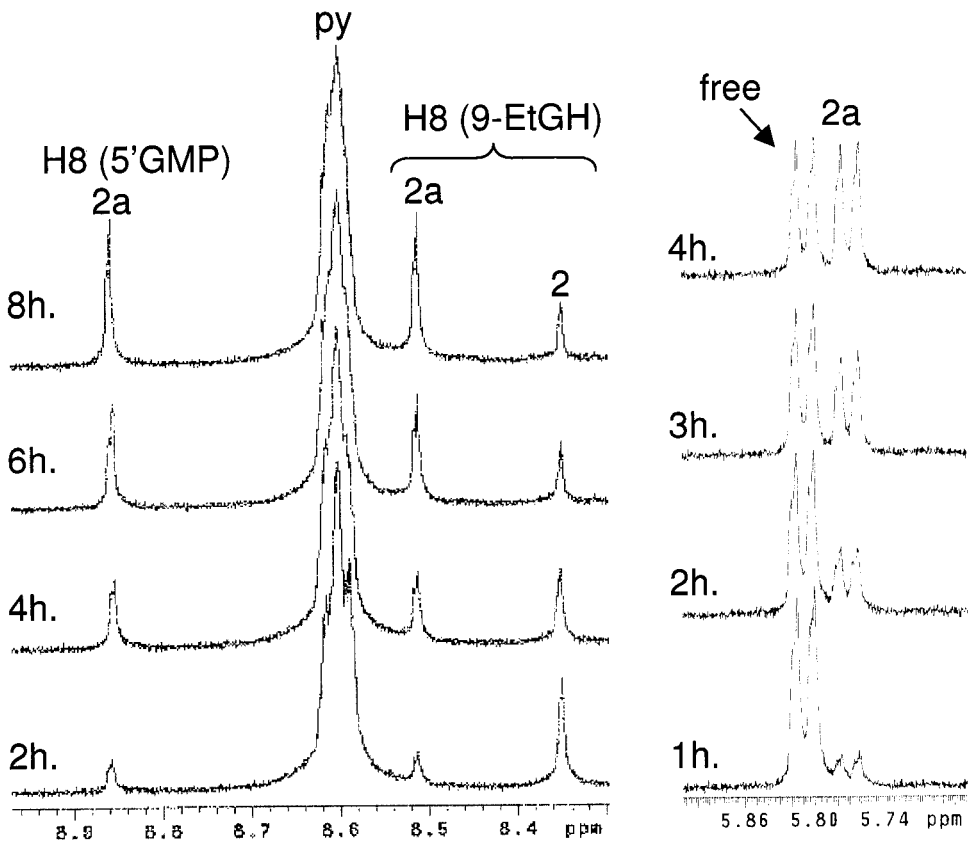

Figure 7.2. Time dependent changes in the ^{1}H-NMR spectrum from a 1:1 solution of *trans*-[PtCl(9-EtGua)(py)$_2$]$^+$ / 5'GMP due to formation of **2a.** Zoom of H8 signals including pyridine ortho hydrogens (left) and H1' from free and coordinated 5'-GMP (right).

The new compound *trans*-[Pt(9-EtGua)(5'-GMP)(py)$_2$]$^+$ shows peaks for coordinated 9-EtGua and 5'-GMP at 8.52 and 8.86 respectively – the latter is split into a doublet suggesting some hindered rotation around the N-Pt-N axis. The H1" of the sugar again undergoes an upfield shift.

For both **1** and **2**, plotting the appearance and intensity of new non-exchangeable peaks attributable to product allowed an estimate of $t_{½}$ for formation of **1a** and **2a** of 7.4 and 4.9 h respectively. The value for **1a** is somewhat smaller than that noted previously (17h) .[10] However in the latter case the pH was maintained constant by use of 0.1M DCl solution and in the present case no free Cl^- was present in solution – since aquation is the rate-limiting step in nucleobase substitution, the differences are reasonably attributed to this cause. The results suggest that the quinoline ligand exerts a more sterically demanding role than that of pyridine, even in a *trans*-$Pt(py)_2$ species. Attempts to compare effects of other planar ligands were not successful – the product of the reaction with *SP*-4-2-[PtCl(9-EtGua)(NH_3)(thiazole)]$^+$ precipitated from solution and no comparative data could be obtained.

The progress of substitution reactions of **1** and **2** with N-acetylmethionine can be followed in a similar manner by ^{1}H-NMR spectroscopy. The ^{1}H NMR spectrum of **1b** is complicated due to the presence of diastereomers and multiple peaks are observed through both the slow interconversion of the *R* and *S* forms of the chiral sulfur center as well as restricted rotation around the Pt-$N7_{gua}$ and Pt-$N1_{quin}$ bonds. The kinetics of substitution could be followed by monitoring signals in the aromatic region – especially the H4 of quinoline ligand shifted downfield in a systematic manner and was free of overlap, Figure 7.2. Quantitation of the substitution reaction, however, has to be made with caution as 9-EtGua is labilized in the presence of the strongly *trans*-influencing sulfur of the methionine ligand and approximately 25-30% of free nucleobase is observed in the course of the reaction leading to presumably an aquated species:

Cl-Pt-N7(9EtGua) → (N-AcMet)S-Pt-N7(9EtGua) → (N-AcMet)S-Pt-H_2O

In the case of **2**, a rapid reaction takes place. The ^{1}HNMR spectrum of N-Acetylmethionine in D_2O shows two singlets at 2.04 and 2.11 ppm for the N-COCH_3 and S-CH_3 respectively. The S-CH_3 signal of N-Acetylmethionine undergoes a small downfield chemical shift to 2.3 ppm upon platination – this effect is not as pronounced as in other Pt-methionine complexes,[10,14,15] possibly due to ring current effects of the *cis*-oriented pyridine ligands as well as the electron-withdrawing properties of the pyridine ligands compared to that of NH_3. No evidence for diastereomers was observed for **2b**. As can be seen from Figure 7.3., product and reactant are in equal proportions after only 45min but some free 9-EtGua also begins to appear. The estimated $t_{½}$ of formation of the ternary [Pt(9-EtGua)(N-Ac-Met)(L)(L')] species are 2.3 h and < 0.75h for **1** and **2** respectively. The results are again consistent with a more sterically demanding role of the quinoline ligand. Table 7.I. summarizes the data. An approximate estimate of sulfur selectivity can be gauged by comparing the $t_{½}$ ratios and it is of interest to note that, despite the more rapid reactions, a higher S/N selectivity is obtained for Complex **2**.

Table 7.I. Half-times for substitution reactions of solutions of monofunctional platinum complexes **1** and **2** with 5'-GMP and N-AcMet[a]

Complex	5'-GMP (h)	*N*-AcMet (h)	S/N
1	7.4 (0.2)	2.3	3.2
2	4.90 (0.02)	<0.75	>6.5

[a] S/N ratio estimated by $t_{1/2}$(5'-GMP)/$t_{1/2}$(*N*-AcMet).

Figure 7.3. Differences in chemical shifts from aromatic signals in complexes **1** (left) and **2** (right) upon chloride substitution by N-AcMet, which can be used to follow the kinetics of the reaction.

Aquation of Mononucleobase Compounds. Substitution of an ammine group by a planar amine in $[PtCl(9\text{-}EtGua)(L)(L')]^+$ dramatically alters the hydrolytic behavior of the cation and **1** undergoes extremely slow hydrolysis.[10] The aquation of *trans*-$[PtCl(9\text{-}EtGua)(NH_3)_2]^+$ proceeds at 37°C with a half-time of approx. 6.5 h. Under similar conditions no measurable aquation was seen for **1**.[10] In attempts to quantify the aquation of **1** and **2**, ^1H NMR spectra were followed with time. The extent of aquation could be measured by the appearance of new peaks in the spectrum attributed to the loss of Cl^-. After 14 days only 11 and 34 % of **1** and **2** were hydrolysed, figure 7.4. Thus, while there

is some variation with structure the remarkable stability to aquation of this class of compounds is confirmed. No detailed kinetic studies have yet been performed on these species – the observed lack of aquation could be due to a very high k_{-1} as observed for dinuclear compounds [16] but it is clear that under physiological conditions the cations will be essentially in the chloride form. A major difference between the requirements for nucleotide and sulfur binding to Pt(II) is that the latter substitution proceeds *via* direct substitution of chloride whereas N7 binding usually requires prior hydrolysis of the chloride.[17] In the present case, comparison of the rates of substitution by 5'-GMP and estimated aquation also suggests direct displacement rather than a solvent-assisted pathway. This reactivity feature, and choice of planar amines, suggests there is considerable scope for tuning the substitution kinetics in terms of changing the ratio of nitrogen to sulfur binding - monofunctional DNA adducts of this type should favor DNA-Pt-protein rather than bifunctional DNA-Pt-DNA crosslink formation.

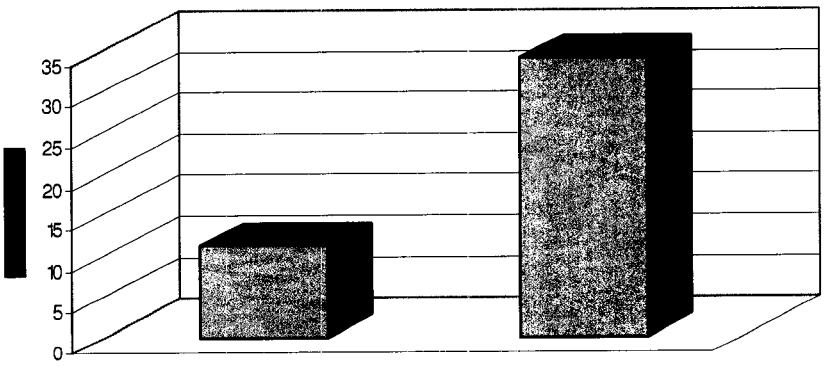

Figure 7.4. Percentage hydrolysis of complexes **1** and **2** after two weeks at 37 °C.

Protein Reactions. To extend these results to protein binding, the interactions of **1** and **2** with Ubiquitin (Ub) were studied. Ub is a good model for protein binding because its structure is well characterized by x-ray crystallography and there are only two major potential platinum binding sites, one methionine in the *N*-terminus (Met1) and one histidine on the surface (His68).[18] The competitive DNA-protein interactions of *cis* and *trans*-DDP with Ubiquitin have been studied.[19] Despite the higher kinetic reactivity of *trans*-DDP due to the mutually *trans* chlorides, the *cis* geometry reacts faster with the protein and predominantly at methionine whereas the *trans* geometry appears to have multiple binding sites In this case, it can be argued that since cisplatin binds mainly to Met1 while transplatin does not, the faster binding kinetics of cisplatin results from the fact that soft ligands like the thioether of Met1 bind Pt(II) faster than harder nitrogen ligands. The nature of L in *trans*-$[PtCl_2(NH_3)(L)]$ also makes a significant difference to kinetics of binding to Ub.[12] When L = quinoline binding is slower than for 4-picoline or piperazine, albeit similar to *trans*-DDP itself .[12] The precursor of **2,** *trans*-$[PtCl_2(py)_2]$, shows minimal reactivity with the protein (data not shown). Replacement of the NH_3 ligand with a bulky amine does not seem to affect the mode of binding of the complexes and all the major products is mainly the monofunctional adduct *trans*-[PtCl(L)(L')(Ub)] Comparison of rates of reaction on selectively blocked protein (i.e. oxidation of the sole methionine residue) again indicates that there are multiple binding sites for the *trans* geometry.[12]

For **1** and **2**, reactions were carried out as previously.[12] The ESIMS (positive mode) of a protein is characterized by a distribution of peaks that corresponds to the different

charge states of the same intact protein. For free ubiquitin the envelope centered at 8565 amu disappears and a new envelope centered at 9090 amu appears in both cases with an isotopic distribution indicative of platinum. The atomic mass of this new peak corresponds approximately to a 1:1 species between Ub and [Pt(9-EtGua)(NH_3)(quin)] and [Pt(9-EtGua)$(py)_2$] {coincidentally these two fragments have the same mass – $PtC_{17}H_{18}N_9O$}. Thus it is reasonable to conclude that the products are 1:1 adducts formed by chloride substitution.

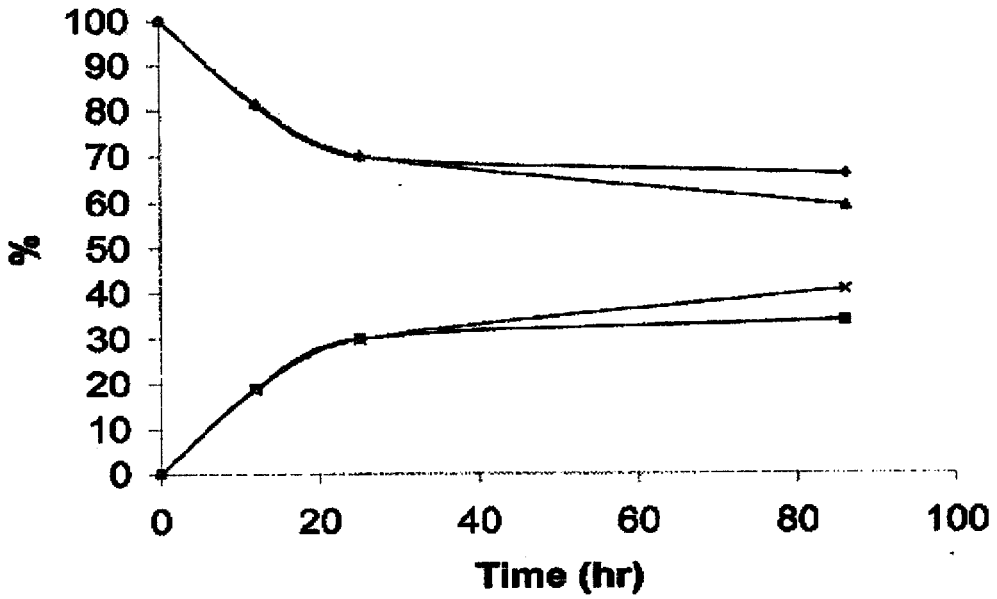

Figure 7.5. Plots of disappearance of free Ubiquitin with time in the presence of **1** (♦) and **2** (▲) and appearance of the platinated product of **1** (■) and **2** (x).

Figure 7.5. shows the rate of disappearance of free protein and appearance of the new product. Interestingly there is little difference in rate between **I** and **2** and 30% binding is achieved within 24 h. This is faster than that observed for the parent dichlorides and

similar to *cis*-DDP.[19] The combined results suggest binding of **1** and **2** to the methionine residue.

7.4. Experimental Section.

Synthesis and Characterization. All platinum compounds were prepared by the published method and characterized by ^{1}H and ^{195}Pt NMR Spectroscopy and ESI-MS .[10] Their purity was assessed by elemental analysis and HPLC. All other reagents and solvents were purchased from common vendors and used without prior purification. N-acetyl-L-methionine was the free acid from Sigma and the mononucleotide 5'-guanosinemonophosphate from Aldrich was used as the disodium salt.

Physical measurements. ^{1}H NMR spectra for the characterization of the compounds were obtained on a Varian Gemini 400 MHz NMR spectrometer equipped with a variable temperature unit. The kinetic results were obtained at constant 37 ^{o}C using appropriate software for arrayed kinetic experiments. Quantitation of the progress of the reactions was achieved by integration of signals of appropriate non-exchangeable protons of the product. Half-lives of reactions were plotted using SCIENTIST software.

Platination reactions and ESI-Mass Spectrometry. The experimental detail followed published work.[12] Platination reactions were carried out at 1-2 mM concentrations of both protein and platinum complexes, in 10 mM phosphate buffer, pH 6.4 at 37 ^{0}C. Excess platinum was removed by ultra-filtration using Microcon YM-3 centrifugal filter devices at $4^{0}C$ and 12,000 rpm, prior to all adduct reactivity studies. Protein binding profiles by ESIMS were measured directly on the reaction mixtures following ZipTip™ (C18,

Millipore) treatment. ESIMS spectra were measured on triplicates of the reaction mixtures; the standard deviation of these measurements was less than ± 2%. Electrospray ionization mass spectrometry was measured on a ThermoQuest Finnigan LCQ- Duo in the positive ion mode. In most cases, elution was in a mixture of 49:49:2 water:methanol:acetic acid at a flow rate of 15 μL/minute. Samples of the platination reactions and adduct reactivity studies were diluted by a 100 fold prior to ESIMS analysis. Data were processed using ThermoQuest Finnigan's Xcalibur™ Biomass Calculation and Deconvolution software. To observe the mass spectra of ubiquitin in its native, folded, state elution was carried out in 1% acetic acid in water.

7.5. Conclusions.

Design of platinum-based chemotherapeutic agents acting through DNA-protein crosslinking may produce a biological profile complementary to the currently used agents. DNA-protein ternary adduct formation may, in principle, arise from protein binding to a monofunctional Pt-DNA site. It is of interest that the model complexes **1** and **2** show some evidence of selective protein binding, whereas the parent dichlorides do not. Thus displacement of Cl by a purine base alters dramatically the chemical and biological properties. Whether this chemistry is a critical feature of the incipient antiviral activity of **1** and **2** is worthy of exploration. The small molecule studies (5'-GMP, N-AcMet) summarized here suggest that systematic enhancement of the S/N ratio is possible by choice of suitable planar amines. The rates and mode of reaction with protein of **1** and **2** and their parent dichlorides do not directly parallel that seen for the small molecules. For example, no demonstrable adducts are found for the reaction of *trans*-

$[PtCl_2(NH_3)(quinoline)]$ with methionine itself (in contrast to **1**) whereas *trans*-$[PtCl_2(pyr)_2]$ reacts readily with L-Met. In contrast the pyridine complex does not react with Me_2SO, except under forcing conditions[20] but Me_2SO reacts at intermediate rates with *trans*-$[PtCl_2(NH_3)(quinoline)]$, but significantly slower than with *trans*-DDP itself. [21] With respect to protein binding other factors besides donor affinity such as accessibility of binding sites must be considered. Other subtle electronic factors may be responsible for some differential reactivity toward S-donors. The results presented here do show that the *trans*-$[PtCl(9\text{-EtGua})(L)(L')]^+$ chemotype is capable of systematic modification to enhance S and hence specific protein binding. Such chemical properties would be expected to result in novel biological activity.

7.6. References.

(1) Van Beusichem, M.; Farrell, N. *Inorg. Chem.*, **1992**, 31, 634.

(2) Farrell, N.; Kelland, L.R.; Roberts, J.D.; Van Beusichem, M. *Cancer Res.*, **1992**, 52, 5065

(3) Fojo, T.; Farrell, N.; Ortuzar, W.; Tanimura, H.; Weinstein, J.; Myers, T.G. *Crit. Revs. Oncol./Hematol.*, **2005**, 53, 25.

(4) Farrell, N.; Povirk, L.F.; Dange, Y.; Gupta, M.S.; Kohlhagen, G.; Pommier, Y. ; Gewirtz, D. *Biochem. Pharmacol.*, **2004**, 68, 857.

(5) Kasparkova, J.; Novakova, O.; Farrell, N.; Brabec, V. *Biochemistry*, **2003**,42, 792.

(6) Marini, V.; Christofis, P.; Novakova, O.; Kasparkova, J.; Farrell, N.; Brabec, V. *Nuc. Acids Res.*, **2005**, 33, 5819.

(7) Darlix, J.L.; Gabus, C.; Nugeyre, M.T.; Clavel, F.; Barre-Sinoussi, F. *J. Mol. Biol.*, **1990**, 216, 689.

(8) Tukalo, M.A.; Kubler, M.D.; Kern, D.: Mougel, M.; Ehresmann, C.; Ebel, J.P.; Ehresmann, B ; Giege, R. *Biochemistry*, **1987**, 26, 5200.

(9) Bierbach, U.; Farrell, N. *J. Biol. Inorg. Chem.*, **1998**, 3, 570.

(10) Sartori, D.A.; Miller, B.; Biebach, U.; Farrell, N. *J. Biol. Inorg. Chem.*, **2000**, 5, 575.

(11) Liu, Q.; Golden, M.; Darensbourg, M.Y.; Farrell, N. *Chem. Commun.*, **2005**, 34, 4360.

(12) Najajreh, Y.; Peleg-Shulman, T.; Moshel, O.; Farrell, N.; Gibson, D. *J. Biol. Inorg. Chem.*, **2003**, 8, 19.

(13) Bierbach, U.; Farrell, N. *Inorg. Chem.*, **1997**, 36, 3657.

(14) del Socorro, M.P.; Ranford, J.D.; Sadler, P.J.; Berners-Price, S. *J. Inorg. Chem.*, **1993**, 32, 2249.

(15) Quintal, S.M.O.; Qu, Y.; Gomez-Quiroga, A.; Moniodis, J.; Nogueira, H.I.S.; Farrell, N. *Inorg. Chem.*, **2005**, 44, 5247.

(16) Davies, M.S.; Thomas, D.S.; Hegmans, A.; Berners-Price, S.J.; Farrell, N. *Inorg. Chem.*, **2002**, 41, 1101.

(17) Djuran, M.I.; Lempers, E.L.M.; Reedijk, J. *Inorg Chem.*, **1991**, 30, 2648.

(18) Vijay-Kumar, S.; Bugg, C.E.; Cook, W.J. *J. Mol. Biol.*, **1987**, 194, 531.

(19) Peleg-Shulman, T.; Gibson, D. *J. Am. Chem. Soc.*, **2001**, 123, 3171.

(20) Fontes, A.P.S.; Oskarsson, Å.;Lövquist. K.; Farrell, N. *Inorg. Chem.*, **2001**, 40, 1745.

(21) Farrell, N. Unpublished Results.

CHAPTER 8 Molecular Dynamics Simulations on DNA Adducts of *t*-$PtCl_2(NH_3)$(thiazole) or ATZ complex.

8.1. Abstract.

Features of DNA adducts with a new generation of platinum complexes exhibiting planar amines in a *trans* geometry, are modeled through 1.2 ns. The molecular dynamics of two free DNA 20-mer is compared with the corresponding metallated-adducts, namely monofunctional, 1,2-bifunctional interstrand and 1,3-bifunctional intrastrand. The differences in terms of structure and energy are ompared for these systems, in general the monofunctional adduct exhibited the most interesting feature in terms of structural change in the DNA double strand causing the destacking of the metallated nucleobase. Bifunctional adducts exhibited loss of Watson-crick bonds and localized change in sugar puckering

8.2. Introduction.

Platinum complexes with a *trans* geometry exhibiting anti-tumor activity defies the initial structure-activity relationships initially established for *cisplatin*.[1] Due to the trans effect (Cl >N >O) the favored specie observed in *transplatin* hydrolysis is the monoaquo (*t*-$[PtCl(NH_3)_2(H_2O)]^+$), which binds to DNA in a monofunctional manner. This type of adduct is very reactive towards nucleophiles, such as the sulphur atom in the protein residues cysteine and methionine. Notably the substitution of chloride by sulphur in the platinum's coordination sphere does not require an aquo intermediate as in the case of

nitrogen,[2] thus the ternary metal-DNA-protein adduct is favored compared to the bifunctional metal-DNA observed on platinum complexes with *cis* geometry. This fact is highly relevant because in the former case the result is a displacement of the platinum complex and DNA repair, while in the second case the whole metabolism of the cell can be disrupted leading to apoptosis.

A way to modulate this outcome is by using a bulky subtituent in place of one or two of the mutually *trans* ammine ligands, this concept has been proven true for a variety of complexes that incorporate planar amines such as pyridine, thiazole or quinoline (see Chapter 1). The presence of the planar amine decrease the reactivity of the complex towards substitution reactions, [3] modifying hydrolysis profiles and increasing the lifetime of monofunctional DNA adducts such that they can exert an appreciable biological effect. As a matter of fact these modified *trans*-planar amine platinum complexes (TPAs) are capable of exhibiting high cytotoxicity being sometimes higher than the corresponding *cis*-analog.[4] Moreover as mentioned before (Chapter 1), the biological reactivity exhibited by these complexes is significantly different when compared to classical *cisplatin* derivatives. Briefly the production of a different DNA-adduct profile with induction of strand breaks, in addition to the possibility of forming ternary adducts with proteins confer to this class of complexes a novel cytotoxicity profile. [5]

In order to understand the molecular basis for this different biological outcome produced specifically by TPAs, several spectroscopic techniques, as well as biochemical and biophysical methods have been employed. The use of computational methods or an *in silico* approach to this end has been rather modest. Early modeling studies comparing

transplatin with *t*-[$PtCl_2(NH_3)$(quinoline)] revealed that the presence of the bulky planar amine gives rise to conformers not present initially for *transplatin*. [6] As shown on figure 8.1., substitution of one chloride by a nucleobase such as 9-ethylguanine (9-EtGH), mimicking the first step in DNA binding, increases the steric demand for the resulting *t*-[$PtCl(NH_3)$(quinoline)(9-EtGH)]$^{2+}$ compared to *t*-[$PtCl(NH_3)_2$(9-EtGH)]$^{2+}$.

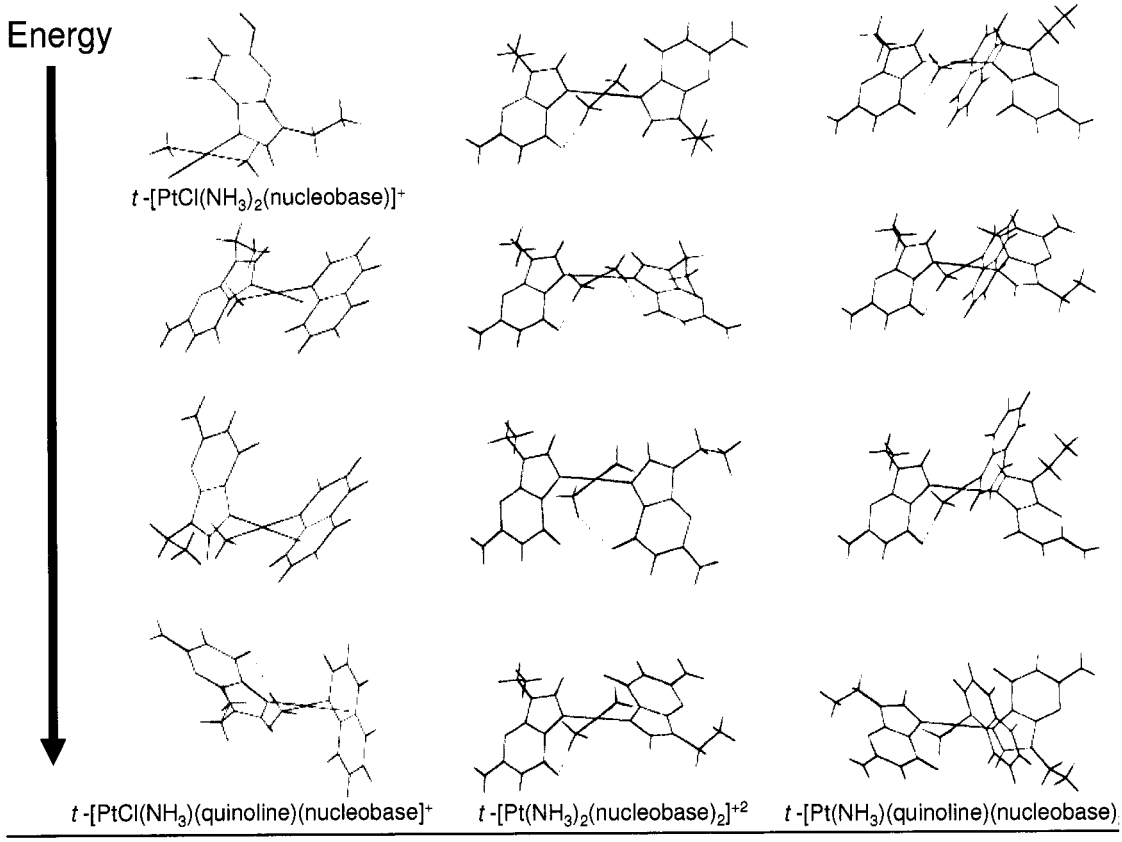

Figure 8.1. Structure of conformers calculated for the step-wise substitution of chloride ligands in trans position by 9-EtGH. Hydrogen bonds are drawn as a dashed line.

Therefore producing three different conformers in which the orientation of the quinoline and the nucleobase will be differentiable, i.e. head to head orientation (HH) vs. head to tail (HT), in terms of energy due to limited rotation around the Pt-N bond (first two

columns of figure 8.1.). The use of 9-EtGH as nucleobase also introduces the possibility of hydrogen bond formation via the exocyclic oxygen in position 6 with one of the ammine ligands, which is another factor to take into consideration for the energetic stability.

Importantly when the substitution of a second chloride is made, mimicking the second step in DNA binding, the presence of four different conformers was obtained, again depending on relative spatial orientation of the ligands and number of hydrogen bonds present. In general for the bis-nucleobase complexes the most stable conformations correlated with the number of hydrogen bonds formed, confirming a stabilizing interaction. This initial conformational search was carried out based on a usage-directed scheme of the Monte Carlo multiple-minimum method, and the obtained structures were in good agreement with experimental observations (^{1}H-NMR one-dimensional and NOE correlations).

An additional study employed molecular mechanics (MM) to further understand the DNA binding mode of the complex *trans*-[$PtCl_2(NH_3)$(quinoline)]. Specifically the conformation of a mono-functional adduct was compared for two different sequences in a short DNA duplex, 9 base pairs long (fig. 8.2.).[7] Results from this study provided a good explanation to the fact that mono-functional adducts of TPA are recognized by cisplatin-specific antibodies and not by trans-platin specific antibodies. The minimized models showed an overall stability when the planar amine (quinoline in this case) was able to stack with the DNA, than otherwise. This stacking interaction bends the double helix in a similar way to the 1,2-intrastrand adduct in cisplatin producing very close conformational change in DNA, this resulting topology could potentially mimic classical cisplatin adducts.

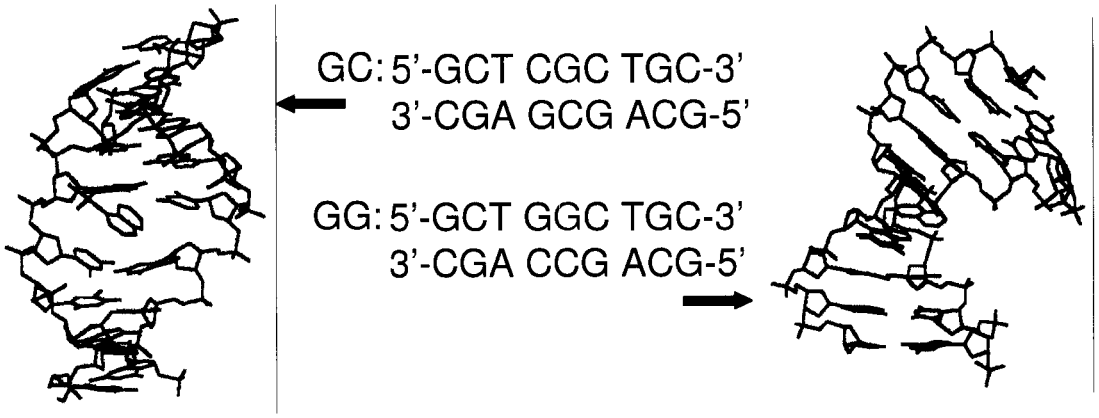

Figure 8.2. Sequences employed for molecular mechanics study of mono-functional adducts of *trans*-[$PtCl_2(NH_3)$(quinoline)], platination sites are highlighted in red. The corresponding minimized conformations obtained are also shown.

In order to expand the current knowledge on modeling of TPA-DNA interaction, we considered of interest to use molecular dynamics (MD) as a way to explore different conformations attainable by the mono- and bi-functional adducts in the potential energy surface of a model system. In MD, the time evolution of a set of interacting atoms is followed by integrating their equations of motion, using Newton's law (F = ma).[8] One of the big advantages of MD is the possibility of studying large systems involving a big number of atoms in an adequate amount of time, which is beyond the possibilities of quantum mechanical methods such as *ab initio* or density functional. In contrast to MM, the forces determined are not minimized but used to calculate changes in the inter- and intra-molecular velocities of the system. MD has been applied previously to other platinum related systems including the major DNA adduct observed for cisplatin (intrastrand), the

study correlated well with existent NMR data and also provide indications of an increased conformational flexibility at the platination site.[9]

On this contribution we aimed to study the interaction of the representative TPA complex *trans*-[$PtCl_2(NH_3)$(thiazole)] or ATZ with a relatively long DNA oligomer containing 20 base pairs (bp). The oligomer sequences were chosen due to its relevance to previous biochemical/biophysical studies that considered the three potential DNA-adducts of ATZ, namely mono-funtional (*mono*), bi-functional 1,3-intrastrand (*bintra*) and bi-functional 1,2-interstrand (*binter*) (fig. 8.3.). [10,11] Table 8.I. presents a summary of the data found compared to *cis*- and *trans*-platinum complexes, in general bi-functional complexes exhibited a significantly different behaviour compare to the mono-functional. They bent DNA at the opposite side (minor grove) with the biological implications of a decreased recognition by HMG proteins. In addition, according to DNA-conformation probing experiments *bintra* and *binter* adducts distort the DNA double helix over a greater number of base-pairs compared to the *mono*, being the intrastrand adduct the more important with a distortion extending 6 bp long.

Table 8.I. Summary and comparison of basic characteristics of DNA adducts for ATZ (*t*PtTz), transplatin and cisplatin.[10]

	1,3-Intrastrand CL of *t*PtTz	Interstrand CL of *t*PtTz	Monofunctional adduct of *t*PtTz	Interstrand CL of transplatin	Interstrand CL of cisplatin	1,2-Intrastrand CL of cisplatin
Frequency (%)	20–40	30–40	30–40	~12	~6	~90
Reactivity of chemical probes (bp)	6	4	2	4	ND	ND
DNA bending	40° toward minor groove	22° toward minor groove	34° toward major groove	~20° toward minor groove	40–45° toward minor groove	32–34° toward major groove
DNA unwinding	15°	20°	12°	~12°	76–79°	13°
HMGB1a recognition	≫1.5 μM	≫1.5 μM	38.5 nM	ND	≫1.5 μM	30.8 nM
HMGB1b recognition	≫30 μM	13.40 μM	2.05 μM	ND	4.60 μM	1.85 μM
Translesion synthesis	No	ND	20%	ND	ND	6%
NER by eukaryotic excinuclease (% excision)	1.0	No	1.4	no	no	1.5

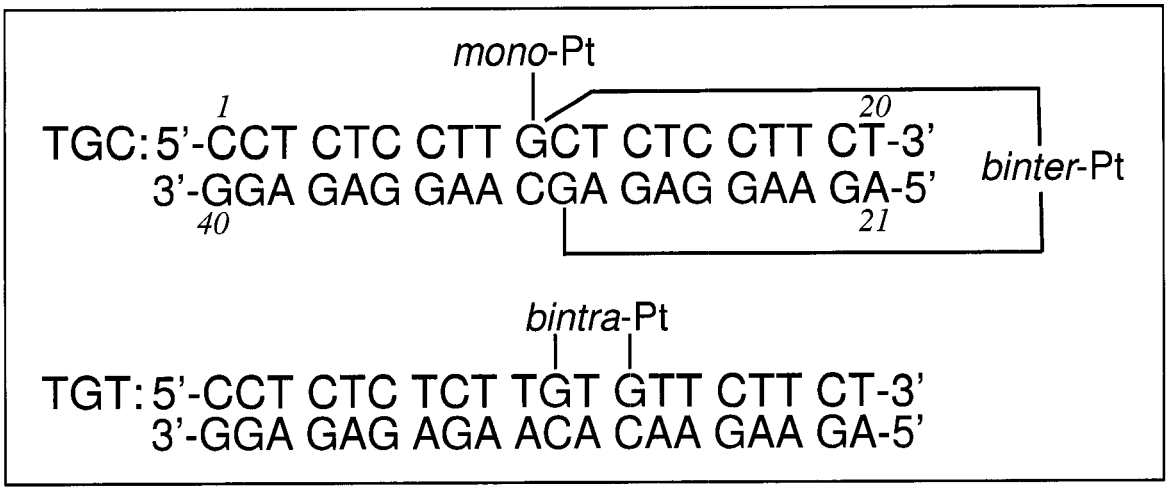

Figure 8.3. Sequence for the 20 bp oligomers used to study monofunctional and bifunctional interstrand (top); and bifunctional intrastrand adducts of ATZ (bottom). Platination sited are indicated in red and nucleobase numbering in italics.

The oligomer sequences will be noted as TGC and TGT in order to facilitate notation, TGC was used for modeling of the monofunctional and the 1,2-interstrand adduct due to the appropriate placement of guanine nucleobases. Sequence TGT was used for the 1,3-intrastrand adduct (fig. 8.3.). A combination of MM and MD will be performed on the three different adducts and on the free oligomers in order to compare qualitatively the influence of the platinum complex on the system dynamics.

8.3. Results and discussion.

8.3.1. Equilibration. Using the program *mdout* the total energy of the system was followed every 0.1 ps in all cases. A plot comparing the different systems studied can be seen in figure 8.5., generally the systems proceeded to the last 20 ps of the equilibration step with a small fluctuation (109 – 45 cal/mol) around a constant mean value, fluctuations

around 100 cal/mol have seen frequently in related systems prior to the production step. The mono-functional adduct was an exception presenting a moderate variation in total energy throughout the equilibration and specifically fluctuations in the order of 600 cal/mol in the last 20 ps of equilibration can be seen as peaks in figure 8.4.

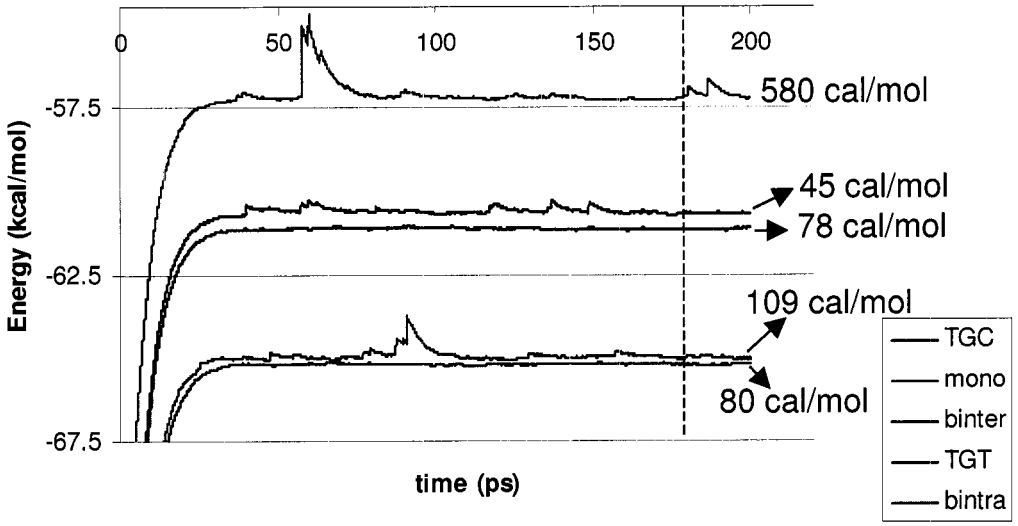

Figure 8.4. Plots of total energy for the systems studied in the equilibration step 0 -200 ps. Last 20 ps are highlighted with a dashed line; numbers indicate fluctuations in this last period.

On the other hand plots obtained for temperature showed that this system fluctuated around the specified temperature (300 °K), and pressure and density also were equilibrated over time (fig. 8.5.), according to these criteria the *mono* system was considered adequate to start the production dynamics.

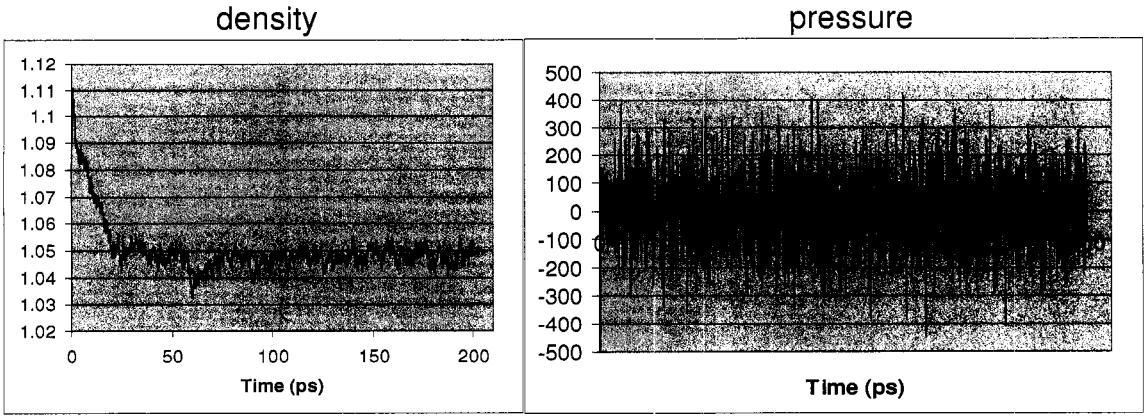

Figure 8.5. Plots of density and pressure for the mono-functional adduct in the equilibration step 0 -220 ps.

In order to better understand the changes in conformation that are producing the energy peaks in the systems, the *.pdb files corresponding to a time span of 10 ps were visualized and compared with the help of the program swiss pdb viewer. For *mono*, a comparison between the period 51 - 60 ps exhibiting a local maximum around -54.7 kcal/mol and the period 151 – 160 ps, with a local minimum around -57.3 kcal/mol showed clear evidence of a deformation in the platinum complex. As can be seen in figure 8.6. after the DNA strands in both files were fitted, a zoom in the platinum complex showed a significant elongation of the coordination bonds, in particular for the thiazole ligand, (up to 3.0 Å), also the ammine-Pt-thiazole angle exhibited deviations from the square planar geometry (122.08°). In addition the thiazole ligand appeared greatly distorted compared to the stable conformation obtained in the local minimum. All these facts coupled with the relative small RMS observed for DNA fitting for DNA backbone (2.79 Å), indicates that the increase in energy is due in part to these rearrangements in the platinum coordination sphere.

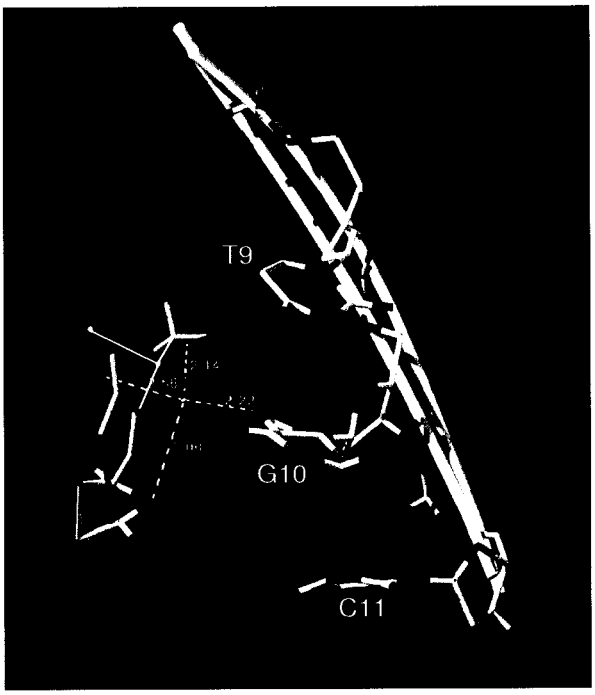

Figure 8.6. Monofunctional adduct of ATZ showing bond distances to the central platinum ion. The high energy conformation is compared with the lower energy counterpart (in magenta). The DNA backbone presented as a white tube is compared also for the platinated strand at local maximum and minimum for equilibration.

The conformation of the *mono* system was also monitored for stacking interactions, at the beginning of the equilibration 1 – 50 ps., a potential interaction between the thiazole ring to stack between A29 and G30 was observed. This interaction was monitored through the distances between H4 in the thiazole ring and A29(N7)/G30(O6), this interaction changed abruptly from an average of 2.8 Å around 50 – 59 ps (in agreement with the local maximum), to 6.0 and 4.7 Å for A29(N7) and G30(O6) respectively after 60 ps. At the same time, the thiazole ring flipped and improved its position for stacking between nucleobases G30 and C31, this configuration of the system resembled closely to the one obtained for the complex *t*-[$PtCl_2(NH_3)$(quinoline)] (Fig. 8.2.). An additional interaction between the ammine ligand and the phosphate in G10 (2.9 Å) was generated that did not existed before (6.0 Å).

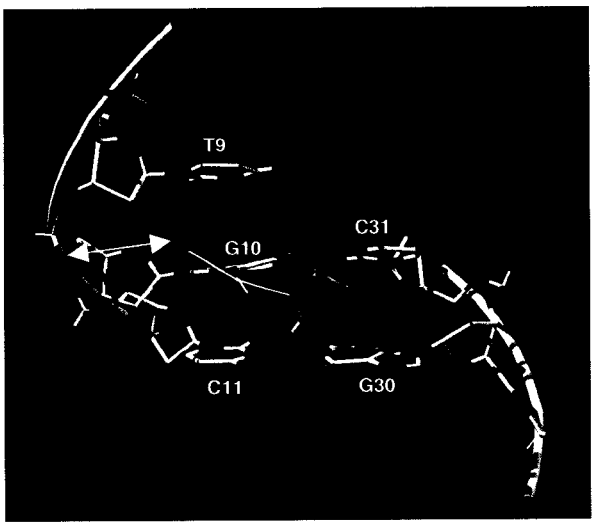

Figure 8.7. pseudo-stacking of the monofunctional adduct of ATZ in G30/C31. Distance between G10 phosphate and ammine ligand is shown by the double arrow.

Monitoring through time shows that the thiazole ring approaches the space between nucleobases G30 - C31 in several occasions, the most favored was found in the period 141 – 150 ps. (which is the previous period to the local minimum observed). The C31 nucleobase seem to be opening creating a site for the thiazole to stack, but probably due to the non-parallel position of the ligand the interaction did not occur in the simulation. The bouncing of the thiazole towards the interbase space was also monitored by the aforementioned distance between the phosphate at G10 and the ammine ligand, this distance (white double arrow in figure 8.7.) varied from 2.9 Å up to 4.3 Å. The failure to appreciate a stacking of the thiazole into DNA is associated with the inherent limitation of the force field, since even when considering non-covalent contributions the complicate nature of aromatic stacking are generally not properly modeled.

The *binter* adduct did proceed to production with a good equilibration, relative minor energy peaks (max. 0.4 kcal/mol) were seen during the equilibration step therefore the conformation will be briefly commented here. At the last stage of equilibration the

Watson-Crick H-bonds were totally lost in the base pair G10/C31 due to the platinum coordination in G10, this interaction was also heavily disrupted for the next base pair C11/G30 with only one H-bond left between C11(C4-NH_2) with G30(O6). It is interesting to note on the other hand an interaction between G10(O6) and the ammine ligand in ATZ (Fig. 8.8., NH_3...O 2.70 Å).

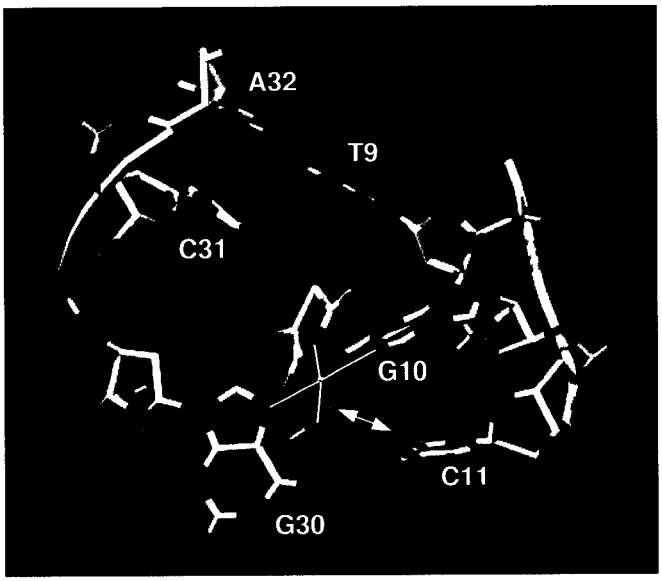

Figure 8.8. binter adduct after equilibration, it can bee seen the lost of base pairing for G10/C31 and C11/G30. Double arrow highlights the interaction between the ammine ligand and G10.

The *bintra* adduct also exhibited a local maximum in the period 91 – 100 ps which was compared with a local minimum 121 – 130 ps., the difference between both being 1.2 kcal/mol was almost half the difference for the *mono* exhibiting a difference of 2.6 kcal/mol, this can be correlated to a higher degree of freedom for the *mono* adduct which can rotate around its single coordination bond, whereas *binter* is held in a more constrained position by the bifunctional coordination. A DNA fit between the two conformations indicated a moderate displacement in the atom positions RMS = 2.17 Å. The conformation in the local maximum showed a break in H-bonds for the base pair G11/C30 due to the

presence of the platinum adduct which causes G11 to step out of the DNA helix. C30 exhibits H-bonds with T12 instead altering also the normal watson-crick pairing between T12/A29 (Fig. 8.9.). A29(N1) on the other hand could be interacting with the ammine ligand since a distance of 2.06 Å was observed.

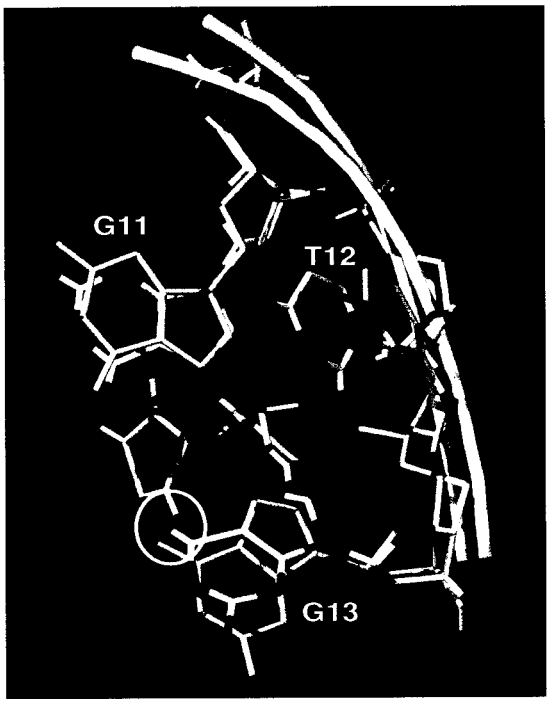

Figure 8.9. Conformational differences between local maximum and local minimum (magenta) of energy in *bintra* equilibration step. The interaction of the thiazole ligand with G13(O6) is highlighted within a white circle. Position of platinum ions is indicated.

In the local minimum conformation basically all the features for the maximum were conserved except that the thiazole ring changed position in such a way that the distance between G13(O6) with the H2 proton goes from 5.09 to 2.96 Å indicating an interaction between these two atoms, this interaction is highlighted in figure 8.9. where the relative positions of the thiazole ligand can be appreciated.

8.3.2 Production.

For tthis step of the simulation the total energy was monitored every 0.1 ps and plotted with the help of the *mdout* program. Energy profiles for the free sequences TGC and TGT showed little variation, they mostly fluctuate around a certain value - 61,17 (± 0,03) kcal/mol and - 65,23 (± 0,03) kcal/mol respectively (figure 8.10.).

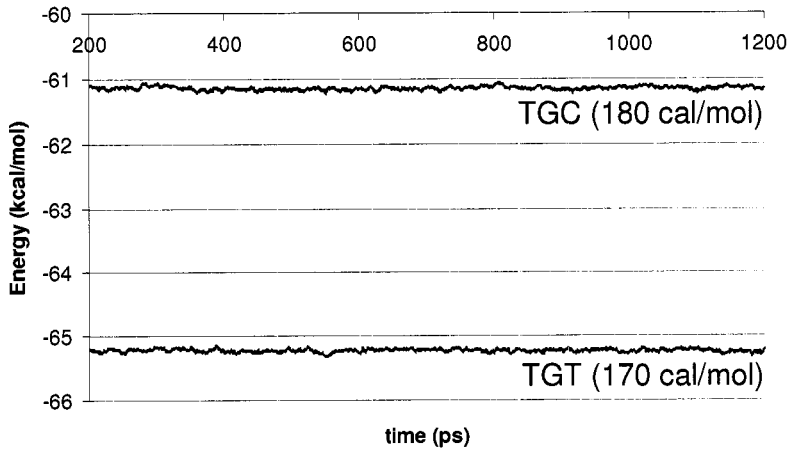

Figure 8.10. Energy profile obtained for free sequences TGC and TGT during the 1.0 ns period of MD. The fluctuation between maxima and minima is indicated.

For sequence TGC one H-bond was broken during the first 100 ps of production, this happened in the last base pair T20/A21 due to a destacking of the adenine nucleobase. A/T base pairs are inherently less stable than G/C mainly due to the number of hydrogen bonds present (2 vs. 3, Fig. 8.11.), real oligomers are less stable at the ends and a terminal A/T could be prone to initiate strand separation. On the other hand the sequence TGT exhibited all base-pair hydrogen bonding interactions during the production.

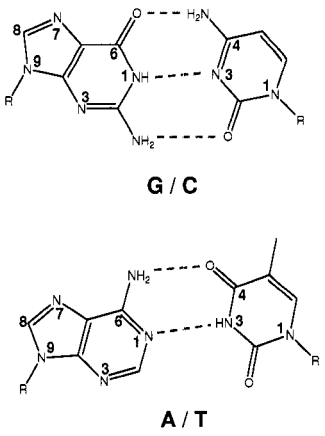

Figure 8.11. Watson-Crick hydrogen bonds (red) exhibited in DNA base pairs.

8.3.2.1. Monofunctional adduct: Figure 8.12. shows the energy profile for the *mono* adduct, during the middle stage of the production rotations around the Pt-guanine bond caused maxima in energy of about 1 kcal/mol (597 ps.). This conformational change placed the thiazole in a solvent exposed position, while the smaller ammine ligand was placed closer to the DNA. According to the energy profile though, there was not net gain in energy from this change in conformation and the high-energy state is probably derived from clashings of the thiazole ligand with the phosphate backbone in DNA when changing positions (A and B in Fig. 8.12.). The interaction between the ammine ligand with the phosphate in G10 was also lost due to this rotation.

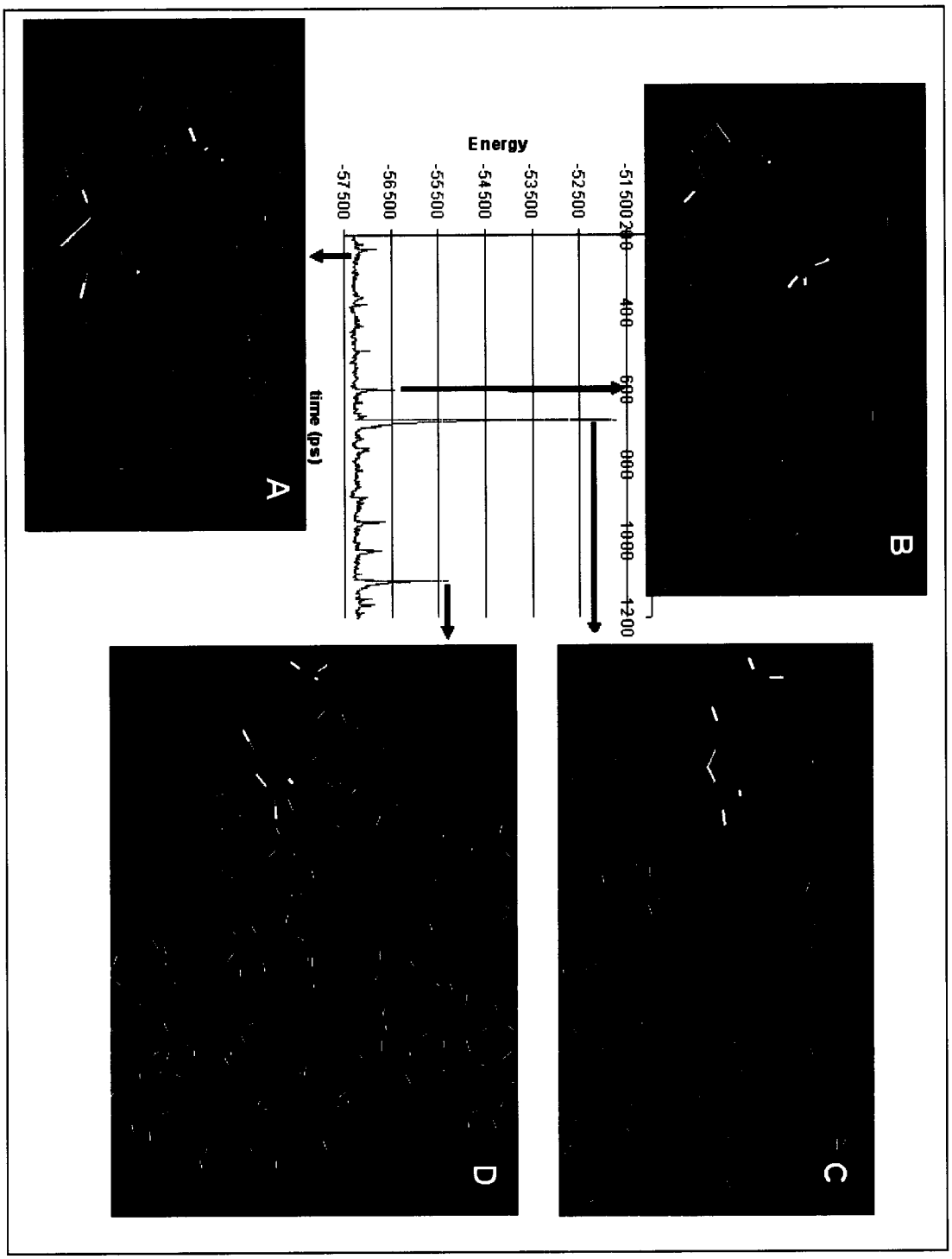

Figure 8.12. Energy profile obtained for the monofunctional adduct of ATZ to the 20-bp oligomer during the 1.2 ns of MD. Conformation for the different high energy states is presented (A – D).

A second and larger maximum in energy was caused by the destacking of the platinated guanine base (G10) from the double helix at aprox. 680 ps. This distortion produced a 6.5 kcal/mol maximum in the energy profile losing all the Watson-Crick interactions for the base pair G10/C31 (C in Fig 8.12.). The new placement of the ammine ligand from ATZ allowed it to be again in close proximity to the phosphate in G10 (2.83 Å). This severe conformational change caused a further distortion in the preceding base pair A9/T32 as measured through the program X3DNA, confirming the appearance of a different helical region compared with the starting right-handed nucleic acid structure. The last important maximum in energy occurred at aprox. 1102 ps and basically the movement of the destacked nucleobase apart from the helix can be accounted for the 2 kcal/mol maximum (D in Fig. 8.12.). Fitting of only the DNA backbone in the different 100 ps periods resulted in a RMS plot like the one seen in figure 8.12. It can be appreciated in the plot that a major displacement registered in DNA conformation can be correlated with the energy peaks previously seen in the energy profile (ca. 400 – 600 ps), after destacking of G10 the net conformational changes in DNA conformation diminished indicated by the presence of two minima, 600 ps and 800 ps., with RMS = 2.6 – 2.7 Å. Then again in the last part of the production there was a second major net maximum probably corresponding with the effect of the ATZ-G10 adduct drifting apart from the double strand. The average RMS registered during the production step for *mono* was 3.2 ± 0.5 Å, this value for TGC was very similar, 3.2 ± 0.6 Å indicating that conformations in both systems did vary at a same extent during the 1.0 ns of production dynamics. However when the last 100 ps

production for mono were compared with the analog production step in TGC a rather high RMS of ca. 4.8 Å. was found, indicating a significant different conformation for the 20-mer when is monofunctionally coordinated by the platinum ion in ATZ. This fact confirmed that the presence of the monofunctional adduct can introduce significant conformational changes in the DNA sequence even at very short times of simulation < 1 ns.

It is worthwhile to mention that the destacking of the nucleobase can be related to the inherent instability of monofunctionally platinated DNA adducts, this fact was reported by a study with complexes closely related to ATZ and TPAs in general.[12] Basically the destacking of one of the nucleobases as it was observed in the present study could create a weak point constituted by unpaired nucleobases or "bubble" inside the double helix, the net effect is similar to the relative instability observed for the ends of the sequence. For the monoadduct the destacking of G10 would decrease the net stability of the TGC sequence, suggesting a potential strand separation for longer simulation periods (> 2 ns).

8.3.2.2. Bifunctional interstrand (*binter*) adduct:

The energy profile for *binter* showed basically two big maxima at 270 (ca. 3.0 kcal/mol) and 570 ps. (1.1 kcal/mol). During the first 100 ps of production dynamics the only remaining H-bond between G30 and C11 was broken, therefore the hydrogen bond interaction between the base pairs G10/C31 and G30/C11 was totally disrupted, in addition A29 was placed almost perpendicularly to the corresponding T12 thus minimizing their Watson-crick interaction interaction (Fig. 8.14.A). Besides from these energy contributing features related to the platinum complex, changes in the DNA sequence proven to be more

relevant for the maxima observed later on the simulation (i.e. 570 ps). RMS values obtained (Fig 8.13.) for this system indicated an appreciable increase in conformational change for the DNA from 600 ps, also a qualitative comparison of the DNA backbone using the program Swiss PDB viewer between the system before and after the energy maximum served to provide a good indication of the extent of DNA deformation (Fig. 8.14., A and B). An additional increase of RMS values were observed in the last 200 ps of production which did not generate a significant increase in total energy, only three minor fluctuations (1059 ps, 1100 ps. and 1170 ps.) around 0.5 kcal/mol were observed during this period.

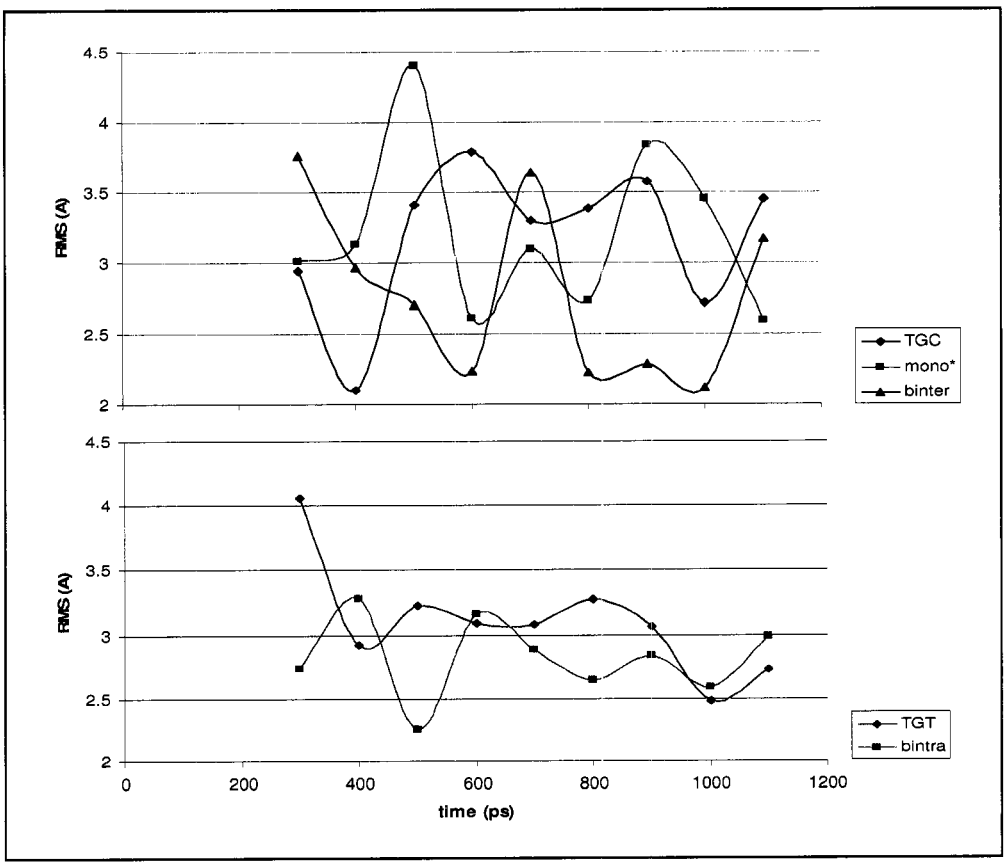

Figure 8.13. RMS values obtained for different systems studied.

Again another picture of the last 100 ps in production show how the complex is out of the plane of the DNA backbone, folding the 20-mer to some extent (Fig. 8.14, C). During the production the ammine ligand in ATZ exhibited close contacts (2.7 – 2.4 Å) with both G10 and C11 and this interaction could stabilize to some extent the adduct formed. The interaction of ammine ligands have been shown to account for more than 70% of the H-bond energy in the case of DNA-cisplatin adducts, therefore the ammine ligand is expected to play a significant role also in the case of ATZ.

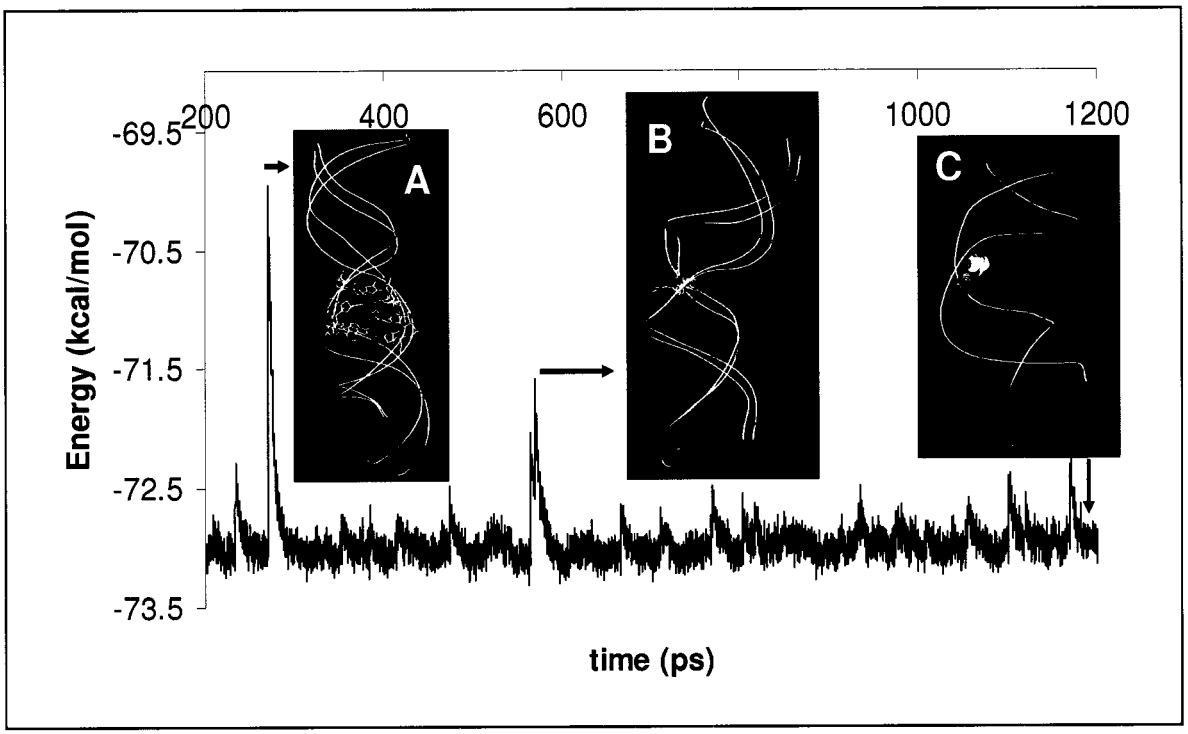

Figure 8.14. Energy profile obtained for the *binter* adduct of DNA-ATZ displaying the change in conformation for the energy maxima.

The average change in conformation for binter alone measured through RMS value (2.8 ± 0.6 Å) was not significantly different when compared to *mono* or TGC, according to

t-test criteria (P = 0.1765). However the net effect of the bifunctional adduct on the free sequence can be appreciated when comparing the last 100 ps. for these two systems: RMS = 4.9 Å. This value is comparable to the one obtained for the mono system even when in this case no nucleobase was destacked from the DNA sequence, probably the DNA bending observed and the additional disruption of Watson-crick interaction can be accounted for the difference (1 bp *mono* vs. 3 bp *binter*).

8.3.2.3. Bifunctional intrastrand (*bintra*) adduct:

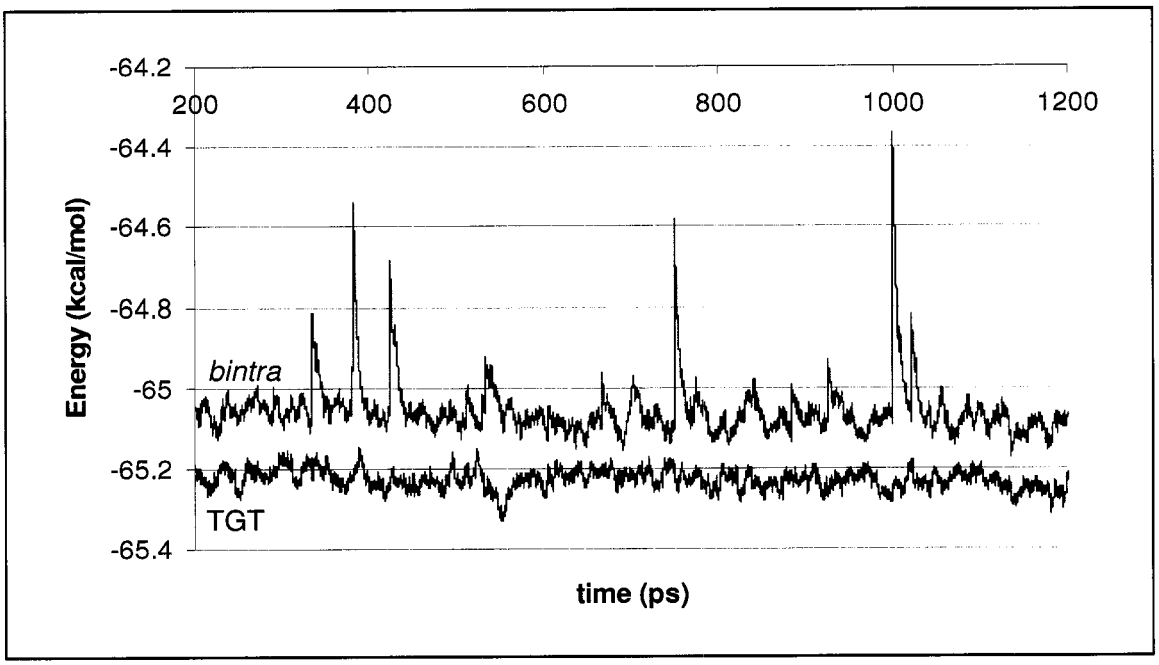

Figure 8.15. Energy profile obtained for the *bintra* adduct of DNA-ATZ (in purple), compared with the free TGT sequence used as a reference (green).

The energy profile for *bintra* during the production exhibited only minor maxima being the larger of them at 1000 ps. (1.1 kcal/mol, fig 8.15.), this was relatively small in contrast to the other adducts studied. RMS for *bintra* was concordantly low with an

average of 2.8 ± 0.3 Å, which is comparable with the free TGT (3.1 ± 0.3 Å) according to t-test criteria (P = 0.0907). This system did not diplay any significant difference during the production step, but minor displacements of the metal complex and the DNA sequence in agreement with the low RMS values observed for this system (Fig. 8.15.).

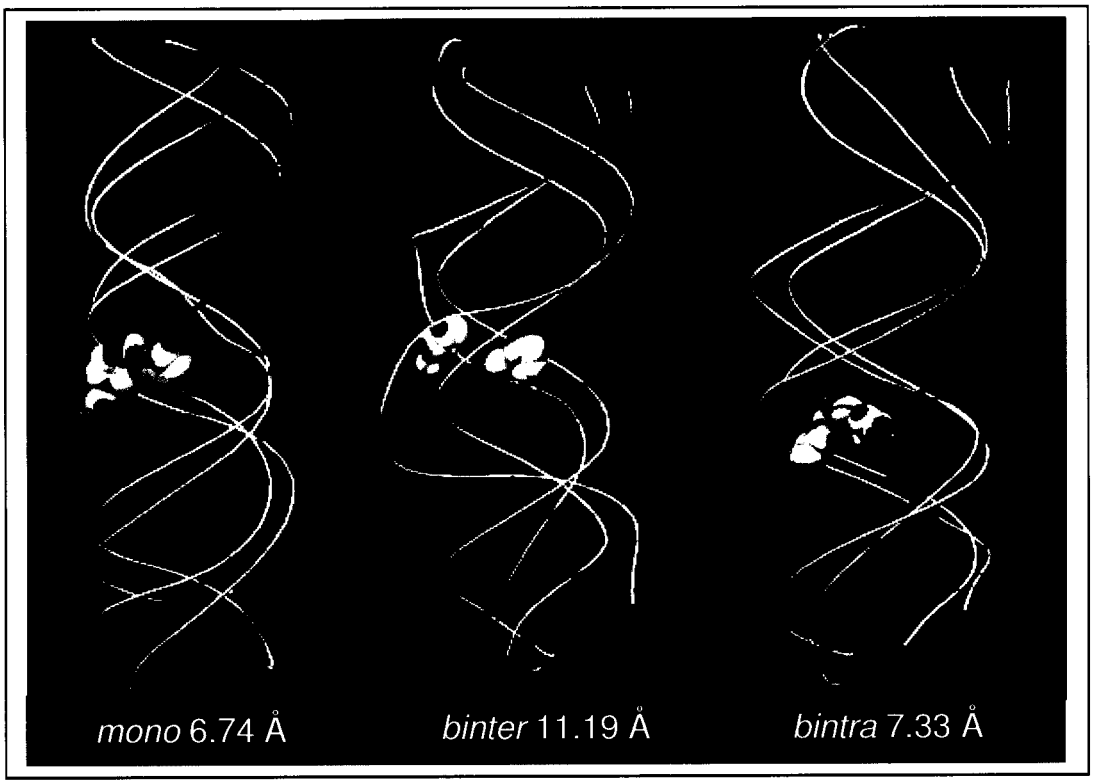

Figure 8.16. Comparison of DNA conformation and platinum complex displacement before and after 1.2 ns of simulation for the platinated adducts studied. Initial structure is colored white and final structure in yellow, also initial complex is indicated with the arrow. RMS between structures is presented.

The net comparison of structural conformation at the initial and final stages of the MD study can be seen in Fig. 8.16. for the platinated systems and Fig 8.17. for the free DNA sequences including RMS values obtained by comparing the DNA backbone in the

first step of equilibration with the last step in production. For the free TGC and TGT sequences it was found that due to the flexibility of DNA inside the waterbox and the temperature employed in the simulation experiments a certain RMS was associated with the system in a range between 5.30 to 7.45 Å. The only platinated adduct that was different into this regard was the *binter* exhibiting an unusually high RMS value that can be correlated to the bending of the DNA.

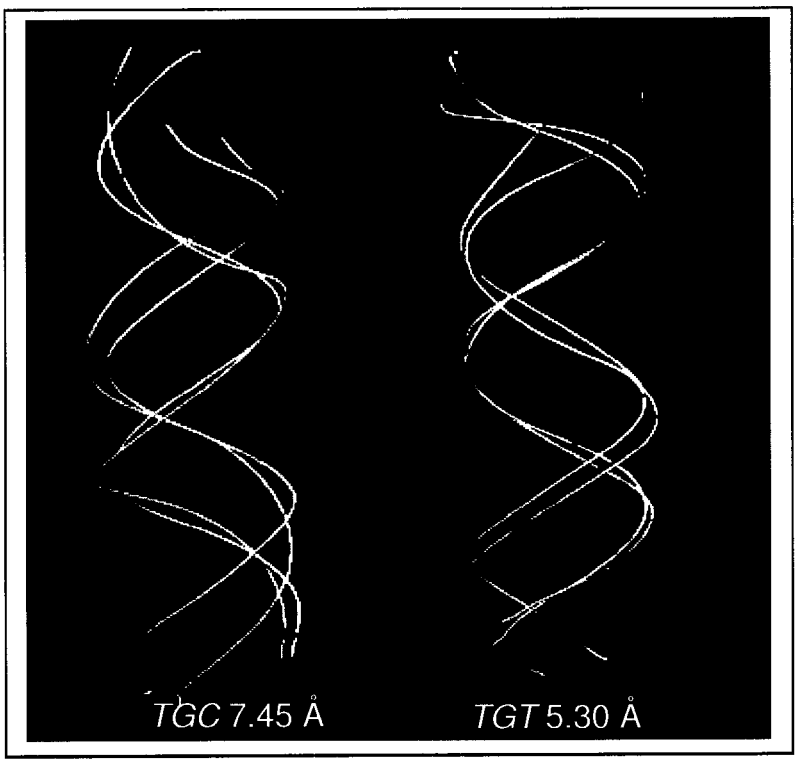

Figure 8.17. Comparison of DNA conformation before and after 1.2 ns of simulation for the free DNA sequences studied. Initial structure is colored white and final structure in yellow, RMS between the structures is presented

In terms of base pairs affected the analysis of H-bonds using the program X3DNA provided indication that *mono* disrupted basically the T9/A32 bp in a moderate extent and G10/C31 strongly due to destacking of G10. For *binter* there were three disrupted base

pairs: T9/A32 moderate, G10/C31 strong and C11/G30 moderate. For *bintra* on the other hand T10/A31 appears as moderately disrupted, while G11/C30 and T12/A29 are strongly disrupted.

8.3.2.4. Analysis of root mean square value using *ptraj*:

A different RMS analysis can be performed with the sub-program *ptraj* included in the program AMBER 7, which process the coordinates of the heavy atoms (all atoms except hydrogens) in DNA (Fig. 8.18.). The analysis performed in the preceding sections is based on DNA backbone only and was done with the program Swiss PDB viewer, *ptraj* on the other hand provides a different approach since considers sugars and nucleobases as well. In general for the production step in the simulation a higher RMS for the *mono* adduct can be observed, specifically an increase can be noted around 700 ps correlating with the nucleobase destacking observed previously for this system.

It is interesting to note that the RMS profile for *mono* obtained with *ptraj* exhibits a higher correlation with the screenshots produced for the system, the increase in conformation flexibility after nucleobase destacking and drifting is better seen in figure 8.18., with an RMS that exhibits the higher values after 700 ps., average was 2.1 ± 0.7 Å. This can be understood since *ptraj* considers more atoms and the monitoring of the system is performed every 5 ps., with the previous method only 100 ps. periods are available to compare changes in conformation.

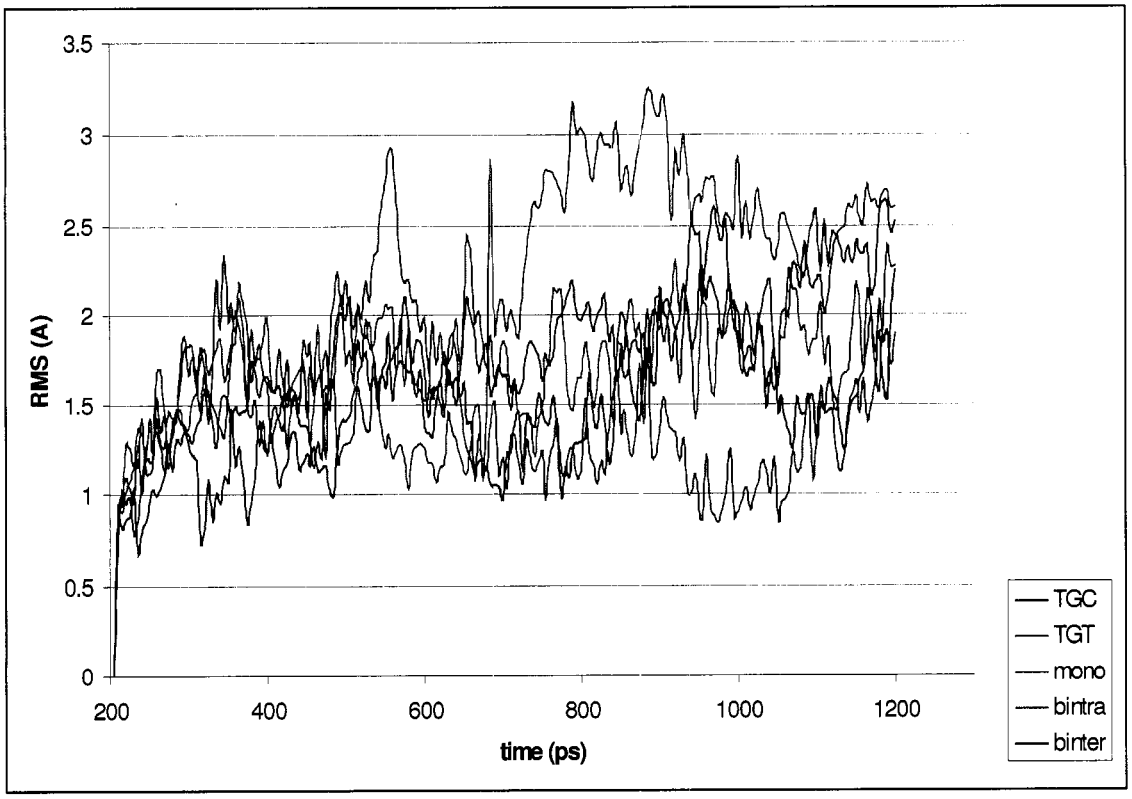

Figure 8.18. RMS displacement of the heavy atoms in DNA for the systems studied during the production step as measured through the program *ptraj*.

The bifunctional platinum adducts *binter* and *bintra* did not exhibited appreciable differences on this profile and in fact their RMS was very similar 1.8 ± 0.4 Å and 1.7 ± 0.3 Å respectively. The RMS average for the free TGC and TGT sequences was the same 1.5 ± 0.4 Å (fig. 8.19.), even though when local maximum (560 ps.) and minimum (1000 ps.)can be observed. If the number of measurements for the production is taking into consideration (n =200) in a t-student test, then the platinated adducts will be significantly different compared with the free sequences. In addition *bintra* and *binter* will also exhibit a significant statistical difference ($P = 0.0049$).

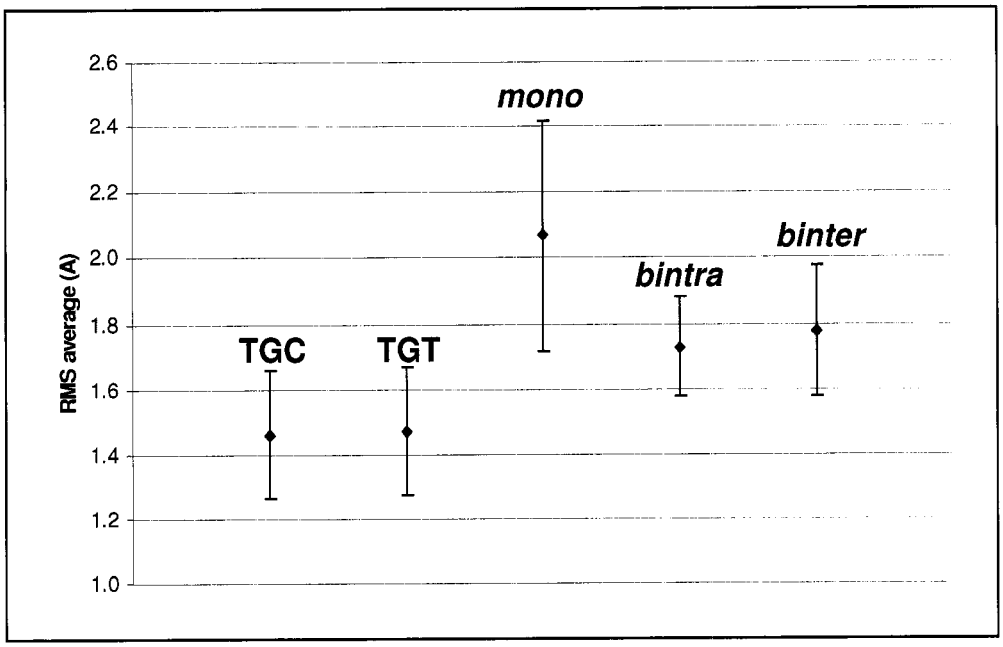

Figure 8.19. RMS average and standard deviation observed for the systems studied during the production step (n = 200) as measured through the program *ptraj*.

A comparison between experimental findings for 1,2-interstrand and 1,3-intrastrand bifunctional ATZ adducts and results on this work can be done even when the relative short simulation time is considered. Briefly, using chemical probes such as $KMnO_4$ that react preferentially with single stranded DNA it was found previously that base-pair disruption involved more nucleobase pairs for 1,3-intrastrand adducts (6) than for 1,2-interstrand adducts (4). In addition the degree of conformational distortion was more pronounced in the intrastrand adduct as seen in figure 8.20. From this study, the 1,2-interstrand adduct *binter* caused one strong disruption of Watson-crick pairing and moderate disruption in the adjacent base pairs. In the case of *bintra*, platination in positions 1,3- caused strong disruption in two bp while in the same side that strong reactivity is

observed in experimental conditions. A further moderate disruption was observed in the bp on the side that weak reactivity was observed. In addition results of RMS analysis performed with *ptraj* could indicate a greater DNA deformation for *bintra* than *binter*.

8.4. Experimental Section (Desription of the method).

The simulations consisted of three consecutive parts where the system were gradually built and minimized in order to proceed with the MD study:

8.4.1. Preparation: The 20-bp oligomer sequences were built in the right handed B DNA conformation using the program *nukit*,[13] included in the AMBER7 suite. The sequences were minimized in vacuo using the *sander* program and the AMBER force field parameters (specifically the force field 99 or *ff99*). The minimization consisted of 2500 cycles using the steepest descent method followed by another 2500 cycles with the conjugated gradient method; the system was minimized before and after the addition of counter ions (Na^+) to neutralize the charge. In both cases the heavy atoms (not H) in DNA were restrained. A third minimization was performed for the entire system with a generalized Born solvation model. After this step the complete system (DNA + nNa^+ / PtDNA + nNa^+) was placed inside a waterbox with periodic boundary conditions to proceed with the equilibration.

In order to build the platinated sequences, the geometry of the fragments $[PtCl(NH_3)(thiazole)]^+$ and $[Pt(NH_3)(thiazole)]^{2+}$ was optimized using the Amsterdam Density Functional software, considering relativistic scalar ZORA basis sets for all atom types. Another important result obtained were the partial charges for the atoms in the fragments, these charges were manually added to the system producing a net charge of +1

or +2 for monofunctional and bifunctional adducts respectively (fig 8.20.). After obtaining the optimized fragments, they were bound to the nitrogen 7 in the appropriate guanine nucleobase using the graphical interface *xleap* from AMBER7.

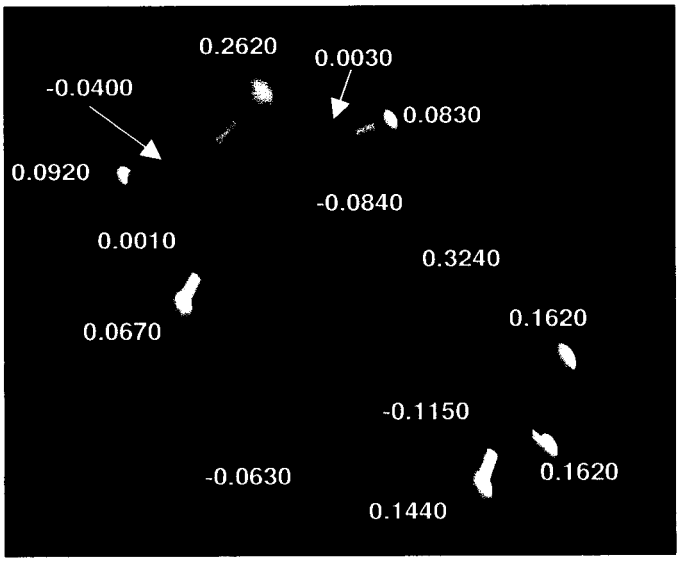

Figure 8.20. Geometry and charges obtained for mono-functional platinated fragment using DFT calculations.

The use of the metallic fragments involves parameters not existent in the force field employed, such as bond lengths/strengths, angles and torsions relating to the platinum atom. These values were introduced with the help of a previous force field used in similar calculations,[14,15] together with information from crystal structures for the ATZ complex.[16]

8.4.2. Equilibration: The five model systems: free TGC, free TGT, *mono*, *bintra* and *binter* adducts were equilibrated inside the water box for 220 picoseconds at constant pressure and temperature of 300 °K. During the first 20 picoseconds heavy atoms in DNA were constrained and then gradually released in two MM/MD alternating steps, followed by 8 MM minimization cycles in order to proceed with the final equilibration (MD). The programs *mdout* and *ptraj* supplied by AMBER7 were used to analyze the data. The first

of the programs process all the MD files and produce a series of summary files, each associated with a different property of the system including total volume, density, energy and temperature. The second of these programs return the root mean square of the distance for the heavy atoms in DNA in the simulation; this will provide a criterion for achievement of a conformationally rigid structure or a minimum in the simulation.

8.4.3. Production:

After a stabilization of the initial model systems additional 1000 ps of MD at constant pressure and 300 °K were followed, the simulation was performed in ten steps of 100 ps each. Data was again processed using the programs *mdout* and *ptraj*.

Programs X3DNA[17] and Swiss PDB viewer[18] were used to visualize, compare and fit the conformation of the different systems studied in periods of 10 ps. for the equilibration and 100 ps. for production steps. The difference between the net displacement of every atom will be expressed in root mean square (RMS) values (Å). The criteria employed for H-bond detection was 1.20 – 2.76 Å and 120°.

Figures and movies of the MD simulations were produced with the program VMD[19] and POV-ray 3.6.[20]

8.5. Conclusions.

The study of the different DNA adducts formed by relevant platinum complexes has been an area of increasing research interest, since it is proposed that this event will dictate the subsequent cascade of cellular events and biological outcomes of the chemotherapeutic agent. In other words the proposed concept of transition-metal drugs that

bind to DNA in a fundamentally different manner to that of "classical" platinum complexes like cisplatin may have altered pharmacological properties.[21, 22]

Specifically for active TPA complexes; this is the first application of molecular dynamics to platinated DNA adducts. Despite the short simulation period, important features for these adducts could be seen. First mono- and bi-functional platinum adducts can alter the conformation of free DNA as compared with the free sequences. Second, a comparison between bifunctional platinum adducts indicate that the differences in base pair disruption can be originated during the first nanosecond of reaction. To this regard two approaches for monitoring the net displacement of the system (RMS) were employed. Third, the monofunctional complex showed possibility of destacking of the platinated nucleobase within one nanosecond with the implications of further destabilize DNA as has been observed experimentally.

Therefore these features can be related to real behavior for the DNA adducts of the representative complex ATZ, and could be worthwhile pursuing longer simulations.

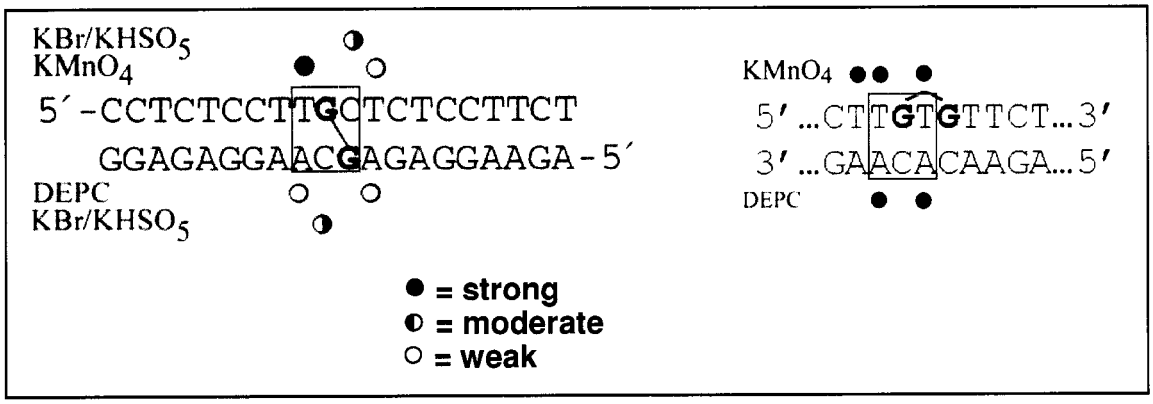

Figure 8.21. Results from probing DNA conformation for interstrand (left) and intrastrand adducts (right) of ATZ. Platinated bases are bold and degree of reactivity is explained in legend.

8.6. References.

(1) Natile, G.; Coluccia, M., *Coord. Chem. Rev.*, **2001**, 216-217, 383-410.

(2) Djuran, M.I.; Lempers, E.L.M.; Reedijk, J., *Inorg. Chem.*, **1991**, 30, 2648-2652.

(3) Anzellotti, A.; Stefan, S.; Gibson, D.; Farrell, N., *Inorg. Chim. Acta.*, **2006**, 359, 3014 -3019.

(4) Van Beusichem, M., Farrell, N., Inorg. Chem., **1992**, 31, 634 – 639.

(5) Fojo, T.; Farrell, N.; Ortuzar, W.; Tanimura, H.; Weinstein, J; Myers, T.G., Crit. Rev. Oncol. Hematol., **2005**, 53, 25 – 34.

(6) Bierbach, U; Farrell, N., *Inorg. Chem.*, **1997**, 36, 3657-3665.

(7) Zakovska, A.; Novakova, O.; Balcarova, Z., *et. al*, *Eur. J. Biochem.*, **1998**, 254, 547-557.

(8) *Haile, J.M.* Molecular Dynamics Simulations: Elementary Methods; Wiley: New York, 1992.

(9) Elizondo-Rojas, M-. A.; Kozelka, J., *J. Mol. Biol.*, **2001**, 314, 1227 – 1243.

(10) Marini, V., Christofis, P., Novakova, O., Kasparkova, J., Farrell, N., Bravec, V., *Nucl. Acids Res.*, **2005**, 33, 5819 – 5828.

(11) Kasparkova, J.; Novakova, O.; Farrell, N.; Brabec, V., *Biochemistry*, **2003**, 42, 792 – 800.

(12) Pearlman, D.A.; Case, D.A.; Caldwell, J.W.; Ross, W.S.; Cheatham, T.E. III; DeBolt, S.; Fergusson, D.; Seibel, G.; Kollman, P., *Comp. Phys. Commun.*, **1995**, 91, 1 – 42.

(13) Yao, S; Plastaras, J.P.; Marzilli, L.G., *Inorg. Chem.*, **1994**, 33, 6061 – 6077.

(14) Hambley, T.W.; Jones, A.R., *Coord. Chem. Rev.*, **2001**, 212, 35 – 39.

(15) Bierbach, U.; Qu, Y.; Hambley, T.W.; Peroutka, J.; Nguyen, H.L.; Doedee, M.; Farrell, N., *Inorg. Chem.*, **1999**, 38, 3535 – 3542.

(16) Lu, X-.J.; Olson, W.K., *Nucleic Acids. Res.*, **2003**, 31, 5108-5121.

(17) N. Guex, M.C. Peitsch, Electrophoresis, 1997, 18, 2714 – 2723.

(18) Humphrey, W.; Dalke, A.; Schulten, K., *J. Molec. Graphics*, **1996**, 14, 33-38.

(19) http://www.povray.org/

(20) Bauer, C.; Peleg-Shulman, T.; Gibson, D.; Wang, A.H. *Eur. J. Biochem.*, **1998**, 256, 253 – 260.

(21) Robertazzi, A., J.A. Platts, *Chem. Eur. J.*, **2006**, 12, 5747 – 5756.

(22) Farrell, N., Kelland, L.R., Roberts, J.D., Van Beusichem, M., *Cancer Res.*, **1992**, 52, 5065 – 5072

CHAPTER 9 General Conclusions

Nucleobases play a central role in chemical-biology. Their unique chemical properties have made of these particular purines and pyrimidine derivatives, the chosen building blocks to store and transfer genetic information. Metal -nucleobases coordination complexes have been studied for the last two decades as initial models to understand the mechanism of action or biological properties of certain transition metals, particularly platinum. New and exciting chemical features can be observed when nucleobases are coordinated to metal ions, and this is due to a specific modulation of electronic and steric properties in the nucleobase that are only achievable upon coordination. A previously reported strengthening of H-bond capability for nucleobases is important for DNA/RNA recognition since can lead to more robust Watson-Crick (or Hoogtseen type) pairing, which together with the coordination geometry in the metal center can generate versatile and novel structures (fig. 9.1).[1-4]

In this work an initial, though important, "proof-of-concept" was shown regarding the role of metallated nucleobases as motifs for molecular recognition in terms of π-stacking interaction (Chapter 3 - 5). This case represent a complementary non-covalent interaction to the previous strengthening of H-bond, which is also exhibited by free nucleobases, but enhanced by the coordination to a metal ion such as Pt(II) or Pd(II). This particular interaction is interesting because it also allows recognition of aromatic aminoacid residues present in proteins like tryptophan, thus its importance in the study of non-covalent interactions in ternary systems composed of Proteins, DNA/RNA, and a

metal ion such as Pt(II)/Pd(II). Molecular recognition of specific substrates using only π-stacking interactions was proven to be very modest as per the value of association constants obtained, however its reinforcement with other non-covalent interactions as H-bonding or cation-π are not negligible for more complex *in vivo* systems.

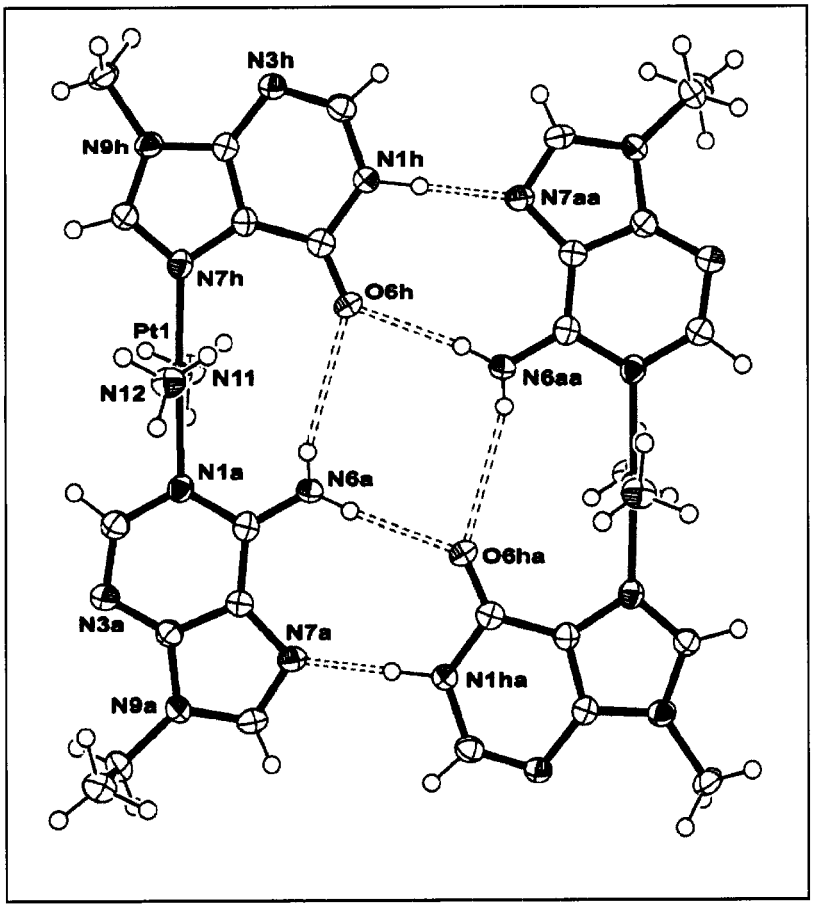

Figure 9.1. Dinuclear, hydrogen bonded cation *trans*-[$(NH_3)_2$-Pt(9-EtA-*N1*)(9-MeHx-*N7*)]$(NO_3)_2$, where 9-EtA = 9-ethyladenine and 9-MeHx = 9-methylhypoxanthine)[4]

Adducts obtained for metal-nucleobase complexes with tryptophan and the C-terminal zinc finger (NCp7) *via* ESI-MS experiments indicated a high stability given the relatively harsch experimental conditions to its detection and study. Also the trend

observed for association constant when the zinc finger was used confirms that other types of non-covalent motifs could be helping the recognition process. It is very probable that the use of a short oligomer instead of a single nucleobase would increase even by order(s) of magnitude this process, especially when the two zinc fingers in NCp7 will be involved. In this case, then the anti-viral activity for these complexes can be improved significatively.

The enhancing effect that nucleobase metallation induces on π-stacking interactions can be ultimately linked to the role of the interacting frontier molecular orbitals (HOMO-LUMO) as showed through density functional theory calculations, this finding showed a common factor invoved also for the broadly known process of nucleobase alkylation and could indicate new modes of interaction for metal-nucleobase complexes with alternative signal-processing mechanism in the cell (see introduction chapter 6).

The role of the nucleobase as ligands involves also modulation of reactivity as was shown in (Chapter 7) which will affect directly in the covalent interaction on the metal-nucleobase complex. Results obtained in Chapter 4 could suggest the use of Pd(II)-nucleobase complexes to specifically interact and cleave peptides and proteins at aromatic residues, in another possibility that remain to be explored in the future and was opened in the present work.

To finish metal-nucleobase or metal-oligonucleotide complexes with specific sequences could be designed to not only increase the half time of the oligo in the body (already reported)[5,6] but to recognize with a reasonable specificity relevant biological substrates.

(1) Roitzsch, M; Lippert, B. *Angew. Chem. Int. Ed.*, **2006**, 45, 147 – 150.

(2) Roitzsch, M; Anorbe, M.G.; Miguel, P.J.S.; Muller, B.; Lippert, B. *J. Biol. Inorg. Chem.*, **2005**, 10, 800 – 812.

(3) Shen, W.; Gupta, D.; Lippert, B. *Inorg. Chem.*, **2005**, 44, 8249 – 8258.

(4) Roitzsch, M; Lippert, B. *Inorg. Chem.*, **2004**, 43, 5483 - 5485.

(5) Perrier, S.; Seela, F.; Schwartz, A.; Leng, M; Chottard, J.C. *Eur. J. Inorg. Chem.*, **2003**, 8, 1641 – 1644.

(6) Muller, J.; Drumm, M.; Boudvillain, M.; Leng, M.; Sletten, E.; Lippert, B. *J. Inorg. Biochem.*, **2001**, 86, 79-79.

VITA

EDUCATION

- **Doctor of Philosophy in Chemistry**, Virginia Commonwealth University (VCU). Richmond, Virginia. **GPA : 3.92**
  Thesis Advisor: Dr. Nicholas P. Farrell
  "Study of covalent and non-covalent interactions on ternary systems involving metal-DNA/RNA-proteins, where metal = Pt(II),Pd(II)"

- **Magister Scientiarum in Chemistry**, Venezuelan Institute for Scientific Research (IVIC). Caracas, Venezuela. May 2004.
  Thesis Advisor: Dr. Roberto Sanchez-Delgado
  "On the understanding of the mode of action of Ru – azole compounds as antichagasic drugs"

- **Bachelor of Science in Chemistry**, University of Los Andes (ULA). Merida, Venezuela. October 1997.
  Thesis Advisor: Dr. Bernardo Fontal
  "Ruthenium Complexes in Biphasic Catalysis"

RELEVANT WORK EXPERIENCE

Research Assistant, VCU, Richmond, VA, 01/03 - 03/07

- Synthesize and characterize metal complexes of Pt(II), Pd(II), Au(III) and Ru (II)/(III).
- Study of the interaction DNA-metal-protein using different spectroscopic techniques.

NMR facility assistant, VCU, Richmond, VA, 01/04 - 03/07

- Perform general maintenance of NMR equipment (N_2/He).
- Installation of Pt probe for ^{195}Pt-NMR.

Intern Chemist, Eastern Isotopes, Inc., Richmond, VA, 08/05 - 03/06

- Synthesize and characterize radiolabeled drugs for use in Positron Emission Tomography.
- Develop and deploy quality control procedures in the laboratory.

Teacher Assistant, VCU, Richmond, VA, 01/04-12/05

▪ Assisted in teaching Quantitative Analysis Laboratory, General Chemistry I, and Introductory Chemistry.

Research Assistant, Procter & Gamble, Caracas, Venezuela, 02/98-09/00

▪ Performed and wrote technical assessment for P & G and competition products.

▪ Assisted in evaluate cases of patent infringement for the area of Latin-America.

▪ Performed technical tests for demo development.

▪ Maintained and updated consumer complain system.

Research Assistant, Los Andes University, Merida, Venezuela, 01/96-12/97

▪ Synthesized and characterized Organometallic catalysts to be used in amine synthesis.

Industrial Intern, LAGOVEN – Oil refinery plant, Punto Fijo, Venezuela, 07/96-08/96

▪ Fine-tuned method for analysis of gasoline batches using gas chromatography/mass spectrometry (GC/MS).

Teacher Assistant, Los Andes University, Merida, Venezuela, 02/93-12/94

▪ Assisted in teaching and preparing General Chemistry I laboratory classes.

PRESENTATIONS & WORKSHOP EXPERIENCE

• Gordon Research Conference – Metals in Biology (2007)	"Effects of Nucleobase Metallation on Frontier Molecular Orbitals: Potential Implications for π-stacking Interaction with Tryptophan"
• Biomedical Imaging Research Opportunities Workshop 4 (2006)	"Iodine-124 produced by the Te-124(p.n)I-124 reaction: Specific Activity and Te(IV) determination"
• International Conference in Biological Inorganic Chemistry (2005)	"Toward Selective Zinc Finger Recognition. Use of Pt- and Pd-nucleobase complexes to enhance specificity"

• U.S.-JAPAN COOPERATIVE CANCER RESEARCH PROGRAM SEMINAR (2005)	"Study of covalent and non-covalent interactions in $[Pd(dien)nucleobase]^{2+}$/ l-tryptophan(N-Acetyl-tryptophan) systems: Formation of metal-tryptophan species by nucleobase substitution under biologically relevant condition"
• 2nd Gordon Research Conference – Metals in Medicine (2004)	"Study of the mechanism of action of ruthenium-azole complexes against the *Trypanosoma cruzi*"
• 9th International Symposium on Platinum Coordination Compounds in Cancer Chemoptherapy (2003)	"Study of Pt(II) and Pd(II) coordination on tryptophan-nucleic base stacking interaction"
• V Venezuelan Chemistry Congress (2001)	"Synthesis and Characterization of $[Ru(MeCN)_6][ZnCl_4]$"
• Iberoamerican Catalysis Symposium (1998)	"$RuCl_2(DMSO)_4$ - Study of the catalytic activity in Biphasic and Homogeneous system"
• VI Iberoamerican Congress in Inorganic Chemistry (1997)	"Derivatives of $Ru_3(CO)_{12}$ with polydentate phosphines. Catalytic Activity"
• III Venezuelan Chemistry Congress (1996)	"Study of the catalytic properties of the cluster $Ru_3(CO)_{10}(\mu$ - dppm)"

SEMINARS

- Actinide Chemistry and Catalytic Applications, IVIC- Venezuela, Dr. Moris Eisen (Technion Institute of Technology – Israel), Jul. 2002.
- II School in Environmental Chemistry, U.L.A. – Venezuela, Dr. Miguel Alonso (U.L.A. – Venezuela), Nov. 2001.
- Organometallic Chemistry for Organic Synthesis, IVIC – Venezuela, Dr. Henri Arzoumanian (CNRS, Université aix-Marseille – France), Nov. 2001.
- Enantioselective Catalysis, IVIC – Venezuela, Dr. Serafino Gladiali (Sassari Univ. – Italy), Nov. 2000.
- Silicone Seminar, P & G – Venezuela, Dr. Adam Peterson (Dow Corning – U.S.A.), Sept. 99.
- Single Crystal Difractometry, U.L.A. – Venezuela, Dr. Graciela Delgado (U.L.A.-Venezuela), Nov. 94.

PUBLICATIONS

- Anzellotti, A.I.; Liu, Q.; Bloemink, M.J.; Scarsdale, N.; Farrell, N.P., "Targeting the Retroviral Zinc finger-DNA interactions. A small molecule approach utilizing the electrophilic nature of trans-platinum-nucleobase compounds" (*In Press Chemistry & Biology*, 2006).

- Anzellotti, A.; Stefan, S.; Gibson, D.; Farrell, N., "Donor atom preferences in substitution reactions of trans-platinum mononucleobase compounds. Implications for DNA-protein selectivity" (Published on Web 2006 doi:10.1016/j.ica.2005.12.060, *Inorg. Chim. Acta.*).

- Anzellotti, A. I.; Sabat, M.; Farrell, N. P., "Covalent and non-covalent interactions for [Metal(dien)nucleobase]$^{2+}$ complexes with l-tryptophan derivatives: Formation of palladium-tryptophan species by nucleobase substitution under biologically relevant conditions", *Inorg. Chem.,* (**2006**), 45, 1638-1645.

- Anzellotti, A. I.; Ma, E. S.; Farrell, N. P., "Platination of nucleobases to enhance non-covalent recognition in protein-DNA/RNA complexes", *Inorg. Chem.*, (**2005**), 44, 483-485.

- Rieber, M.S.; Anzellotti, A.; Sánchez-Delgado, R. A.; Rieber, M., "Tumor apoptosis induced by ruthenium(II)-ketoconazole is enhanced in nonsusceptible carcinoma by monoclonal antibody to EGF receptor", *Int. J. Cancer.* (**2004**), 112, 376-384.

- Sánchez-Delgado R.A.; Anzellotti, A., "Metal Complexes as Chemotherapeutic Agents Against Tropical Diseases: Trypanosomiasis, Malaria and Leishmaniasis". *Mini Rev. in Med. Chem.*, (**2004**), 4, 159-165.

- Cabrera, E.; Cerecetto, H.; González, M.; Gambino, D.; Noelia, P.; Otero, L., Parajón-Costa, B.; Anzellotti, A.; Sánchez-Delgado, R.; Azqueta, A.; López de Ceráin, A.; Monge A., "Ruthenium(II) Nitrofurylsemicarbazone Complexes: New DNA Binding Agents", *Eur. J. Med. Chem.* (**2004**), 39, 377-382.

- Sánchez-Delgado,R. A.; Anzellotti, A.; Suarez, L., " Metal Complexes as Chemotherapeutic Agents Against Tropical Diseases: Malaria, Trypanosomiasis and Leishmaniasis", Metal Ions in Biological Systems, **2003**, Vol. 41, Siegel, A., Siegel, H. Eds., Marcel Dekker Inc: New York, 380-419.

- Anzellotti A., Briceño, A., Delgado G., Díaz-de-Delgado G.; Fontal B., "*cis*-dichloro[tris(diphenylphosphinoethyl)amine] ruthenium (II)-chloroform-water (1/2.5/1)". *Acta Cryst.* (**2002**). C58, m355 – m357.

- Anzellotti A.; Briceño A., "Hexakis(acetonitrile)ruthenium(II) tetrachlorozincate 2.55-hydrate". *Acta Cryst.* (**2001**). E57, m538-m540.

- Fontal B.; Anzelotti A.; Reyes M.; Bellandi F; Suarez T., "Catalytic Activity of $RuCl_2(DMSO)_4$ in Biphasic and Homogeneous Systems". *Catalysis Letters*, (**1999**), 59: (2-4), 187 –190.

IN PREPARATION

- Farrell, N.P; Anzellotti, A., "Zinc Metalloproteins as Medicinal Targets." (Submitted to *Chem. Soc. Rev.* 2007)

- Anzellotti, A.; Bayse, C; Farrell, N.P., "Effects of Nucleobase Metallation on Frontier Molecular Orbitals: Potential Implications for π-stacking Interaction with Tryptophan" (To be submitted to *J. Am. Chem. Soc.*, 2007)

AWARDS AND SCHOLARSHIPS

- Dr. Susan and Gerald Bass Scholarship, Chemistry Department-Virginia Commonwealth University. (2005)
- Fellowship for Ph.D. studies from the Chemistry Department- Virginia Commonwealth University. (2004 – 2005)
- American Chemical Society, International Activities Fellowship (2003)
- Fellowship for M.Sc. studies from the Venezuelan Academy of Physical, Mathematical and Natural Sciences. (2001-2003)
- "Outstanding Performance" from Los Andes University, Chemistry Dept. (1992 – 1994)

LANGUAGES

Spanish, English & Italian: Written and Spoken fluently.

ADDITIONAL SKILLS

- Synthetic Laboratory Techniques: Inert gas synthesis and high-pressure batch reactors.
- Spectroscopic methods of characterization: NMR, FT-IR, UV-vis, Fluorescence, AE-ICP, Gas Chromatography, HPLC.
- Computer working environments: Windows /Linux.
- Molecular Dynamics: AMBER package and ab-initio: Gaussian98.
- Docking programs: GOLD and FleXX.
- Visualization packages: Swiss PDB, WebLab, POV, Mercury, Ortep 3.

ASSOCIATIONS

- Venezuelan Chemical Society (2000-2002).
- Venezuelan Scout Association (1988 –1990).